Pharmacological modulation of mitochondrial dysfunction by Dimebon and Olesoxim in cellular and murine models of Alzheimer`s Disease

Dissertation
zur Erlangung des Doktorgrades
der Naturwissenschaften,
vorgelegt beim Fachbereich
Biochemie, Chemie und Pharmazie
der Johann-Wolfgang-Goethe Universität
in Frankfurt am Main

von
Schamim Eckert
aus Neu-Anspach
Frankfurt 2016

D30

… for my beloved mother ☺

Table of Contents

List of Abbreviations

ACh acetylcholine

AD Alzheimer's Disease

ADP adenosine diphosphate

AFM atomic force microscopy

AMPK adenosine monophosphate-activated protein kinase

ANT ATP–ADP translocase

ApoE apolipoprotein E

APP amyloid precursor protein

ATP adenosine triphosphate

APS Ammonium persulfate

Aβ β-amyloid

BCA bicinchoninic acid

b.w. body weight

cAMP cyclic adenosine monophosphate

cLSM confocal laser scanning microscopy

CS citrate synthase

DBC dissociated brain cells

DMEM Dulbecco's Modified Eagle Medium

DMSO dimethyl sulfoxide

DNA deoxyribonucleic acid

Drp1 dynamin-related protein 1

ETC electron transport chain

ETS electron transport system

FAD flavin adenine dinucleotide

FCCP carbonyl cyanide-4-(trifluoromethoxy)phenylhydrazone

FCS fetal calf serum

fis1 fission 1

GTP guanosine triphosphate

IU international units

i.p. intraperitoneal

i.v. intravenous

H2O2 hydrogen peroxide

HBSS Hank's Balanced Salt Solution

HEK Human embryonic kidney

HS horse serum

LOAD late onset Alzheimer disease

LPO lipid peroxidation

MDA malondialdehyde

Mfn1 Mitofusin 1

Mfn2 Mitofusin 2

MMP mitochondrial membrane potential

MPTP mitochondrial permeability transition pore

mtDNA mitochondrial DNA

NMDA N-methyl-D-aspartat

Opa1 optic atrophy 1

OXPHOS oxidativ phosphorylation

PCR polymerase chain reaction

PBS Phosphate buffered saline

PBR peripheral benzodiazepine receptor

PGC1α peroxisome proliferator-activated receptor gamma coactivator 1-α

PI protease inhibitor

P$_i$ inorganic phosphate

PMSF Phenylmethylsulfonylfluorid

PPARγ peroxisome proliferator-activated receptor γ

ppm parts per million

R123 Rhodamine-123

RCR respiratory control ratio

ROS reactive oxygen species

ROX residual oxygen consumption

TIMM translocase of the inner mitochondrial membrane

TOMM translocase of the outer mitochondrial membrane

Tris tris(hydroxymethyl)aminomethan

tRNA transfer ribonucleic acid

VDAC voltage dependent anion channel

Summary

To understand neurodegenerative diseases is one of the major challenges of the 21st century. This also includes Alzheimer´s disease (AD), which represents a chronic neurodegenerative disorder, with long preclinical and prodromal phases (approx. 20 years) and an average clinical duration of 8–10 years. In the early phase of this disease, patients show deterioration of memory, difficulties in finding the right words for everyday objects or mood swings. The risk of AD grows exponentially with age, doubling approximately every 5 to 6 years. AD may contribute to 60–70% of all dementia cases, being the most common cause of this disease. Dementia is one of the major causes of disability and dependency among older people worldwide.

The causes of the sporadic form of AD with late onset (LOAD) are not yet known, but it seems to be a result of multiple factors. Neuropathological features are extracellular senile plaques, containing beta-amyloid peptides (Aβ) and intracellular neurofibrillary tangles, containing paired helical tau proteins, which have been associated with neuronal loss and atrophy of the cerebral cortex. Thus, misfolded proteins seem to contribute to the pathogenesis, but are not the only players in the disease process.

Developing feasible therapies is difficult due to the multifactorial pathology of AD. Currently approved drugs only attenuate symptoms, but do not cure the disease. Research into AD also has had several failures in terms of developing disease-modifying therapies. Thus, new therapeutic targets in order to develop a causal therapy are desperately needed. Since AD starts many years far before the first symptoms occur, new scientific approaches focus on the early stage, which are discussed to be important in aging and the onset of AD.

Today, the hypothesis of the advanced mitochondrial cascade becomes more and more the leading model for LOAD, integrating physiological aging as the main risk factor. Thus, new interventions targeting mitochondrial dysfunction are of substantial interest. Accordingly, the efficacy of Dimebon and TRO19622 to ameliorate mitochondrial dysfunction in cellular and murine models of AD were investigated.

Dimebon (Latrepirdine) was, originally developed in Russia as an H1-antiallergic drug. It might specifically interfere with mechanisms relevant for the cognitive decline, especially by improving impaired mitochondrial function and/or dynamics in AD.

TRO19622 (Olesoxim) has been identified in a phenotypic screening approach to promote the survival of primary motor neurons. Olesoxim is easily absorbed by cells and accumulates in mitochondria. Olesoxim's mode of action is not fully understood, however it has been shown to modulate mitochondrial membranes and interact with the voltage-dependent anion channel (VDAC) and the translocator protein (TSPO; also known as PBR). Thereby it inhibits mitochondrial permeability transition.

In this study, the effects of Aβ overproduction on mitochondrial function were investigated. The effects of Dimebon and Olesoxim were examined, using a HEK cell line stably transfected with the Swedish APP double mutation (HEKsw) and un-transfected control cells (HEKut).

Mitochondrial membrane potential, ATP concentrations, and respirometry were measured. Western Blot analysis of marker proteins for fission & fusion, autophagy, mitogenesis and mPTP formation were performed. Confocal laser scanning microscopy was introduced as a novel method to visualize mitochondrial dynamics. Olesoxim was also tested in Thy-1-C57BJ/6-APPSL mice representing a murine model of AD. For the *in vivo* model mitochondria from brain tissue were isolated and dissociated brain cells were prepared to determine respiration, lipid peroxidation, MMP, and ATP-levels.

Both, the *in vitro* and *in vivo* models were compared and discussed in relation to human post-mortem data. The research was conducted in frame of the EU-project entitled „MITOTARGET" (Mitochondrial dysfunction in neurodegenerative diseases: towards new therapeutics) funded under FP7-Health (http://cordis.europa.eu/result/rcn/54471_en.html).

HEKsw cells showed an overall reduction in the mitochondrial respiration, a significant lower MMP, and significantly reduced ATP levels compared to HEKut cells. Mitochondrial mass was equal in both cell lines. In addition most mitochondria in HEKsw cells showed truncated morphology, followed by punctuated mitochondria.

Levels of the fission related protein Drp were significantly elevated in HEKsw cells whereas protein levels of fusion related OPA were strongly reduced, leading to a shift in the distribution pattern towards shorter mitochondria. Moreover, HEKsw cells showed reduced mitochondrial density. Protein levels of the translocase of the inner mitochondrial membrane (TIMM50) were strongly diminished in HEKsw cells. The OXPHOS machinery is located in the inner membrane, where the MMP is build up and ATP is generated. Reduced TIMM50 levels in HEKsw indicated a reduction of the inner mitochondrial membrane, which could

explain the described deficits in OXPHOS, MMP, ATP and mitochondrial morphology and density. Concentration of both mPTP markers, the voltage-depended anion channel (VDAC) and the peripheral benzodiazepine receptor (PBR), were broadly increased in HEKsw cells.

Thy1-APP$_{SL}$ transgenic mice were characterized as *in vivo* model of AD. Those mice are modified to express the human form of APP, containing both, the Swedish (KM670/671NL) and the London (V717L) double mutations under the murine Thy1 promotor. Beginning at the age of 3 months, Thy1-APP$_{SL}$ mice develop elevated Aβ levels and mitochondrial dysfunction. Mitochondria isolated from brains of Thy-1-C57BJ/6-APP$_{SL}$ mice showed significant impaired respiration, resulting in a reduced MMP. However, ATP levels in dissociated brain cells did not differ compared to controls.

Protein levels of FIS were unchanged, whereas Drp levels were significantly increased. Levels of the mitochondrial fusion marker optic atrophie-1 (Opa) protein were significantly reduced. Peroxisome proliferation-activated receptor gamma coactivator 1-alpha (PGC1) is a transcription factor, which represents a master regulator of mitochondrial biogenesis. PGC1 expression was significantly elevated in brains of Thy-1-C57BJ/6-APP$_{SL}$ mice. However, mitochondrial mass seemed to be equal in both mouse lines. Both LC3-Isoforms, the cytosolic and the autophagosomal form, were not changed in brains of Thy-1-C57BJ/6-APP$_{SL}$ mice, which indicates equal mitophagic activity. In brain homogenates, isolated from Thy-1-C57BJ/6-APP$_{SL}$ mice, both mPTP marker, VDAC and PBR, were considerably increased, which is in accordance with the findings in HEKsw cells.

In conclusion, both, the cellular (HEKsw) and the animal model of AD (Thy1-APP$_{SL}$) broadly match pathophysiological features, which have been found in post-mortem samples from AD patients. Thus, HEKsw cells and Thy1-APP$_{SL}$ mice seem to be suitable models to study new treatments against AD.

Incubation of HEKsw cells with Dimebon resulted in a remarkable increase in respiratory activity and restored the MMP after impairing the cells with rotenon. Dimebon had no effects on ATP levels in both cell lines, neither after challenging cells with rotenon, nor under basal conditions.

By adding Dimebon, citrate synthase (CS) activity in HEKsw cells was increased and mitochondrial morphology was shifted to a tubular shape. Dimebon further enhanced protein levels of Drp and resulted in the compensation of reduced OPA levels. Moreover, Dimebon restored the increased expression levels of the mPTP markers VDAC and PBR. Aβ$_{1-40}$ levels

were significantly decreased in HEKsw cells. However, changes in $A\beta_{1-40}$ levels seemed to be too small, to solely explain the much larger effects of Dimebon on impaired mitochondrial function.

In conclusion, Dimebon treatment restored diverse defects in $A\beta$ overexpressing cells: $A\beta$ levels were reduced, autophagy marker were increased, mitophagy as repair and renewal mechanism was elevated, mitochondrial mass and density were increased, OXPHOS capacity was restored, mitochondrial dynamics were balanced, mitochondrial shape showed a normal distribution, expression levels of the mPTP constituents were reduced, TIMM50 levels augmented to control levels and stress induced MMP and ROS levels were reduced. All these effects were observed after incubation of cells with a rather low concentration of 100 nmol/L.

Based on these findings and in addition to already existing literature, Dimebon presents a potential therapeutic option for diseases with accompanied mitochondrial dysfunction. Although, clinical findings published so far are inconsistent.

Olesoxim induced a general increase in respiratory activity and enhanced the electron transport (ETS) capacity in HEKsw cells. In addition it normalized the OXPHOS activity almost to control levels. However, incubation using different Olesoxim concentrations led to a dose independent decline in the MMP and decreased ATP levels.

Adding Olesoxim caused a dose-dependent change in the length of mitochondria strongly shifting the pattern towards longer mitochondria. In HEKsw cells a reduced mitochondrial density was observed which was reversed by Olesoxim dose-dependently. Olesoxim completely compensated the severely reduced expression levels of TIMM50, but had no effects on TOMM22 levels.

An unexpected finding was that 10 µM Olesoxim significantly increased Aβ1-40 levels.

Effects of Olesoxim were also tested *in vivo*. Treatment of Thy-1-C57BJ/6-APP$_{SL}$ mice with Olesoxim restored the impaired MMP in dissociated brain cells, but had no effects on ATP-levels.

Olesoxim increased the respiratory activity in isolated brain mitochondria and restored impaired respiration complex activities almost to control levels, without having an effect on CS activity. However, treatment with Olesoxim caused an increase of PGC1 protein levels in brains of Thy-1-C57BJ/6-APP$_{SL}$ mice,beyond basal levels of littermate controls. The mPTP marker proteins voltage-depended anion channel (VDAC) and peripheral benzodiazepine receptor (PBR) were significantly reduced.

As well as in the cell models, treatment of Thy-1-C57 BJ/6-APP$_{SL}$ mice with Olesoxim significantly enhanced total human, soluble human and soluble mouse Aβ1-40 levels.

Further investigation needs the observation that Olesoxim caused partly negative effects in controls. For instance, Olesoxim reduced the OXPHOS capacity and enhanced protein levels of VADAC and PBR in brains of C57BJ/6 littermate control mice, which could limit the applicability of Olesoxim in further preclinical studies.

Zusammenfassung

Eine der größten Herausforderungen des 21. Jahrhunderts stellt das Verständnis von neurodegenerativen Erkrankungen dar. Hierzu gehört auch die Alzheimer`sche Krankheit (AD), die eine langes präklinisches Prodromalstadium von ungefähr 20 Jahren aufweist. Die klinische Phase, welche durchschnittlich 8 bis 10 Jahre dauert, ist charakterisiert durch Gedächtnisstörungen, Schwierigkeiten bei der Wortfindung oder auch Stimmungsschwankungen. Das Risiko an AD zu erkranken steigt exponentiell mit dem Lebensalter und verdoppelt sich ab dem 65 Lebensjahr alle 5 bis 6 Jahre. AD ist mit 60 bis 70% die häufigste Ursache für eine Demenz. Die Demenz repräsentiert die Hauptursache für eine eingeschränkte Lebensführung bei Älteren.

Die kausalen Ursachen der sporadischen AD mit spätem Krankheitsbeginn (LOAD) sind bislang unbekannt. Es wird davon ausgegangen, dass es sich bei LOAD um eine multifaktorielle Erkrankung handelt. Neuropathologisch finden sich extrazelluläre Ablagerungen von senilen Plaques, die Beta-Amyloid Protein (Aβ) enthalten und intrazelluläre sind Bündel von Tau-Proteinen vorzufinden. Diese Peptid-Ablagerungen wurden mit dem Verlust von Neuronen und der Atrophie des zerebralen Kortex in Verbindung gebracht. Allerdings scheinen solche missgefaltete Peptide nicht die einzige Ursache der Krankheit zu sein.

Zugelassene Medikamente wirken rein symptomatisch, ohne die Krankheit zu heilen. Die multifaktorielle Pathologie erschwert die Entwicklung kausaler Behandlungsstrategien und die Forschung musste in jüngster Zeit zahlreiche Rückschläge bei der Entwicklung von Krankheit-modifizierenden Medikamenten hinnehmen. Dementsprechend besteht ein großer Bedarf an neuen Zielstrukturen, um kausale Therapien zu entwickeln. Da die Krankheit viele Jahre vor den ersten Symptomen ausbricht, fokussiert sich die Wissenschaft heute auf die frühen Phasen der Erkrankung, die auch für die Alterungsprozesse relevant sind.

Die erweiterte Mitochondrien-Kaskaden-Hypothese rückt als Erklärungsansatz für die sporadische AD mit spätem Krankheitsbeginn LOAD immer stärker in den Fokus. Diese stellt die mitochondriale Dysfunktion, als eine der wesentlichen Faktoren für die Entstehung der Erkrankung, in den Mittelpunkt und integriert die physiologische Alterung des Gehirns, als den wesentlichen Risikofaktor. Folglich treffen neue Interventionsmöglichkeiten, die die mitochondriale Dysfunktion bekämpfen, auf substantielles Interesse. Im Rahmen dieser Arbeit wurde getestet, inwieweit die beiden Wirkstoffe Dimebon und TRO19622, die

mitochondriale Dysfunktion im zellulären und im murinen Modell der AD beeinflussen können.

Dimebon (Latrepridine) wurde ursprünglich in Russland als H_1-Antiallergikum entwickelt. Befunde, dass der Wirkstoff mitochondriale Funktionen verbessert und mit relevanten Mechanismen der Kognition interagieren kann, haben Dimebon als mögliches Therapeutikum bei Alzheimer identifiziert.

TRO19622 (Olesoxim) wurde in einem Screening-Verfahren identifiziert, bei dem die Fähigkeit zur Verbesserung des Überlebens von primären Motoneuronen untersucht wurde. Olesoxim wird bereitwillig von Zellen aufgenommen und reichert sich in Mitochondrien an. Der Wirkmechanismus der Substanz ist noch nicht vollständig aufgeklärt. Es wurde gezeigt, dass Olesoxim mitochondriale Membranen moduliert und mit bestimmten Proteinen (VDAC und TSPO) interagiert, die an der Ausbildung der mitochondrialen Transitionspore (mPTP) beteiligt sind.

Die beiden Wirkstoffe wurden in einem zellulären Modell der AD getestet. Hierfür wurde eine HEK-Zelllinie benutzt, die in der Vergangenheit stabil mit der schwedischen Doppelmutation des APP Gens transfiziert wurde (HEKsw Zellen), was zu einer verstärkten Bildung von Aβ führt. Es wurden unter anderem das mitochondriale Membranpotential (MMP), die Spiegel an ATP und die Respiration in HEK Zellen gemessen, die humanes APP mit entsprechenden Mutationen exprimieren. Weiterhin wurden Markerproteine für Fission & Fusion, Autophagie, Mitogenese und mPTP bestimmt. Die konfokale Laser-Scanning-Mikroskopie wurde als neue Methode um dynamische Prozesse von Mitochondrien zu messen, eingeführt. Olesoxim wurde zusätzlich an Thy1-APPSL Mäusen, einem murinen Modell der AD, getestet. Für die Untersuchungen wurden aus dem Gehirn der Mäuse Mitochondrien und dissoziierte Gehirnzellen isoliert, um unter anderem MMP, ATP Spiegel und die Respiration zu messen.

Beide Krankheitsmodelle wurden miteinander verglichen und in Relation zu humanen post-mortem Daten diskutiert. Die wissenschaftliche Arbeit fand im Rahmen des Projektes „MITOTARGET" statt, das unter dem Aufruf FP7-Health (http://cordis.europa.eu/result/rcn/54471_en.html) von der EU finanziert wurde.

Im Vergleich zu Kontrollzellen zeigen HEKsw Zellen eine generelle Reduktion der mitochondrialen Respiration, ein signifikant reduziertes MMP und signifikant erniedrigte ATP Spiegel. Die mitochondriale Masse unterschied sich nicht zwischen den Zelllinien. In

HEKsw Zellen zeigten die meisten Mitochondrien eine verkürzte Morphologie, viele Mitochondrien wiesen eine punktförmige Form auf.

Das an Fission-Prozessen beteiligte Drp Protein wurde verstärkt von HEKsw Zellen gebildet. Wohingegen eine verminderte Produktion des mit Fusions-Prozessen assoziierten OPA Proteinen festgestellt wurde, was wohl insgesamt zu kürzeren Mitochondrien geführt hat. Mitochondrien in HEKsw Zellen zeigten zudem eine reduzierte Dichte. Die Proteingehalte des Proteins „Translokase der inneren mitochondrialen Membran" (TIM50), waren stark vermindert in HEKsw Zellen. Die innere mitochondriale Membran ist der Ort, an dem die OXPHOS Maschinerie lokalisiert ist und somit das MMP aufgebaut und letztlich ATP gebildet wird. Reduzierte TIM50 Gehalte deuten auf eine reduzierte innere Membran hin, die zu den beobachteten Veränderungen hinsichtlich OXPHOS, MMP, ATP und Morphologie beigetragen haben könnte. Beide Marker-Proteine (VDAC und PBR) der mPTP waren in HEKsw Zellen deutlich erhöht.

Thy1-APPSL transgene Mäuse wurden als in vivo Modell der AD charakterisiert. Diese Mäuse exprimieren unter der neuronenspezifischen Kontrolle des murinen Thy-1 Promotors, die humane Form des APP, welche sowohl die Schwedische- (KM670/671NL), als auch die London-(V717L) Mutation exprimieren. Im Alter von 3 Monaten lassen sich im Gehirn dieser Mäuse erhöhte Aβ Gehalte, sowie mitochondriale Dysfunktion nachweisen. Isolierte Mitochondrien weisen eine beeinträchtigte Respiration auf, die in einem reduzierten MMP resultiert. Allerdings waren die ATP-Spiegel in dissoziierten Gehirnzellen nicht verändert.

Die Proteingehalte an FIS waren nicht verändert, während die Drp Spiegel signifikant erhöht waren. Beide Proteine sind an Fission-Prozessen beteiligt. Auf der anderen Seite war der Gehalt des Fusion-Markers Opa deutlich vermindert. Signifikant erhöht waren im Gehirn der Mäuse die Gehalte an PGC1alpha, einem Transkriptionsfaktor, der bei der Neubildung von Mitochondrien eine Schlüsselrolle spielt. Dennoch scheint diese Veränderung sich nicht in der mitochondrialen Masse niederzuschlagen. Ebenso unverändert scheint die Mitophagie. Wie im zellulären Modell, finden sich im Gehirn des murinen Modells erhöhte Gehalte der mPTP Marker VDAC und PBR.

Beim Vergleich mit der Literatur findet man, dass sowohl das zelluläre als auch das murine Modell pathophysiologische Merkmale abbilden, die man in post-mortem Gehirngewebe von

Alzheimer Patienten gefunden hat. Dementsprechend scheinen HEKsw Zellen und Thy1-APPSL Mäuse brauchbare Modellsysteme zu sein, um neue Therapien für AD zu testen.

Die Inkubation von HEKsw Zellen mit Dimebon induzierte einen bemerkenswerten Anstieg der mitochondrialen Respiration und stellte das MMP nach Schädigung mit Rotenon wieder her. Dimebon hatte allerdings keine Effekte auf die ATP Gehalte, weder unter basalen Bedingungen, noch nach Schädigung mit Rotenon.

Dimebon erhöht die Aktivität der Citratsynthase und sorgt für eine tubuläre Struktur der Mitochondrien. Der Wirkstoff erhöht die Drp-Proteingehalte und kompensiert die erniedrigten Opa-Gehalte. Darüber hinaus kompensiert Dimebon die erhöhen Gehalte der mPTP Marker Proteine VDAC und PBR und erniedrigt die Gehalte an Aβ. Allerdings scheinen die Effekte auf die Aβ Gehalte zu moderat, als dass diese die positiven Effekte auf die mitochondriale Funktionen von Dimebon alleine erklären könnten.

Zusammenfassend lässt sich sagen, dass Dimebon diverse Defekte in Aβ über exprimierenden Zellen kompensieren kann: Aβ Gehalte wurden erniedrigt, Markerproteine der Autophagie wurden erhöht, die Mitophagie als Reparatur- und Erneuerungsprozess wurde verstärkt, die mitochondriale Masse und Dichte wurden erhöht, die mitochondriale Dynamik ausbalanciert und die Menge an mPTP Markerproteinen wurde erniedrigt. Die Gehalte an TIM50 wurden auf das Maß der Kontrolle gehoben und der Stress-induzierte Abfall des MMP wurde kompensiert. All diese Effekte wurden nach Inkubation mit einer relativ geringen Konzentration von 100 nmol/l beobachtet.

Auch wenn die bisherigen klinischen Befunde sich als inkonsistent erweisen, stellt sich Dimebon in den durchgeführten Untersuchungen, als mögliche therapeutische Option für Krankheiten, die mit einer mitochondrialen Dysfunktion einhergehen dar.

Olesoxim verbesserte in HEKsw Zellen die respiratorische Aktivität weitgehend auf Kontrollniveau. Allerdings verursachte Olexoxim in dem zellulären Modell einen konzentrationsabhängigen Abfall des MMP und der ATP Spiegel.

Hinsichtlich der mitochondrialen Dynamik verschob Olesoxim das mitochondriale Muster hin zu deutlich längeren Mitochondrien. Die reduzierte mitochondriale Dichte wurde durch Olesoxim kompensiert, genauso wie die erniedrigten TIM50 Gehalte.

Unerwarteter Weise erhöhte allerdings 10 μM Olesoxim signifikant den Gehalt an Aβ.

Die Effekte von Olesoxim wurden auch in vivo getestet. Die Behandlung von Thy1-APPSL Mäusen mit Olesoxim stellte das beeinträchtigte MMP in dissozierten Gehirnzellen wieder her, hatte allerdings keine Auswirkung auf die ATP Gehalte.

Olesoxim erhöhte die respiratorische Aktivität in isolierten Mitochondrien und stellte die beeinträchtigten Komplexaktivitäten wieder her, ohne einen Effekt auf die Citratsynthase-Aktivität zu haben. Allerdings wurden durch die Behandlung, die erhöhten Gehalte an PGC1 Protein gesenkt und das noch unter das Niveau der Kontrolltiere. Ebenso reduziert wurden die Gehalte der mPTP-Markerenzyme VDAC und PBR.

Wie schon im zellulären System, erhöhte die Behandlung von Mäusen mit Olesoxim die Bildung von Aβ.

Eine weitere interessante Beobachtung, die weitere Untersuchungen erfordert war, dass Olesoxim in Kontrollmäusen zum Teil negative Effekte hatte, die so im Krankheitsmodell nicht auftraten. Zum Beispiel reduzierte Olesoxim die OXPHOS Kapazität und erhöhte die Proteingehalte der mPTP-Marker VDAC und PBR in nicht transgenen C57BJ/6 – Wurfgeschwistern, was eine mögliche Anwendbarkeit von Olesoxim in weiteren präklinischen Studien limitieren könnte.

Introduction

Alzheimer`s disease

Epidemiology

Research and treatment of neurodegenerative diseases is one of the major challenges, we face in the 21st century. Population ageing has become a worldwide demographic trend. According to the WHO, the global population aged 65 and over is believed to reach 1.3 billion (14%) of the total population by 2040 and, consequently, the prevalence of chronic age-related conditions like cardiovascular diseases or cognitive decline will increase significantly (WHO 2015b). This also includes Alzheimer´s disease (AD), which represents a chronic neurodegenerative disorder, with long preclinical and prodromal phases (20 years) and an average clinical duration of 8–10 years. The disease has an estimated prevalence of 10–30% in the population >65 years of age with an incidence of 1–3% (Masters et al. 2015). In 2015, worldwide nearly 47.5 million people had dementia with 7.7 million new cases every year. AD is the most common cause of dementia and may contribute to 60–70% of cases. It is one of the major causes of disability and dependency among older people worldwide. Dementia has physical, psychological, social and economic impact on caregivers, families and the society (WHO 2015a). The incidence rate of dementia increases exponentially with age and is quite similar across regions (Qiu et al. 2007; Qiu et al. 2009). The risk of AD also grows exponentially with age, doubling approximately every 5 to 6 years (Ziegler-Graham et al. 2008). The total number of people with dementia is projected to be 75.6 million in 2030 and almost double by 2050 with 135.5 million. The major reason for this increase is attributable to the rising number of people with dementia, living in low- and middle-income countries (WHO 2015a). Hence, the global trend in the phenomenon of an ageing population, has dramatic consequences for public health, healthcare financing and delivery systems worldwide (International 2015b).

Clinical manifestation

In the early phase of the disease, patients show deterioration of memory, difficulties in finding the right words for everyday objects or mood swings. As Alzheimer's progresses, patients forget recent events, names and faces, have difficulties in understanding the context

of a conversation and become confused when handling money or driving a car. They undergo personality changes, appearing not to care anymore about themselves and those around them. Patients sometimes burst into tears for no apparent reason, or become convinced that someone is trying to harm them. As the disease progresses, people may also adopt unsettling behavior, such as getting up in the middle of the night or wander off and become lost. Moreover, they lose their capability and sense for a suitable behavior, undress in public or make inappropriate sexual advances (Perry et al. 2006; Alzheimer`s Disease International 2015a).

Most patients with AD (>95%) suffer from the sporadic form, which is characterized by a late onset (65–90 years of age) (LOAD). Investigations have supported the concept, that LOAD is a complex disorder, that may involve multiple susceptibility genes (Masters et al.). A small proportion of patients (1-5%) have inherited mutations in genes, which affect the processing of Aβ, resulting in the development of AD at a much younger age (mean age of ~45 years) (Masters et al. 2015). The search for the genetic factors contributing to AD, has evolved tremendously throughout the past years. Starting with the discovery of fully penetrant mutations in the amyloid precursor protein (APP), Presenilin-1, and -2 (PS-1, PS-2) as a cause of autosomal dominant AD. Followed by the indentification of the ε4 allele of Apolipoprotein E, as a strong genetic risk factor for both, early-onset and LOAD. Recently, genome-wide association studies and massive parallel re-sequencing efforts have evolved to the detection of at least 21 additional genetic risk loci for the genetically complex form of AD (Van Cauwenberghe et al. 2015).

Etiology

The causes of the sporadic forms of AD with late onset are not yet known, but it seems to be a result of multiple factors (Association 2012). Ageing and Apo E genotype are strongly associated with AD (Saunders et al. 1993; Michaelson 2014; Reitz and Mayeux 2014). High blood pressure, high blood levels of homocysteine and cholesterol, diabetes mellitus, adiposity, depression and smoking are other – modifiable - risk factors (Kidd 2008; Barnard et al. 2014; Beydoun et al. 2014).

Neuropathological hallmarks of the disease are extracellular senile plaques containing beta-amyloid peptides (Aβ) and intracellular neurofibrillary tangles containing paired helical tau

proteins, which have been associated with neuronal loss and atrophy of the cerebral cortex (Selkoe et al. 1982; Rozemuller et al. 1989). Thus, misfolded proteins seem to contribute to the pathogenesis, but are not the only factors in the disease process.

The isolation of Aβ from senile plaques (Glenner and Wong 1984) and the identification of mutations in genes, encoding for the processing of Aβ from its precursor protein (APP) in families with early disease onset (Citron et al. 1992), led to the amyloid cascade hypothesis (Hardy and Higgins 1992). In a nutshell this hypothesis states, that an elevated secretion of Aβ, which has been shown to be neurotoxic (Pike et al. 1991; Ueda et al. 1994), is the initial cause of this disease. First transgenic mouse models harboring human genes, inherited in an autosomal dominant manner, showed elevated Aβ production, amyloid plaques, and memory deficits and thus were in confirmation with the hypothesis (see table 1) (Hsiao et al. 1996). Subsequently, several transgenic mouse models harboring different human mutations were introduced and widely used in the field (Emilien et al. 2000; Kitazawa et al. 2012; Bilkei-Gorzo 2014). Pathology varies depending on the transgene, the promoter and the stain used to produce those mouse models (table 1).

Behavioral deficits are probably more related to synaptic deficits, than to plaque formation and synaptic loss seems to represent a common hallmark in AD mouse models (Kitazawa et al. 2012; Bilkei-Gorzo 2014). On the other site, one must be aware of the limitations of any research tool, and there are many important issues to keep in mind when evaluating data from mouse models of AD: There may be limitations in applying data from AD mouse models to sporadic AD in humans, since the mice most closely develop autosomal dominant AD (Hall and Roberson 2012). There are certain pathophysiological differences between autosomal dominant and sporadic AD. The most important fact is that one is primarily driven by Aβ overproduction and the other one not. In the extreme, a treatment that acts by neutralizing the preference of βsecretase for the Swedish mutation in APP might have significant benefits in a mouse model with that mutation, but none in sporadic AD (Hall and Roberson 2012). On the other hand, both conditions seem to be characterized by high Aβ levels, so treatments that reduce Aβ or block its detrimental effects, may be equally effective in both conditions. The degree on how treatments for autosomal dominant and sporadic AD should overlap is a current issue in the field. This includes clinical research, as there is increasing interest in

studying patients, suffering from autosomal dominant AD, as a pool of subjects, for testing AD treatments in the pre-symptomatic phase of the disease (Hall and Roberson 2012).

The role of amyloidosis as a causative agent in sporadic AD remains undefined. For this reason, new hypotheses about the causes of this disease and their corresponding animal models are under investigation. For instance, loss-of-function of presenilins have been claimed to explain both, familiar and sporadic forms of AD. The pathogenic contribution of the ε4 isoform of Apolipoprotein E in late-onset forms is also actively studied. Other processes such as calcium dysregulation, disturbed autophagy, aberrant proteasome function, mitochondrial failure, and many other alterations are under investigation and will lead to new mouse models of sporadic AD (Torres-Aleman 2008).

Table 1. Transgenic APP mouse models of Alzheimer`s disease. Table was adopted from Kitazawa et al. (Kitazawa et al. 2012). Models presented in the following table represent inherited forms of AD.

Abbr.	Transgene	Promoter	Strain	Pathology
-	Wildtype human APP	Yeast artificial (YAC) APPpromoter	C57BL/6J	No Aβ or AD-like pathology at 3 months
-	Wildtype human APP	YAC APP promoter		Increased APP expression. No Aβ - or AD-like pathology
PDAPP	Human APP (Indiana) minigene	PDGFb	Swiss Webster × B6D2F1	Aβ plaques at 6-9 months. Gliosis, synaptic loss. Neuronal loss in hippocampus and dentate gyrus at 3-4 months. Behavior deficits.
Tg2576	Human APP695 (Swedish)	Hamster PrP	C57BL/6J	Aβ plaques at 10-12 months. Oligomeric Aβ species. Synaptic loss at 15-18 months. Behavior deficits.
APP23	Human APP751 (Swedish)	Mouse Thy-1.2	C57BL/6J	7-fold APP expression over endogenous levels Aβ - plaques by 6 months. Gliosis. Increased phospho-tau at 6 months. Phospho-tau deposits around plaques at 12 months. CA1 neuronal loss at 14-18 months. Behavior deficits.
APP22	APP751 (Swedish/London)	Human Thy-1	C57BL/6J	2-fold APP expression over endogenous levels. Aβ plaques at 18 months. Tau phosphorylation and dystrophic neurites around plaques.
J20	Human APP (Swedish/Indiana) minigene	PDGFb	C57BL/6 × DBA/2 F2	Aβ plaques at 4-5 months. Pospho-neurofilaments. Synaptic loss behavior.
I5	Human wildtype APP	PDGFb	C57BL/6 × DBA/2	No plaques even at 24 months. Mild synaptic loss

			F2	
	minigene			
TgCRND8	Human APP695 (Swedish/Indiana)	Hamster PrP	C3H/He × C57BL/6	Aβ plaques (Thioflavin S positive) at 3 months. Dense core plaques at 5 months. Dystrophic neurites around plaques 50% mortality at ~150 days. Behavior deficits by 3 months.
Arc6, Arc48	Human APP (Arctic) minigene	PDGFb	C57BL/6N	Aβ plaques by 2 months (Arc48) or 4-6 months (Arc6). Increased Aβ fibrillar formation. Decreased Aβ oligomers which correlate with attenuating behavior deficits.
TBA2	mTRH-Aβ3Q-42	Mouse Thy-1	C57BL/6J	Mean survival around 70 days. Massive Purkinje cell loss. Diffuse plaques. No phospho-tau.
-	Human APP695 (E693D)	Mouse PrP	B6C3F1 (back-crossed to C57BL/6)	Increased Aβ oligomer intracellular deposits in hippocampus and cortex at 8 months. No Aβ plaques. PHF1-phospho-tau deposits in mossy fibers at 8 months. Synaptic loss at 8 months. Microglial activation at 12 months. Astrocyte activation at 18 months. Neuronal loss at 24 months. Behavior deficits at 8 months.
APP/PS1	Mouse/human chimeric APP695 (Swedish) Human PS1 (A246E)	Mouse PrP (APP and PS1)	C3H/HeJ × C57BL/6J	Increased Aβ42/Aβ40 ratio Accelerated Aβ plaques at 9 months Dystrophic neurites and gliosis at 12 months
rTg4510	Human tau (P301L) (0N4R)	CaMKIIa (tTA) TRE (tau)	129S6 × FVB/N	Massive neuronal loss and forebrain atrophy by 5-6 months Phospho-tau deposits by 2.5 months NFT-like pathology at 4 months (cortex) to 5.5 months (hippocampus) Cognitive and motor impairments by 4 months Cognitive impairments but not NFT formation is rescued following transgene suppression

However, a recent review examined the relationship between Aβ levels and cognitive deficits in AD transgenic mice. The overall result revealed no statistically significant correlation between quantified Aβ levels and experimental measures of cognitive function (Foley et al. 2015).

Over time, the long-standing emphasis on fibrillar Aβ deposits and neuronal death, slowly gave way to a new paradigm, involving soluble oligomeric forms of Aβ, which play a prominent role in triggering the cognitive deficits by specifically targeting synapses and disrupting synaptic signaling pathways at a morphological and functional level (Pozueta et al. 2013). The Aβ oligomer-centric hypothesis is widely accepted today in the AD field, although the molecular details have not been fully elucidated (Pozueta et al. 2013).

Table 2: Progress of late-phase clinical trials targeting the Amyloid Cascade Hypothesis. Table was adopted from (Lansdall 2014).

Drug type	Drug name	Phase	Reason for failure
Aβ aggregation inhibitor	AlzhemedTM (Tramiprosate)	III	Results obtained could not support a claim for clinical efficacy (ClinicalTrials.gov Identifier: NCT00088673)
γ-Secretase Inhibitor	Semagacestat	III	Evaluated in two Phase III trials, the Interrupting Alzheimer's dementia by evaluating treatment of amyloid pathology (IDENTITY) trial and the IDENTITY-2 trial (ClinicalTrials.gov identifier: NCT00594568 and NTC00762411). Patients receiving Semagacestat displayed an increased deterioration in cognition and activities of daily living compared to placebo- treated controls. Semagacestat was also found to be associated with an increased risk of skin cancer compared to placebo.
γ-Secretase modulators	FlurizanTM (tarenflurbil)	III	No statistically significant effect in co-primary outcome measures of cognition and activities of daily living was observed (ClinicalTrials.gov Identi er: NCT00105547)
Aβ active immunotherapy	AN1792	III	Safety findings were reported, including the development of aseptic meningoencephalitis and leukoencephalopathy in 6% of vaccinated patients (ClinicalTrials.gov Identifer: NCT00021723)
Aβ passive immunotherapy	Bapineuzumab	III	No significant efficacy found. Furthermore, vasogenic oedema was reported during the study, particularly in ApoE4 carriers. Due to these safety findings, the highest dose was discontinued (ClinicalTrials.gov Identifier: NCT00575055 and NCT00574132)
Soluble Aβ immunotherapy	Solanezumab	III	Failed to reach its cognitive or functional endpoints in either of two double-blind, placebo-controlled trials in patients with mild to moderate Alzheimer's disease EXPEDITION and EXPEDITION-2 (ClinicalTrials.gov Identifier: NCT00905372 and NCT00904683), despite acute and sub-chronic treatment attenuating or reversing memory deficits in transgenic mice.
Soluble Aβ immunotherapy	Gantenerumab	II/III	Ongoing (Clinical Trials.gov identified NCT01224106, NCT02051608 and NCT01760005).

The Aβ hypothesis and its enhancements have emerged preclinical concepts that were translated into clinical settings. However, numerous failures and discontinuations (see table 2) have further highlighted possible inconsistencies in the Amyloid Hypothesis (Lansdall 2014). Thus, growing amounts of data have accumulated, that are inconsistent with the basically linear structure of this hypothesis and its general rejection is currently debated (Drachman 2014; Herrup 2015; Musiek and Holtzman 2015).

Brain imageing data of LOAD patients show the presence of Aβ plaques decades before first cognitive symptoms arise. Aβ plaques seem to be stable over time and rather decrease when cognitive dysfunction occurs (Swerdlow et al. 2014; Mueller et al. 2016) (Sperling et al. 2011). This might also be true for early, heritable forms of AD (Mueller et al. 2016). Although mutations in the relevant risk genes result in massive Aβ plaques – one of the main arguments for the amyloid cascade hypothesis - recent data question this direct relationship (Mueller et al. 2016). For instance there is evidence that mutations in the PS-1 gene, directly induce neurodegeneration, independently from Aβ (Baki et al. 2008; Barthet et al. 2013) (Bruban et al. 2015) (Schuessel et al. 2006).

Thus, there is an urgent need to explore targets other than Aβ. There is now increasing interest in inhibiting tau pathology, which seems to have a far more compelling rationale than Aβ (Giacobini and Gold 2013; Iqbal et al. 2014). Tau-based strategies have received little attention until recently, despite the fact that the presence of extensive tau pathology is a central feature to the disease. The discovery of mutations within the tau gene, that cause fronto-temporal dementia, demonstrated that tau dysfunction, in the absence of amyloid pathology, is sufficient to cause neuronal loss and clinical dementia (Medina and Avila 2014). However, AD is multifactorial and over 95% of the cases belong to the sporadic form of the disease.

Ageing of the brain represents the most important risk factor for LOAD and is a major contributor to dementia in the elderly (Drachman 2006). Decline of cognition and loss of synapses, are well-documented concomitants of normal ageing (Drachman 2014). It has been postulated, that LOAD results from multiple age-associated processes, that erode brain structure and function gradually, making it vulnerable to degeneration. The vulnerable aged brain, with normal age-associated changes, may be affected by an additional precipitating

event, that transforms it from normal ageing to AD, resulting in accelerated neuronal and synaptic loss, and cognitive decline (Drachman 2014). Accordingly, gradual loss of energy in association with elevated oxidative stress links mitochondrial dysfunction in ageing to AD (see below) (Reddy et al. 2010).

In 2004, the „**mitochondrial cascade hypothesis**" was proposed, that comprehensively combines seemingly disparate histopathologic and pathophysiologic features in LOAD (Swerdlow and Khan 2004). In this model, the inherited, gene-determined make-up of an individual's electron transport chain sets basal rates of reactive oxygen species (ROS) production. Oxidative damage amplifies ROS production and triggers the response to elevated ROS by generating Aβ, induction of apoptosis, and disturbing the cell cycle (Swerdlow and Khan 2004). Additionally, new mitochondria related targets, such as the synaptic vesicle protein 2A (SV2a protein) have been identified which might play a role in ageing and LOAD (Stockburger et al. 2015). Thus, mitochondrial dysfunction may represent the missing link between ageing and sporadic AD, and serves an attractive target against neurodegeneration (Muller et al. 2010; Grimm et al. 2015; Friedland-Leuner et al. 2014).

Nowadays, the hypothesis of the advanced mitochondrial cascade is more often regarded as the leading model for LOAD (Mueller et al. 2016). It also integrates physiological ageing as the main risk factor for LOAD. Advanced age enhances ROS production which directly stimulates gamma-secretase activity (Leuner et al. 2012a; Leuner et al. 2012c), finally leading to enhanced Aβ production. This may lead to a vicious cycle, in which ageing and amyloid toxicity exaggerates each other (Stockburger et al. 2014; Mueller et al. 2016) (see also chapter "Mitochondrial Targeted Therapy").

Treatment

The current standard of care for mild AD includes standardized extracts of **Ginkgo biloba** (e.g. EGb761). For mild to moderate AD, **acetylcholine esterase inhibitors** (Galantamine, Donezepil and Rivastigmine) are the usual medication, to improve cognitive function (Eckert 2010). The **NMDA** (N-methyl-D-aspartate) **receptor modulator** memantin has also been shown to improve cognitive function in patients with moderate to severe AD (Citron 2010). Additionally, a number of anti-dementia drugs (**Nootropics**), such as Nimodipine, Nicergolin, Hydergine or Piracetam are in clinical use. All these aforementioned drugs act

symptomatically and do not cure the disease. Thus, new therapeutic strategies for the development of disease-modifying drugs are under investigation.

Ginkgo biloba

Originally, **Ginkgo biloba** (Coniferae) has been used for respiratory disorders in China and to improve memory loss associated with abnormalities of blood circulation in Iran (Howes et al. 2003; Eckert 2010; Mueller et al. 2016). This herbal drug has been subjected to numerous investigations, regarding its potential in cognitive disorders. Standardized extracts, particularly EGb 761, derived from the leaves of the Ginkgo tree are successfully used as herbal drug for the improvement of cognitive and memory impairment (Eckert 2010).

Numerous experimental evidences document EGb 761[®]'s protective efficiency *in vitro* and *in vivo* (Bedir et al. 2002; Sastre et al. 2002; Abdel-Kader et al. 2007; Mueller et al. 2016). EGb761[®] contains 24% of flavonoids and 6% of terpens, which have been identified as the active ingredients. Beside its effects on monoaminergic neurotransmission (Fehske et al. 2009), several terpene lactones (Ginkgolides, Bilobalide) showed substantial mitochondria-protecting properties (Abdel-Kader et al. 2007; Eckert et al. 2012a).

The flavonoid fraction of EGb761[®] seems to be mainly responsible for the free radical scavenging characteristics. The effects of oxidative stress were reduced in lymphocytes and brain cells derived of EGb761[®]-treated AD-transgenic and non-transgenic mice (100 mg/kg b.w. p.o. for 14 days) (Schindowski et al. 2001; Abdel-Kader et al. 2006; Abdel-Kader et al. 2007). Data indicate, that EGb 761[®] also affects the production of neurotoxic Aβ, for example by up-regulating α-secretase activity, both, in cells and animals (Abdel-Kader et al. 2007). In aged and/or AD transgenic mice, EGb 761[®] treatment resulted in improved memory compared to control animals (Stoll et al. 1996; Tang et al. 2002).
EGb761[®] also has been shown to improve all aspects of impaired neuroplasticity, following oxidative stress, including reduced long-term potentiation, reduced spine density, impaired neuritogenesis and even reduced neurogenesis (Mueller et al. 2012)(Eckert et al. 2012a).

Placebo-controlled clinical trials proved *Ginkgo biloba* to be a useful herbal remedy for attenuating symptoms in dementia, with an efficiency comparable to those of standard drugs in AD treatment (Le Bars 2003). This finding has been confirmed in a 3-month study in

comparison to donepezil (Mazza et al. 2006). Furthermore, EGb 761[®] has been suggested to prevent neurodegenerative pathologies (Christen 2004). The clinical usefulness of EGb761[®] in dementia has been proven in clinical trials (Eckert 2010; Wang et al. 2010; Weinmann et al. 2010). Accordingly, EGb761[®] has been included in the guidelines for treatment of Alzheimer's disease of the World Federation of Societies of Biological Psychiatry (Ihl et al. 2011). Its efficacy and good tolerability in patients with dementia was confirmed by recent published meta-analysis (Ihl 2013; Gauthier and Schlaefke 2014).

The possible benefit of EGb 761[®] in long-term treatment to prevent dementia is more controversial. While the GEM study in cognitively very healthy elderly participants did not show any preventive effect (DeKosky et al. 2008), the GUIDAGE study reported a significant protection against the development of dementia in elderly having problems with their memory (Vellas et al. 2010). However, at the end of the trial, the long-term use of a standardized ginkgo biloba extract did not reduce the risk of the progression of Alzheimer's disease compared to placebo (Vellas et al. 2012). However, a statistical re-evaluation adopting the data to the real situation (e.g. absent conversion to dementia), showed a significant risk reduction for patients, who were treated with *Ginkgo biloba* at least for four years (Vellas et al. 2012; Mueller et al. 2016).

AchE-Inhibitors

Loss of cholinergic neurons in the basal forebrain represents a hallmark of AD pathology (Anand et al. 2014). Cholinergic neurons are involved in cortical activity, in cerebral blood flow, in learning, task and memory related activities, in the development of the cerebral cortex and the regulation of the sleep-wake cycle (Berger-Sweeney 2003; Schliebs and Arendt 2006). The dysfunction of the cholinergic system in AD is characterized by a decreased choline acetyltransferase activity, reduced choline uptake, a decrease in acetylcholine synthesis (Slotkin et al. 1990) and altered levels of acetylcholine receptors (AChRs) (Xu et al. 2012; Anand et al. 2014).

Donepezil, rivastigmine and galantamine are the three acetylcholinesterase inhibitors (AChEIs) approved by the EMA for the treatment of AD (Anand et al. 2014). AChEIs inhibit the enzyme acetylcholinesterase (AChE) and enhance cholinergic neurotransmission by reducing the degradation of acetylcholine. Elevated levels of acetylcholine activate

cholinergic acetylcholine receptors (AChRs) and increase the long-term potentiation (Anand et al. 2014). Cholinergic AChRs are expressed on principal and inhibitory interneurons, at both pre- and post-synaptic sites in most regions of the hippocampus. Thus, elevation of acetylcholine levels in the synaptic cleft can have bidirectional effects (Drever et al. 2011). Galantamine also possesses agonist activity at the nicotinic α4β2 receptor subtype and its clinical benefits are probably related to both mechanisms (Coyle and Kershaw 2001; Anand et al. 2014).

It has been shown recently, that muscarinic M1 AChRs are involved in the regulation of long- term potentiation and synaptic plasticity (Anisuzzaman et al. 2013). Cholinergic transmission also plays a role in modulating the mechanisms involved in adult neurogenesis (Bruel-Jungerman et al. 2011). In addition, studies do suggest, that AChEIs alleviate oxidative stress (Klugman et al. 2012; Anand et al. 2014).

Various short-term trials with AChEI monotherapy have shown clinically apparent and encourageing improvement in cognitive function, to slow down the pace of functional decline or clinical worsening, compared to placebo and reduced behavioral symptoms in mild-to-moderate and moderate-to-severe AD patients (Anand et al. 2014). Data from meta-analyses confirm that donepezil, galantamine and rivastigmine are efficacious for mild-to-moderate AD. There is no evidence of any difference between the drugs with respect to efficacy, although the compounds have slight variations in their mode of action (Birks 2006) (Tan et al. 2014; Birks and Grimley Evans 2015).

NMDA-Receptor Modulators

Glutamate is the primary excitatory neurotransmitter in the hippocampal and neocortical regions of the brain, which play a significant role in cognition, learning and memory processes (Anand et al. 2014). The post-synaptic membrane has a high density of the glutamatergic N-methyl-D-aspartate (NMDA) receptor, that is coupled with an ion-channel, preferably permeable for Ca^{2+}-ions (Anand et al. 2014).

Glutamatergic neurons are involved in the regulation of synaptic plasticity, neuronal growth and differentiation, in cognition, learning and memory (Butterfield and Pocernich 2003). The glutamatergic system is involved in the pathology of AD at a later stage of the disease (Anand et al. 2014). Studies have shown that there is excess of extracellular

glutamate in AD, which contributes to both, an increased presynaptic glutamate release and a decreased re-uptake. Subsequently this leads to a tonic activation of NMDA receptors (Revett et al. 2013; Anand et al. 2014).

Memantin is a non-competitive, voltage dependent NMDA receptor antagonist, with rapid blocking kinetics and moderate affinity. Memantin blocks the NMDA-channel by trapping it in the open conformation (Gilling et al. 2009). In contrast Mg^{2+} ions block the NMDA channel under resting conditions (Anand et al. 2014). When glutamate binds to its receptor the blockade is relieved and the NMDA channel is open for Ca^{2+} influx. In a pathological state such as AD, there is a low and persistent activation of NMDA channels, even at resting periods (Anand et al. 2014). During this activation, Mg^{2+} ions are excluded from the channel, thereby, allowing continuous Ca^{2+} flow across the membrane. The moderate affinity and voltage dependent property of Memantin allows it to block the persistent NMDA activation and is thus, beneficial in AD (Anand et al. 2014). Evidences also indicate that Memantin mediated blockade is relieved by high glutamate concentrations in the synaptic cleft. Hence, when a physiological impulse arrives, glutamate overrides the Memantin blockade, and physiological transmission can continue without interference (Parsons et al. 2013; Anand et al. 2014).

Currently, memantin is the only drug approved for clinical use in moderate to severe AD in the USA and Europe (Anand et al. 2014). Studies show convincing evidence of memantin's value (McShane et al. 2006; Hellweg et al. 2012; Tan et al. 2014). Although the effect of memantin is evident in late stages, its role is unclear in early AD. Studies that have investigated the role of memantin in mild to moderate AD, show some beneficial effects on the cognitive and global functioning status, but it does not impede the progression of the disease (Peskind et al. 2006; Bakchine and Loft 2008; Porsteinsson et al. 2008; Schneider et al. 2011; Anand et al. 2014).

Studies that evaluated new doses, indications and dose formulations remain a large part of the current literature (Ehret and Chamberlin 2015). Donepezil gained approval for the treatment of severe AD and became available in a 23-mg/d dose formulation. Rivastigmine became available in a patch formulation while memantin became available as an extended-release capsule. A combination product containing memantin as extended release and donepezil was recently approved in the USA. Among clinicians it is controversly discussed when the

therapy should be initiated, how long this product should be taken and when it should be discontinued (Ehret and Chamberlin 2015).

Other approved anti-dementia drugs (Nootropics)

Piracetam basically completes the list of approved drugs to treat AD, that essentially act symptomatically and in the majority lack clinical efficacy.

Piracetam, a nootropic drug, which was approved in the early 1970s, is used since many years to treat cognitive impairment in ageing, brain injuries, as well as dementia (Muller et al. 1999; Winblad 2005; Eckert et al. 2012a). A comprehensive meta-analysis, including all published and not-published clinical studies, provided compelling evidence for the global clinical efficacy of Piracetam in a diverse group of older patients with cognitive impairment (Waegemans et al. 2002). However, its clinical use for the treatment of AD is controversially discussed, because clinical trials with convincing evidence are missing (Eckert et al. 2012a).

In addition, common non-cognitive neuropsychiatric symptoms, such as mood disorder, agitation and psychosis often require adequate psychopharmacological medication, even though no existing drug is specifically indicated for their management (Eckert et al. 2012a).

New therapeutic strategies

Currently, there is no treatment available with a proven disease-modifying effect (Citron 2010). Interventions with approved drugs, if started early enough, may at best slow down the fatal pathophysiological alterations leading to the manifestation of clinical AD. Current drugs are unable to reverse the neurodegenerative process (Eckert 2010). Thus, new therapeutic strategies are in the focus of drug discovery programs (see table 2). As discussed above, numerous failures and discontinuations have highlighted possible inconsistencies in the Amyloid Hypothesis (Lansdall 2014). Thus, there is increasing interest in inhibiting tau pathology (Giacobini and Gold 2013; Iqbal et al. 2014) and other therapeutic strategies. A mitochondrial restorative mechanism of antioxidants in AD, including coenzyme Q10, idebenone, mitoQ, mitovitE, and MitoTEMPOL has been recently reviewed regarding the mitochondrial cascade hypothesis (Kumar and Singh 2015). This thesis focuses on mitochondria targeted strategies, especially on Dimebon and Olesoxim, which are discussed in detail below. Regarding other therapeutic strategies, the reader is referred to relevant recent reviews (Giacobini and Gold 2013; Anand et al. 2014; Iqbal et al. 2014; Lansdall 2014; Medina and Avila 2014; Heneka et al. 2015; Wisniewski and Goni 2015).

Mitochondrial Targeted Therapy

Mitochondrial dysfunction

Mitochondria are essential organelles for all living cells, as they provide the majority of cellular energy in form of adenosine triphosphate (ATP) (Muller et al. 2010; Eckert et al. 2012b). The electron transfer chain (ETC) in the inner mitochondrial membrane transfers electrons through protein complexes (complex I-IV) and generates an electrochemical proton gradient across the membrane (mitochondrial membrane potential, MMP). Complex V (ATP-synthase) in turn, uses this gradient to produce ATP, as the main source of cellular energy (Figure E1) (van den Heuvel and Smeitink 2001). Under physiological conditions, this process also produces low levels of ROS, which are important in signaling processes (Valko et al. 2007).

Age-related dysfunction of mitochondrial ETC proteins with concomitant increased ROS-levels, has been observed in studies on mammals (Benzi et al. 1992; Petrosillo et al. 2008; Muller et al. 2010; Paradies et al. 2011). Dysfunctions of single complexes, such as complex I and IV, are often accompanied by the loss of MMP and subsequently reduced ATP levels as shown in brains of age-related mouse models (Afshordel et al. 2015; Hagl et al. 2015b; Hagl et al. 2016). Mitochondrial dysfunction is also present in AD mouse models (Abdel-Kader et al. 2007; Hauptmann et al. 2009; Kurz et al. 2010; Mao and Reddy 2011). Thus, mitochondrial dysfunction represents an early common event in brain ageing and AD (Lynn et al. 2010; Eckert et al. 2013). Accordingly, a defective energy metabolism was stated, to be a fundamental component of AD (Valla et al. 2001; Manczak et al. 2004; Manczak et al. 2006; Schioth et al. 2012). Notably, genes in mitochondrial complexes I-V subunits are extensively downregulated in the AD brain, most evident in the hippocampus (Berchtold et al. 2014).

As major consequences of mitochondrial dysfunction, enhanced depletion of mitochondria in axons and dendrites, synaptic dysfunction, loss of synapses and finally neuronal loss occurs (Li et al. 2004a; Reddy and Beal 2008; Muller et al. 2010).

Increasing evidences suggest an important role of mitochondrial dysfunction for **oxidative stress** in AD (Hirai et al. 2001; Mattson et al. 2008; Wang et al. 2009; Swerdlow et al. 2014). Mitochondrial dysfunction associated with elevated reactive oxygen species (ROS) levels, can damage mitochondrial structures, such as nucleic acids, proteins or phospholipids,

affecting mitochondrial integrity. Early defects in the expression of several subunits of respiratory chain complexes (Rhein et al. 2009), decreased mitochondrial respiration, mainly mediated by a decline in complex I and complex IV function, reduced MMP and ATP levels were detected in several AD cell and animal models (Keil et al. 2006; Rhein et al. 2009; Wang et al. 2009; Leuner et al. 2012b; Stockburger et al. 2014; Hagl et al. 2015a).

Moreover, data indicate that superoxide-dismutase-2 (SOD2) deficiency induces oxidative stress in an AD mouse model (Lee et al. 2012). Early deficits in synaptic mitochondria in an Alzheimer's disease mouse model were reported (Du et al. 2010). Compared to non-synaptic mitochondria, synaptic mitochondria showed a greater degree of age-dependent accumulation of Aβ and mitochondrial alterations. The synaptic mitochondrial pool of Aβ was detected at an age, as young as four months, well before the onset of non-synaptic mitochondrial and extensive extracellular Aβ accumulation occurs (Du et al. 2010). Aβ triggers mitochondrial dysfunction through a number of pathways, such as impairment of oxidative phosphorylation (OXPHOS), elevation of ROS production, alterations of mitochondrial dynamics, and interaction with mitochondrial proteins. Aβ interacts with different mitochondrial targets, including the outer mitochondrial membrane, the intermembrane space, the inner mitochondrial membrane and the matrix (Pagani and Eckert 2011; Pinho et al. 2014). Mitochondria-derived ROS are sufficient to trigger amyloidogenic APP-processing *in vitro* and *in vivo* and Aβ itself leads to mitochondrial dysfunction and increased ROS levels. Based on recent findings, it was proposed, that starting from mitochondrial dysfunction, a vicious cycle is triggered, that contributes to the pathogenesis of sporadic AD (Leuner et al. 2012b). Increasing evidence suggests, that mitochondrial dysfunction in AD is originated not only from the deleterious impact of APP/Aβ, but also from its interplay with hyperphosphorylated Tau protein at the level of mitochondria (Keil et al. 2006).

To fulfill the complex demands of providing the neuron with ATP, not only at the level of the cell body, but also at the synapses, mitochondria are dynamic cell organelles with the abilities to undergo constant **fission and fusion** and to migrate from cell body to synapses and *vice versa*. The latter being quite important, considering the substantial lengths of some axons (Knott et al. 2008). Moreover, mitochondria may vary in localization, shape, size, and number. In response to environmental stimuli, mitochondria fuse and divide constantly, in order to meet changes in cellular metabolic needs and to distribute the chondriom among the

cell (Griparic et al. 2004). Several proteins control the fission and fusion processes. Mitofusin 1 (Mfn1), Mitofusin 2 (Mfn 2) and optic atrophy 1 (Opa 1) are regulators of the fusion machinery, and dynamin-related protein 1 (Drp 1) and fission 1 (Fis 1) determine the fission events (Griparic et al. 2004). The relevance of mitochondrial fission and fusion to underlying mechanisms of ageing and AD has not been fully investigated yet. The best-studied proteins involved in fusion are Mfn1, responsible for the tethering of opposing mitochondrial membranes and Opa1 responsible for cristae junction of the inner membrane of mitochondria. Reduced fusion and/or enhanced fission can contribute to further mitochondrial dysfunction, that is possibly associated with ageing and AD (Reddy and Beal 2008). In line with the large body of evidence, indicating mitochondrial dysfunction as one of the major pathomechanisms in AD (Reddy and Beal 2005; Friedland-Leuner et al. 2014), several reports indicate deficits of mitochondrial dynamics in this disease, including impaired balance between fission and fusion mechanisms and reduced mitochondrial trafficking (Trimmer et al. 2000; Rui et al. 2006; Wang et al. 2008; Reddy 2009; Wang et al. 2009). This imbalance results in a pronounced fragmentation of mitochondria, which is a correlate for the enhanced fission processes taking place in AD (Reddy and Beal 2008; Leuner et al. 2012b). Moreover, interfering with impaired mitochondrial dynamics has been proposed as novel strategy, for anti-dementia drugs (Moreira et al. 2010; Muller et al. 2010; Su et al. 2010).

Concomitant with disturbed dynamic proteins, **mitophagy** (a protective cellular mechanism to sort out damaged or energy-deficient mitochondria) seemed to be dysregulated. During ageing or in AD, enhanced autophagy is observed, which is responsible for apoptotic neuronal cell loss (Green et al. 2011; Cai and Tammineni 2016). It has been speculated, that changes in mitochondrial dynamics and biogenesis are also senescence related and are considered as another important parameter of mitochondrial dysfunction, associated with ageing (Green et al. 2011).

  Autophagy is a quality control system of eminent importance, to degrade damaged proteins and dysfunctional organelles and to reintroduce their constituents back to the cytosol as nutrients for renewal (Mizushima et al. 2008; Barnett and Brewer 2011). Since energy is needed to elongate autophagosomal membranes during autophagic processes (Tanida et al. 1999), a depletion or lack of ATP could inhibit autophagy (Plomp et al. 1989). Overexpression of LC3 induces autophagy, extends lifespan by 50% and increases resistance to ROS cytotoxicity in Drosophila (Simonsen et al. 2008). In cortex post-mortem samples of AD patients autophagy mediators are reduced, which was interpreted as an inhibition of

autophagy in AD (Pickford et al. 2008). Evidence suggests that dysfunctional mitochondria can be selectively removed by mitophagy (Cai and Tammineni 2016).In consequence, the degradation of dysfunctional mitochondria might be reduced (Pickford et al. 2008). If damaged mitochondria are not degraded, their increased ROS production might have adverse effects to cells (Barnett and Brewer 2011).

Mitochondrial membranes play a key role in **apoptosis** (Azarashvili et al. 2010). Pro-apoptotic proteins, such as Bax, induce the assembly of the **mitochondrial permeability transition pore (mPTP)** in mitochondrial membranes, that consists of VDAC, PBR, ANT, and other components, such as the matrix protein cyclophillin D (Cyp D) (Figure E1). Proteome analysis of post-mortem brain tissue from subjects with mild cognitive impairment, early stage, and late stage Alzheimer's disease, identified increased VDAC and ANT levels as early marker of mitochondrial dysfunction (Lynn et al. 2010). Interaction of Aβ with Cyp D also caused disturbances of mitochondrial function, increasing ROS production or deregulation of the mPTP (Du et al. 2008; Du and Yan 2010; Repalli 2014). Thus, it has been proposed, that Cyp D-mediated mitochondrial membrane permeability transition pore formation contributes to mitochondrial and neuronal failure in an Aβ-rich environment (Du et al. 2011). Blockade of Cyp D protects mitochondria from Aβ toxicity (Du and Yan 2010) and Aβ decreased the threshold of mPTP formation, by interacting with CypD (Du et al. 2011). Opening of the mPTP is sensitive to the fluidity of mitochondrial membranes. Enrichment of isolated mitochondria with cholesterol, that reduces mitochondrial membrane fluidity, impairs the ANT-mediated mPTP opening (Eckmann et al. 2013). This opening is particularly induced by an excess of calcium, but also by several effectors and is followed by a sudden increase of permeability, which allows solutes of up to 1,5 kDA to equilibrate between mitochondrial matrix and cytosol (Azarashvili et al. 2010). In consequence, uncoupling of oxidative phosphorylation system, mitochondrial matrix swelling and release of cytochrome *c*, initiate apoptosis (Azarashvili et al. 2010; Rasola et al. 2010; Martinou and Youle 2011).
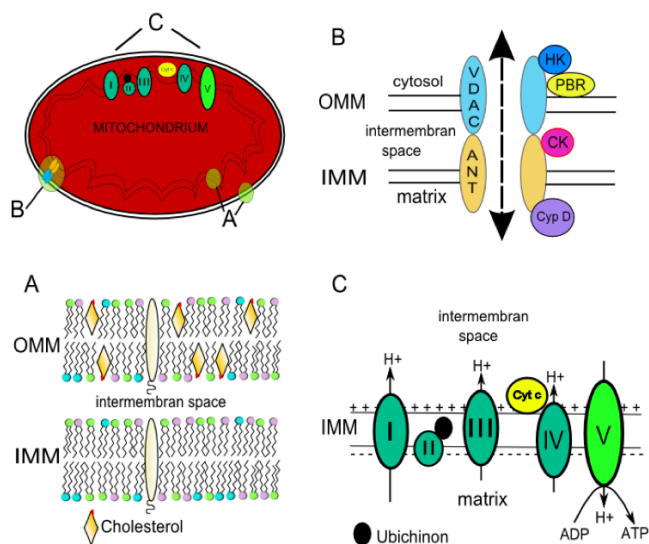
Figure E1. Mitochondria – composition and function. A. Mitochondria are composed of outer (OMM) and inner mitochondrial membranes (IMM). Both membranes are highly dynamic phospholipid bilayers and substantially differ in their composition. Cholesterol is almost exclusively found in OMM, whereas cardiolipin represents a unique phospholipid of IMM. OMM contains porins that are responsible for its high permeability. IMM, in contrast, harbors many proteins responsible for oxidative phosphorylation and ATP production**. B.** The mitochondrial permeability transition pore (mPTP) opening is a key event in apoptosis. The mPTP spans inner and outer mitochondrial membranes. Main mPTP components are VDAC in the OMM and ANT in the IMM, forming the central core together with Cyc D, a matrix protein. Hexokinase II (HK), mitochondrial creatine kinase (CK), and the peripheral benzodiazepine receptor (PBR) are considered as possible regulatory components. **C.** The oxidative phosphorylation system is located in the IMM. Respiratory complexes I, III and IV build up a mitochondrial membrane potential by pumping protons (H^+) from the matrix into the intermembrane space. This proton gradient is the driving force for complex V (ATP-synthase) to produce ATP from ADP (Nijtmans et al. 2004). Picture taken from (Eckmann et al. 2013).

The relationship between mitochondrial energy production and mitochondrial network organization is mutual (Benard and Rossignol 2008). As major consequences, enhanced depletion of mitochondria in axons and dendrites leads to synaptic dysfunction, loss of synapses and neurites, and finally neuronal loss occurs (Li et al. 2004b; Reddy and Beal 2008; Muller et al. 2010).

Mitochondrial dysfunction is an early feature of AD, that contributes to an impairment of the energy metabolism, defects in key respiratory enzyme activity/function, accumulation/generation of mitochondrial ROS, formation of mPTP, altered mitochondrial biogenesis and dynamics (Picone et al. 2014; Schuh et al. 2014). Thus, mitochondria offer multiple points to develop strategies against mitochondrial dysfunction (Picone et al. 2014).

Beside natural occurring antioxidants and active molecules, such as curcumin (Hagl et al. 2014; Hagl et al. 2015b), omega-3 fatty acids (Afshordel et al. 2015), vitamin E (Hagl et al. 2013; Hagl et al. 2015a; Hagl et al. 2016), Gingko biloba (Abdel-Kader et al. 2007), chemical derived molecules such as Piracetam (Leuner et al. 2010), MH48 (Pohland et al. 2016), Idebenone, MitoQ or SkQ (James et al. 2007; McManus et al. 2011; Kumar and Singh 2015; Zhang et al. 2016) have been investigated.

Mitochondrial cascade hypothesis

A reduction in the cerebral metabolic rate of glucose is one of the most predominant abnormalities, generally found in the Alzheimer brain, whereas the cerebral metabolic rate of oxygen is diminished only slightly or not at all, at the beginning of AD (Hoyer 1993). One of the first who related mitochondrial dysfunction to AD were Hoyer et al., who calculated the cerebral ATP-formation rate from the cerebral metabolic rates of oxidized glucose and oxygen in AD patients (Hoyer 1993). Patients with incipient early-onset, incipient late-onset and with stable advanced dementia, showed a graduated reduction of the ATP-formation in their brains (Hoyer 1993). The most severe loss was calculated for patients with stable advanced dementia (Hoyer 1993). In 2004, Swerdlow and Khan proposed the „mitochondrial cascade hypothesis", that comprehensively brings together seemingly disparate histopathologic and pathophysiologic features in LOAD (Swerdlow and Khan 2004). In their model, the inherited, gene-determined make-up of an individual's electron transport chain, sets basal rates of ROS production, which determines the pace at which acquired mitochondrial damage accumulates. Oxidative mitochondrial DNA, RNA, lipid, and protein damage amplifies ROS production and triggers three events: (1) cells respond to elevated ROS by generating Aβ, which further perturbs mitochondrial function, (2) compromised cells undergo apoptosis and (3) a disturbed cell cycle, with results in aneuploidy, tau phosphorylation and neurofibrillary tangle formation (Swerdlow and Khan 2004). Since then, several investigations reported data, consistent with or supportive of this hypothesis (Swerdlow and Khan 2009; Swerdlow et al. 2010, 2014). Additionally, new mitochondria related targets, such as the synaptic vesicle protein 2A (SV2a protein) have been identified, which might play a role in ageing and LOAD (Stockburger et al. 2015). Thus, mitochondrial dysfunction may represent the missing link, between ageing and sporadic AD and serves an attractive target against neurodegeneration (Muller et al. 2010; Grimm et al. 2015) (Friedland-Leuner et al. 2014).
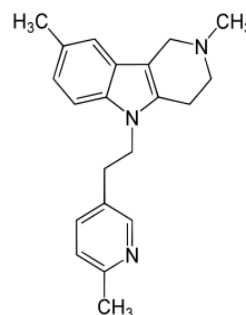
The advanced mitochondrial cascade hypothesis dominates more and more as the leading model for LOAD (Mueller et al. 2016). It also integrates physiological ageing as the main risk factor for LOAD. Advanced aged enhances ROS production, which directly stimulates gamma-secretase activity (Leuner et al. 2012a; Leuner et al. 2012c), finally leading to enhanced Aβ production. This probably leads to a vicious cycle, in which ageing and amyloid toxicity exaggerates each other (Stockburger et al. 2014; Mueller et al. 2016).

In frame of this thesis, the efficacy of Dimebon and Olesoxim to affect mitochondrial dysfunction, in cellular and animal models of AD, which might target the prodromal stage of AD (Caldwell et al. 2015), were investigated.

Dimebon

Dimebon (latrepirdine; 2,3,4,5-Tetrahydro-2,8-dimethyl-5-(2-(6-methyl-3-pyridyl)ethyl)-1H-pyrido[4,3-b]indol) with a molecular weight of 319,44 Da ($C_{21}H_{25}N_3$), represents an old antiallergic drug, originally developed in Russia as H_1-antihistaminicum (Figure E2) (Bachurin et al. 2001; Sachdeva and Burns 2011). Based on preliminary findings about cognition enhancing properties in a small group of AD patients (Bachurin et al. 2001), a large placebo controlled phase II trial was carried out

Figure E2: Chemical structure of Dimebon

in nearly 200 AD patients, indicating a substantial therapeutical benefit over placebo after 24 weeks (Doody et al. 2008). However, most of the beneficial effects in AD patients (Doody et al. 2008) could not be reproduced in a subsequent large-scale multicenter phase III trial (Jimeson and Machado 2010).

Several plausible explanations for the failure of Dimebon in Phase III trials are desrcibed, despite promising Phase II data (Sabbagh and Berk 2010). The most likely reasons include the failure of the placebo group to decline, as expected and a potentially invalid data set resulting from the Russian Phase II trials or differences in the Russian patients compared to typical western cohorts (Sabbagh and Berk 2010). Recent meta-analyses concluded, that while not associated with an increased risk of adverse events, there is no effect of Dimebon on cognition and function in mild-to-moderate AD patients compared to placebo, although it tended to improve cognitive scores (Cano-Cuenca et al. 2014; Chau et al. 2015).

Dimebon's potential use in geriatric memory disorders was also supported by studies about similar effects in Huntington disease patients (Kieburtz et al. 2010) and cognition improving properties in several animal models, including young and adult mice (repeated (0.1 mg/kg) and acute (0.5 mg/kg) i.p. treatment) (Vignisse et al. 2011), mice transgenic for mutant human APP (12 mg/kg b.w. Dimebon for 4 months delivered through their drinking water) (Wang et al. 2011), rats (0.1-30 mg/kg b.w. i.p.) (Schaffhauser et al. 2009; Giorgetti et al. 2010) and rhesus monkeys (3.9-118 µg/kg b.w.) (Webster et al. 2011).

Quantitative immunohistochemistry revealed a significant reduction in hippocampal APP/Aβ in male and female 3xTg-AD mice, that received a daily intraperitoneal injection of 0.1 %

Dimebon for 1.5 months. However, protein bioassays found no change in full length APP, soluble $A\beta_{1-40}$ and $A\beta_{1-42}$, $A\beta$ oligomers, BACE1 and GFAP levels between the groups. Interestingly, the number of the hippocampal APP/$A\beta$ plaques in female and male Dimebon-treated mice, was higher compared to gender-matched control mice (Perez et al. 2012). Accordingly, a recent *in situ* study using immunoblotting and atomic force microscopy (AFM) showed a modest increase in both, the formation and size of $A\beta$ aggregates (Porter et al. 2016).

In another study, Dimebon administration resulted in increased levels of autophagy biomarkers in brains of TgCRND8 (APP K670M, N671L, V717F) or wild-type mice. The treatment was associated with abrogation of behavioral deficits, reduction in $A\beta$ neuropathology and prevention of autophagic failure among TgCRND8 mice (Steele et al. 2013a). Dimebon was also found to partially protect against the progressive decline in motor function and accumulation of tau-positive dystrophic neurons, characteristic of tauP301S mice (Peters et al. 2013a). However, Dimebon was not found to improve neither the general health or motor behavior, nor prevent accumulation of $A\beta$ peptides in the brain of mice harboring five familial mutations associated with hereditary AD (5xFAD line) (Peters et al. 2013a).

Regardless the final proof of Dimebon's clinical efficacy, Dimebon might specifically interfere with mechanisms, relevant for the cognitive decline, especially by improving impaired mitochondrial function and/or dynamics in AD (Moreira et al. 2010; Su et al. 2010). This mechanism represent the most relevant driving force in the vicious cycle between $A\beta$ production, mitochondrial dysfunction and neurodegeneration, including loss of synapses, neurits and nerve cells (Leuner et al. 2012b; Reddy 2014).

Findings that Dimebon (25 μmol/l) protects against the neurotoxic effects of $A\beta$ (Bachurin et al. 2001; Lermontova et al. 2001), together with many observations of mitochondria as major target for the cell toxicity of $A\beta$ (Reddy 2009; Leuner et al. 2012c), led to the assumption that mitochondrial protection might be a major mechanism for the beneficial effects of Dimebon in neurodegenerative diseases. Cerebral glucose utilization (CGU) was assessed in young and aged mice *in vivo,* using [18F]-fluorodeoxyglucose positron emission tomography (FDG-PET), after acute treatment with Dimebon. Two ages of B6SJLF2 mice (5 and 20 months old) were tested. Three test-retest FDG-PET baseline scans were assessed across all subjects. As

CGU was heterogeneous in aged mice, compared to young mice, aged subjects were rank ordered and then counterbalanced into two CGU homogenous groups. In studies 1 and 2, Dimebon (1.0 mg/kg) significantly enhanced CGU in aged mice. In contrast, study 3 revealed that Dimebon did not modulate CGU in young mice (Day et al. 2011).

A few recent publications reported additional evidence for mitochondrial protection by Dimebon. In micromolar concentrations (1–50 μmol/l), Dimebon protects against L-glutamate neurotoxicity in a cellular model of Huntington's disease (Wu et al. 2008) and inhibits calcium-induced swelling of rat brain mitochondria, without affecting cytochrome *c* release or calcium retention (Zhang et al. 2010). More importantly, Dimebon at nanomolar concentrations (0.1-10 nmol/l), improved several measured parameters of mitochondrial function, such as membrane potential, ATP production, MTT reduction and apoptosis in human SH-SY5Y neuroblastoma cells and primary rat cortical neurons (Zhang et al. 2010). Protective effects were observed in both cell lines after treatment with Dimebon alone, but were more pronounced when the cells were additionally stressed, e.g. by serum deprivation (Zhang et al. 2010). Furthermore, Dimebon protects SH-SY5Y neurons against Aβ toxicity and promotes GFAP expression in primary mouse astrocyte cultures (Perez et al. 2012). Recent data from our laboratory showed that nanomolar concentrations (100 nmol/l) of Dimebon restored morphologic changes and function of mitochondria, mainly by increasing the amount of ETS in a cellular model (HEK-APP$_{sw}$ cells) that produces excess of Aβ (see result section (Eckert et al. 2012b). Recently, Pohland et al. reported that Dimebon reduced levels of soluble Aβ$_{1-42}$ and protects HEK-APPwt cells from sodium nitropurssid induced mitochondrial dysfunction, indicated by elevated MMP and ATP levels (Pohland et al. 2016).
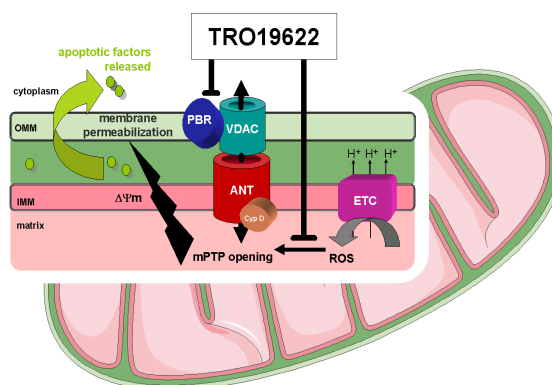
Olesoxim

Olesoxim (Trophos code: TRO19622; chemical name: cholest-4-en-3-one-oxime) is a cholesterol-like compound with a molecular weight of 399.65 Da ($C_{27}H_{45}NO$), which exists as a stable mixture of *syn* and *anti* isomers of the oxime in the 3-position (Figure E3). Olesoxim as a crystalline powder, is stable for more than 36 months under conditions described in regulatory guidelines. Due to its
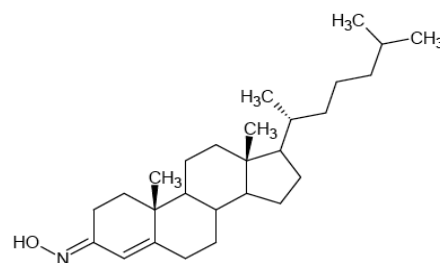
Figure E3: Chemical structure of Olesoxime (cholest-4-en-3-one).

lipophilic properties, oily excipients can be used to prepare solid and liquid oral dosage forms for preclinical and clinical studies (Bordet et al. 2010).

Olesoxim has been identified in a phenotypic screening approach to promote the survival of primary motor neurons (Bordet et al. 2007). Olesoxim is easily absorbed by cells and accumulates in mitochondria (Bordet et al. 2010). Olesoxim's mode of action is not fully understood, although it has been shown to modulate mitochondrial membranes (Eckmann et al. 2014) and interact with the voltage-dependent anion channel (VDAC) and the translocator protein (TSPO; also known as PBR) (Bordet et al. 2007). Thereby it inhibits mitochondrial permeability transition (Bordet et al. 2010; Gouarné et al. 2013; Gouarne et al. 2015). VDAC and TSPO are two proteins of the outer mitochondrial membrane that are involved in Ca^{2+}-homeostasis (Gincel et al. 2001), metabolite (Shoshan-Barmatz and Ben-Hail 2012) and cholesterol transport (Hu et al. 2010). Both proteins are further involved in mitochondrial permeability transition (mPTP). Olesoxim was also able to rescue cortical neurons from apoptotic cell death, induced by camptothecin (Gouarné et al. 2013) or occipital lesions (Martin et al. 2011). Morover, Olexoxim protects human neuronal differentiated SHSY-5Y cells against wild-type α-synuclein-induced

Figure E4. Targets of Olesoxime (TRO19622). Olesoxime reduces ROS formation and interacts with the peripheral benzodiazepine receptor (PBR), which is also named translocator protein (TSPO) [Source: Trophos S.A.]

toxicity (Gouarne et al. 2015) and may ameliorate the function and resilience of dopaminergic neurons in vivo (Richter et al. 2014).

Olesoxim has demonstrated therapeutic efficacy in disease models of amyotrophic lateral sclerosis (Bordet et al. 2007; Sunyach et al. 2012), Huntington (Clemens et al. 2015) and peripheral neuropathies (Bordet et al. 2008; Xiao et al. 2009; Rovini et al. 2010; Xiao et al. 2012) by targeting mitochondria-related defects. Furthermore, Olesoxim accelerated myelination and induced repairs in models of demyelination (Li et al. 2013). Accordingly, Olesoxim promoted myelin formation with consequent functional improvement in a rat model of demyelination (Magalon et al. 2012).

Olesoxim, although well tolerated, did not show significant beneficial effect in ALS patients treated together with riluzole in a phase II-III trial (ClinicalTrials.gov Identifier: NCT00868166)(Lenglet et al. 2014). However, Olesoxim recently yielded impressive beneficial effects on motor function in a phase II clinical trial in spinal muscular atrophy patients (ClinicalTrials.gov Identifier: NCT01302600) (http://www.roche.com/media/store/releases/med-cor-2015-01-16.htm)(Zanetta et al. 2014).

Problem statement & work plan

AD has a multifactorial pathology making it difficult to develop feasible therapies. Currently approved drugs attenuate symptoms, but do not cure the disease. Research into AD also has had several failures in terms of developing disease-modifying therapies. Since AD starts many years far before the first symptoms occur, new scientific approaches focus on the early stage, which are discussed to be important in ageing and the onset of AD. Since mitochondrial dysfunction seems to occur early in AD pathogenesis, new approaches targeting mitochondrial dysfunction are of substantial interest. The aim of this thesis was to investigate the efficacy of the mitochondria targeting drugs, Dimebon and Olesoxim, to ameliorate mitochondrial dysfunction in HEK-cells harboring the Swedish mutation in the APP gene (HEKsw), that represent a cellular model of LOAD. Therefore, mitochondrial membrane potential, ATP concentrations and respiration were measured beside others,. Western Blot analysis of marker proteins for fission & fusion, autophagy, mitogenesis and mPTP formation were also performed. Confocal laser scanning microscopy was introduced as a novel method to visualize mitochondrial dynamics. Olesoxim was studied in Thy-1-C57BJ/6-APPSL mice representing a murine model of AD. For the in vivo model, mitochondria from brain tissue were isolated and dissociated brain cells were prepared to determine respiration, lipid peroxidation, MMP, ATP-levels and other parametes. Both, the in vitro and in vivo models were compared and discussed in relation to human post-mortem data. The research was conducted in frame of the EU-project entitled „MITOTARGET" (Mitochondrial dysfunction in neurodegenerative diseases: towards new therapeutics) funded under FP7-Health (http://cordis.europa.eu/result/rcn/54471_en.html).

Materials and Methods

The country in which a company is based is only specified, if it is not Germany.

Devices

- Autoclave *Bioklav* (Schütt Labortechnik, Göttingen)
- Cell culture equipment (Greiner, Frickenhausen)
- Centrifuges *GS-6R* and *Microfuge R* (Beckman, Krefeld)
- Confocal Laserscan Microscope TCS SP5 (Leica, Wetzlar)
- Fluorescence spectrometer *SLM Aminco Bowman Series 2* (Thermo Fisher, Waltham, USA)
- Gel electrophoresis and blotting systems *Novex Mini-Cel l* (invitrogen, Carlsbad, USA) and *Mini Protean Tetra Cell* (Bio-Rad, München)
- Incubator *BB6220* (Heraeus, Hanau)
- Microscope *TCS SP5* (Leica, Solms)
- *Milli-Q Academic* water filtration system (Millipore, Billerica, USA)
- *Molecular Imager Gel Doc XR System* (Bio-Rad, München)
- Multi-gel casting chamber and gel casting stands (Bio-Rad, München)
- *NuPAGE Novex 4-12% Bis-Tris gels* (life technologies, Carlsbad, USA)
- *Oxygraph-2k* (Oroboros Instruments, Innsbruck, Austria)
- pH meter *inoLab pH level 1* (WTW, Weilheim)
- Photometer *Digiscan* (Asys Hightech, Eugendorf)
- Photometer *Genesys 5* (Spectronic *via* Thermo Fisher, Waltham, USA)
- Pipetting aid *accu-jet* (Brand, Wertheim)
- Pipets *Pipetman* (Abimed, Langenfeld)
- Plastic labware (Greiner, Frickenhausen)
- Potter homogenizer *Potter S* (B. Braun, Melsungen)
- Quartz cuvette *101-QS* 10mm (Zeiss, Jena)
- Safety cabinet *DLF/Rec4 Kl. 2A* (Heraeus, Hanau)
- Scales *AB204* and *AT261 Delta Range* (Mettler-Toledo, Gießen)
- Shaker plate *Promax 1020* (Heidolph, Schwabach)
- *SNAP i.d.* incubation system for Western Blots (Millipore, Billerica, USA)
- Sonifier *Cell Disruptor B15* (Branson, Danbury, USA)
- Thermal shaker *Thermomixer comfort* (Eppendorf, Hamburg)
- Thermal cycler *Advanced primus 25* (peqlab, Erlangen)
- Ultracentrifuge *I8-70M* (Beckmann, Krefeld)
- *Victor X3 2030* multilabel counter (Perkin Elmer, Rodgau-Jügesheim)
- Water bath *1002* (GFL, Burgwedel)

Chemicals

- 1,4-diazabicyclo[2.2.2]octane (DABCO) (Sigma-Aldrich, Steinheim)
- 4-(2-hydroxyethyl)-1-piperazineethanesulfonic acid (HEPES) (Merck KGaA, Darmstadt)
- 5,5'-dithiobis-(2-nitrobenzoic acid) (DTNB) (Sigma-Aldrich, Steinheim)
- Acetyl coenzyme A, trilithium salt (Sigma-Aldrich, Steinheim)
- Adenosine diphosphate (ADP) (Sigma-Aldrich, Steinheim)
- Antimycin A (Sigma-Aldrich, Steinheim)
- Aprotinin (Sigma-Aldrich, Steinheim)
- Ammonium persulfate (APS) (Bio-Rad, München)
- Bovine serum albumine, essentially fatty acid free (BSA) (Sigma-Aldrich, Steinheim)
- Calcium chloride (Merck KGaA, Darmstadt)
- Carbonyl cyanide 4-trifluoromethoxyphenylhydrazone (FCCP) (Sigma-Aldrich, Steinheim)
- Citrate synthase from porcine heart (Sigma-Aldrich, Steinheim)
- Cyclosporin A (Sigma-Aldrich, Steinheim)
- Cytochrome c from equine heart (Sigma-Aldrich, Steinheim)
- Digitonine (Sigma-Aldrich, Steinheim)
- Dimethylsulfoxid (DMSO) (Merck KGaA, Darmstadt)
- Disodium phosphate (Merck KGaA, Darmstadt)
- Dithionite (Merck KGaA, Darmstadt)
- Dulbecco's Modified Eagle Medium (DMEM) (invitrogen, Carlsbad, USA)
- Dulbecco's phosphate buffered saline (PBS) (Gibco, Darmstadt)
- Ethanol (>99%) (Merck KGaA, Darmstadt)
- Ethanol (70%) (Roth, Karlsruhe)
- Ethidium bromide solution (10 mg/ml) (Bio-Rad, München)
- Ethylenediaminetetraacetic acid (EDTA) (Merck KGaA, Darmstadt)
- Ethylene glycol tetraacetic acid (EGTA) (Sigma-Aldrich, Steinheim)
- Fetal calf serum (FCS) (Sigma-Aldrich, Steinheim)
- Formaldehyde (Roth, Karlsruhe)
- G418 (gibco, Carlsbad, USA)
- Glucose (Merck KGaA, Darmstadt)
- Glutamate (Sigma-Aldrich, Steinheim)
- Glycine (Roth, Karlsruhe)
- Glycerol (Alfa Aesar, Karlsruhe, Germany)
- Hanks' balanced salts (Sigma-Aldrich, Steinheim)
- Horse serum (Sigma-Aldrich, Steinheim)
- Hydrochloric acid 37% (HCl) (Merck KGaA, Darmstadt)
- Isopropanol (Merck KGaA, Darmstadt)
- Iron (II) chloride tetrahydrate (Merck KGaA, Darmstadt)
- K-lactobionate (Sigma-Aldrich, Steinheim)
- Leupeptin (Sigma-Aldrich, Steinheim)
- Magnesium chloride hexahydrate (Merck KGaA, Darmstadt)
- Malate (Sigma-Aldrich, Steinheim)

- MES SDS Running Buffer (20x) (life technologies, Carlsbad, USA)
- Methanol (Merck KGaA, Darmstadt)
- MitoTracker CMXRos (life technologies, Carlsbad, USA)
- Monopotassium phosphate (Merck KGaA, Darmstadt)
- Mowiol 4-88 (Sigma-Aldrich, Steinheim)
- Non-fat dried milk powder (AppliChem, Darmstadt)
- N,N,N',N'-tetramethyl-p-phenylenediamine (TMPD) (Sigma-Aldrich, Steinheim)
- NuPage Antioxidant (life technologies, Carlsbad, USA)
- NuPage LDS Sample Buffer (4x) (invitrogen, Carlsbad, USA)
- NuPage Sample Reducing Agent (10x) (invitrogen, Carlsbad, USA)
- NuPage Transfer Buffer (20x) (life technologies, Carlsbad, USA)
- Oligomycin (Sigma-Aldrich, Steinheim)
- Oxalacetate (Sigma-Aldrich, Steinheim)
- Penicillin/Streptomycin (PenStrep) (PAA, Cölbe)
- Pepstatin (Sigma-Aldrich, Steinheim)
- Percoll (Sigma-Aldrich, Steinheim)
- Phenylmethylsulfonylfluorid (PMSF) (Sigma-Aldrich, Steinheim)
- Potassium chloride (Merck KGaA, Darmstadt)
- Protease Inhibitor Cocktail Complete (Roche, Basel, Switzerland)
- Pyruvate (Sigma-Aldrich, Steinheim)
- Rhodamine-123 (Sigma-Aldrich, Steinheim)
- Rotenon (Sigma-Aldrich, Steinheim)
- Sodium ascorbate (Sigma-Aldrich, Steinheim)
- Sodium azide (Sigma-Aldrich, Steinheim)
- Sodium chloride (Merck KGaA, Darmstadt)
- Sodium dodecyl sulfate (SDS) (Merck KGaA, Darmstadt)
- Sodium orthovanadate (> 90 %) (Sigma-Aldrich, Steinheim)
- Succinate (Sigma-Aldrich, Steinheim)
- Sucrose (Roth, Karlsruhe)
- Taurine (Sigma-Aldrich, Steinheim)
- tetramethylethylenediamine (TEMED) (Bio-Rad, München)
- Triethanolamine (Sigma-Aldrich, Steinheim)
- Tris(hydroxymethyl)aminomethan (Tris) (Merck KGaA, Darmstadt)
- Triton X-100 (Merck KGaA, Darmstadt)
- Trypan blue (Sigma-Aldrich, Steinheim)
- Trypsin/EDTA (PAA, Cölbe)
- Tween20 (Sigma-Aldrich, Steinheim)
- Urea (Merck KGaA, Darmstadt)

Buffer

All buffers were produced in ultrapure water (Milli-Q, Millipore, Billerica, USA).

Tris(hydroxymethyl)aminomethane (Tris) [20 mM]
To obtain a 20 mM solution, 2.42 g of Tris were dissolved in 1000 ml H_2O. pH was adjusted to 7.4 at 4 °C using HCl (1 N).

Phosphate buffered saline (PBS)
100 ml of 10x Dulbecco's PBS were diluted in 900 ml H_2O to obtain a ready-for-use 1x PBS solution.

PBS/PI
One tablet of protease inhibitor cocktail was dissolved in 50 ml of PBS (1x). The solution was stored at 2 to 8 °C for no longer than 4 weeks.

Formaldehyde solution
A 0.4 % solution of formaldehyde was prepared using 1x PBS solution. Prior to use, pH of the solution was adjusted to 7.4 at 37 °C.

Mowiol solution for cell fixation
6 g glycerol and 2.4 g Mowiol 4-88 were mixed for 1 h at room temperature and 6 ml of water was added to the solution. The solution was stirred for another hour. Afterwards, 12 ml Tris-HCl solution (0.2 M, pH=8.5) were added and the mixutre was stirred at 50 °C for 2 h. When the Mowiol was completely dissolved, the solution was aliquoted (1 ml) and stored at −20 °C. Shortly before use, 25 mg of DABCO were added to the aliquot.

MIR05

Substance	Concentration
EGTA	0.5 mM
$MgCl_2 \cdot 6\,H_2O$	3 mM
K-lactobionat	60 mM
Taurine	20 mM
KH_2PO_4	10 mM
HEPES	20 mM
BSA	100 mM
	1 g/l

pH of MIR05 was adjusted to 7.1 at 30 ◦C using KOH (5 N) and MIR05 was stored at −20 ◦C.

Medium 1

Substance	Concentration
NaCl	138 mM
KCl	5.4 mM
Na_2HPO_4	0.17 mM
KH_2PO_4	0.22 mM
Glucose $\cdot$ H_2O	5.5 mM
Sucrose	58.4 mM

pH of medium 1 was adjusted to 7.35 at 4 $^\circ$C using HCl (1 N) and NaOH (1 N). Medium 1 was stored at 4 $^\circ$C not exceeding 14 days.

Medium 2

Substance	Concentration
NaCl	110 mM
KCl	5.3 mM
$CaCl_2 \cdot 2H_2O$	1.8 mM
$MgCl_2 \cdot 6H_2O$	1 mM
Glucose $\cdot$ H_2O	25 mM
Sucrose	70 mM
HEPES	20 mM

pH of medium 2 was adjusted to 7.4 at 4 $^\circ$C using HCl (1 N) and NaOH (1 N). Medium 2 was stored at 4 $^\circ$C not exceeding 14 days.

Hanks' balanced salt solution (HBSS)

Substance (for 1 litre)	
HEPES	2.400 g
$CaCl_2 \cdot 2H_2O$	0.147 g
$MgSO_4 \cdot 7H_2O$	0.246 g
H_2O ad	1000 ml

pH of HBSS was adjusted to 7.4 at 37 $^\circ$C using HCl (1 N) and NaOH (1 N). HBSS was stored at 4 $^\circ$C.

Citrate synthase (CS) reaction medium

Substance	Concentration
DTNB	0.1 mM
Triton X-100	10 %
Oxaloacetic acid	10.0 mM
Acetyl coenzyme A	12.2 mM

Running buffer for gel electrophoresis

Substance	Concentration
H_2O	950 ml
MES SDS Running Buffer (20x)	50 ml
NuPage Antioxidant	1 ml

Running buffer was used for gel electrophoresis with ready-bought gels.

Electrode buffer (10x) for gel electrophoresis

Substance	Concentration
Tris	30.3 g
SDS	10.0 g
Glycin	144.7 g
H_2O ad	1000 ml

Electrode buffer (1x) was used for gel electrophoresis with self-casted gels.

Lower buffer for gel casting

Substance	Concentration
Tris	18.17 g
SDS	0.80 g
H_2O ad	1000 ml

pH was adjusted to > 8.8 in a cool water bath using HCl (37 %).

Upper buffer for gel casting

Substance	Concentration
Tris	3.02 g
SDS	0.20 g
H_2O ad	50 ml

pH was adjusted to > 6.8 in a cool water bath using HCl (37 %).

Transfer buffer for Western Blotting

Substance	Concentration
H_2O	850 ml
Methanol	100 ml
NuPage Transfer Buffer (x20)	50 ml
NuPage Antioxidants	1 ml

Stripping buffer

Substance	Concentration
Glycin	8.0 g
HCl (37%)	2.5 ml
H_2O ad	1000 ml

TBST (10x)

Substance	Concentration
Tris (base)	24.2 g
NaCl	80.0 g
HCl (37%)	13.0 ml
H_2O ad	1000 ml

TBST (10x) was stored at room temperature and diluted 1 : 10 prior to use.

Lysis Buffer

Buffer 1

Substance	Concentration
EDTA	1.0 mM
Triton X-100	0.5 %
PBS (1x) ad	250 ml

Buffer 2

Substance	Concentration
Urea	6.0 M
Sodium pyrophosphate	2.5 mM
Sodium orthovanadate	1.0 mM
Sodium deoxycholate	0.5 %
Sodium dodecyl sulfate	0.5 %

Shortly before using the buffer, Aprotinin (1.7 mg/ml), Leupeptin (5 mg/ml), Pepstatin (5 mg/ml) and PMSF (100 mM) were added to an appropriate amount of buffer 2.

Kits

- ViaLight Plus bioluminescence kit (Lonza, Walkersville, USA)
- BioRad DC Protein Assay (Bio-Rad, Munich, Germany)
- BCA Protein Assay Kit (Pierce, Rockford, USA)
- Colorimetric Lipid Peroxidation Microplate Assay Kit (Oxford Biomedical Research, Oxford, USA)
- Protein Carbonyl Content Assay Kit (Sigma Aldrich, Steinheim, Germany)

Antibodies

Primary antibodies were purchased from Abcam (Cambridge, UK), Millipore (Billerica, USA), Adipogen (Liestal, Switzerland), Bethyl Laboratories (Montgomery, USA) or proteintech (Chicago, USA). All primary antibodies and their respective secondary antibodies are listed in table M.1.

Table M.1: Primary antibodies used for Western Blot experiment

primary antibody (order number)	secondary	primary	antibody	band size
PGC1α (ab106814)	goat	1:500		100kDa
TOMM22	mous	1:1000		15kDa
TIMM50 (ab109436)	rabbit	1:1000		40kDa
Mitofusin1 (ABC41)	rabbit	1:2000		86kDa
Fis1 (AG-25B-0007)	rabbit	1:500		17kDa
GAPDH (MAB374)	mouse	1:300		37kDa
Tubulin (ab6160)	rat	1:10000		52kDa
LC3 (ab48394)	rabbit	1:500		17kDa (LC3-II); 19kDa (LC3-I)
Opa1 (ab42364)	rabbit	1:800		92kDa; 88kDa
Drp1 (A303-410A)	rabbit	1:1000		80kDa; 82kDa
PBR (ab109497)	rabbit	1:100		19kDa
VDAC1/Porin (ab14734)	mouse	1:1000		39kDa

Cell culture media

HEKut:	substance	amount
	DMEM with Glutamax	500 ml
	fetal calf serum (FCS)	10 %
	horse serum (HS)	5 %
	Penicillin	50 U/ml
	Streptomycin	50 µg/ml

HEKsw:	substance	amount
	DMEM	500 ml
	FCS	10 %
	HS	5 %
	Penicillin	50 U/ml
	Streptomycin	50 µg/ml
	G418	0.4 mg/ml

The above mentioned medium mixtures refer to full cell culture medium. To produce reduced cell culture media, FCS content was lowered to 2 % and HS content was lowered to 1 % while the amount of all other ingredients remained unchanged.

Cell line (HEK293)

All cell lines were cultured in a humidified incubator at 37 °C and a CO_2 concentration of 5 %. HEK cells are human embryonic kidney cells, which were transformed with fragments of adenovirus type 5 DNA [Graham et al. 1977]. HEK293 untransfected cells (HEKut) were used as a model for the healthy condition. HEKsw cells were transfected with

DNA constructs harboring human mutant APP (APPsw, KM670/671NL) gene, inserted downstream of a cytomegalovirus promoter, using the FUGENE 6 technology (Roche Diagnostics) (Eckert et al. 2001; Keil et al. 2004). The stably expressing APPsw HEK 293 cells were cultured in Dulbecco's modified Eagle's medium supplemented with 10% heat-inactivated fetal calf serum, 50 units/ml penicillin, 50 μg/ml streptomycin and 400 μg/ml G418. Untransfected HEK 293 cells were cultured in Dulbecco's modified Eagle's medium supplemented with 10% heat-inactivated fetal calf serum, 50 units/ml penicillin and 50 μg/ml streptomycin. Both cell lines were cultured at 37 °C in a humidified incubator containing 5% CO_2. There was no need to use trypsin when splitting the cells since cells could be detached easily from the culture flask by rinsing with cell culture medium.

Mice strain (Thy1-APPSL transgenic mice)

Thy1-APPSL transgenic mice express the human form of APP containing both the swedish (KM670/671NL) and the London (V717L) double mutations under the murine Thy1-promotor (Blanchard et al. 2003). The Thy1 promotor leads to an increased and selective expression of APP in neurons. Beginning at the age of 3 months, Thy1-APPSL mice exhibit elevated Aβ levels and mitochondrial dysfunction. The first Aβ plaques can be found at the age of 6 months (Blanchard et al. 2003) (Hauptmann et al. 2009). Thy1-APPSL transgenic mice were reared at the animal facility of the Pharmacological Institute in Frankfurt. A PCR method was used to assess the genotype of young mice.

Genotyping of Thy1-APPSL transgenic mice

A mouse-tail biopsy (length approx. 1 mm) was taken from mice aged 6 weeks or older and stored at −20 °C. To isolate deoxyribonu- cleic acid (DNA), the tail samples were laced with 100 μl of a 1:40 dilution of 1N NaOH in H_2O and incubated at 98 °C for 20 min. Afterwards, 100 μl of non-buffered Tris buffer (40 mM) were added to each sample before 1 μl of each sample was mixed with 24 μl of the polymerase chain reaction (PCR) master mix (see table 2.2). Nucleotide sequence of primer A was 5'-GTA GCA GAG GAG GAA GAA GTG-3' and nucleotide sequence of primer B was 5'-CAT GAC CTG GGA CAT TCT C-3'. All samples were put in a thermal cycler using the

program depicted in table 2.3. Afterwards samples were laced with 2 µl blue juice (Peqlab, Erlangen) and applied onto a 1.5 % agarose gel spiked with ethidium bromide. Gel electrophoresis was carried out at 90 V for 2 min and subsequently at 120 V for 45 min. The gel was detected *via* ultraviolet (UV) light, using a Molecular Imager Gel Doc XR system. Samples from tail biopsies of transgenic mice produced a band at 500 bp while wildtype mice samples were blank at 500 bp. After completion of the feeding study, new tail biopsies of all participating mice were taken to confirm the results of the first genotyping.

Table M.2: creation of master mix used for PCR experiments; nucleotide sequence of primer A was 5'-GTA GCA GAG GAG GAA GAA GTG-3' and nucleotide sequence of primer B was 5'-CAT GAC CTG GGA CAT TCT C-3'

Compound	amount	manufacturer
DEPC treated water	444 µl	Invitrogen (Carlsbad, USA)
Taq Master Enhancer (5x)	150 µl	Peqlab (Erlangen)
Reaction Buffer	75 µl	Peqlab (Erlangen)
dNTP Mix	15 µl	Peqlab (Erlangen)
Primer A	15 µl	Eurofins MWG (Ebersberg)
Primer B	15 µl	Eurofins MWG (Ebersberg)
Taq polymerase	6 µl	Peqlab (Erlangen)

Table M.3: PCR program used for genotyping of Thy1-APPSL transgenic mice; steps 2-4 were repeated 35 times; lid temperature was 99 °C.

step	temperature	duration
1	94 °C	15 min
2	94 °C	20 s
3	65 °C	40 s
4	72 °C	1 min
5	72 °C	10 min
6	22 °C	forever

Cell Culture

Thawing cells

Cells were removed from liquid nitrogen and gently thawed in a water bath (37 °C). 1 ml of pre-heated cell culture medium (37 °C) was quickly added to the cell suspension, which was then transferred into a Falcon tube, containing 10 ml of cell culture medium. The suspension was centrifuged (1000 rpm, 5 min, room temperature), the supernatant aspirated and the remaining cell pellet was dissolved in 12 ml of fresh cell culture medium. Cells were allowed to rest for 24 h before they were split for the first time.

Splitting cells

When cells attained a confluence of 70 to 80 %, they were split to ensure constant growing of cells. Cell culture medium was aspirated and 10 ml of cell culture medium was added into the dish. The resulting 10 ml of cell suspension were divided into new culture dishes, containing 12 ml of fresh cell culture medium each. Cells were split between 1 : 3 and 1 : 8, depending on the confluence of the cells.

Seeding cells

Prior to measurement of mitochondrial membrane potential (MMP) and ATP concentrations, cells had to be seeded into 24-well plates or 96-well plates to be able to incubate them with either Dimebon or Olesoxim. Culture dishes with a confluence of 70 to 80 % were used for seeding cells. The old cell culture medium was aspirated and 10 ml of fresh medium was added to the cell suspension, which was then centrifuged (1000 rpm, 5 min, room temperature). The resulting pellet was re- solved in 1 ml of fresh cell culture medium. 10 µl of this solution were used to dye cells with trypan blue (0.4 %) and to count them using a Neubauer improved counting chamber. Cell count was adjusted to 1 million cells per ml, using fresh culture medium. 300 µl of cell culture medium was put into each well of a 24-well plate, before 200 000 cells per well were added. 20 000 cells were put in each well of a 96-well plate. The plated were allowed to

rest in the incubator for 48 h, before they were incubated with the respecting test substances.

Harvesting cells for western blot analysis

Cells were detached in 10 ml of ice-cold PBS. The cell solution was centrifuged (300 g, 5 min) and the cell pellet was re-dissolved in 1 ml of PBS/PI. The cell solution was centrifuged (300 g, 5 min) and the cell pellet was stored at $-80\,°C$.

Harvesting cells for Respirometry measurements

Cells were detached from the flask by rinsing with cell culture medium. The cell suspension was centrifuged (1000 rpm, 5 min) and the pellet was redissolved in 1 ml of pre-heated MIR05 (37 °C). 10 µl of this cell suspension were used to dye cells with trypan blue (0.4 %) and to count them with a Neubauer improved counting chamber. Cell count was adjusted to 1 mio cells per ml by dilution with MIR05.

Determination of protein content

Protein levels in isolated mitochondria, cell or brain homogenates were determined either by the Lowry or by the bicinchoninic acid (BCA) method, using a ready-made kit. The Lowry method includes a Biuret reaction, followed by the reduction of copper and a sub- sequent reduction of the Folin-Ciocalteau reagent [Lowry et al. 1951]. The concentration of reduced Folin is measured photometrical at 750 nm and is proportional to the protein content of the sample. The BCA method is based on a reduction of copper by protein residues. Reduced copper(I) reacts with bicinchoninic acid to give a violet complex, whose absorption can be measured photometrical at 562 nm. Lowry and BCA protein assays were conducted, according to the instructions of the respective manufacturer. Bovine serum albumin was used to create a standard curve in both assays.

Isolation of mitochondria from brain tissue

To isolate mitochondria, 1/4 of a mouse brain (around 80 mg) was used. For isolation of mitochondria, a protease inhibitor (PI, complete tablets, Roche, Mannheim, Germany) was added to the medium. The brain was homogenized in 2 ml of MiR05+PI using a Potter homogenizer (800 rpm). After homogenization, the sample was centrifuged to remove cell debris (1400 g, 7 min, 4 °C). The supernatant was then centrifuged once for washing (1400 g, 3 min, 4 °C) and once again (10.000 g, 5 min, 4 °C) to collect the mitochondria in the pellet. Afterwards the pellet was re-dissolved in 1 ml of MIR05+PI and centrifuged once for washing (1400 g, 3 min, 4 °C) and once again to collect the mitochondria in a pellet (10.000 g, 5 min, 4 °C). The pellet was then dissolved in 250 µl MIR05+PI. 80 µl of this solution were injected into one chamber of the Oxygraph-2k (Oroboros, Innsbruck, Austria). The remainder of the isolated mitochondria was stored at −80 °C for analysis of protein content and citrate synthase (CS) activity.

Preparation of dissociated brain cells

DBC were prepared using 1/2 of a mouse brain. The brain was washed once in medium 1. Afterwards it was cut into small pieces in 2 ml of medium 1 using a scalpel. The chopped brain was then pressed through a 200 µm nylon mesh into a beaker containing 16 ml of medium 1 using a plastic Pasteur pipette with a wide opening. In the last step the brain homogenate was filtered through a 102 µm nylon mesh. The resulting brain homogenate was centrifuged (2000 rpm, 5 min, 4 °C) before the pellet was re-dissolved in 20 ml of medium 2. The centrifugation step was repeated twice; after the last centrifugation the pellet was re-dissolved in 4.5 ml of Dulbecco's Modified Eagle Medium (DMEM) (without any supplements). Replicates of six were seeded into 24 well- plates (250 µl for measurement of MMP) or 96 well-plates (50 µl for measurement of ATP). Afterwards the cells were cultured at 37 °C in a humidified incubator under 5 % CO_2.

Measurement of mitochondrial membrane potential

In dissociated brain cells

MMP was measured using the fluorescence dye Rhodamine-123 (R123). DBC were incu- bated in an incubator (37 $^{\circ}$C, 5 % CO_2) for 15 min with 0.4 μM R123. Afterwards, the reaction was stopped by adding Hank's Balanced Salt Solution (HBSS) into the wells. DBC were centrifuged (3000 rpm, 5 min, room temperature), the medium was aspirated and DBC were supplemented with new HBSS. DBC were triturated to obtain a homogenous sample. Subsequently MMP was assessed by reading the R123 fluorescence at an excitation wavelength of 490 nm and an emission wavelength of 535 nm (Victor X3 multilabel counter). The fluorescence in each well was read in four consecutive runs. The fluorescence values were then normalized to protein content.

In cell culture

MMP was measured using the fluorescence dye R123. DBC were incubated in an incubator (37 $^{\circ}$C, 5 % CO_2) for 15 min with 0.4 μM R123. Afterwards, the reaction was stopped by adding HBSS into the wells. DBC were centrifuged (1500 rpm, 5 min, room temperature), the medium was aspirated and DBC were supplemented with new HBSS. MMP was assessed by reading the R123 fluorescence at an excitation wavelength of 490 nm and an emission wavelength of 535 nm (Victor X3 multilabel counter). The fluorescence in each well was read in four consecutive runs.

Measurement of ATP concentrations

The ViaLight Plus bioluminescence kit (Lonza, Walkersville, USA), which is based on the production of light from ATP and luciferin in the presence of luciferase, was employed for assessing ATP concentrations. At the end of the incubation, the 96-well plate was removed from the incubator and allowed to cool to room temperature for 10 min. Thereafter, all wells were incubated with lysis buffer (25 μl for DBC and 50 μl for measurement of cell culture experiments) in the dark for 10 min. In the next step,

the wells were incubated for 5 min with monitoring reagent (50 µl for DBC and 100 µl for measurement of cell culture experiments). The emitted light (bioluminescence), which is linearly related to ATP con- centration, was recorded using a luminometer (Victor X3 multilabel counter). The ATP concentrations in the wells were determined using a standard curve; ATP concentrations of DBC were additionally normalized to protein content.

Respirometry measurements

To analyze mitochondrial respiration, an Oxygraph-2k system (Oroboros Instruments, Innsbruck, Austria) was used. Before starting the measurement, 2.4 ml of MIR05 (preheated to 37 °C) was filled into the two chambers of the Oxygraph and allowed to equilibrate for approximately 30 min.

Isolated mitochondria

The schematic view of a measurement protocol is depicted in figure 2.1, a representative example of a measurement at the Oxygraph-2k is shown in figure 2.2. After signal stabilization, isolated mitochondria (80 µl) were added directly into the chamber and the oxygen signal was allowed to equilibrate. Complex I substrates pyruvate [5 mM and malate [2 mM] were added (leak respiration in the absence of ADP, leak (P/M)). Afterwards, adding ADP [2 mM] resulted in complex I respiration (CI). Addition of the complex II substrate succinate [10 mM] lead to maximal physiological respiration (CI+CII). Afterwards, addition of cytochrome c [10 mM] served as quality control for mitochondrial integrity. Thereafter, oligomycin [2 µg/ml] inhibited complex V respiration (leak respiration, leak (omy)), before FCCP [steps of 0.5 µM] was used to uncouple respiration (ETS). After uncoupling, rotenon [0.5 µM] was added to inhibit complex I (CII$_{ETS}$) before antimycin A [2.5 µM] inhibited complex III to unveil residual oxygen consumption (ROX). TMPD [0.5 mM], an artificial complex IV substrate, was added together with ascorbate [2 mM] which was needed to recycle TMPD (complex IV respiration, CIV). In the last step, sodium azide [> 100 mM], a complex IV inhibitor, was added to measure oxygen consumption unrelated to

mitochondrial respiration. ROX was subtracted from all raw data values, respiration after addition of sodium azide was additionally subtracted from complex IV respiration. Mitochondrial integrity was considered to be good if the increase in respiration after addition of cytochrome c did not exceed 10 %. To ensure adequate oxy- gen concentration in the chambers of the Oxygraph-2k during the measurement, chambers were opened from time to time to increase oxygen concentration. Usually chambers were opened after addition of oligomycin, antimycin A and TMPD/ascorbate.

Intact cells

For measurement of whole cell respiration, MIR05 was aspirated and 2.4 ml of a cell suspension containing 1 mio cells/ml was put into the chambers. The oxygen consumption signal was allowed to equilibrate to give endogenous cell respiration. The measurement protocol was identical to that used with isolated mitochondria, with only some minor changes. Cells were permeabilized with digitonin [10 μg/mio cells] after equilibration of endogenous respiration, glutamate [10 mM] was used instead of pyruvate and cytochrome c was left out of the protocol.

<u>Measurement of citrate synthase activity</u>

Isolated mitochondria from brain tissue or cultured cells (1 mio/ml) were frozen in liquid nitrogen and stored at −80 °C before measurement. CS reaction medium (see section 2.1.3) was mixed and the solution was pre-heated to 30 °C for 5 min. 200 μl of cell suspension or 10 μl of isolated mitochondria were added to the reaction medium to give a total volume of 1 ml. Afterwards, the mixture was transferred into a quartz cuvette and CS activity was assessed spectrophotometrically at 412 nm.
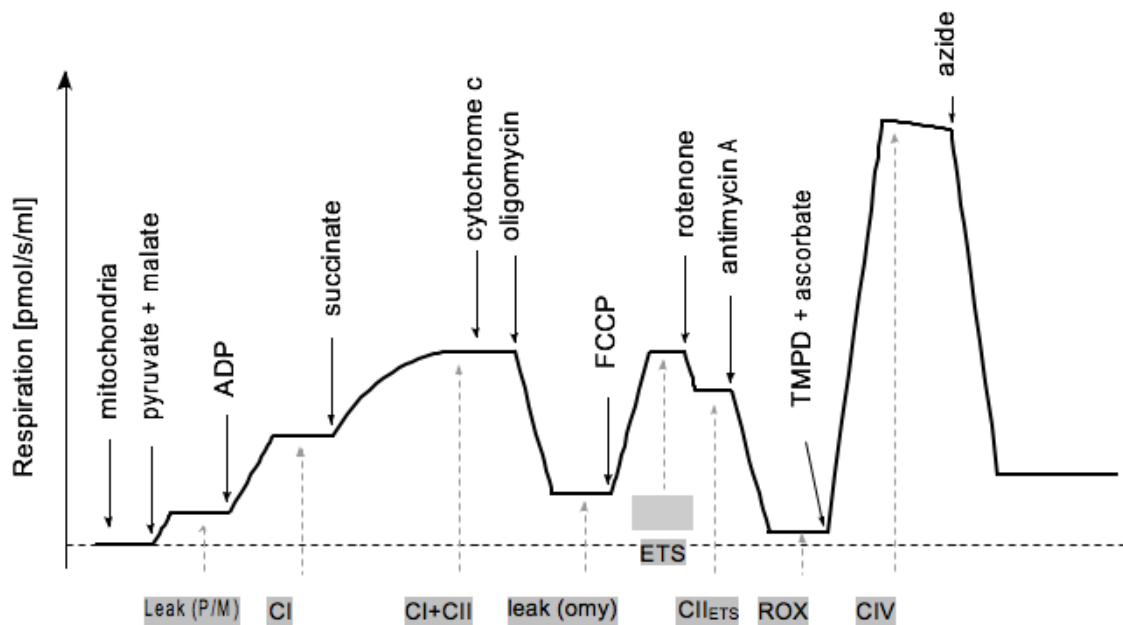
Figure M.1: schematic view of an Oxygraph-2k measurement protocol for isolated mitochondria; substrates and inhibitors of the respiratory system are depicted in black, respiratory states are depicted in the grey boxes; CI: complex I; CII: complex II; ETS: electron transport system, uncoupled respiration; CII_{ETS} : uncoupled complex II respiration; ROX: residual oxygen consumption; CIV: complex IV; modified after (Hagl et al. 2013).
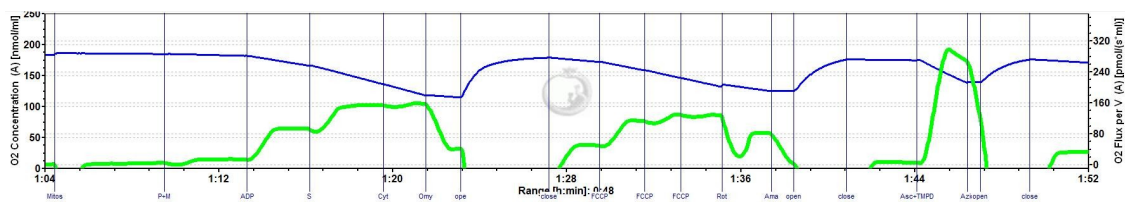
Figure M.2: example of a typical Oxygraph-2k measurement with isolated mitochondria; the oxygen concentration in the Oxygraph chamber is depicted in blue, the oxygen consumption in the Oxygraph chamber is depicted in green; the time scale of the measurement is depicted on the x-axis; Mitos: addition of isolated mitochondria into the chamber; P+M: addition of pyruvate and malate; ADP: addition of ADP; S: addition of succinate; Cyt: addition of cytochrome c; Omy: addition of oligomycin; FCCP: addition of FCCP; Rot: addition of rotenon; Ama: addition of antimycin A; Asc+TMPD: addition of TMPD and ascorbate; Azid: addition of sodium azide; open: chamber was opened to increase oxygen concentration; close: chamber was closed.

Brain homogenate for Western Blot analysis

One 1/8 of a mouse brain (approx. 40 mg) was snap-frozen immediately after harvesting and stored at -80 $^{\circ}$C. After thawing the brain on ice, it was homogenized in 2 ml of lysis buffer in a Potter homogenizer (10 strokes, 800 rpm). Afterwards, protein content of the samples was measured using BCA protein assay and samples were diluted in Tris buffer to obtain protein concentrations of 1 to 1.5 mg/ml.

Gel electrophoresis

Western Blot samples were thawed on ice and homogenized by sonication. Samples were diluted in Tris [20 mM] to adjust protein content to 10 µg or 20 µg. Sample buffer was added at the ratio of 1 : 3, reducing agent at the ratio of 1 : 9. The samples were incubated for 10 min at 95 $^{\circ}$C to disintegrate secondary, tertiary and quaternary structure of the proteins. After spinning them down shortly in a centrifuge, protein samples were loaded into the gels. To assure proper identification of the bands, a protein standard (Precision Plus Protein WesternC Standards, BioRad, Hercules, USA) was added into one pocket of the gel. Pre-cast gels were run at 60 V for 8 min to allow sample assemblage and afterwards at 190 V for 40 min to separate proteins in the gel.

Western Blot

After finishing the gel electrophoresis, proteins were blotted onto a PVDF membrane (30 V, 90 min) using a Blotting system by Invitrogen (Carlsbad, USA). Afterwards, the membranes were blocked for 30 min in a solution of skimmed milk powder (75 mg/ml H_2O).

Antibody incubation

Western Blots were incubated with all primary antibodies on a shaker plate overnight at 4 $^{\circ}$C. The only exceptions were GAPDH which was incubated on a shaker plate at room temperature for 15 min and tubulin which was incubated on a shaker plate at room

temperature for 30 min. Secondary antibodies (see table 2.1) were incubated using the SNAP i.d. device. Blots were washed with 50 ml TBST, incubated with the secondary antibody for 10 min and once again washed with 50 ml TBST.

Lipid peroxidation

Lipid peroxidation was assessed as malondialdehyde (MDA), an end product derived from peroxidation of polyunsaturated fatty acids and related esters present in lipid mem- branes. MDA concentration was measured by a colorimetric reaction using the Colori- metric Lipid Peroxidation Microplate Assay Kit (Oxford Biomedical Research, Oxford, USA). Brain homogenate was incubated for 3 h with either H_2O to measure basal MDA level or $FeCl_2$ [50 µM] to measure MDA level after insult. After the reaction, 200 µl of the reaction mixture were transferred in triplicate into a 96-well plate. Absorbance of the chromophore was measured at 570 nm (ASYS Hitech Digiscan, Eugendorf, Germany).

1,1,3,3-Tetramethoxypropane in Tris-HCl buffer was used as MDA standard.

Confocal laser scanning microscopy

Three days before incubation HEK cells were seeded on 0.1 % gelatin coated cover slips. For morphological analyses, cells were incubated for 4 hours with 25nM Mito Tracker CMXRos and fixed with 4% formalin in phosphate-buffered saline (PBS) (pH7.4, 37°C) for 20 min at RT and washed 3 times with PBS. The samples were embedded in Mowiol containing 2.5 % DABCO and analyzed with the confocal laser scan microscope TCS SP5 from Leica, Germany. For analyses of mitochondrial morphology and density, Image J 1.43u (National Institutes of Health, USA) was used.

Animal studies

Female mice at the age 3 months were kept in the animal facility of the Pharmacological Institute. No more than 10 mice were housed in Makrolon cages with stainless steel covers equipped with bedding, paper towels and plastic tubes. In the

animal rooms, standard conditions (room temperature: 22 °C, air moisture: 55 %, 12h light-dark cycle) were applied. During the study in which Olesoxim, corresponding to about a 100mg/kg dose using oral gavage, was administered via a pelletized diet or Placebo-loaded food pellets, animal had free access to these pellets and water. During the three month study period, animals were checked daily to assure proper health and they were weighed once a week to monitor food intake. The protocols for the animal feeding study and tissue collection were approved by the local authorities for animal welfare and all experiments were carried out according to the European Communities Council Directive (86/609/EEC) by individuals with appropriate training. Mice were sacrificed by cervical dislocation and decapitation. Blood was centrifuged in heparinized vials at 3000 rpm. The obtained plasma samples were immediately frozen at −80 °C for further experiments. The brain was quickly dissected on ice after removal of the cerebellum and brain stem.

Table M.4: group names, genotype and substances applied to Thy1-APPSL mice during the feeding study; test substances were contained in the pelleted diet while control group animals received pelleted diet without addition.

group name	genotype	number	diet
wt	wildtype	8	placebo pellets
wt TRO	wildtype	11	TRO pellets
tg	transgenic	7	placebo pellets
tg TRO	transgenic	10	TRO pellets

Study schedule

- Dissociated brain cells (DBC)
  - MMP
    - 3 hrs stimulation with Rot 50µM
  - ATP
    - 1,5 hrs stimulation with Rot 25nM
  - LPO
    - 4 hrs stimulation with Fe^{2+} 50µM

- Respirometric analysis
- CS activity

- Aß-level

- Western Blots

- Body weight (once a week)

- Plasma levels of TRO19622
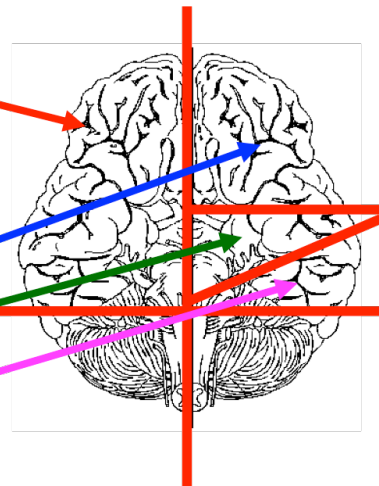
Results

<u>Characterization of a cellular model for LOAD</u>

A HEK cell line, stably transfected with the Swedish APP double mutation (HEKsw) and un-transfected control cells (HEKut) have been used to study the effects of Aβ overproduction on mitochondrial function and to examine the effects of Dimebon and Olesoxim.

HEKsw cells produce high amounts of Aβ and thus served as a model for the detrimental effects of intracellular generated Aβ on mitochondrial function, mirroring the situation in AD brain (Keil et al. 2005; Leuner et al. 2012b). In turn HEKut cells were described to mirror healthy conditions (Keil et al. 2005; Leuner et al. 2012b). Both cell lines, HEKsw and HEKut, are well established in our group (Keil et al. 2004; Peters et al. 2009a; Kurz et al. 2010; Pohland et al. 2016). The following experiments were conducted with the aim to expand the method portfolio, especially regarding the correlation between the mitochondrial form and function.

A

	Digitonin	Glutamat/Malat	ADP	Succinat	Oligomycin	FCCP	Rotenon	Antimycin A	Ascorbat/TMPD
Digitonin	+								
Glutamat/Malat		+							
ADP			+						
Succinat				+					
Oligomycin					+				
FCCP						+			
Rotenon							+		
Antimycin A								+	
Ascorbat/TMPD									+

B

HEK$_{ut}$

C

HEK$_{sw}$
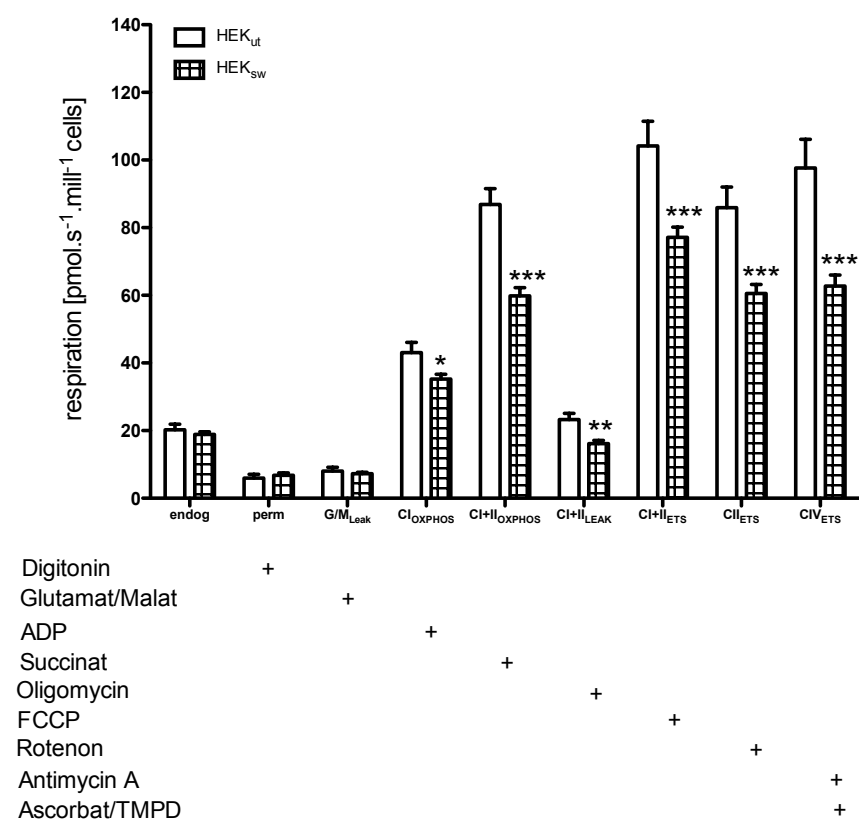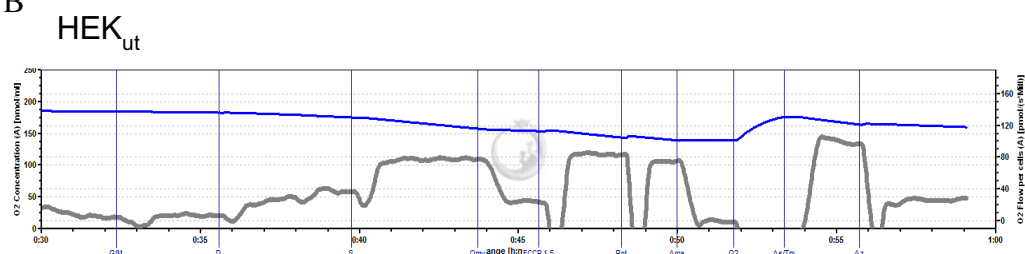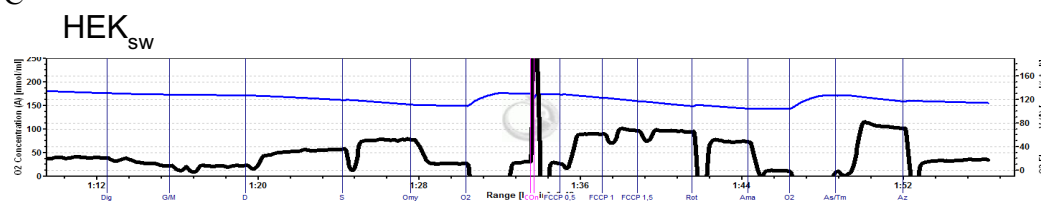
Figure 1. Mitochondrial respiration. Oxygen consumption was measured using a clark – electrode (Oxygraph-2k, Oroboros, Innsbruck, Austria). (**A**) Respiration was measured in different mitochondrial stages after injection of several substrates and inhibitors. Endogen respiration was determined after injecting the samples (endog) into the chambers. Digitonin was used for permeabilizing the cell membranes (perm). Glutamat and Malat supplementation served as complex I substrates (G/M$_{Leak}$). Due to the lack of ADP this

experimental stage was still leaky; ADP was the driving force to initiate the electron transport chain to build the proton gradient among the inner mitochondrial membrane. ADP injection fulfilled the demands for CI dependent oxidative phosphorylation (CI_{OXPHOS}) (OXPHOS stands for oxidative phosphorylation). Adding succinat, finally provided a CII substrate and enables CI+II oxidative phosphorylation ($CI+II_{OXPHOS}$). By adding oligomycin, the ATP synthase, (complex V), was inhibited, making it possible to detect the respiratory capacity on CI+II substrates to compensate for proton leak ($CI+II_{Leak}$) through the membrane. Using stepwise injection of FCCP, which is a ionophor that uncouples the respiratory chain, non-coupled respiration with CI and CII substrates ($CI+II_{ETS}$) was measured, which is considered as maximum capacity of the ETS (ETS stands for electron transport system). Rotenon was inhibiting complex I, hence non-coupled CII respiration (CII_{ETS}) was detected. Antimycin A was blocking the electron transport chain, by inhibiting Cytochrom C, thus electrons could not be transferred from complex III to complex IV. By supplementation of CIV substrates Ascorbat/TMPD, non-coupled respiration of complex IV was accessible (CIV_{ETS}). Values represent the means $\pm$ SEM from n = 6-9 experiments per protocol, data represent two protocols, Two-way ANOVA with Bonferroni posttests, *$p<0.05$, **$p<0.01$, ***$p<0.001$. Representative graphs of oxygen consumption measurements in (**B**) HEKut (grey) and (**C**) in HEKsw cells (black). Total oxygen concentration is indicated as blue line.

Compared to HEKut cells, HEKsw cells showed an overall reduction in the mitochondrial respiration (Figure 1). Oxidative phosphorylation capacity was significantly diminished, as well as the capacity of CIV and the electron transfer system in the non-coupled state. In nearly all test settings the reduction showed values between 20 % to 30 %, except for CI which maintained the oxidative phosphorylation (CI_{OXPHOS}).

In general, mitochondrial respiration is the driving force to build up a proton gradient across the inner mitochondrial membrane, leading to an enhanced mitochondrial membrane potential (MMP)(Nijtmans et al. 2004).
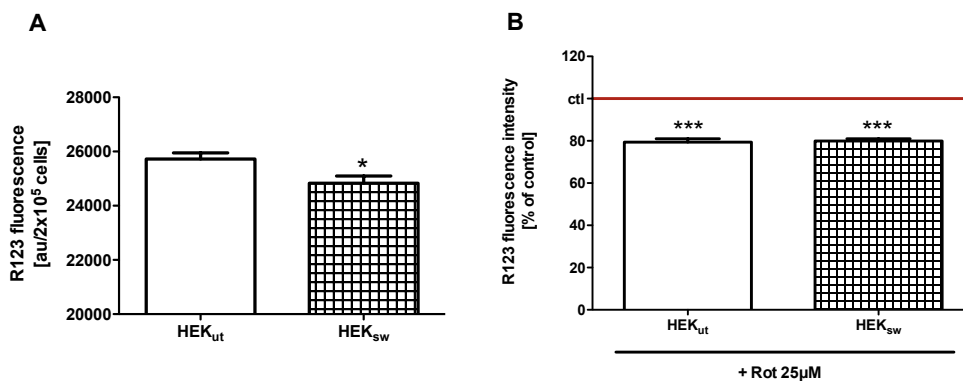
Figure 2. Mitochondrial membrane potential (MMP). (**A**) Basal MMP was measured using the fluorescence dye Rhodamin 123 (R123) in $2x10^4$ HEK-cells, harboring the Swedish mutation in the APP gene (HEKsw) or in controls (HEKut) as described in material &

methods. (**B**) MMP after rotenon insult. Cells were incubated with 25 µM rotenon and MMP was measured after 6 hours. Results were normalized to untreated HEKsw- and HEKut-cells (ctl = 100%), respectively. Data represent the means ± SEM; n=6 independent experiments; p*<0,05, p***<0,001; Student`s t-test.

HEKsw cells showed a significant lower MMP compared to control cells (Figure 2). Thus, the dysfunctional respiratory chain in HEKsw (Figure 1 A) resulted in a reduced MMP. ATP levels were measured, since the MMP provides the power for complex V that finally generates ATP. Rotenon has an equal effect in both cell lines, regarding MMP measurements (Figure 2 B).
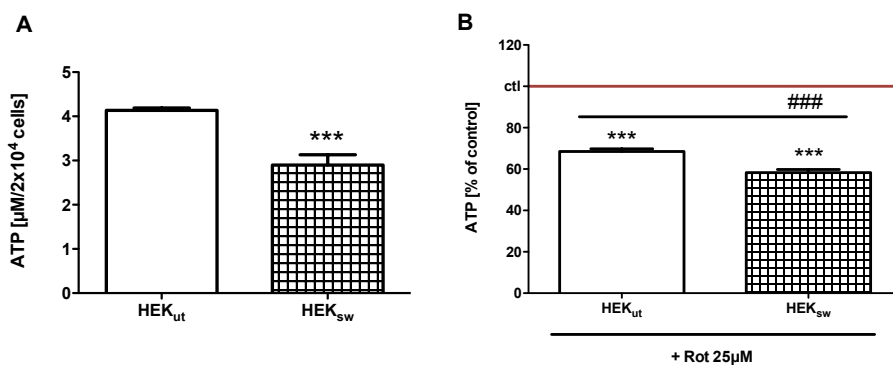
Figure 3. Adenosine triphosphate (ATP) levels. (**A**) Basal ATP levels were determined using a luminescence kit in 2×10^4 HEK-cells, harboring the Swedish mutation in the APP gene (HEKsw) or in controls (HEKut) as described in material & methods. N=6 independent experiments; (**B**) ATP levels after rotenon insult. Cells were incubated with 25 µM rotenon and ATP levels were determined after 6 hours. Results were normalized to untreated HEKsw- and HEKut-cells (ctl = 100%), respectively. N=6-12 independent experiments; Data represent the means ± SEM; p***<0,001 vs. ctl; p[###]<0,001 HEKsw + Rot 25 µM vs. HEKut + Rot 25 µM. Student`s t-test.

HEKsw cells have significantly reduced ATP levels (Figure 3A). In addition, these cells react more vulnerable in response to rotenon mediated complex I inhibition (Figure 3B).

To establish, whether the detected dysfunctional parameters (OXPHOS, MMP, ATP) were related to deficient mitochondria itself, or are merely due to a loss of mitochondrial mass, the citrate synthase (CS) activity was measured. As part of the Krebs-cycle CS is constantly expressed in mitochondria. Thus, CS activity is highly correlated with mitochondrial mass and represents a reliable marker (Larsen et al. 2012).
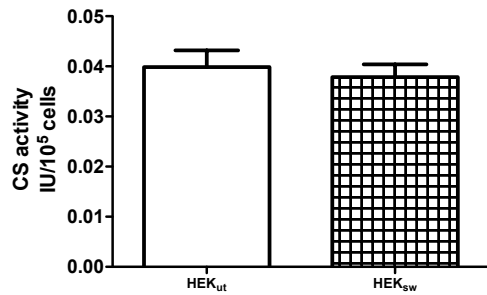
Figure 4. Citrate synthase (CS) activity. Enzyme activity was determined in HEK-cells harboring the Swedish mutation in the APP gene (HEKsw) or in controls (HEKut) using a spectrophotometric method at 412nm and 30°C as described in material & methods. Data represent the means ± SEM, n = 6, each experiment was measured as duplet.

CS activity is not altered in HEKsw cells (Figure 4). Thus, it can be concluded that mitochondrial mass is equal in both cell lines.

Since mitochondrial mass is unchaged in HEKsw cells, the underlying processes for the mitochondrial dysfunction were further investigated. Beside impaired function of mitochondrial respiratory chain complexes, mitochondrial dysfunction includes deficits of mitochondrial dynamics, such as impaired balance between fission and fusion mechanisms, abnormal shaping of mitochondria, and reduced mitochondrial trafficking.
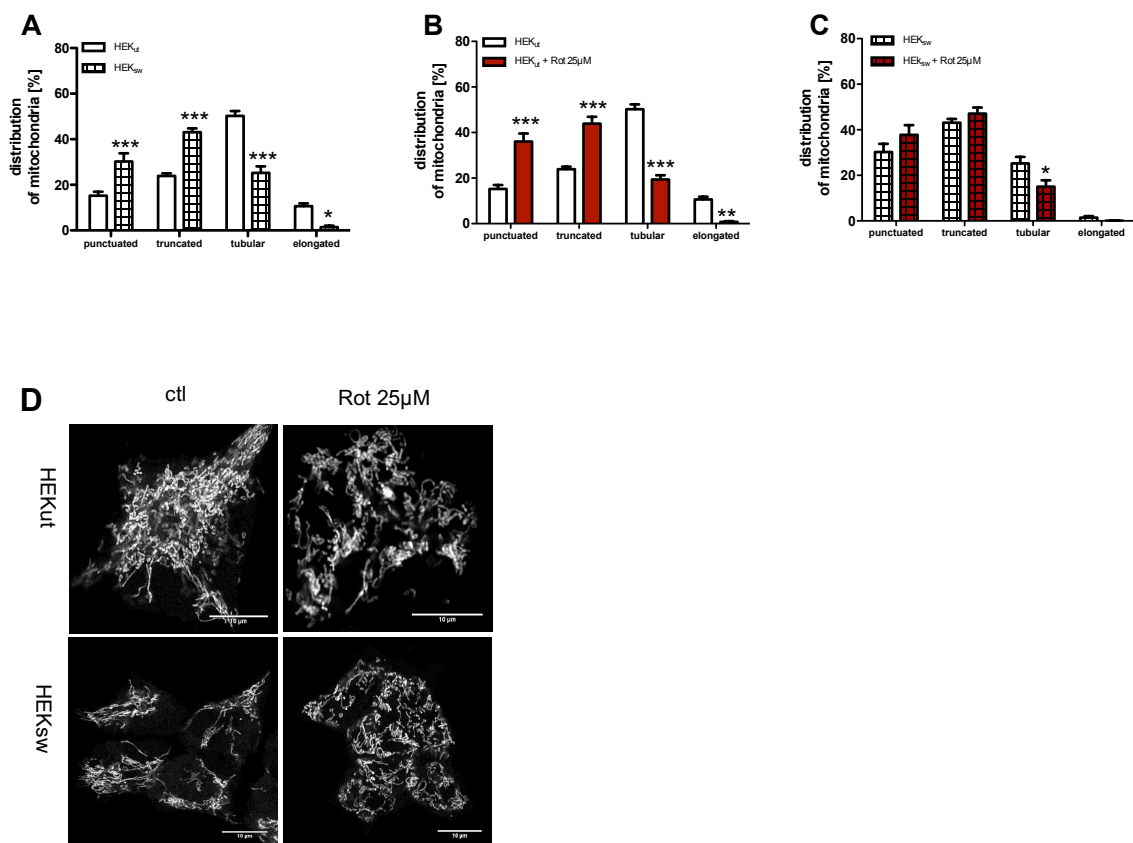
Figure 5. Morphological changes of mitochondria. Using the fluorescence marker Mito Tracker CMXRos, mitochondria were labeled in HEK controls (HEKut) or in HEK cells harboring the Swedish mutation in the APP gene (HEKsw) (**A**) under basal conditions or after 6 hours incubation with 25 µM rotenon in (**B**) HEK controls or in (**C**) HEKsw cells. (**D**) Representative images of HEKut and HEKsw cells in the absence and presence of rotenon, respectively. After fixation with PFA, cells were examined using confocal laser-scanning microscopy. Mitochondrial lengths were quantified with Image J and classified as punctuated, truncated, tubular, and elongated. Data represent the means ± SEM with at least 100 measured mitochondria per experiment, n = 8-9, Two-way ANOVA with Bonferroni posttests, $*p < 0.05$, $**p < 0.01$, $***p < 0.001$.

To characterize changes in mitochondrial morphology a novel methodology to categorize mitochondrial shape was introduced. Mitochondria were classified by assigning mitochondrial lengths into 4 groups: punctuated (<2um), truncated (2-4um), tubular (4-10um) and elongated (>10um). Substantial differences between controls and HEKsw cells were detected (Fig 5 A), supporting previous findings about pronounced effects of Aβ on mitochondrial dynamics (Eckert et al. 2012b). In control cells the tubular shape represented the largest fraction, followed by truncated mitochondria. Additionally, there were minor fractions of punctuated and elongated mitochondria (Figure 5 A). This pattern is completely opposite in HEK$_{sw}$ cells,

most mitochondria showed truncated morphology, followed by punctuated mitochondria. The amount of tubular shaped mitochondria was divided in half and the elongated shape nearly disappeared (Figure 5 A). After induction of complex I dysfunction with rotenon, HEKut cells were highly fragmented. The distribution shifted completely to shorter mitochondria, comparable to the pattern in HEKsw cells (Figure 5 B). Since mitochondria in HEKsw cells almost did not change their form after inducing complex I dysfunction, they seemed to be already maximal stressed (Figure 5 C).
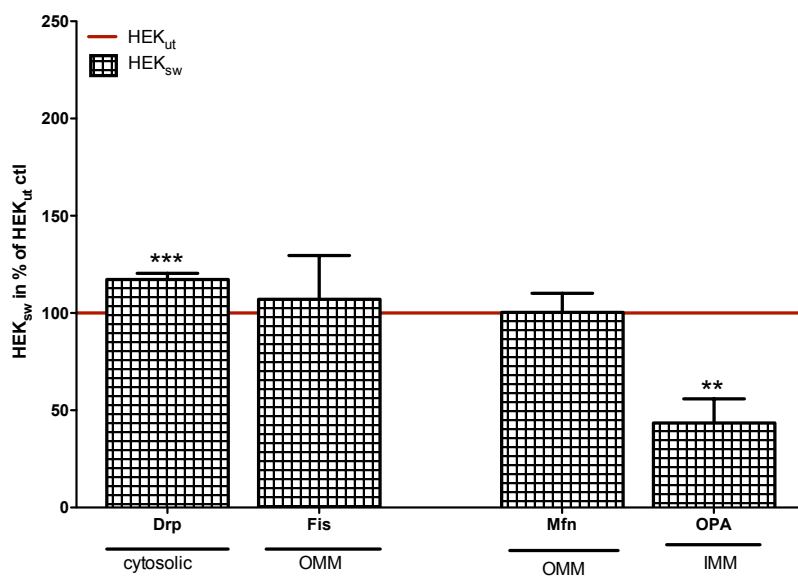
Figure 6. Mitochondrial Fission & Fusion proteins. In HEK-cells harboring the Swedish mutation in the APP gene (HEKsw) and in controls (HEKut), marker proteins for fission dynamin related protein1 (Drp) and fission 1 related protein (Fis) as well as markers for fusion were measured, using western blot analysis after electrophoretic separation and using specific antibodies in the total cellular homogenates. Data were normalized to HEKut (100%) and represent the means ± SEM, n = 8-9, Two-way ANOVA with Bonferroni post-tests, **p<0,01, ***p<0,001. Representative Western Blots, see figure 20 C.

Fission dynamin related protein1 (Drp) and fission 1 related protein (Fis) are marker proteins for mitochondrial fission. Protein levels of Fis were unchanged, whereas Drp levels were significantly elevated in HEKsw cells (Figure 8). Mitochondrial fusion protein 1 (Mfn) and optic atrophie-1 (Opa) protein are markers for mitochondrial fusion. Mfn levels were unchanged, whereas protein levels of OPA were strongly reduced (Figure 8). Both changes led to the shift in the distribution pattern towards shorter mitochondria (see figure 5).

To further examine the dynamic machinery mitochondrial densities were determined.
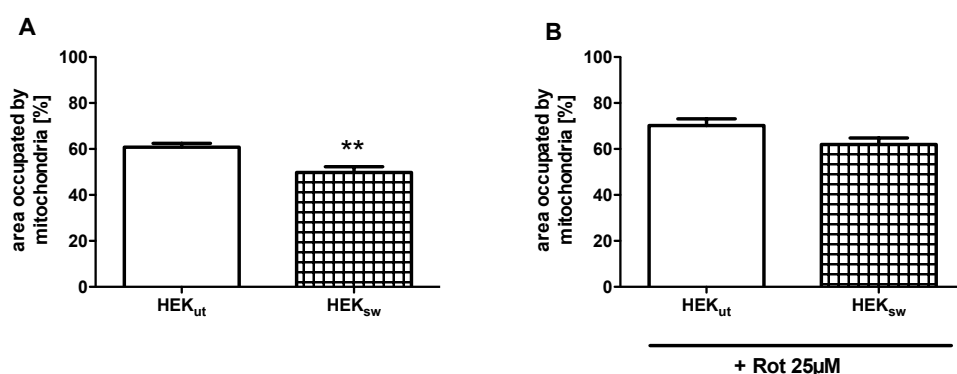
Figure 7. Mitochondrial density. (**A**) Mitochondria were labeled in HEK-cells harboring the Swedish mutation in the APP gene (HEKsw) or in controls (HEKut) using the fluorescence marker Mito Tracker CMXRos. Following fixation with PFA, cells were examined using confocal laser-scanning microscopy. Mitochondrial densities were quantified, based on fluorescence intensities with Image J and expressed as area occupied by mitochondria (%). Compared to HEKut cells, HEKsw cells have impaired mitochondrial density. (**B**) The same procedure was followed after 6 hours incubation with 25 µM rotenon. Data represent the means ± SEM with at least 100 measured mitochondria per experiment, n = 4-10, p**<0,01 Student`s t-test.

HEKsw cells showed reduced mitochondrial density (Figure 7 A), which could be referred to an altered inner mitochondrial membrane, as well as the to the fact that the dye Mito Tracker CMXRos attaches voltage dependently to the inner mitochondrial membrane. Thus, the reduced MMP in HEKsw cells (Figure 2), could have contributed to a lower dye load, that in turn would have led to lower measures of density.

Aforementioned mitochondrial parameters are related to the inner mitochondrial membrane (Eckmann et al. 2013). To clarify the impact of mitochondrial membranes on impaired functionality and/or lower density, appropriate markers were measured.
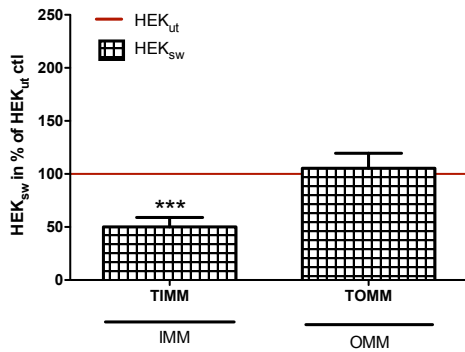
Figure 8. Mitochondrial membrane markers. In HEK-cells harboring the Swedish mutation in the APP gene (HEKsw) and in controls (HEKut), marker proteins for the inner (IMM) and the outer mitochondrial membrane (OMM) were measured in total homogenates, using western blot analysis after electrophoretic separation and using specific antibodies against translocator proteins of the inner (TIMM50) and outer (TOMM22) mitochondrial membrane in total cellular homogenates. Data were normalized to HEKut (100%) and represent the means $\pm$ SEM, n = 8-9, Two-way ANOVA with Bonferroni post-tests, ***p<0,001. Representative Western Blots, see figure 21 C.

Protein levels of the translocase of the outer mitochondrial membrane (TOMM22) were not altered in HEKsw cells. On the other side, protein levels of the translocase of the inner mitochondrial membrane (TIMM50) are strongly diminished in HEKsw cells (Figure 8). In the inner membrane the OXPHOS machinery builds up the MMP, which represents the driving force for the generation of ATP. Depending on the MMP, Mito Tracker CMXRos attaches to the inner mitochondrial membrane and enables the visualization of mitochondria's morphology. Thus, a deficient inner mitochondrial membrane perfectly matches the data presented so far: Reduced TIMM50 level in HEKsw indicate less inner mitochondrial membrane, which could explaine the described deficits in OXPHOS (Figure 1), MMP (Figure 2), ATP (Figure 3), mitochondrial morphology (Figures 5&6) and density (Figure 7).

To evaluate the observed changes in mitochondrial length (Figure 5) in more detail, protein levels of the fission & fusion machinery, as well as markers for mitophagy and swelling were measured. Fragmented mitochondria could either enforce autophagosomal activity or enhance apoptosis (Griparic et al. 2004).
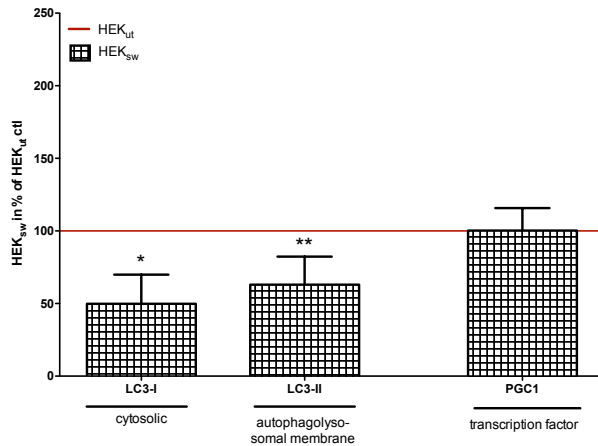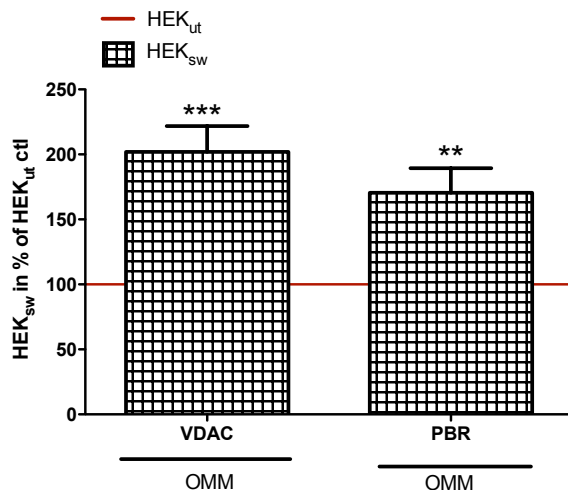
Figure 9. Autophagy marker proteins. In HEK-cells harboring the Swedish mutation in the APP gene (HEKsw) and in controls (HEKut), autophagy marker proteins for the cytosol (LC3-I) and autophagosomal membranes (LC3-II), as well as the transcription marker peroxisome proliferation-activated receptor gamma coactivator 1-alpha (PGC1) were measured using western blot analysis after electrophoretic separation and using specific antibodies in total cellular homogenates. Data were normalized to HEKut (100%) and represent the means ± SEM, n = 8-9, Two-way ANOVA with Bonferroni post-tests, *$p<0,05$, **$p<0,01$. Representative Western Blots, see figure 22 E.

Peroxisome proliferation-activated receptor gamma coactivator 1-alpha (PGC1) represents a transcription factor. PGC1 as a master regulator of mitochondrial biogenesis (Liang and Ward 2006; Wareski et al. 2009) was not altered, which is in line with equal levels of CS in both cell lines (Figure 4). Both LC3-Isoforms, the cytosolic and the autophagosomal form were reduced in HEKsw, which indicate enhanced mitophagic activity (Figure 9). This finding is further supported by a reduced ratio of the LC3- isoforms (Mizushima and Yoshimori 2007), which gives information about the autophagosomal activity (Figure 10). Unchanged PGC1 levels may indicate constant mitochondrial biogenesis, which could explain the equal mitochondrial mass, as detected in both analysed cell lines (Figure 4).

Fragmented mitochondria (figure 5) may induce apoptosis after formation and opening of the mitochondrial transition pore (mPTP).
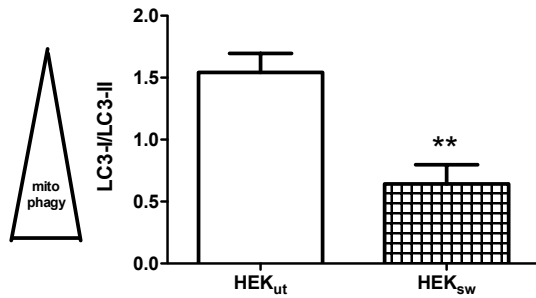
Figure 10. Autophagic activity. In HEK-cells harboring the Swedish mutation in the APP gene (HEKsw) and in controls (HEKut), autophagy marker proteins for the cytosol (LC3-I) and autophagosomal membranes (LC3-II) were measured, using western blot analysis after electrophoretic separation and using specific antibodies in total cellular homogenates (see Figure 9). A low LC3-I/LC3-II ratio indicates a high degree of mitophagy. Data were normalized to HEKut (100%) and represent the means ± SEM, n = 8-9, Two-way ANOVA with Bonferroni post-tests, **p<0,01.

Figure 11. Mitochondrial permeability transition pore (mPTP). In HEK-cells harboring the Swedish mutation in the APP gene (HEKsw) and in controls (HEKut), the mPTP marker proteins, voltage-depended anion channel (VDAC) and peripheral benzodiazepine receptor (PBR), were measured using western blot analysis after electrophoretic separation and using specific antibodies in total cellular homogenates. Both marker proteins are located in the outer mitochondrial membrane (OMM). Data were normalized to HEKut (100%) and represent the means ± SEM, n = 8-9, Two-way ANOVA with Bonferroni post-tests, **p<0,01, ***p<0,001. Representative Western Blots, see figure 23 C.

Both mPTP markers, the voltage-depended anion channel (VDAC) and the peripheral benzodiazepine receptor (PBR) were broadly increased in HEKsw cells (Figure 11). The turnover of mitochondria in HEKsw seemed to be elevated, since they exhibit higher mitophagic processes (Figure 9&10) and in the same time, seemed to be involved in apoptotic processes (Figure 11).

**Effects of Dimebon in a cellular model for LOAD**

Dimebon is an unselective H1-receptor antagonist, that was used as antiallergic drug in Russia (Bachurin et al. 2001; Sachdeva and Burns 2011). Nowadays, Dimebon attracts interest in the AD field, especially since it was reported to improve mitochondrial function in human neuroblastoma cells and primary rat cortical neurons (Zhang et al. 2010).

The pharmacological effects of Dimebon on mitochondria related parameters (respiration, ATP levels, MMP, oxidative stress, citrate synthase activity, fusion & fission and autophagy) were assessed in HEK-cells harboring the Swedish mutation in the APP gene (HEKsw), which represents an established model of LOAD (please refer to 1.1) and in untransfected control cells (HEKut). Therefore, a concentration of 0,1 µM was used, which is above the brain levels of Dimebon in treated TgCRND8 mice(810 pmol/mg brain) (Wang et al. 2011), but much lower than the concentrations used in other in vitro investigations (Bachurin et al. 2001; Lermontova et al. 2001).
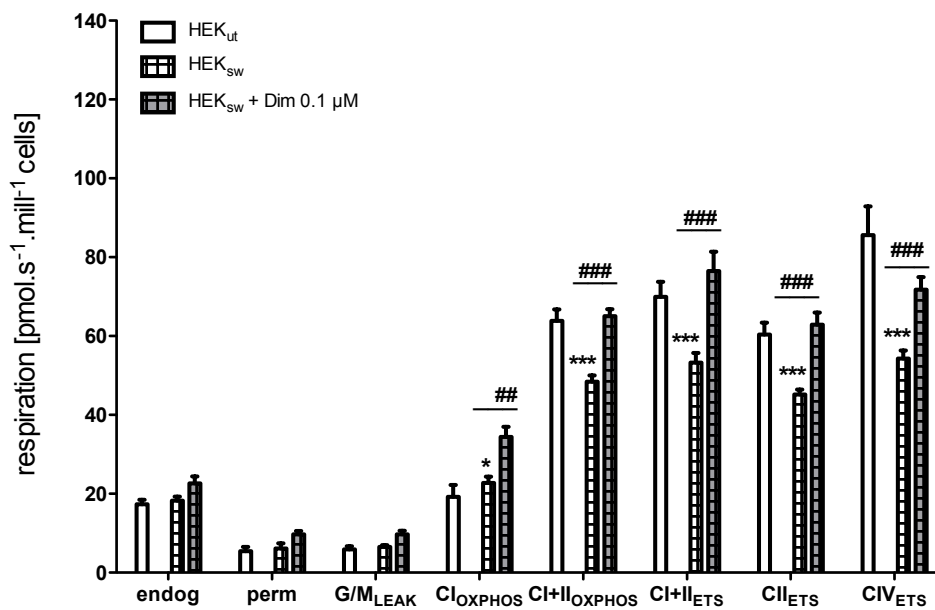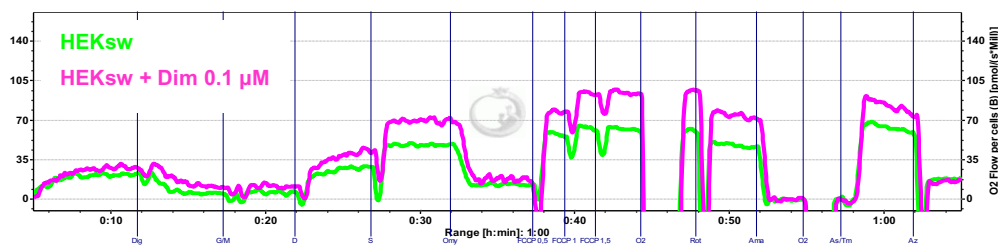
A
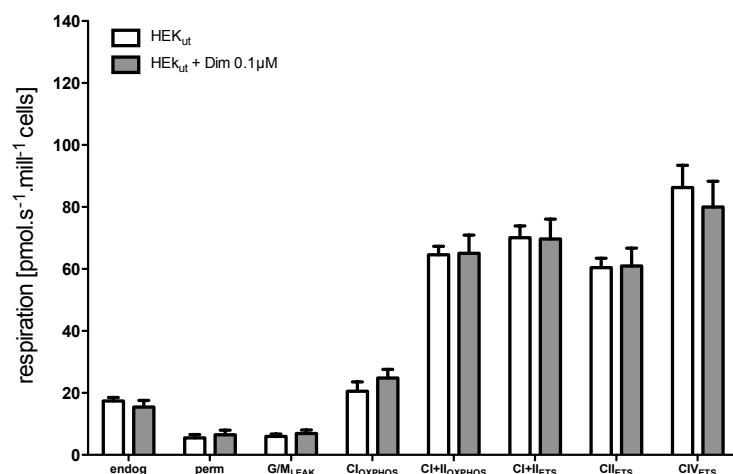
B
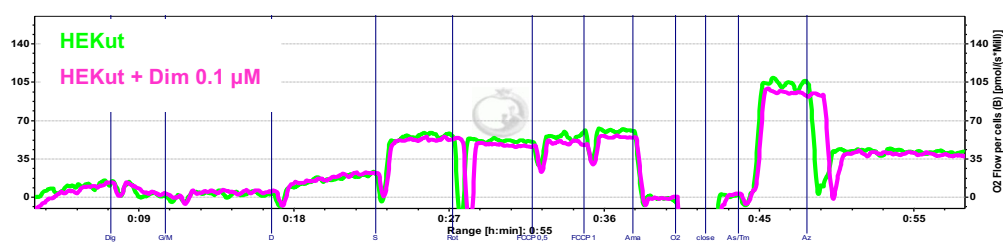
Figure 12. Effects of Dimebon on mitochondrial respiration in HEKut cells. Cells were incubated with 0,1 µM Dimebon for 6 hours. Oxygen consumption was measured using an Oxygraph-2k. Respiration was measured in different mitochondrial stages after injecting several substrates and inhibitors (please refer to material & methods). (**A**) Endogen respiration was determined after injecting the samples (endog) into the chambers. Digitonin was used for permeabilizing the cell membranes (perm). Glutamat and Malat supplementation served as complex I substrates (G/M_{Leak}). Due to the lack of ADP this experimental stage ws still leaky; ADP was the driving force to initiate the electron transport chain to build the proton gradient among the inner mitochondrial membrane. ADP injection fulfilled the demands for CI dependent oxidative phosphorylation (CI_{OXPHOS}) (OXPHOS stands for oxidative phosphorylation). Adding succinat finally provided a CII substrate and enabled CI+II oxidative phosphorylation ($CI+II_{OXPHOS}$). Using stepwise injection of FCCP, a ionophor that uncouples the respiratory chain, non-coupled respiration with CI and CII substrates ($CI+II_{ETS}$) was measured, which was considered as maximum capacity of the ETS (ETS stands for electron transport system). Rotenon was inhibiting complex I, making it possible to detect non-coupled CII respiration (CII_{ETS}). Antimycin A was blocking the electron transport chain by inhibiting Cytochrom C, thus electrons could not be transferred from complex III to complex IV. By supplementation of CIV substrates Ascorbat/TMPD, non-coupled respiration of complex IV was accessible (CIV_{ETS}). Values represent the means ± SEM from n = 8 independent experiments. (**B**) Representative graphs of oxygen consumption measurements in HEKut (pink) and HEKut + Dim 0,1 µM (green).

A

Figure 13. Effects of Dimebon on mitochondrial respiration in HEKsw cells. Cells were incubated with 0,1 μM Dimebon (Dim) for 6 hours. Oxygen consumption was measured using an Oxygraph-2k. Respiration was followed in different mitochondrial stages after injecting several substrates and inhibitors (please refer to material & methods). (**A**) Endogen respiration was determined after injecting the samples (endog) into the chambers. Digitonin was used for permeabilizing the cell membranes (perm). Glutamat and Malat supplementation served as complex I substrates (G/M$_{Leak}$). Due to the lack of ADP this experimental stage was still leaky; ADP was the driving force to initiate the electron transport chain to build the proton gradient among the inner mitochondrial membrane. ADP injection fulfilled the demands for CI dependent oxidative phosphorylation (CI$_{OXPHOS}$) (OXPHOS stands for oxidative phosphorylation). Adding succinat finally provided a CII substrate and enabled CI+II oxidative phosphorylation (CI+II$_{OXPHOS}$). Using stepwise injection of FCCP, a ionophor that uncouples the respiratory chain, non-coupled respiration with CI and CII substrates (CI+II$_{ETS}$) was measured, which was considered as maximum capacity of the ETS (ETS stands for electron transport system). Rotenon was inhibiting complex I, making it possible to detect non-coupled CII respiration (CII$_{ETS}$). Antimycin A was blocking the electron transport chain by inhibiting Cytochrom C, thus electrons could not be transferred from complex III to complex IV. By supplementation of CIV substrates Ascorbat/TMPD, non-coupled respiration of complex IV was accessible (CIV$_{ETS}$). Values represent the means ± SEM from n = 8 independent experiments. Values represent the means ± SEM from n = 6-9

independent experiments. Two-way ANOVA with Bonferroni posttests, *p<0.05, ***p<0.001 HEKsw vs. HEKut; ##p<0,01, ###p<0,001 HEKsw vs. HEKsw + Dim 0,1 µM. (**B**) Representative graphs of oxygen consumption measurements in HEK_{sw} (pink) and HEKsw + Dim 0,1 µM (green).

Firstly, effects of Dimebon on mitochondrial respiration were assessed. Dimebon had no effect on the respiratory capacity in HEKut cells (Figure 12). On the other hand, incubation of HEKsw cells with Dimebon induced a remarkable increase in respiratory activity (Figure 13). Dimebon enhanced CI_{OXPHOS} activity and normalized all measured mitochondrial parameters in HEKsw cells almost to control levels (Figure 13).
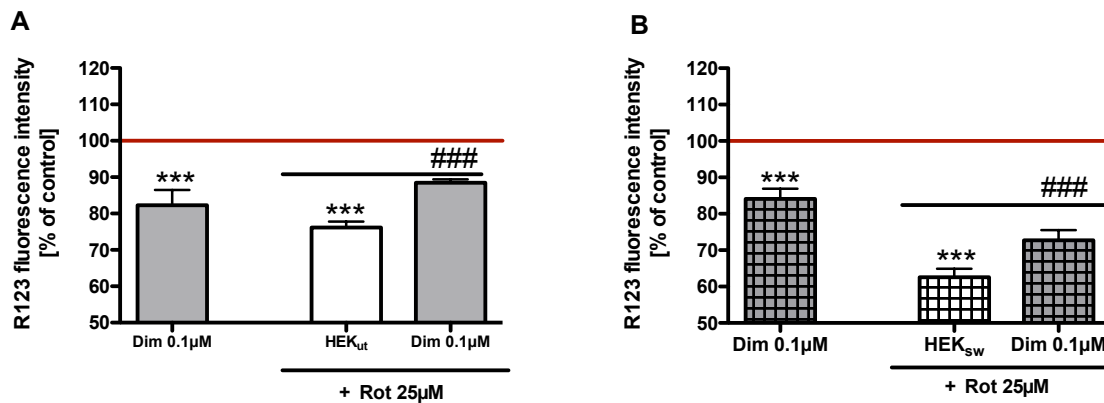

Figure 14. Effects of Dimebon on mitochondrial membrane potential (MMP). Cells were pre-incubated with 0,1 µM Dimebon (Dim) for 1 hour, afterwards cells were challenged using 25 µM rotenon for 6 hours. MMP was measured, using the fluorescence dye Rhodamin 123 (R123) in $2x10^5$ HEK-cells (**B**) harboring the Swedish mutation in the APP gene (HEKsw) or in (**A**) controls (HEKut) as described in material & methods. Results were normalized to untreated HEKsw- and HEKut-cells (ctl = 100%), respectively. Data represent the means ± SEM; n=6 independent experiments; p***<0,001 vs. ctl; ###p<0,001 vs. Rot 25 µM challenged ctl; Student`s t-test.

Mitochondrial respiration builds up a membrane potential (MMP) which represents the driving force for ATP production. Under basal conditions, Dimebon decreased the MMP in both, HEKut and HEKsw cells (Figure 14 A&B). On the other hand, preincubation of cells with Dimebon restored the MMP after challanging the cells with rotenon (Figure 14 A&B).
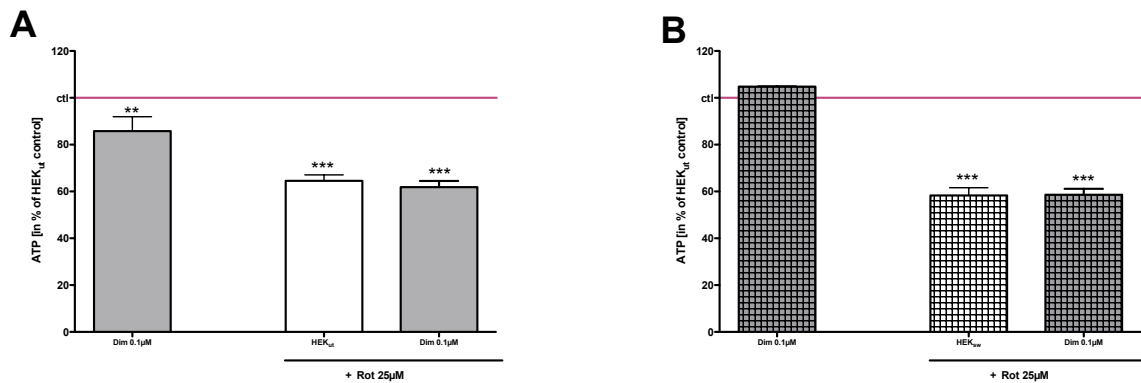
Figure 15. Effects of Dimebon on Adenonsine triphosphate (ATP) levels. Cells were pre-incubated with 0,1 µM Dimebon (Dim) for 1 hour, afterwards cells were challenged, using 25 µM rotenon for 6 hours. ATP levels were determined using a luminescence kit in $2\text{x}10^4$ HEK-cells (**B**) harboring the Swedish mutation in the APP gene (HEKsw) or in (**A**) controls (HEKut) as described in material & methods. Results were normalized to untreated HEKsw- and HEKut-cells (ctl = 100%), respectively. Data represent the means ± SEM; n=4-6 independent experiments; p**<0,01, p***<0,001; Student`s t-test.

Dimebon had no effects on ATP levels, neither under basal conditions, nor after challenging cells with rotenon in both cell lines (Figure 15 A&B).
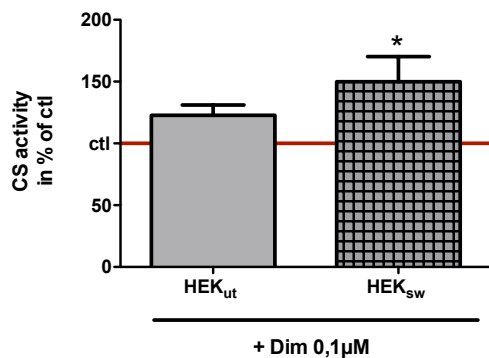

Figure 16. Citrate synthase (CS) activity. Cells were incubated with 0,1 µM Dimebon (Dim) for 6 hours. Enzyme activity was determined in HEK-cells harboring the Swedish mutation in the APP gene (HEKsw) or in controls (HEKut) using a spectrophotometric method at 412nm and 30°C as described in material & methods. Data represent the means ± SEM, n = 6, each experiment was measured as duplet. p*<0,05; Student`s t-test.

Effects on CS activity, a robust marker of mitochondrial mass, were explored during the next step. Dimebon did not interfere with the mitochondrial mass in HEKut cells. CS activity in HEKsw cells was increased by Dimebon (Figure 16). Together with elevated mitochondrial respiratory activity (Figure 12) this increase indicated a higher mitochondrial content. These

83

findings are in line with enlarged area occupied by mitochondria after Dimebon incubation measured, using Confocal Laser Scanning Microscopy, after staining with Mito Tracker CMXRos (Figure 17). A lower mitochondrial density in HEKsw cells was assessed using confocal microscopy and MitoTracker staining (Figure 7). Incubation with Dimebon compensated for this deficiency (Figure 17). Under similar conditions, Dimebon had no effects on mitochondrial density in HEKut cells.
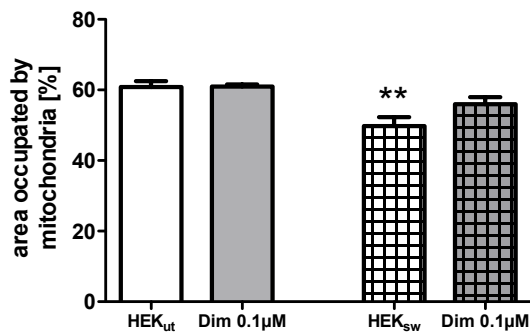
Figure 17. Mitochondrial density. Cells were incubated with Dimebon (0,1 µM) for 6 hours. Mitochondria were labeled in HEK-cells harboring the Swedish mutation in the APP gene (HEKsw) or in controls (HEKut) using the fluorescence marker Mito Tracker CMXRos. Following fixation with PFA, cells were examined using confocal laser-scanning microscopy. Mitochondrial densities were quantified based on fluorescence intensities with Image J and expressed as area occupied by mitochondria (%). Data represent the means ± SEM with at least 100 measured mitochondria per experiment, n = 5-10, **p<0,01, unpaired t-test.
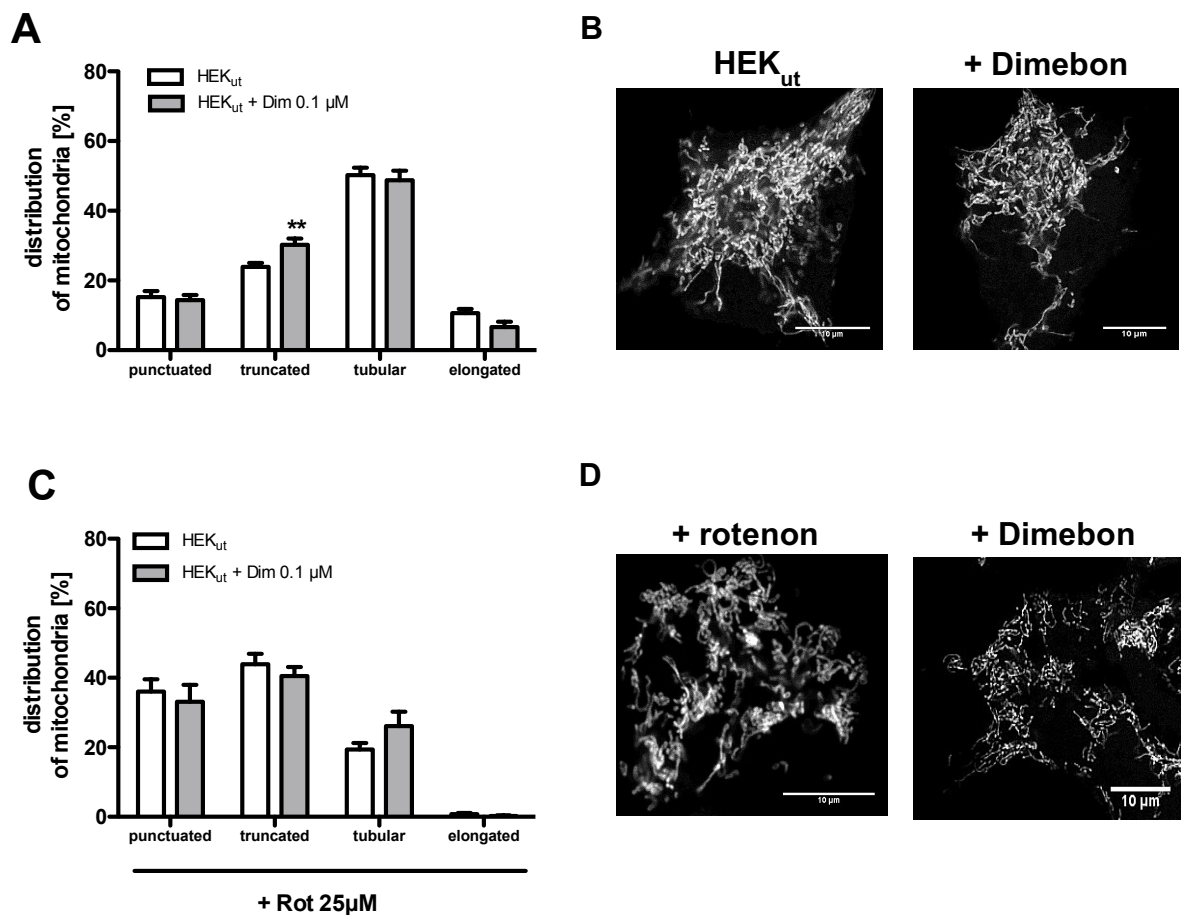
Figure 18. Effects of Dimebon on morphological changes of mitochondria after rotenon insult in HEKut cells. (A) HEKut control cells were incubated for 6 h with Dimebone (0.1 µM). Mitochondria were labelled with Mito Tracker CMXRos, fixed with PFA, and mitochondrial lengths were quantified using Image J. **(B)** Representative images of mitochondria in HEKut cells in the presence and absence of Dimebone. **(C)** HEKut cells were stressed with rotenon (25 µM) for 6 h. Cells were pre-incubated with Dimebone (0.1 µM) for 1 hour to determine possible protective effects. Mitochondria were labeled using Mito Tracker CMXRos, fixed with PFA, and mitochondrial lengths were quantified using Image J. **(D)** Representative images of mitochondria in HEKut cells treated with rotenon in the presence and absence of Dimebone. Data represent the means ± SEM with at least 100 measured mitochondria per experiment, n = 10, Two-way ANOVA with Bonferroni posttests, **$p<0,01$.
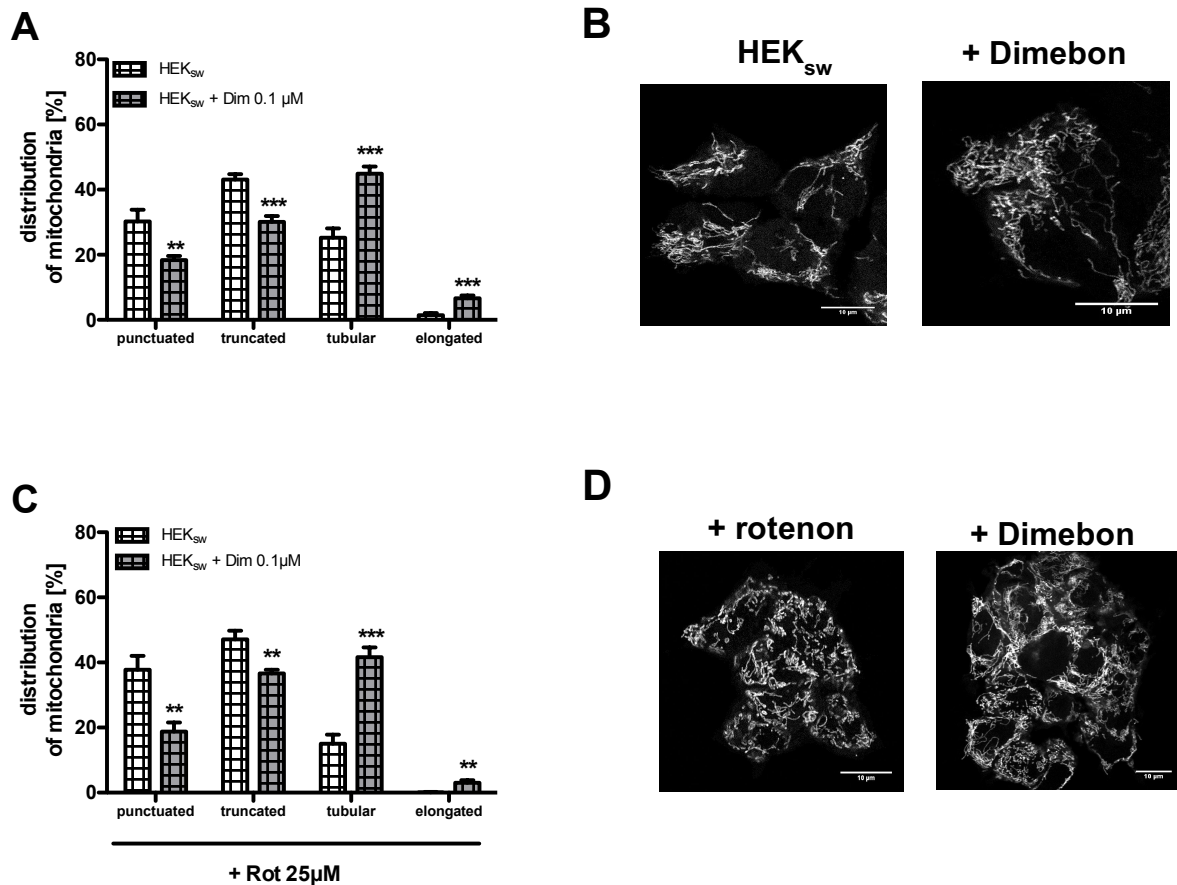
Figure 19. Effects of Dimebon on morphological changes of mitochondria after rotenon insult in HEKsw cells. (A) HEK-cells harboring the Swedish mutation in the APP gene (HEKsw) cells were incubated for 6 h with Dimebone (0.1 µM). Mitochondria were labelled with Mito Tracker CMXRos, fixed with PFA, and mitochondrial lengths were quantified using Image J. (B) Representative images of mitochondria in HEKsw cells in the presence and absence of Dimebone. (C) HEKsw cells were stressed with rotenon (25 µM) for 6 h. Cells were pre-incubated with Dimebone (0.1 µM) for 1 hour to determine possible protective effects. Mitochondria were labelled using Mito Tracker CMXRos, fixed with PFA, and mitochondrial lengths were quantified using Image J. (D) Representative images of mitochondria in HEKsw cells treated with rotenon in the presence and absence of Dimebon. Data represent the means ± SEM with at least 100 measured mitochondria per experiment, n = 9-11, Two-way ANOVA with Bonferroni posttests, **$p < 0,01$, ***$p < 0,001$.

Morphological changes of mitochondria were assessed, after staining with Mito Tracker CMXRos, using confocal laser scanning microscopy. In HEKut cells Dimebon had almost no effects on mitochondrial shape (Fig 18 A+B) and does not protect against rotenon induced mitochondrial fragmentation (Fig 18 C+D). On the other hand, incubation with Dimebon for 6 hours significantly shifted mitochondrial morphology to a tubular shape in HEKsw cells (Fig 19 A+B). Morphology of cells was almost unchanged after challanging the cells with rotenon (Fig 19 C+D).
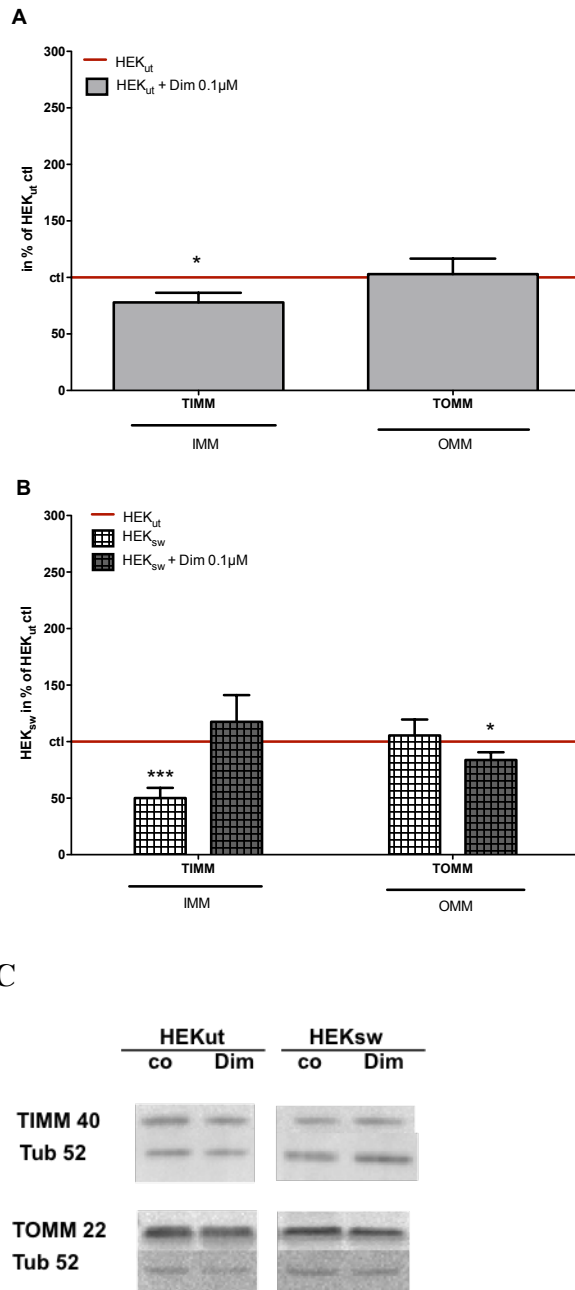
A

B

C
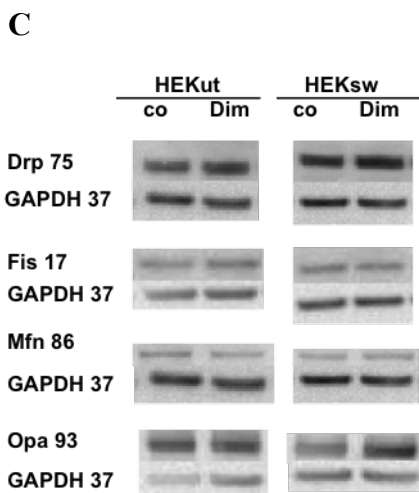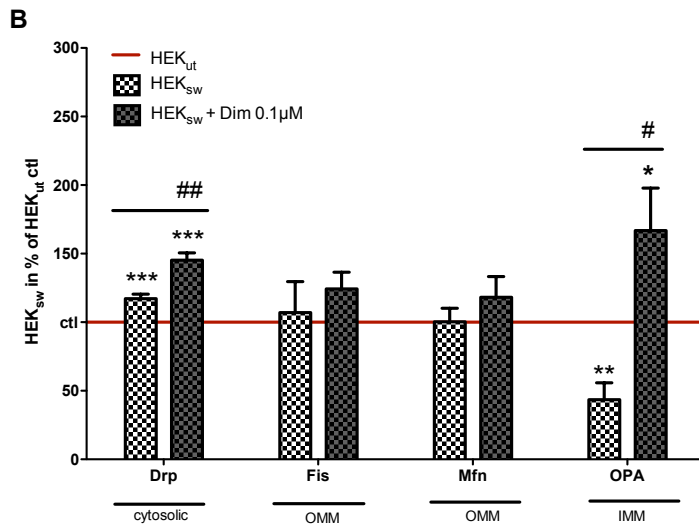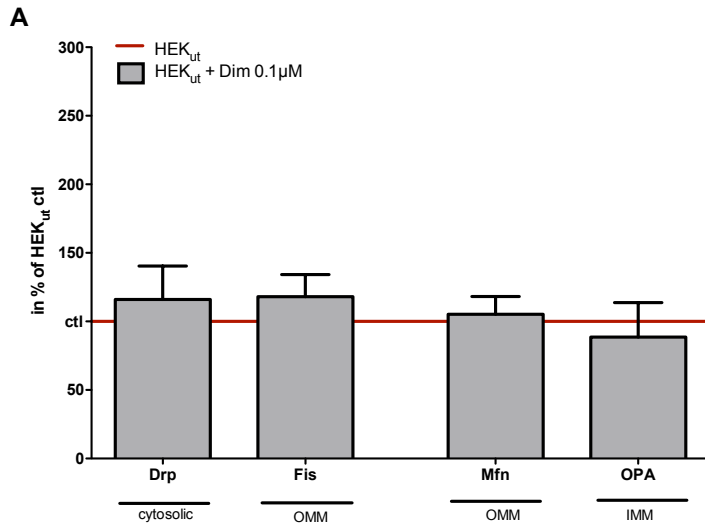
Figure 20. Effects of Dimebon on mitochondrial Fission & Fusion proteins. Cells were incubated with 0,1 μM Dimebon (Dim) for 6 hours. (**B**) In HEK-cells harboring the Swedish mutation in the APP gene (HEKsw) and in (**A**) controls (HEKut), marker proteins for fission

dynamin related protein1 (Drp) and fission 1 related protein (Fis), as well as markers for fusion mitochondrial fusion protein 1 (Mfn) and optic atrophie-1 (Opa) were measured using western blot analysis, after electrophoretic separation and using specific antibodies. Cellular location of the proteins in the cytosolic fraction as well as in inner (IMM) and outer (OMM) mitochondrial membranes was indicated. Data were normalized to HEKut (100%) and represent the means ± SEM, n = 8-9, Two-way ANOVA with Bonferroni post-tests, *$p<0,05$, **$p<0,01$, ***$p<0,001$ vs. ctl; [#]$p<0,05$, [##]$p<0,01$ vs. HEKsw. (**C**) Representative Western Blots.

Dimebon had no effect on protein levels of mitochondrial dynamic markers in HEKut control cells (Fig 20 A). In HEKsw cells Dimebon further enhanced protein levels of Drp and compensated for reduced OPA levels (Fig 20 B).

Incubation of HEKut control cells with Dimebon slightly decreased protein levels of TIMM50 but not of TOMM22 (Figure 21 A). In HEKsw cells Dimebon incubation compensated for significantly reduced TIMM50 protein levels and TOMM22 protein levels were slightly diminished (Figure 21 B).

Figure 21. Effects of Dimebon on mitochondrial membrane markers. Cells were incubated with 0,1 µM Dimebon (Dim) for 6 hours. In (**A**) HEK control cells (HEKut) and (**B**) HEK-cells harboring the Swedish mutation in the APP gene (HEKsw), marker proteins for the inner (IMM) and the outer mitochondrial membrane (OMM), were measured in total homogenates, using western blot analysis after electrophoretic separation and using specific antibodies against translocator proteins of the inner (TIMM50) and outer (TOMM22) mitochondrial membrane in total cellular homogenates. Data were normalized to HEKut (100% in A) and HEKsw (100% in B), respectively. Data represent the means ± SEM, n = 6, Two-way ANOVA with Bonferroni post-tests, *p<0,05, ***p<0,001. (**C**) Representative Western Blots.

Concomitant with disturbed dynamic proteins, mitophagy (a protective cellular mechanism to sort out damaged or energy-deficient mitochondria) seemed to be dysregulated (Cai and Tammineni 2016). This quality control system is of eminent importance, to degrade dysfunctional organelles (Mizushima et al. 2008; Barnett and Brewer 2011). Autophagy can be estimated, using marker proteins for the cytosol (LC3-I) and autophagosomal membranes (LC3-II). Thereby, a low LC3-I/LC3-II ratio indicates a high degree of mitophagy.
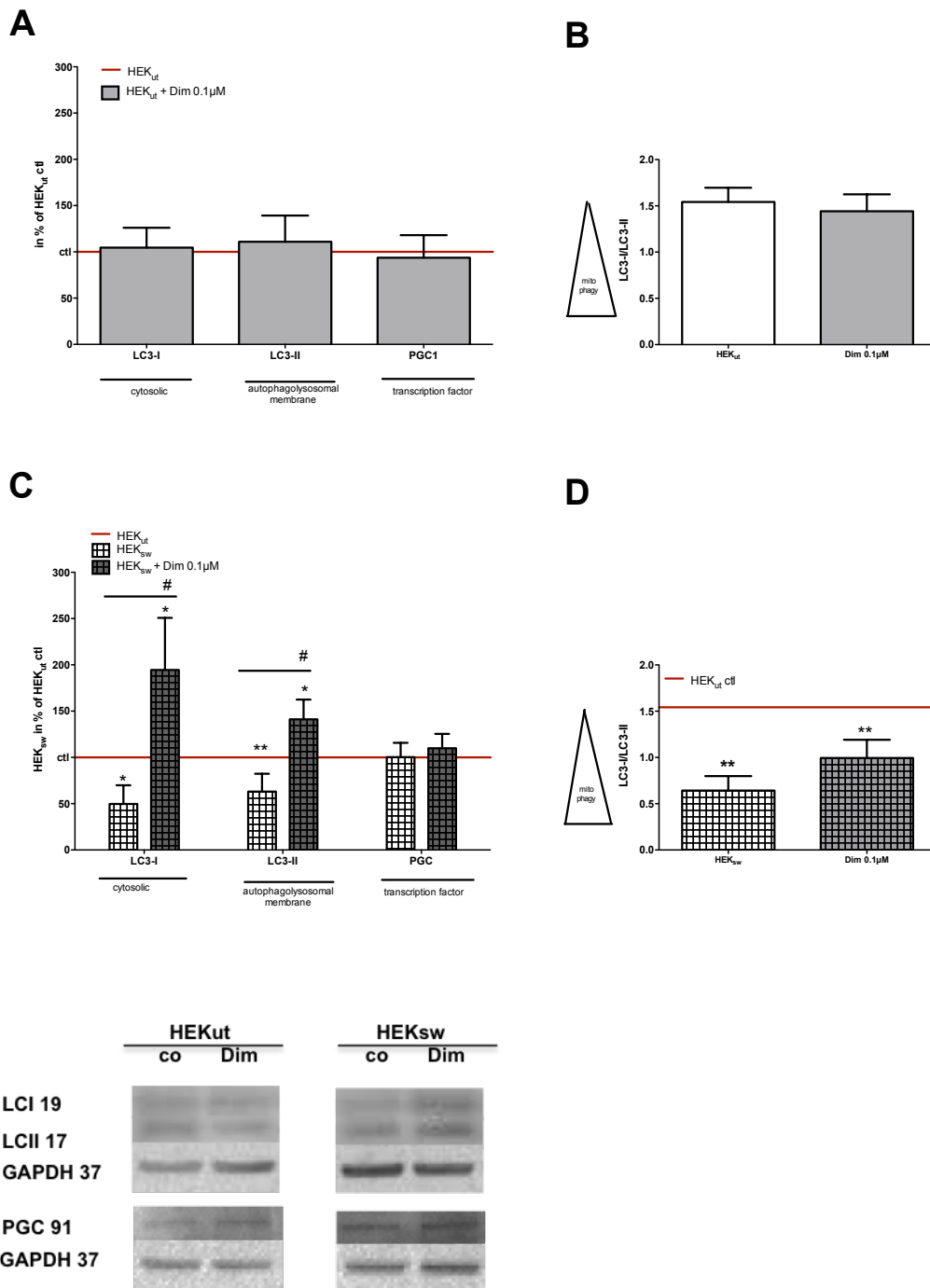
Figure 22. Autophagic activity. (**C**) HEK-cells harboring the Swedish mutation in the APP gene (HEKsw) and (**A**) controls (HEKut) were incubated with 0,1 µM Dimebon (Dim) for 6 hours. Autophagy marker proteins for the cytosol (LC3-I) and autophagosomal membranes (LC3-II) as well as the transcription marker peroxisome proliferation-activated receptor gamma coactivator 1-alpha (PGC), were measured using western blot analysis after electrophoretic separation and using specific antibodies in total cellular homogenates. A low LC3-I/LC3-II ratio indicates high degree of mitophagy. (**B**) Incubation of HEKut cells with Dimebon has no effect on the autophagosomal activity. (**D**) Whereas Dimebon incubation in HEKsw cells highly activates the autophagosomal pathway of mitochondrial renewal. Data

were normalized to HEKut (100%) and represent the means ± SEM, n = 8-9, Two-way ANOVA with Bonferroni post-tests, *p<0,05, **p<0,01 vs. HEKut ctr; #p<0,05 vs. HEKsw ctl. (**E**) Representative Western Blots.

Treatment of HEK control cells with Dimebon did neither influence expression levels of autophagic (LC3-I and LC3-II), nor of mitogensis marker (PGC1 alpha) (Figure 22 A+B). In HEKsw cells protein levels of LC3-I and LC3-II were decreased, which was compensated by Dimebon treatment (Fig 22 C+D). Protein levels of the mitogenesis marker were not influenced by Dimebon in HEKsw cells (Fig 22 C). Although, changes in marker proteins do not necessarily result in changed activity, the results indicated that Dimebon might have reduced autophagy in HEKsw (Figure 22 D), but not in HEKut (Figure 22 B) cells.
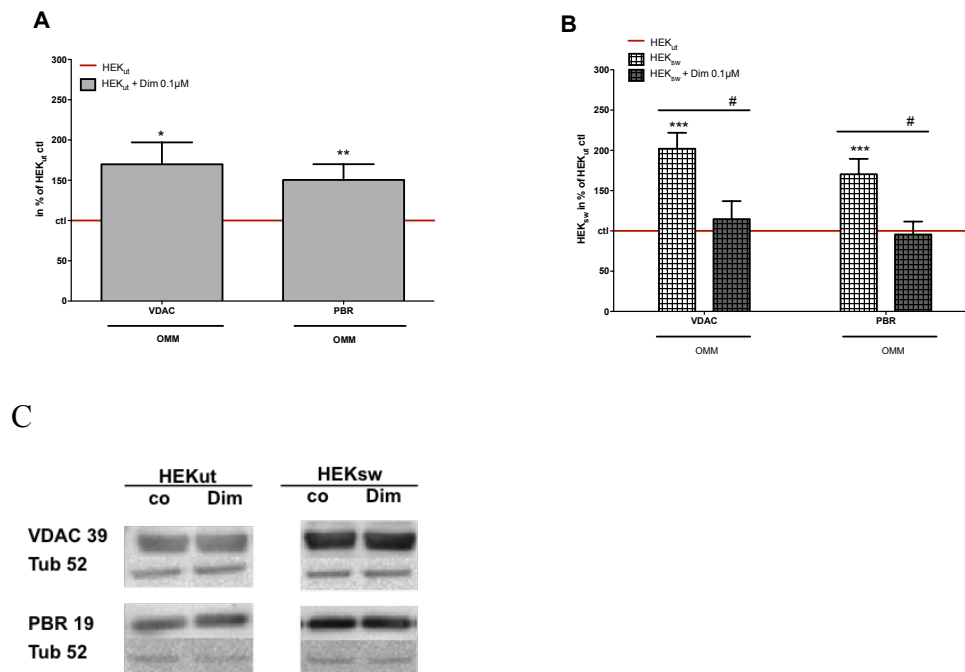
Figure 23. Mitochondrial permeability transition pore (mPTP). Cells were incubated with 0,1 μM Dimebon (Dim) for 6 hours. (**A**) In HEK control cells (HEKut) and in (**B**) HEK-cells harboring the Swedish mutation in the APP gene (HEKsw), mPTP marker proteins of the mitochondrial outer mitochondrial membranes (OMM), voltage-depended anion channel (VDAC) and peripheral benzodiazepine receptor (PBR), were examined using western blot analysis after electrophoretic separation and using specific antibodies in total homogenates. Data were normalized to HEKut (100%) and represent the means ± SEM, n = 8-9, Two-way ANOVA with Bonferroni post-tests, **p<0,01, *p<0,05, ***p<0,001 vs. HEKut ctl; #p<0,05 vs. HEKsw ctl. (**C**) Representative Western Blots.

Mitochondrial permeability transition pore opening seemed to be another parameter, that was differentially regulated by Dimebon, depending on the cell system used: In HEKut cells

Dimebon elevated protein levels of both mPTP marker, VDAC and PBR (Fig 23 A). In HEKsw cells, Dimebon dramatically restored the increased expression levels of these mPTP markers (Fig 23 B). The obvious discrepancy of dimeson's effect in the two cell lines provoke further studies, that also should investigate a relationship between enhanced fission and mPTP-opening markers (Stockburger 2014).
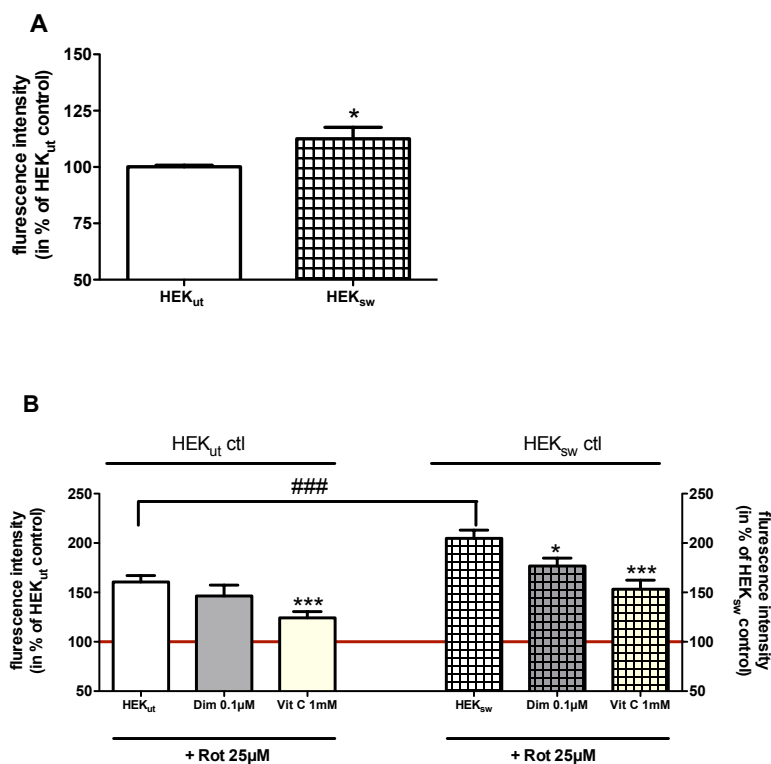
Fig. 24. Effects of Dimebon on intracellular reactive oxygen species (ROS) formation. (**A**) The fluorescence of dihydroethidium (DHE) as an indicator of intracellular ROS was measured using a Beckman fluorescence activated cell counter (FACS) in HEK control cells (HEKut) and in HEK-cells harboring the Swedish mutation in the APP gene (HEKsw). (**B**) HEK cells were pre-treated with Dimebone (0.1 µM) or Vitamin C (1 mM) for 45 min, then rotenon (25 µM) was added for 2 hours. ROS levels were detected using the fluorescent dye dihydroethidium (5 µM). Data represent the means ± SEM with at least 10^4 measured cells per experiment, e*xperiments were done as triplicates,* n = 10, unpaired t-test, *p<0.05, ***p<0.001.

Oxidative stress represents another mitochondrial related parameter, since failures of the interplay of respiration chain complexes generate reactive oxidative species (ROS), which can damage mitochondria itself or surrounding tissue. Compared to HEKut control cells, higher levels of ROS were detected in HEKsw cells (Fig 24 A). Protective effects of Dimebon were observed after challenging with rotenon in HEKsw cells only (Fig 24 B). The

free radical scavenger vitamin C, which was used as positive control, compensated for increased ROS levels in both cell lines (Figure 24 B).
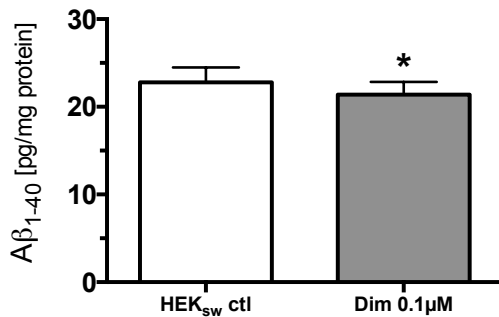
Fig. 25. Effects of Dimebon on β-amyloid protein Aβ_{1-40}. A$\beta_{1-40\ was}$ determined in HEKsw cells after 6 hours incubation with 0.1 µM Dimebon (Dim) using an ELISA as described in material & methods. Data represent the means ± SEM with at least 10^4 measured cells per experiment, e*xperiments were done as dublicates,* n = 6, unpaired t-test, *p<0.05.

HEKsw cells produce an excess of Aβ which is involved in mitochondrial dysfunction and oxidative stress. Therefore, it was investigated if Dimebon alters the production of Aβ to determine if the beneficial effects of Dimebon on mitochondrial dysfunction in HEKsw cells are based on effects on APP processing. Aβ_{1-40} levels were significantly decreased in HEKsw cells that were incubated with 0,1 µM Dimebon for 6 hours (Fig. 24 A). However, changes seemed to be too small, to explain the much larger effects of Dimebon on impaired mitochondrial parameters.

Effects of Olesoxim (TRO) in HEK-cells

Olesoxim is a cholesterol-like compound, which has been identified to promote the survival of primary motor neurons (Bordet et al. 2007). Olesoxim is easily absorbed by cells and accumulates in mitochondria (Bordet et al. 2010). Although Olesoxim's mode of action is not fully understood, evidences indicate that it interacts with mitochondria (Eckmann et al. 2014) (Bordet et al. 2007; Bordet et al. 2010; Gouarné et al. 2013; Gouarne et al. 2015).

The concentration dependent pharmacological effects of Olesoxim on mitochondria related parameters were assessed in HEK-cells harboring the Swedish mutation in the APP gene (HEKsw), which represents an established model of LOAD (please refer to 1.1) and in untransfected control cells (HEKut).
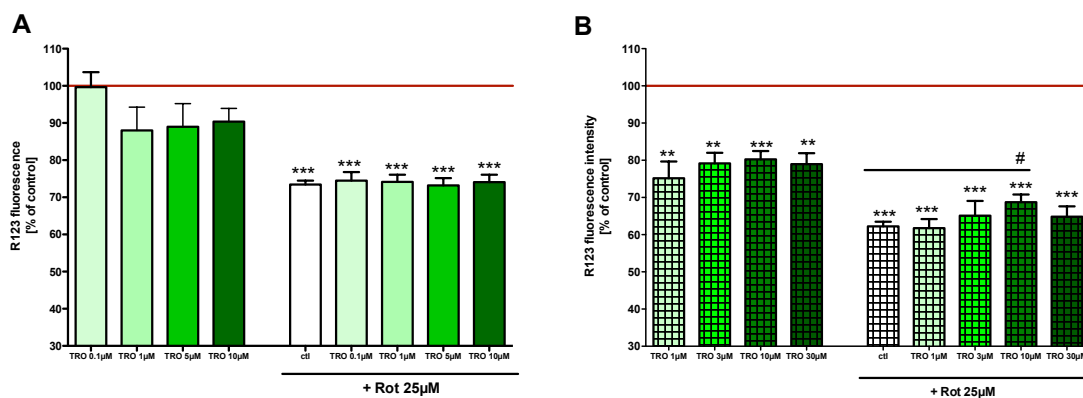
Figure 26. Effects of Olesoxim on mitochondrial membrane potential (MMP). Cells were pre-incubated with 1 - 30 µM Olesoxim (TRO), then challenged using 25 µM rotenon for 6 hours. MMP was measured using the fluorescence dye Rhodamin 123 (R123) in 2×10^5 HEK-cells (**B**) harboring the Swedish mutation in the APP gene (HEKsw) or in (**A**) controls (HEKut) as described in material & methods. Results were normalized to untreated HEKsw- and HEKut-cells (ctl = 100%), respectively. Data represent the means ± SEM; n=6 independent experiments; p**<0,01, p***<0,001 vs. ctl; #p<0,05 HEK+ Rotenon 25 µM vs. HEK+ Rotenon 25 µM + TRO 10 µM; Student`s t-test.

Incubation of HEKut control cells with different concentrations of Olesoxim did neither influence the MMP under basal conditions, nor after rotenon challenging (Figure 26 A). In HEKsw cells incubation with different Olesoxim concentrations (1-30 µM) led to a dose independent decline in the MMP indicating that even concentrations lower than 1 µM would

have the potential to lower MMP. In HEKsw cells 10 µM Olesoxim completely restored complex I respiratory dysfunction (Figure 26 B). Compared to HEKut control cells, the response to rotenon induced complex I dysfunction is more vulnerable in HEKsw cells (Figures 26 A vs. B).
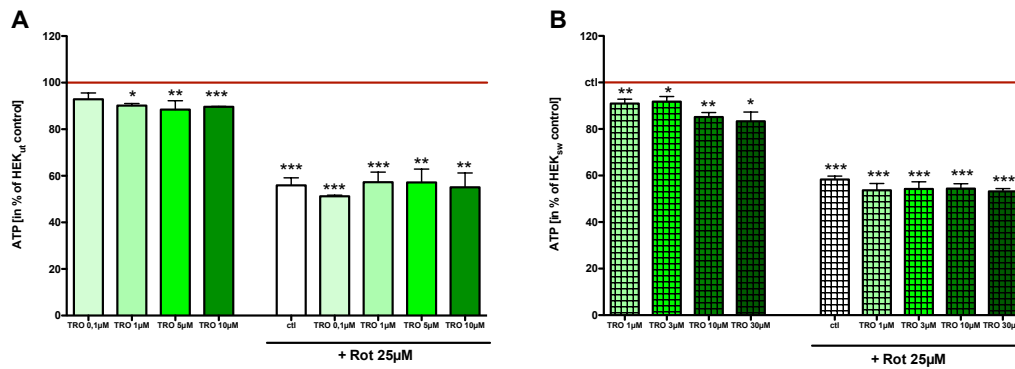
Figure 27. Effects of Olesoxim on Adenonsine triphosphate (ATP) levels. Cells were pre-incubated with 1 - 30 µM Olesoxim (TRO) and then challenged using 25 µM rotenon for 6 hours. ATP levels were determined using a luminescence kit in 2×10^4 HEK-cells (**B**) harboring the Swedish mutation in the APP gene (HEKsw) or in (**A**) controls (HEKut) as described in material & methods. Results were normalized to untreated HEKsw- and HEKut-cells (ctl = 100%), respectively. Data represent the means ± SEM; n=6 independent experiments; p*<0,05; p**<0,01, p***<0,001; Student`s t-test.

In both cell lines incubation with different Olesoxim concentrations decreased ATP levels. Olesoxim had no effect on ATP levels after challenging cells with rotenon (Figures 27A+B).

A
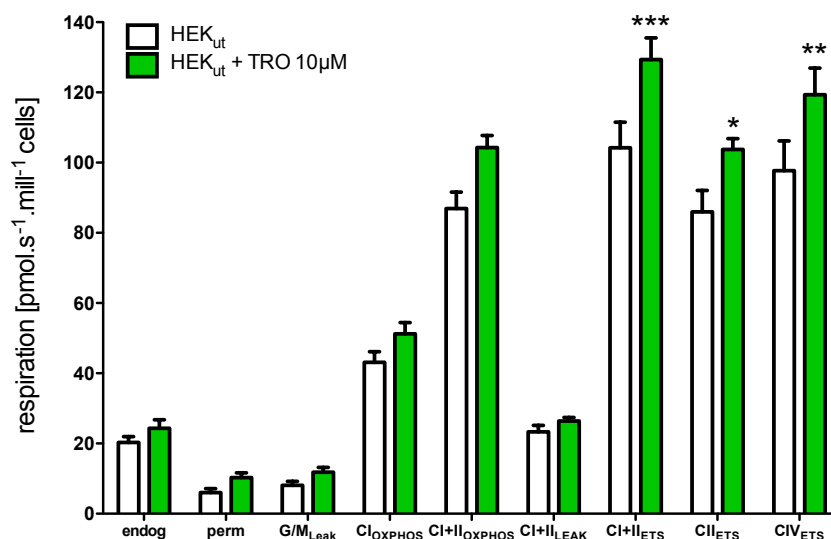
B
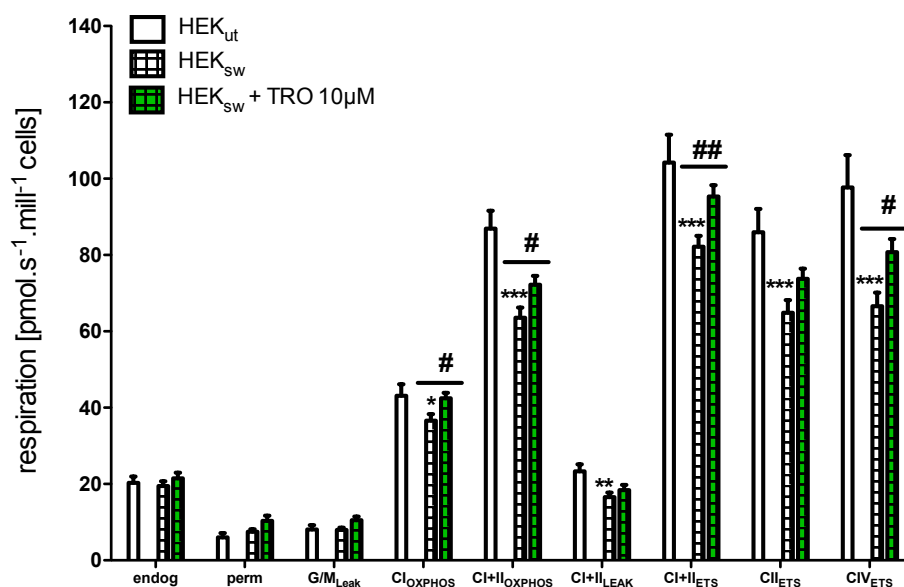
Figure 28. Effects of Olesoxim on mitochondrial respiration in HEK cells. (A) HEKut and **(B)** HEKsw cells were incubated with 10 μM Olesoxim (TRO) for 6 hours, respectively. Oxygen consumption was measured using an Oxygraph-2k. Respiration was determined in different mitochondrial stages after injecting several substrates and inhibitors (please refer to material & methods). Endogen respiration was measured after injecting the samples (endog) into the chambers. Digitonin was used for permeabilizing the cell membranes (perm). Glutamat and Malat supplementation served as complex I substrates (G/M$_{Leak}$). Due to the lack of ADP this experimental stage was still leaky; ADP was the driving force to initiate the electron transport chain to build the proton gradient among the inner mitochondrial membrane. ADP injection fulfilled the demands for CI dependent oxidative phosphorylation (CI$_{OXPHOS}$) (OXPHOS stands for oxidative phosphorylation). Adding succinat finally provided a CII substrate and enabled CI+II oxidative phosphorylation (CI+II$_{OXPHOS}$). By adding oligomycin, the ATP synthase, complex V, was inhibited and it was possible to detect the respiratory capacity on CI+II substrates to compensate for proton leak (CI+II$_{Leak}$) through the membrane. Using stepwise injection of FCCP, a ionophor that uncouples the respiratory chain, non-coupled respiration with CI and CII substrates (CI+II$_{ETS}$) was measured, which was considered as maximum capacity of the ETS (ETS stands for electron transport system). Rotenon was inhibiting complex I, making it possible to detect non-coupled CII respiration (CII$_{ETS}$). Antimycin A was blocking the electron transport chain by inhibiting Cytochrom C, thus electrons could not be transferred from complex III to complex IV. By supplementation of CIV substrates Ascorbat/TMPD, non-coupled respiration of complex IV was accessible (CIV$_{ETS}$). Values represent the means ± SEM from n = 6 independent experiments. Two-way ANOVA with Bonferroni posttests, *$p < 0,05$, **$p < 0,01$. Total oxygen concentration is indicated as blue line.

Olesoxim siginficantly enhanced the electron transport (ETS) capacity upstream of complex II in HEKut cells (Figure 28 A). Compared to HEKut cells, HEKsw cells showed an overall reduction in mitochondrial respiration (Figure 28 B). Incubation of HEKsw cells with

Olesoxim induced a general increase in respiratory activity and normalized CI_{OXPHOS} activity in HEKsw cells almost to control levels (Figure 28 B).
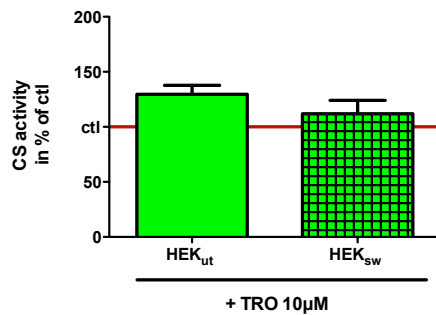
Figure 29. Citrate synthase (CS) activity. Cells were incubated with 10 µM Olesoxim (TRO) for 6 hours. Enzyme activity was determined in HEK-cells harboring the Swedish mutation in the APP gene (HEKsw) or in controls (HEKut) using a spectrophotometric method at 412nm and 30°C as described in material & methods. Data represent the means ± SEM, n = 6, each experiment was measured as duplet.

Olesoxim incubations had no effects on CS activity, neither in HEKut nor in HEKsw cells (Figure 29).
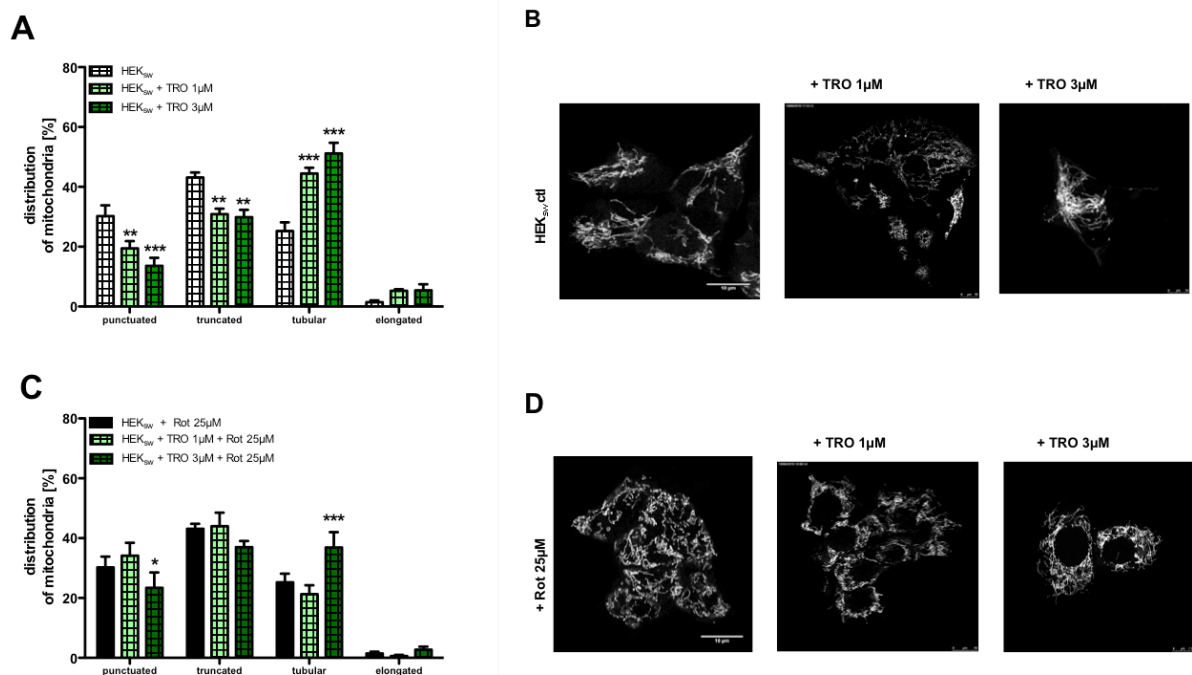
Figure 30. Effects of Olesoxim on mitochondrial morphology. (A) HEK-cells harboring the Swedish mutation in the APP gene (HEKsw) were incubated for 6 hours with Olesoxim (TRO 1 µM and TRO 3 µM). **(C)** HEKsw cells were pre-incubated with Olesoxim (TRO 1 µM and TRO 3 µM) for 1 hour and then stressed with rotenon (25 µM) for 6 hours. Mitochondria were labelled with Mito Tracker CMXRos, fixed with PFA, and mitochondrial

lengths were quantified using Image J. **(B)** Representative images of mitochondria in HEKsw cells in the presence and absence of Olesoxim. **(D)** Representative images of mitochondria in HEKsw cells treated with rotenon in the presence and absence of Olesoxim. Data represent the means ± SEM with at least 100 measured mitochondria per experiment, n = 10, Two-way ANOVA with Bonferroni posttests, *p<0,05, **p<0,01, p***<0,001; unpaired Students t-test.

Mitochondrial lengths were not analyzable in HEKut cells after incubation with Olesoxim (1 μM and 3 μM). In HEKsw cells Olesoxim changed the length of mitochondria in a dose-depend way and strongly shifted the pattern towards longer mitochondria. The amount of punctuated mitochondria was strongly reduced by approximately 50%. On the other hand, the amount of tubular mitochondria was nearly doubled (Figure 30 A). Olesoxim pre-incubation had a moderate protective effect after challenging HEKsw cells with rotenon (Figure 30 C).
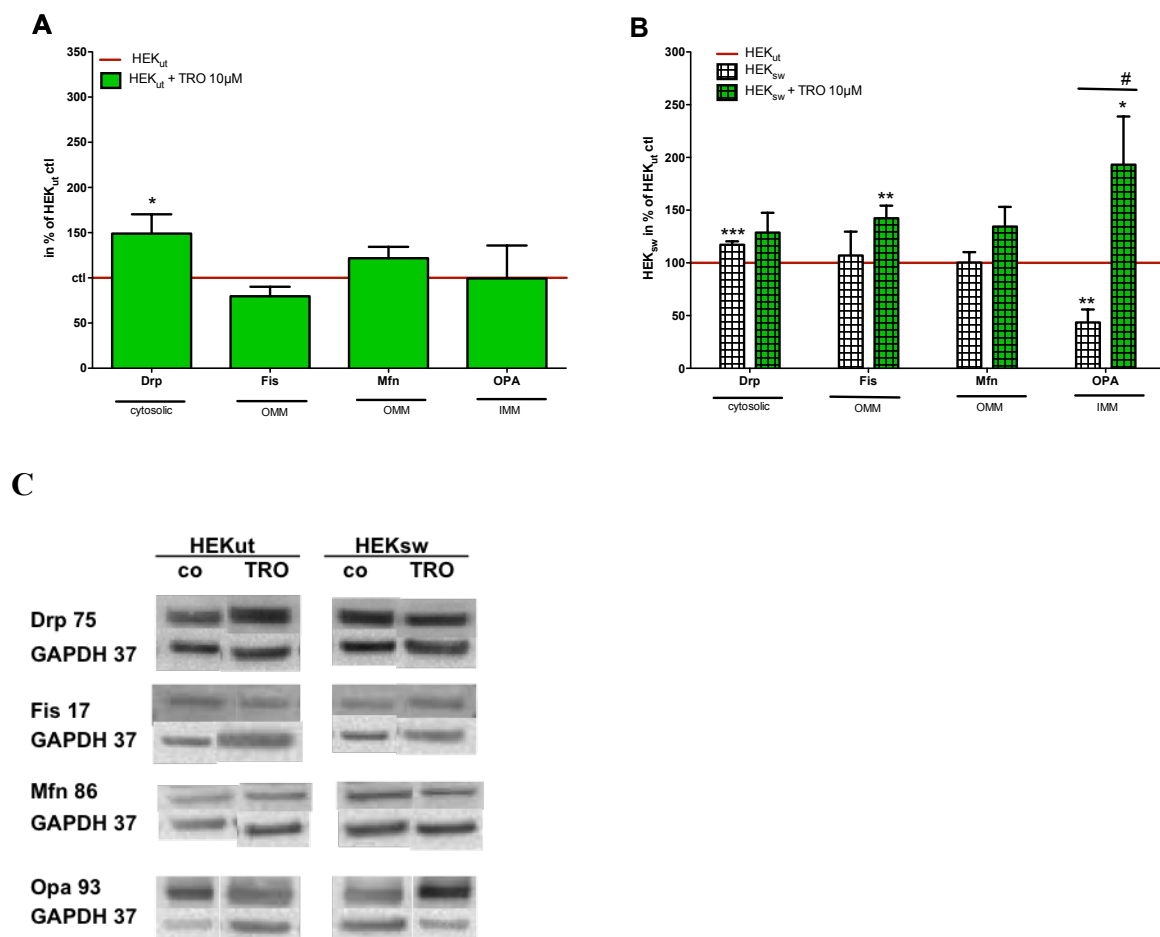
Figure 31. Effects of Olesoxim on mitochondrial Fission & Fusion proteins. Cells were incubated with 10 μM Olesoxim (TRO) for 6 hours. (**B**) In HEK-cells harboring the Swedish mutation in the APP gene (HEKsw) and in (**A**) controls (HEKut), marker proteins for fission

dynamin related protein1 (Drp) and fission 1 related protein (Fis), as well as markers for fusion mitochondrial fusion protein 1 (Mfn) and optic atrophie-1 (Opa) were measured, using western blot analysis after electrophoretic separation and using specific antibodies. Cellular location of the proteins in the cytosolic fraction, in inner (IMM) and outer (OMM) mitochondrial membranes was indicated. Data were normalized to HEKut (100%) and represent the means ± SEM, n = 8-9, Two-way ANOVA with Bonferroni post-tests, *p<0,05 **p<0,01, ***p<0,001 vs. ctl; #p<0,05 HEKsw ctl vs. HEKsw + TRO 10 μM. (**C**) Representative Western Blots.

In HEKut cells 10 μM Olesoxim enhanced Drp protein levels (Figure 31 A). Levels in HEKsw cells showed diminished OPA protein levels, that were strongly increased after incubation with Olesoxim (10 μM) to a degree, far above the levels detected in HEKut control cells (Figure 31 B). Although, all marker proteins of the mitochondrial dynamic machinery were elevated by trend only, changes in Fis and OPA protein level reached significance (Figure 31 B).
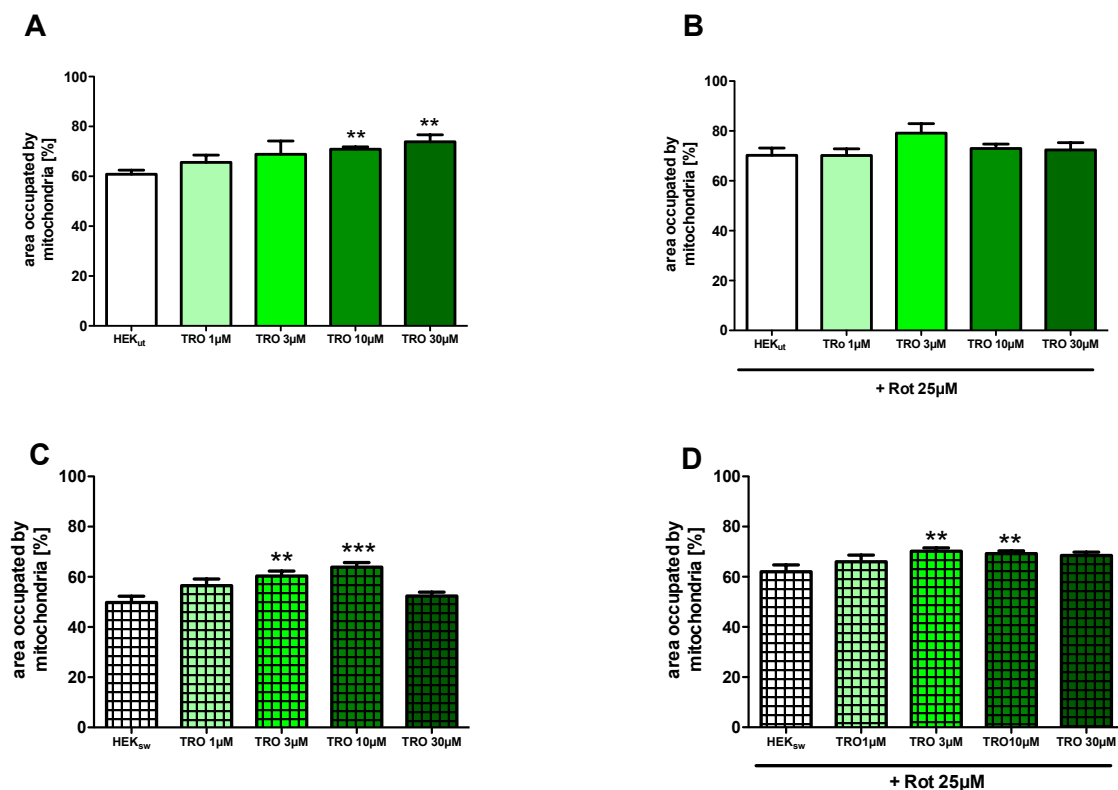
Figure 32. Mitochondrial density. Cells were incubated with Olesoxim (TRO 1-30 μM) for 6 hours (graphs on the left, **A** and **C**) or pre-incubated with Olesoxim (TRO 1-30 μM) and challenged with rotenon (25 μM) for 6 h (graphs on the right, **B** and **D**). Mitochondria were labeled in (**C, D**) HEK-cells harboring the Swedish mutation in the APP gene (HEKsw) or in (**A, B**) controls (HEKut) using the fluorescence marker Mito Tracker CMXRos. Following fixation with PFA, cells were examined using confocal laser-scanning microscopy. Mitochondrial densities were quantified based on fluorescence intensities with Image J and

expressed as area occupied by mitochondria (%). Data represent the means ± SEM with at least 100 measured mitochondria per experiment, n = 7-20, **p<0,01, ***p<0,001; unpaired t-test.

Olesoxim increased the mitochondrial density in HEKut cells in a dose-dependent way (Figure 32 A) and to a degree that made a quantification of mitochondrial length impossible (data not analyzable). Olesoxim showed no effects after challenging HEKut cells with rotenon (Figue 32 B). In HEKsw cells a reduced mitochondrial density was observed (Figure 7A), which was reversed by Olesoxim in a dose-dependent manner (Figure 32 C). However, Olesoxim did not ameliorate the mitochondrial density after challenging HEKsw cells with rotenon (Figure 32 D).
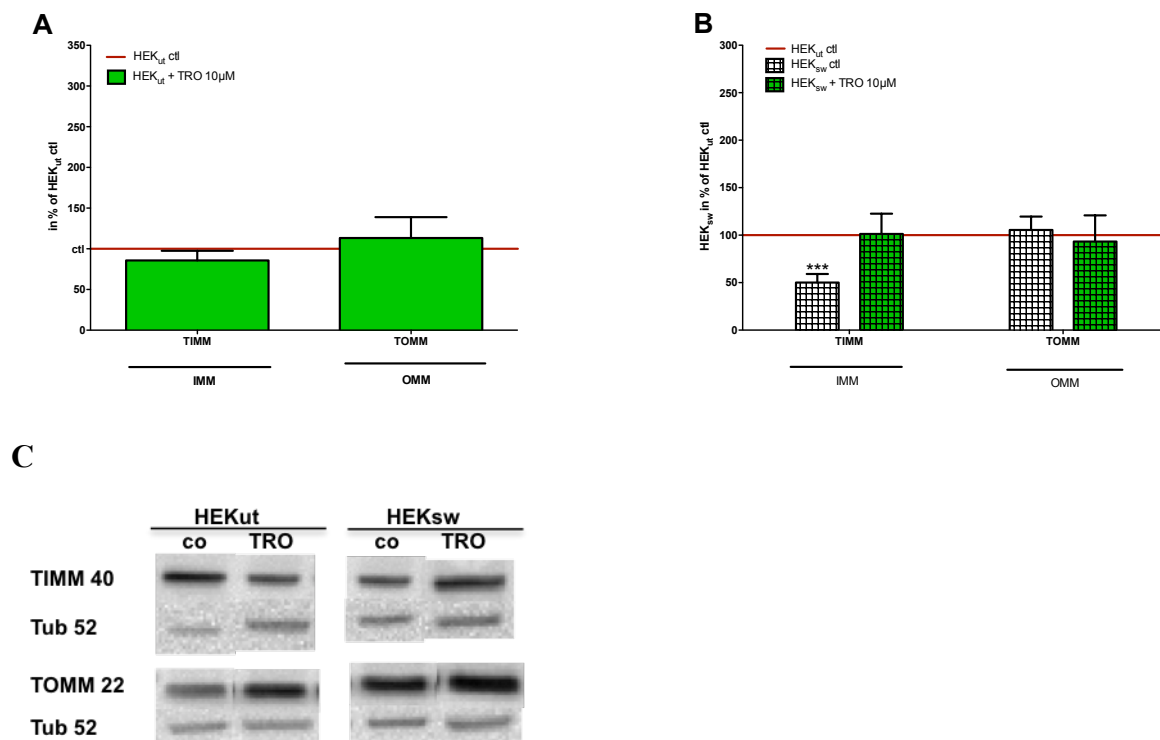
Figure 33. Effects of Olesoxim on mitochondrial membrane markers. Cells were incubated with 10 µM Olesoxim (TRO) for 6 hours. In HEK-cells (**B**) harboring the Swedish mutation in the APP gene (HEKsw) and in (**A**) controls (HEKut), marker proteins for the inner (IMM) and the outer mitochondrial membrane (OMM) were measured in total homogenates, using western blot analysis after electrophoretic separation and using specific antibodies against translocator proteins of the inner (TIMM50) and outer (TOMM22) mitochondrial membrane in total cellular homogenates. Data were normalized to HEKut (100% in A) and HEKsw (100% in B), respectively. Data represent the means ± SEM, n = 6, Two-way ANOVA with Bonferroni post-tests, ***p<0,001. (**C**) Representative Western Blots.

Olesoxim had no effect on the expression of TIMM50 and TOMM22 in HEKut (Figure 33 A). In HEKsw cells on the other hand, Olesoxim completely compensated for the severely reduced expression levels of TIMM50 (Figure 33 B) but had no effect on TOMM22 levels (Figure 33 B).
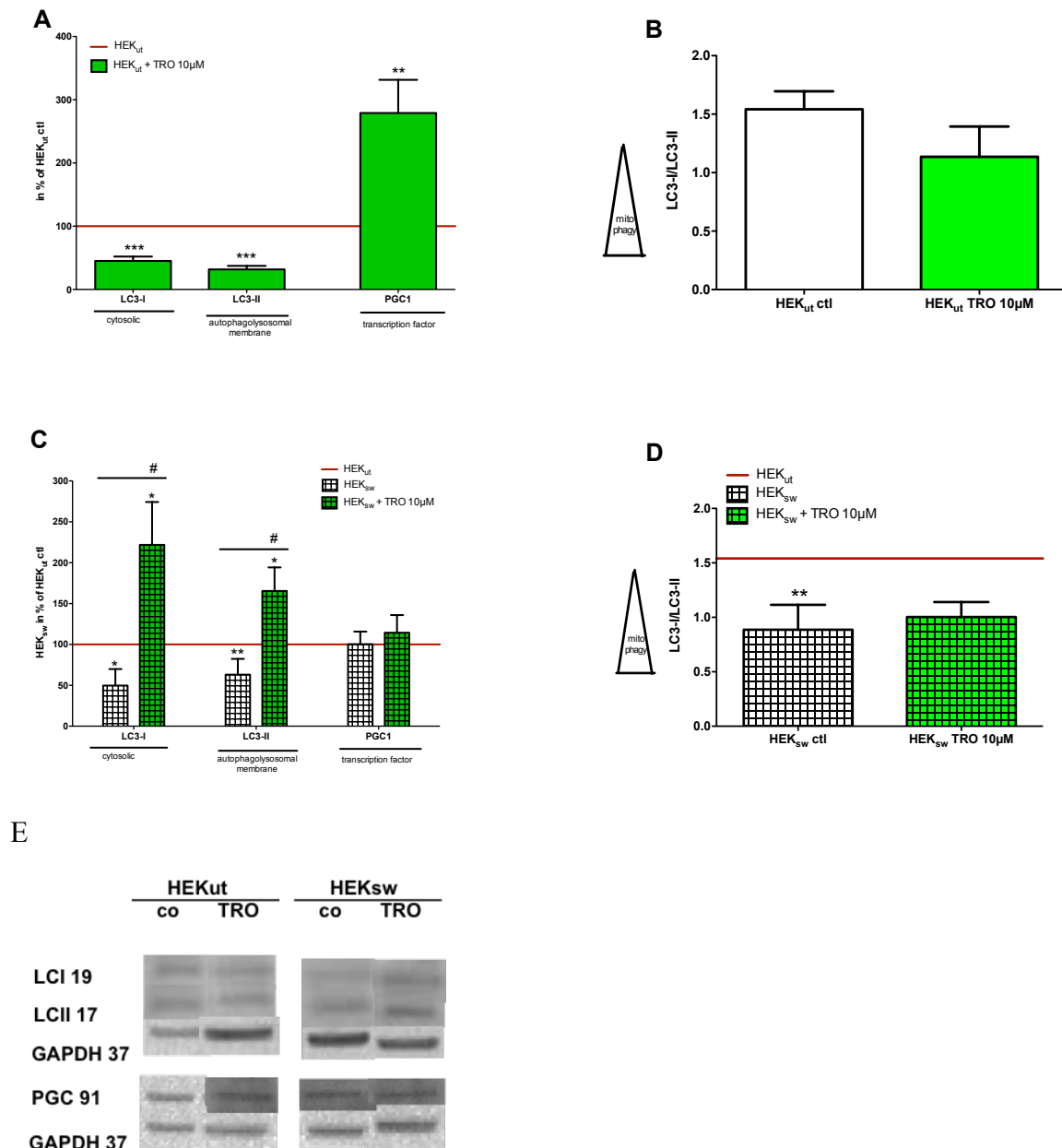
Figure 34. Autophagic activity. (**A**) Control cells (HEKut) and (**C**) HEK-cells harboring the Swedish mutation in the APP gene (HEKsw) were incubated with 10 μM Olesoxim (TRO) for 6 hours. Autophagy marker proteins for the cytosol (LC3-I) and autophagosomal membranes (LC3-II), as well as the transcription marker peroxisome proliferation-activated receptor gamma coactivator 1-alpha (PGC1alpha) were measured, using western blot analysis after electrophoretic separation and using specific antibodies in total cellular homogenates. A

low LC3-I/LC3-II ratio indicated a high degree of mitophagy. Whether in (**B**) HEK control cells, nor in (**D**) HEKsw cells, incubation with TRO effected the autophagosomal activity. Data were normalized to HEKut (100%) and represent the means ± SEM, n = 8-9, Two-way ANOVA with Bonferroni post-tests, *p<0,05, **p<0,01, ***p<0,001 vs. ctl; [#]p<0,05 vs HEKsw ctl. (**E**) Representative Western Blots.

The mitophagy precursor protein marker LC3-I and LC3-II were strongly reduced after Olesoxim incubation in HEKut cells (Figure 34 A). Since both proteins were reduced, the ratio of LC-I to LC-II, which is an indicator for autophagosomal activity, was not significantly changed (Figure 34 B). Under the same conditions a threefold increase in peroxisome proliferation-activated receptor gamma coactivator 1-alpha (PGC1alpha) protein levels was observed (Figure 34 A). In HEKsw cells levels of LC-I and LC-II were significantly decreased. Olesoxim strongly elevated the levels of LC3-I and LC3-II far beyond the levels of control cells (Figure 34 C). Autophagosomal activity, as indicated by LC-I to LC-II ratio (Figure 34 D), as well as PGC1alpha protein levels (Figure 34 C), were not altered by Olesoxim in HEKsw cells.
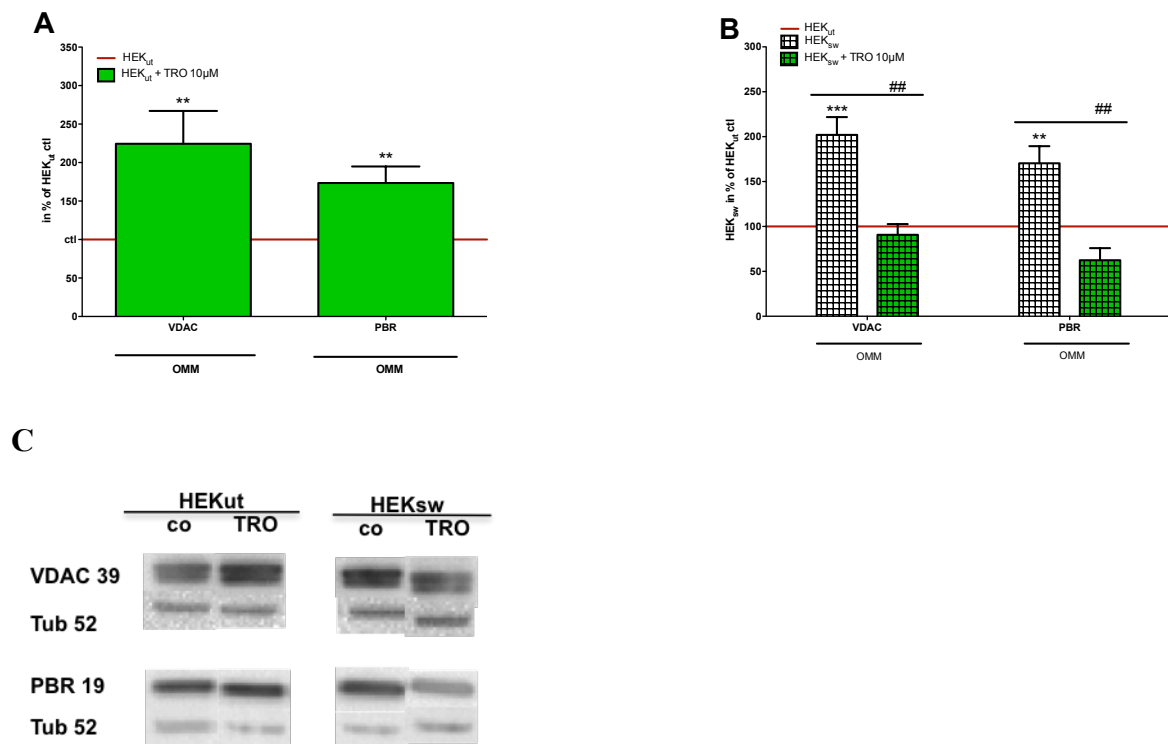
Figure 35. Mitochondrial permeability transition pore (mPTP). Cells were incubated with 10 μM Olesoxim (TRO) for 6 hours. (**A**) In HEK control cells (HEKut) and in (**B**) HEK-cells harboring the Swedish mutation in the APP gene (HEKsw), mPTP marker proteins of the mitochondrial outer mitochondrial membranes (OMM), voltage-depended anion channel (VDAC) and peripheral benzodiazepine receptor (PBR) were examined, using western blot analysis after electrophoretic separation and using specific antibodies in total homogenates.

Data were normalized to HEKut (100%) and represent the means ± SEM, n = 8-9, Two-way ANOVA with Bonferroni post-tests, **p<0,01, ***p<0,001 ws HEKut ctr.; ##p<0,01 vs. HEKsw ctr. (**C**) Representative Western Blots.

Incubation of HEKut cells with Olesoxim strongly increased the protein levels of the mPTP marker, VDAC and PBR (Figure 35 A), indicating a higher vulnerability against mPTP opening to initiate mitochondrial swelling. In HEKsw cells protein levels of the mPTP marker, VDAC and PBR were significantly elevated. Olesoxim incubation abolished the elevated VDAC and PBR protein levels (Figure 35 B).
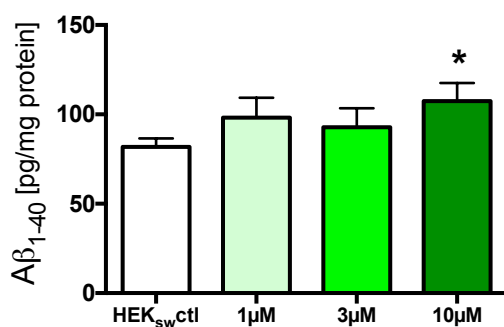
Fig. 36. Effects of Olesoxim on β-amyloid protein levels (Aβ$_{1-40}$). Aβ$_{1-40 \text{ was}}$ determined in HEKsw cells after 24 hour incubation with 1 -10 µM Olesoxim using an ELISA as described in material & methods. Data represent the means ± SEM with at least 10^4 measured cells per experiment, e*xperiments were done as duplicates,* n = 6, unpaired t-test, *p<0.05.

HEKsw cells were incubated with different concentrations of Olesoxim for 24 hours. 10 µM Olesoxim significantly increased Aβ$_{1-40}$ levels (Fig. 36).

Characterization of a mouse model for Alzheimer`s disease

Transgenic mouse models harboring human genes, inherited in an autosomal dominant manner, showing elevated Aβ production, amyloid plaques, and memory deficits, are commonly used in AD research (see table 1). For this study Thy-1-C57BJ/6-APP$_{SL}$ transgenic mice (Thy1-APPSL mice), expressing the human form of APP, containing both the Swedish (KM670/671NL) and the London (V717L) double mutations under the murine Thy1 pro- motor (Blanchard et al. 2003), were used. The Thy1 promotor leads to an increased and selective expression of APP in neurons. Beginning at the age of 3 months, Thy1-APPSL mice exhibit elevated Aβ levels and mitochondrial dysfunction. The first Aβ plaques could be found at the age of 6 months (Blanchard et al. 2003; Hauptmann et al. 2009).
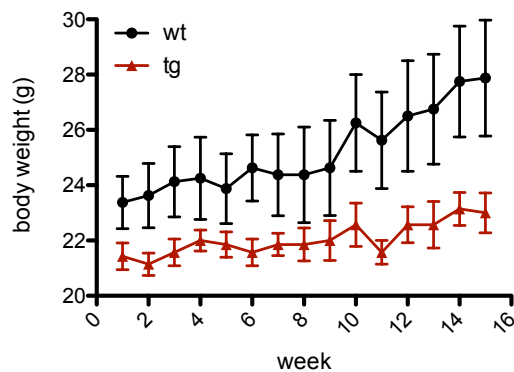
Figure 37. Development of the body weight. Body weight of Thy-1-C57BJ/6-APP$_{SL}$ (tg) and littermate control mice (wt). Body weight was followed every week over a period of of 4 months. Data represent means ± SEM, n = 7-8.

Both mouse strains gained weight over time. A tendency for a lower body weight and a reduced weight gain was observed in Thy-1-C57BJ/6-APP$_{SL}$ (tg), compared to littermate controls (wt) (Figure 37).

A
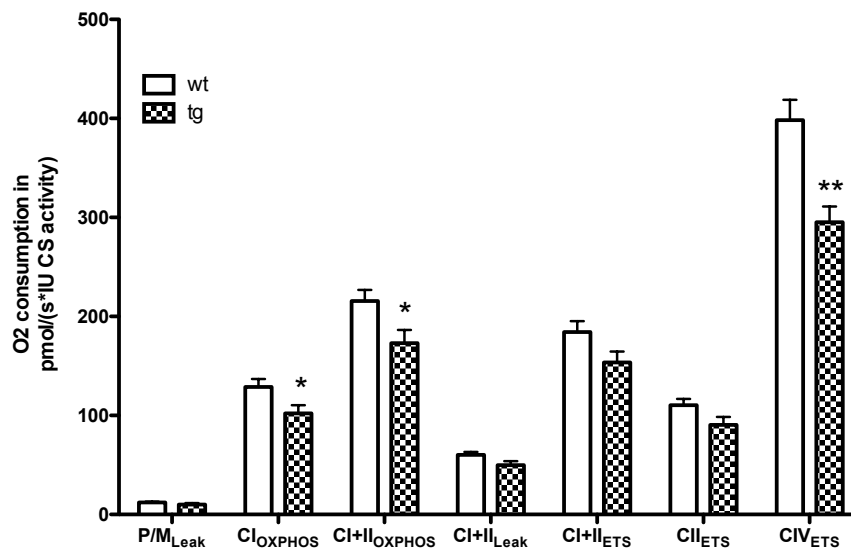
B
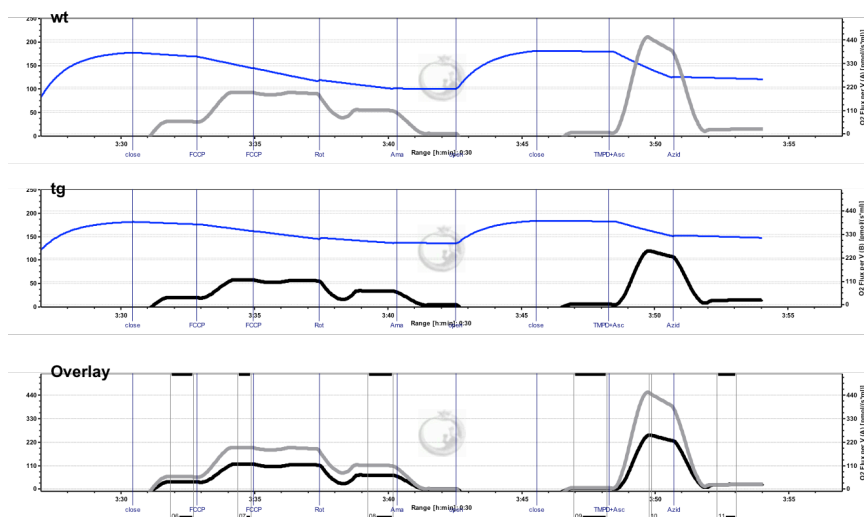
Figure 38. Mitochondrial respiration. (**A**) Oxygen consumption was measured in brain mitochondria isolated from littermate C57BJ/6 control (wt) and Thy-1-C57BJ/6-APP$_{SL}$ (tg) mice (refer to material & methods). Pyruvat and Malat supplementation served as complex I substrates (P/M$_{Leak}$). Due to the lack of ADP this experimental stage was still leaky; ADP was the driving force to initiate the electron transport chain to build the proton gradient among the inner mitochondrial membrane. ADP injection fulfils the demands for CI dependent oxidative phosphorylation (CI$_{OXPHOS}$) (OXPHOS stands for oxidative phosphorylation). Adding succinat finally provided a CII substrate and enabled CI+II oxidative phosphorylation (CI+II$_{OXPHOS}$). By adding oligomycin, the ATP synthase, complex V, was inhibited and it was possible to detect the respiratory capacity on CI+II substrates to compensate for proton leak (CI+II$_{Leak}$) through the membrane. Using stepwise injection of FCCP, a ionophor that uncouples the respiratory chain, non-coupled respiration with CI and CII substrates (CI+II$_{ETS}$) was measured, which was considered as maximum capacity of the ETS (ETS stands for electron transport system). Rotenon was inhibiting complex I, making it possible to detect non-coupled CII respiration (CII$_{ETS}$). Antimycin A was blocking the

106

electron transport chain by inhibiting Cytochrom C, thus electrons could not be transferred from complex III to complex IV. By supplementation of CIV substrates Ascorbat/TMPD, non-coupled respiration of complex IV was accessible (CIV_{ETS}). Values represent the means $\pm$ SEM from n = 6-8 independent experiments. Two-way ANOVA with Bonferroni post-tests, *p<0,05, **p<0,01. (**B**) Representative graphs of oxygen consumption measurements in mitochondria isolated from littermate C57BJ/6 control (wt) and Thy-1-C57BJ/6-APP_{SL} (tg) mice.

Firstly, mitochondrial function in mice brains was investigated. Therefore, mitochondria and dissociated brain cells were isolated. Mitochondria, isolated from brains of Thy-1-C57BJ/6-APP_{SL} mice, showed significant impaired respiration of complex I, complex I+II, and complex IV compared to littermate wild-type control mice (Figure 38 A).

Since mitochondrial respiration was found to be the driving force to build up a proton gradient across the inner mitochondrial membrane, leading to an enhanced mitochondrial membrane potential (MMP) (Nijtmans et al. 2004), the MMP was measured in dissociated brain cells (DBC), isolated from Thy-1-C57BJ/6-APP_{SL} and litter mate wild-type control mice.
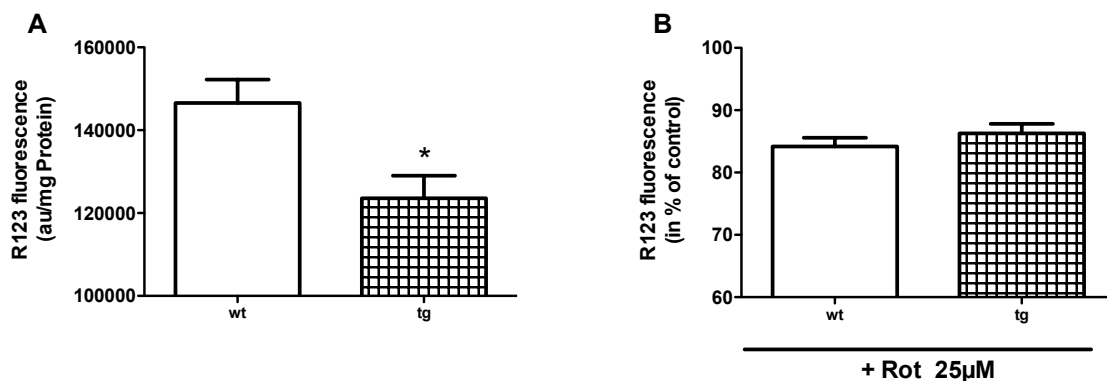
Figure 39. Mitochondrial membrane potential (MMP). (A) MMP was measured using the fluorescence dye Rhodamin 123 (R123) in dissociated brain cells isolated from C57BJ/6 littermate control (wt) and Thy-1-C57BJ/6-APP_{SL} (tg), as described in material & methods. (B) MMP of dissociated brain cells challenged, using 25 µM rotenon (Rot) for 3 hours. Results were normalized to litter mate control. Data represent the means $\pm$ SEM; n=6-7; p*<0,05; Student`s t-test.

In DBC isolated from Thy-1-C57BJ/6-APP_{SL} mice, a significant lower fluorescence of Rhodamin R123 was measured compared to littermate control mice (Figure 39 A), indicating a reduced mitochondrial membrane potential. Thus, the dysfunctional respiratory chain in mitochondria isolated from brains of Thy-1-C57BJ/6-APP_{SL} mice (Figure 38) resulted in a

reduced MMP (Figure 39 A). Regarding MMP measurements, rotenon had an equal impact on DBC isolated from Thy-1-C57BJ/6-APP$_{SL}$ and littermate control mice (Figure 39 B). ATP levels were measured next, since the MMP provided the power for complex V that finally generated ATP (Nijtmans et al. 2004).
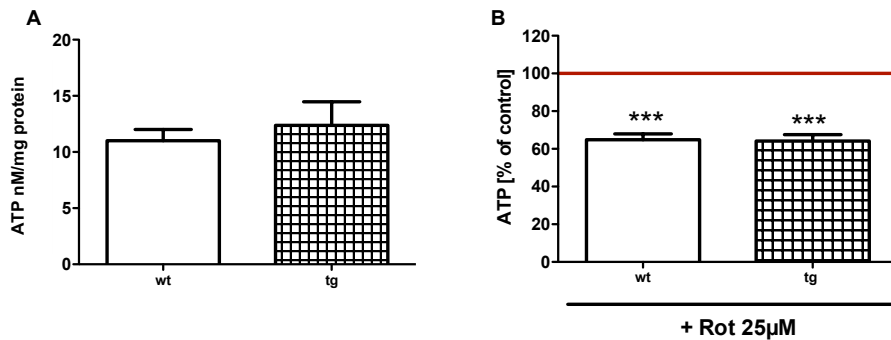
Figure 40. Levels of Adenosine triphposphate (ATP). (**A**) ATP levels (nM/mg protein) were determined using a luminescence kit in dissociated brain cells, isolated from C57BJ/6 litter mate control (wt) and Thy-1-C57BJ/6-APP$_{SL}$ (tg), as described in material & methods. (**B**) ATP levels of dissociated brain cells challenged using 25 nM rotenon (Rot) for 1,5 hours. Results were normalized to litter mate control. Data represent the means ± SEM; n=6-7 independent experiments.

ATP levels in dissociated brain cells did not differ between Thy-1-C57BJ/6-APP$_{SL}$ mice and littermate controls, neither at basal conditions (Figure 40 A), nor under stress conditions (Figure 40 B).
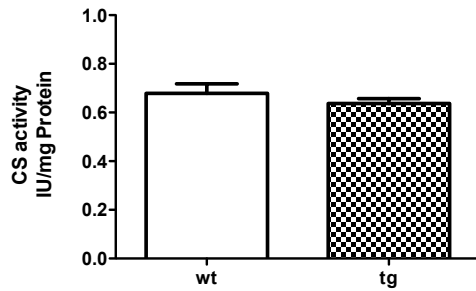
Figure 41. Citrate synthase (CS) activity. CS was determined using a spectrophotometric method at 412nm and 30°C in mitochondria, isolated from C57BJ/6 littermate control (ctl) and Thy-1-C57BJ/6-APP$_{SL}$ (tg), as described in material & methods. Data represent the means ± SEM; n=7-11 independent experiments, each experiment was measured as duplet.

CS activity as marker for the mitochondrial content (Larsen et al. 2012) was not altered in mitochondria isolated from brains of Thy-1-C57BJ/6-APP$_{SL}$, compared to C57BJ/6 littermate control mice (Figure 39). Thus, it can be concluded that the mitochondrial mass was equal in both mouse lines.
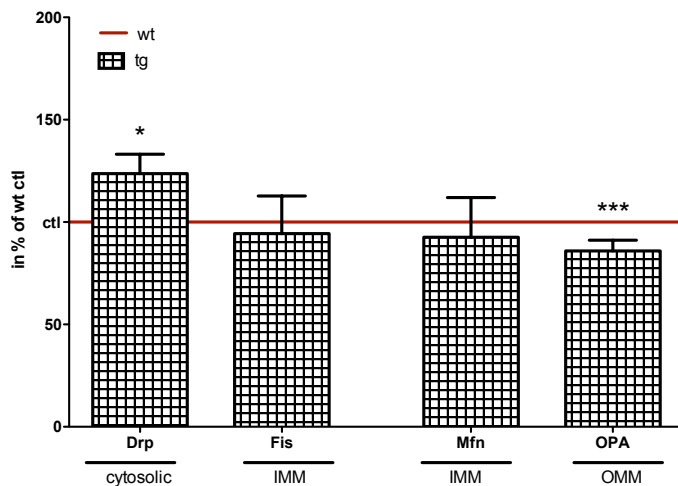
Figure 42. Mitochondrial Fission & Fusion proteins. Marker proteins for fission, dynamin related protein1 (Drp) and fission 1 related protein (Fis), as well as markers for fusion, mitochondrial fusion protein 1 (Mfn) and optic atrophie-1 (Opa), were measured using western blot analysis after electrophoretic separation and using specific antibodies in brain homogenates isolated from C57BJ/6 littermate control (ctl) and Thy-1-C57BJ/6-APP$_{SL}$ (tg) as described in material & methods. Data were normalized to littermate controls. Data represent the means ± SEM, n = 6. Two-way ANOVA with Bonferroni post-tests, *p<0,05, ***p<0,001. Representative Western Blots see figure 58.

Fission dynamin related protein1 (Drp) and fission 1 related protein (Fis) are marker proteins for mitochondrial fission (Griparic et al. 2004). Protein levels of Fis were unchanged, whereas Drp levels were significantly elevated in brains of Thy-1-C57BJ/6-APP$_{SL}$ mice (Figure 41). Mitochondrial fusion protein 1 (Mfn) and optic atrophie-1 (Opa) protein are markers for mitochondrial fission (Griparic et al. 2004). Mfn levels were unchanged, whereas protein levels of OPA were significantly reduced (Figure 42).
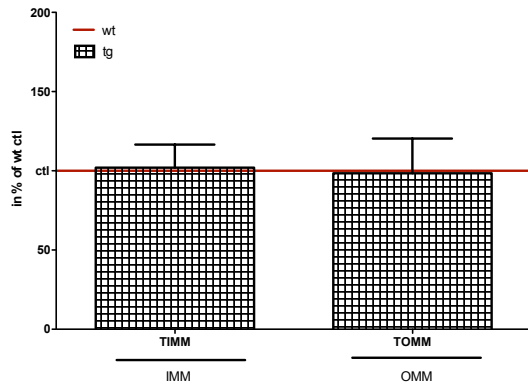
Figure 43. Mitochondrial membrane markers. Marker proteins for the inner (IMM) and the outer mitochondrial membrane (OMM) were measured in total homogenates, using western blot analysis after electrophoretic separation and using specific antibodies against translocator proteins of the inner (TIMM50) and outer (TOMM22) mitochondrial membrane, in brain homogenates isolated from C57BJ/6 littermate control (ctl) and Thy-1-C57BJ/6-APP$_{SL}$ (tg), as described in material & methods. Data were normalized to littermate controls. Data represent the means ± SEM, n = 6. Representative Western Blots see figure 58.

Protein levels of the translocase of the outer (TOMM22) and inner (TIMM50) mitochondrial membrane were not altered in brains of Thy-1-C57BJ/6-APP$_{SL}$ mice (Figure 43).
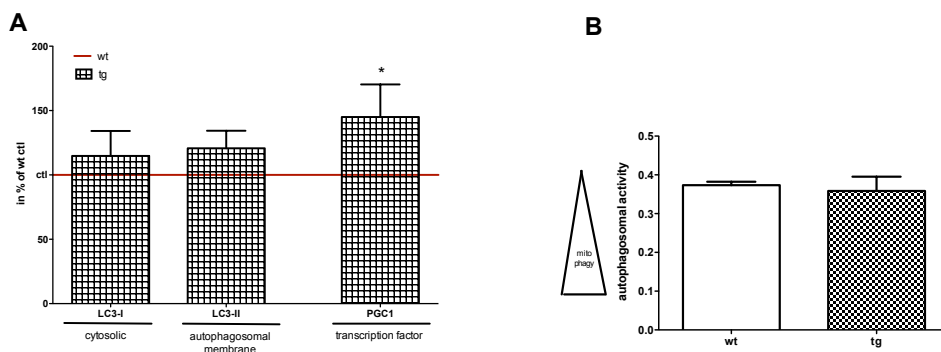
Figure 44. Autophagic activity. (**A**) Autophagy marker proteins for the cytosol (LC3-I) and autophagosomal membranes (LC3-II) as well as the transcription marker peroxisome proliferation-activated receptor gamma coactivator 1-alpha (PGC1), were measured using western blot analysis after electrophoretic separation and using specific antibodies in brain homogenates isolated from C57BJ/6 littermate control (ctl) and Thy-1-C57BJ/6-APP$_{SL}$ (tg),

as described in material & methods. A low LC3-I/LC3-II ratio indicated high degree of mitophagy. (**B**) Both, the wt and the tg model, do not differ in their autophagosomal activity. Data were normalized to littermate controls and represent the means ± SEM, n = 6-9, Two-way ANOVA with Bonferroni post-tests, *p<0,05. Representative Western Blots see figure 58.

Peroxisome proliferation-activated receptor gamma coactivator 1-alpha (PGC1) is a transcription factor, which represents a master regulator of mitochondrial biogenesis (Liang and Ward 2006; Wareski et al. 2009). PGC1 was significantly elevated in brains of Thy-1-C57BJ/6-APPSL mice (Figure 44). To estimate autophagy the marker proteins for the cytosol (LC3-I) and autophagosomal membranes (LC3-II) were determined, using Western Blot analysis. Both LC3-Isoforms, the cytosolic and the autophagosomal form, stayed unchanged in brains of Thy-1-C57BJ/6-APPSL mice, which indicated equal mitophagic activity (Figure 44).
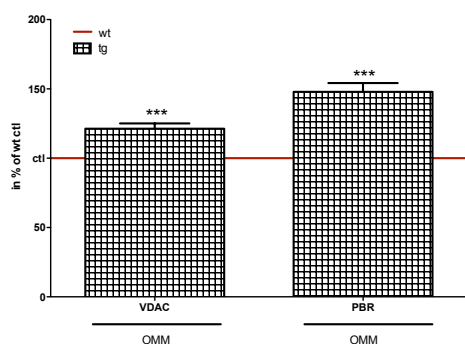
Figure 45. Mitochondrial permeability transition pore (mPTP). The mPTP marker proteins voltage-depended anion channel (VDAC) and peripheral benzodiazepine receptor (PBR), which represent markers of the mitochondrial outer mitochondrial membranes (OMM), were examined using western blot analysis after electrophoretic separation in brain homogenates isolated from C57BJ/6 littermate control (ctl) and Thy-1-C57BJ/6-APP$_{SL}$ (tg), as described in material & methods. Data were normalized to littermate controls and represent the means ± SEM, n = 6-8, Two-way ANOVA with Bonferroni post-tests, ***p<0,001. Representative Western Blots see figure 58.

In brain homogenates, isolated from Thy-1-C57BJ/6-APP$_{SL}$ mice, the concentration of both mPTP marker, VDAC and PBR, was strongly increased (Figure 45), which was in line with recent findings in HEKsw (Figure 11).
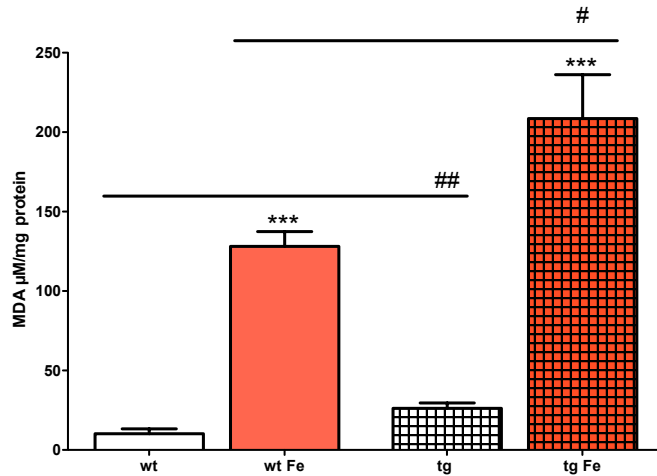
Figure 46. Malondialdehyde (MDA) levels. MDA levels were determined, using a kit based on a modified thiobarbituric-acid method at 60°C in brain homogenates, isolated from C57BJ/6 littermate control (ctl) and Thy-1-C57BJ/6-APP$_{SL}$ (tg). Brain homogenates were additionally challenged using 50 µM Fe^{2+} (Fe) for 4 hours, as described in material & methods. Data represent the means ± SEM, n = 5-6, Two-way ANOVA with Bonferroni post-tests, ***p<0,001 vs. ctl. #p<0,05, ##p<0,01 wt vs. tg.

To determine oxidative stress, the levels of malondialdehyd (MDA) – an endproduct of free radical induced lipid peroxidation - were measured in brain homogenates at basal levels and after iron induced Haber-Weiss-reaction in brain homogenates of Thy-1-C57BJ/6-APP$_{SL}$ and littermate control mice. It can be seen from Figure 46, that MDA levels were significantly higher in brains of Thy-1-C57BJ/6-APP$_{SL}$ mice and that those brains were more vulnerable towards oxidative stress *ex vitro* (Figure 46).

Effects of Olesoxim in a mouse model for Alzheimer`s disease

Olesoxim was administered via a pelletized diet or Placebo-loaded food pellets, corresponding to about a 100mg/kg dose, using oral gavage. During the three months study period, mice were examined daily to assure proper health and weighed once a week to monitor food intake.
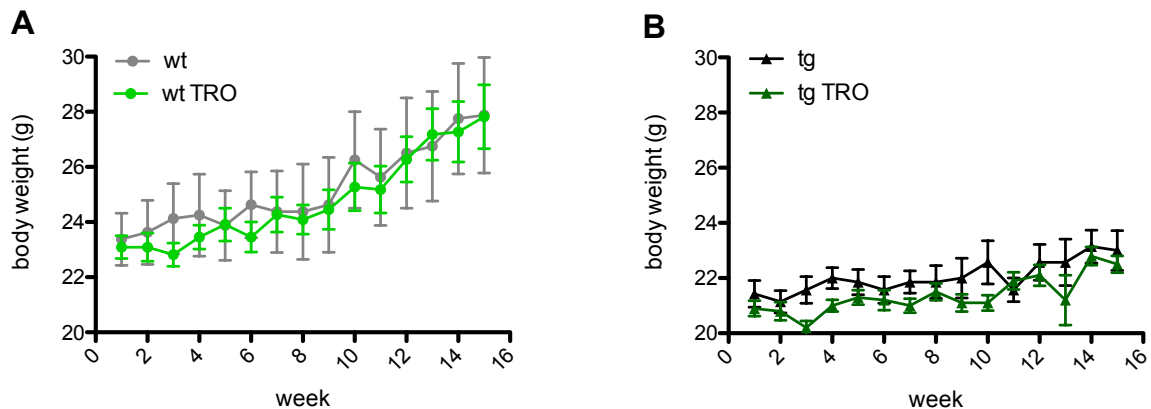
Figure 47. Development of the body weight. Body weight of (**A**) littermate control mice (wt) and (**B**) Thy-1-C57BJ/6-APP$_{SL}$ (tg) mice was followed every week, over a period of of 4 months. Mice were either fed a control diet (Placebo) or a diet containing Olesoxim (TRO), as described in material & methods. Data represent means ± SEM, n = 7-11.

Treatment of mice with Olesoxim for 15 weeks did not affect the body weight of Thy-1-C57BJ/6-APP$_{SL}$ or littermate control mice (Figure 47 A+B).
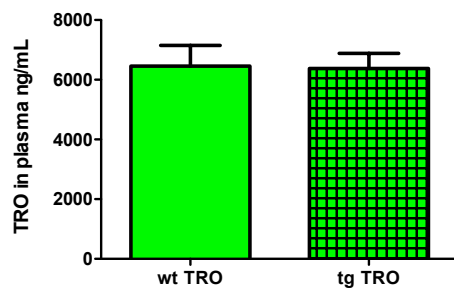
Figure 48. Olesoxim (TRO) plasma levels. Plasma samples were taken from littermate control mice (wt) and Thy-1-C57BJ/6-APP$_{SL}$ (tg) mice that were fed a diet containing Olesoxim (TRO). Olesoxim plasma levels were determined using a HPLC method by Trophos Inc. Data represent means ± SEM, n = 9-10.

Olesoxim was absorbed after oral treatment, which resulted in plasma levels of approximately 6,2 µg/ml in both mouse lines (Figure 48).
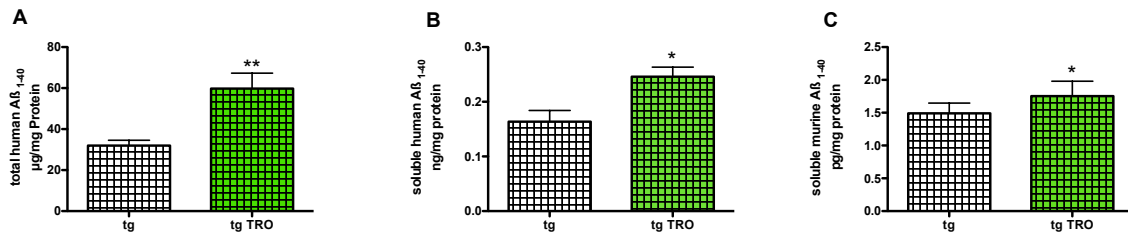
Figure 49. Brain levels of beta-amyloid peptide (Aβ1-40). Levels of (A) Total and (B) soluble human Aβ1-40, as well as (C) soluble murine Aβ1-40 were determined, using ELISA kits in brain homogenates, isolated from Thy-1-C57BJ/6-APP$_{SL}$ (tg) mice. Mice were either fed a control diet (tg) or a diet containing Olesoxim (tg TRO), as described in material & methods. Data represent the means ± SEM, n = 6-8, *p<0,05, **p<0,01, unpaired Students t-test.

Olesoxim treatment significantly enhanced total human (Figure 49 A), soluble human (Figure 49 B), and soluble mouse Aβ$_{1-40}$ levels (Figure 49 C). This finding might indicate either a reduced clearance or enhanced production of amyloid peptide in brains of Olesoxim treated mice (Figure 49). The latter seemed to be more likely, since Olesoxim interacts with cellular membranes, which might interfere with the processing of APP (refer to the discussion part).

A
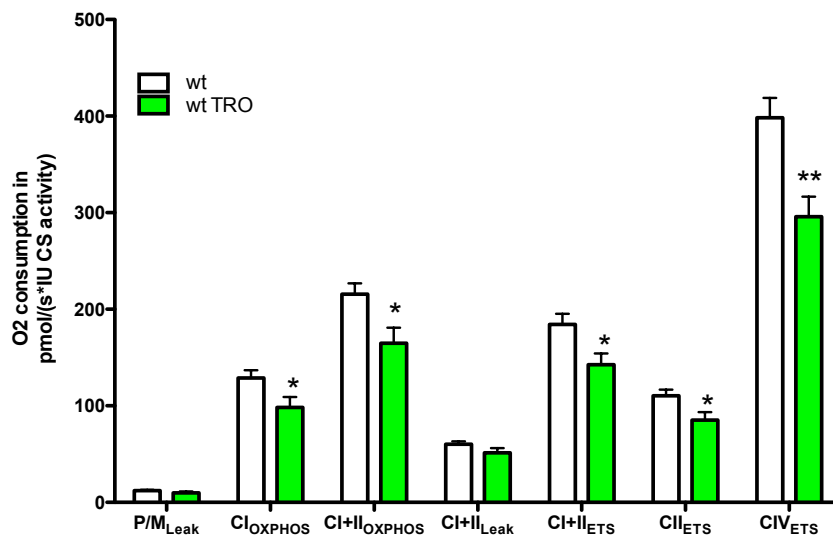
B
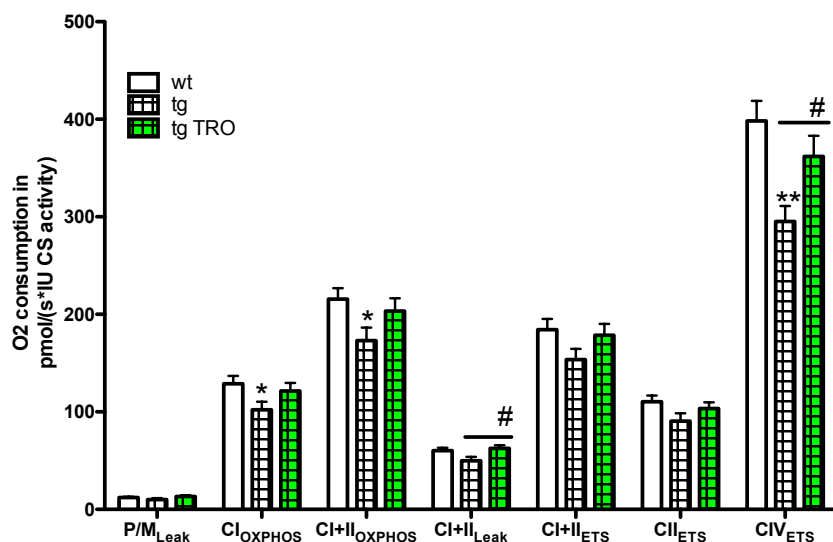
Figure 50. Mitochondrial respiration. Oxygen consumption was measured in brain mitochondria isolated from **(A)** C57BJ/6 control, either fed a control diet (wt) or a diet containing Olesoxim (wt TRO) and **(B)** Thy-1-C57BJ/6-APP$_{SL}$ mice, either fed a control diet (tg) or a diet containing Olesoxim (tg TRO), using an Oxygraph-2k. Respiration was determined in different mitochondrial stages after injecting several substrates and inhibitors (refer to material & methods). Pyruvat and Malat supplementation served as complex I substrates (P/M$_{Leak}$). Due to the lack of ADP this experimental stage was still leaky; ADP was the driving force to initiate the electron transport chain to build the proton gradient

among the inner mitochondrial membrane. ADP injection fulfilled the demands for CI dependent oxidative phosphorylation (CI_{OXPHOS}) (OXPHOS stands for oxidative phosphorylation). Adding succinat finally provided a CII substrate and enabled CI+II oxidative phosphorylation ($CI+II_{OXPHOS}$). By adding oligomycin, the ATP synthase, complex V, was inhibited and it was possible to detect the respiratory capacity on CI+II substrates to compensate for proton leak ($CI+II_{Leak}$) through the membrane. Using stepwise injection of FCCP, a ionophor that uncouples the respiratory chain, non-coupled respiration with CI and CII substrates ($CI+II_{ETS}$) was measured, which was considered as maximum capacity of the ETS (ETS stands for electron transport system). Rotenon was inhibiting complex I, making it possible to detect non-coupled CII respiration (CII_{ETS}). Antimycin A was blocking the electron transport chain by inhibiting Cytochrom C, thus electrons could not be transferred from complex III to complex IV. By supplementation of CIV substrates Ascorbat/TMPD, non-coupled respiration of complex IV was accessible (CIV_{ETS}). Values represent the means $\pm$ SEM from n = 7-9 independent experiments. Two-way ANOVA with Bonferroni post-tests, *$p<0.05$, **$p<0.001$, vs. ctl; [#]$p<0.05$; vs. tg.

Treatment of littermate control mice with Olesoxim significantly reduced the respiration of isolated brain mitochondria (Figure 50 A). Except of the $CI+II_{Leak}$ respiration, all measured activities of the respiratory chain complexes were diminished (Figure 50 A). On the other hand, treatment of Thy-1-C57BJ/6-APP$_{SL}$ mice with Olesoxim increased the respiratory activity in isolated brain mitochondria and resorted impaired respiration complex activities almost to control levels (Figure 50 B).
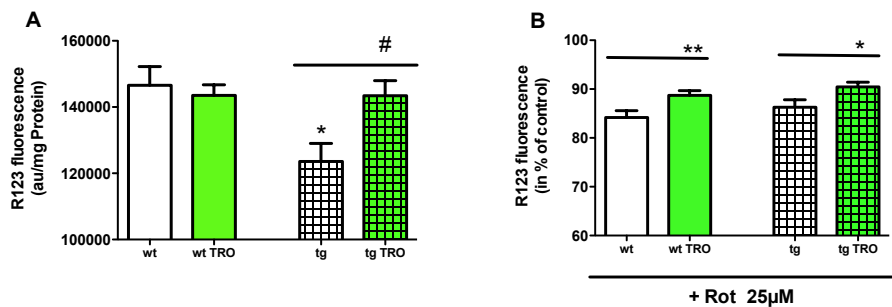
Figure 51. Mitochondrial membrane potential (MMP). (**A**) MMP was measured using the fluorescence dye Rhodamin 123 (R123) in dissociated brain cells, isolated from C57BJ/6 litter mate control (wt) and Thy-1-C57BJ/6-APP$_{SL}$ (tg), either fed a control diet or a diet containing Olesoxim (TRO), as described in material & methods. (**B**) MMP of dissociated brain cells challenged, using 25 µM rotenon (Rot) for 3 hours. Results were normalized to litter mate control. Data represent the means $\pm$ SEM; n=6-11; p*$<0,05$; p**$<0,01$; [#]$p<0,05$ vs. tg. Student`s t-test.

Olesoxim treatment had no effect on the mitochondrial membrane potential (MMP) in dissociated brain membranes, isolated from littermate control mice (Figure 51 A). Treatment of Thy-1-C57BJ/6-APP$_{SL}$ mice with Olesoxim restored the impaired MMP in dissociated

brain cells (Figure 51 A). Dissociated brain cells, isolated from brains of Thy-1-C57BJ/6-APP$_{SL}$ mice, as well as from littermate control mice that received Olesoxim, were protected from rotenon induced inhibition of complex I activity (Figure 51 B).
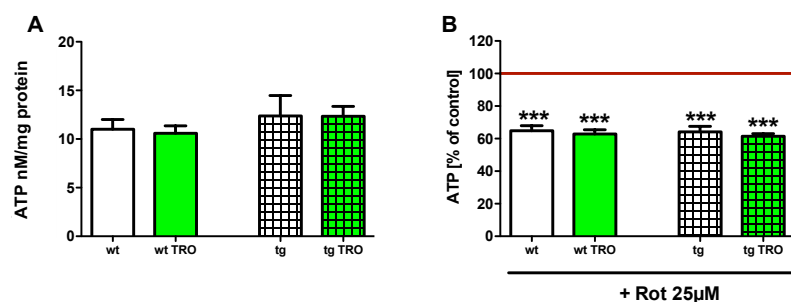
Figure 52. Adenosine triphosphate (ATP) levels. (**A**) ATP levels (nM/mg protein) were determined using a luminescence kit in dissociated brain cells isolated from C57BJ/6 litter mate control (wt) and Thy-1-C57BJ/6-APP$_{SL}$ (tg) either fed a control diet or a diet containing Olesoxim (TRO) as described in material & methods. (**B**) ATP levels of dissociated brain cells, challenged using 25 nM rotenon (Rot) for 1,5 hours. Results were normalized to litter mate control. Data represent the means ± SEM; n=7-11; p***<0,01; Student`s t-test.

Treatment of mice with Olesoxim had no effect on ATP-levels in dissociated brain cells, neither of Thy-1-C57BJ/6-APPSL mice, nor of littermate control mice (Figure 52). Moreover, no effects on rotenon-induced stress were observed (Figure 52 B).
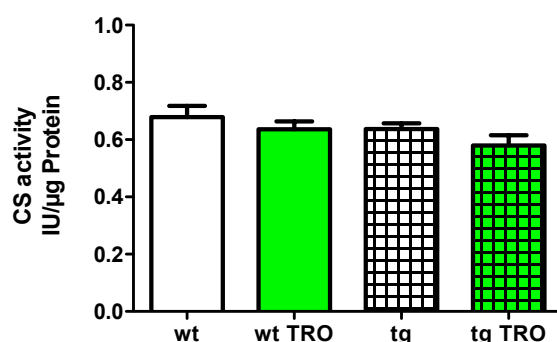
Figure 53. Citrate synthase (CS) activity. CS was determined using a spectrophotometric method at 412nm and 30°C in mitochondria isolated from C57BJ/6 littermate control (ctl) and Thy-1-C57BJ/6-APP$_{SL}$ (tg), either fed a control diet or a diet containing Olesoxim (TRO) as described in material & methods. Data represent the means ± SEM; n=7-11.

Treatment of mice with Olesoxim had no effect on citrate synthase (CS) activity in brain mitochondria, isolated neither of Thy-1-C57BJ/6-APPSL mice, nor from littermate control mice (Figure 53).
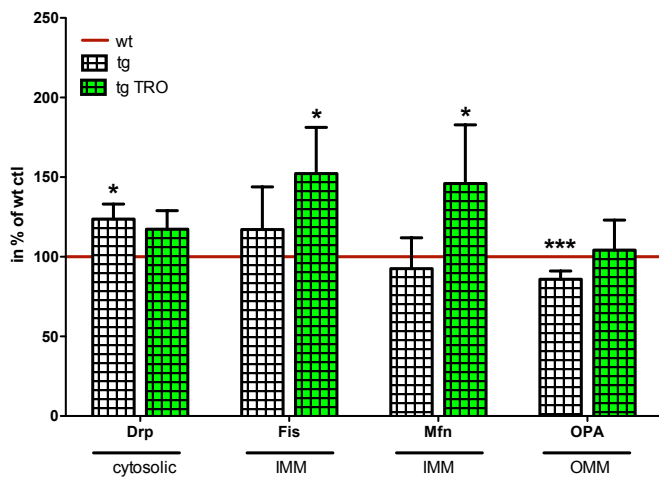
Figure 54. Mitochondrial Fission & Fusion proteins. Marker proteins for fission: dynamin related protein1 (Drp) and fission 1 related protein (Fis), as well as markers for fusion: mitochondrial fusion protein 1 (Mfn) and optic atrophie-1 (Opa), were measured using western blot analysis after electrophoretic separation and using specific antibodies in brain homogenates isolated from C57BJ/6 littermate control (wt) and Thy-1-C57BJ/6-APP$_{SL}$ (tg), either fed a control diet (tg) or a diet containing Olesoxim (tg TRO), as described in material & methods. Data were normalized to littermate controls. Data represent the means ± SEM, n = 6-11. Two-way ANOVA with Bonferroni post-tests, *p<0,05, ***p<0,001. Representative Western Blots see figure 58.

Treatment of Thy-1-C57BJ/6-APP$_{SL}$ with Olesoxim increased the levels of fission 1 related protein (Fis), mitochondrial fusion protein 1 (Mfn), and – to a lower extent - optic atrophie-1 protein (Opa) in brain homogenates, indicating enhanced fission & fusion events (Griparic et al. 2004) (Figure 54).
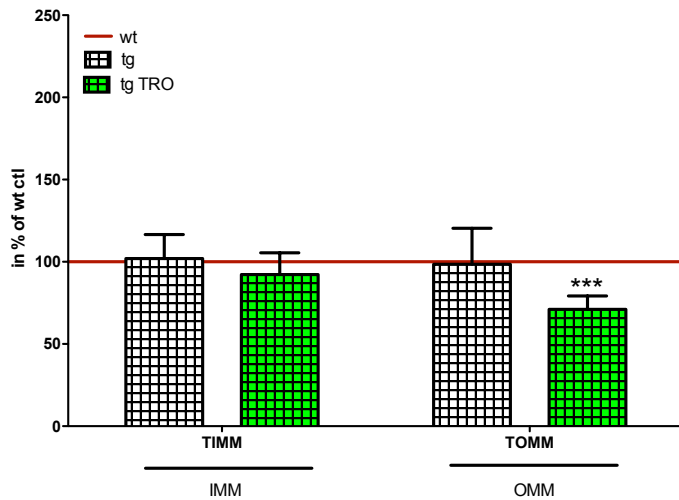
Figure 55. Mitochondrial membrane markers. Marker proteins for the inner (IMM) and the outer mitochondrial membrane (OMM) were measured in total homogenates using western blot analysis after electrophoretic separation and using specific antibodies against translocator proteins of the inner (TIMM50) and outer (TOMM22) mitochondrial membrane in brain homogenates isolated from C57BJ/6 littermate control (wt) and Thy-1-C57BJ/6-APP$_{SL}$ (tg) either fed a control diet (ctl) or a diet containing Olesoxim (TRO), as described in material & methods. Data were normalized to littermate controls (ctl). Data represent the means ± SEM, n = 6. p***<0,01; Student`s t-test. For representative Western Blots see figure 58.

Treatment of Thy-1-C57BJ/6-APP$_{SL}$ mice with Olesoxim significantly decreased protein levels of TOMM20, a marker protein of the outer mitochondrial membrane (Figure 55). Levels of TIMM50, a marker protein for the inner mitochondrial membrane, stayed unchanged (Figure 55).

A
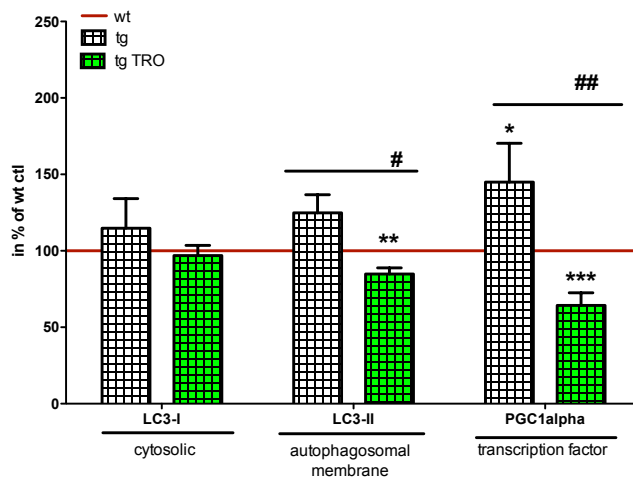
B
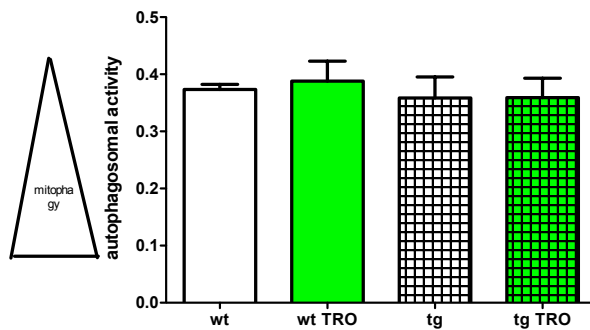
Figure 56. Autophagic activity. (**A**) Autophagy marker proteins for the cytosol (LC3-I) and autophagosomal membranes (LC3-II) as well as the transcription marker peroxisome proliferation-activated receptor gamma coactivator 1-alpha (PGC1alpha) were measured using western blot analysis after electrophoretic separation and using specific antibodies in brain homogenates isolated from C57BJ/6 littermate control (wt) and Thy-1-C57BJ/6-APP$_{SL}$ (tg), either fed a control diet (wt or tg) or a diet containing Olesoxim (wt TRO or tg TRO), as described in material & methods. A low LC3-I/LC3-II ratio indicated a high degree of mitophagy. (**B**) Within the four study groups, there is no difference detectable in the autophagosomal activity. Data were normalized to littermate controls and represent the means ± SEM, n = 5-9, Two-way ANOVA with Bonferroni post-tests, *p<0,05, **p<0,01, ***p<0,001; [#]p<0,05, [##]p<0,01 vs. tg. Representative Western Blots see figure 58.

Elevated LC3-II expression levels in Thy-1-C57BJ/6-APPSL mice were decreased after Olesoxim treatment (Figure 56 A). However, the autophagosomal activity seemed to be unaffected in all study groups, as indicated by unchanged LC-1 to LC-II ratios (Figure 56 B). Increased PGC1 protein levels in brains of Thy-1-C57BJ/6-APP$_{SL}$ mice were diminished beyond basal levels of littermate controls, after treatment with Olesoxim (Figure 56 A).
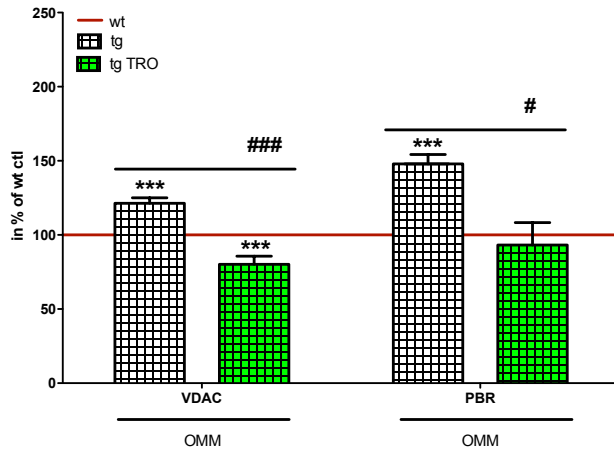
Figure 57. Mitochondrial permeability transition pore (mPTP). The mPTP marker proteins voltage-depended anion channel (VDAC) and peripheral benzodiazepine receptor (PBR) were examined using western blot analysis after electrophoretic separation in brain homogenates isolated from C57BJ/6 littermate control (wt) and Thy-1-C57BJ/6-APP$_{SL}$ (tg), either fed a control diet (wt or tg) or a diet containing Olesoxim (wt TRO or tg TRO), as described in material & methods. Data were normalized to littermate controls and represent the means ± SEM, n = 6-8, Two-way ANOVA with Bonferroni post-tests, ***p<0,001; #p<0,05, ###p<0,01 vs. tg. Representative Western Blots see figure 58.

The mPTP marker proteins voltage-depended anion channel (VDAC) and peripheral benzodiazepine receptor (PBR) were significantly reduced in brain homogenates, isolated from Olesoxim treated Thy-1-C57BJ/6-APP$_{SL}$ mice. Levels of VDAC were even lower than in littermate control mice (Figure 57).
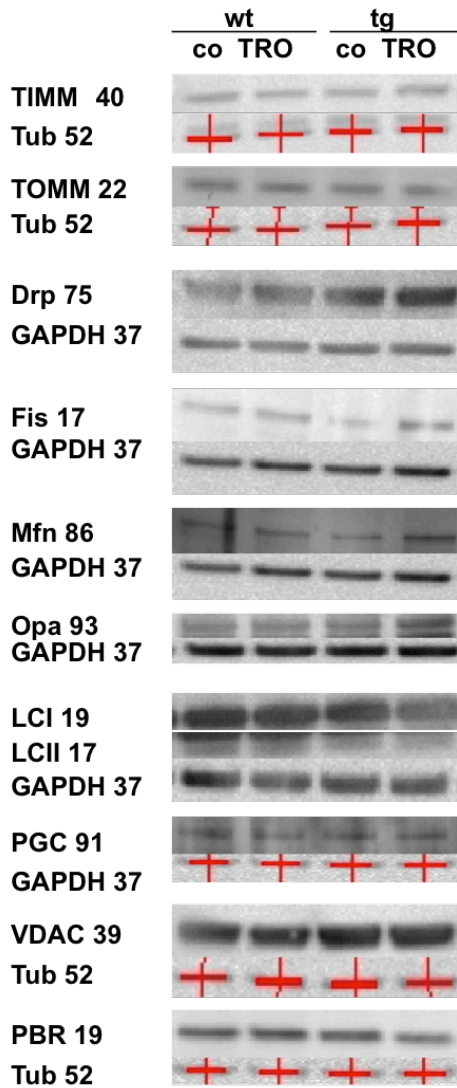
Figure 58. Representative examples of western blot analysis from figures 40-57, after electrophoretic separation in brain homogenates isolated from C57BJ/6 littermate control (wt) and Thy-1-C57BJ/6-APP$_{SL}$ (tg), either fed a control diet (wt or tg) or a diet containing Olesoxim (wt TRO or tg TRO), as described in material & methods. n = 5-11.

Description of the particular marker on the Western Blots, see Figures 40-57.
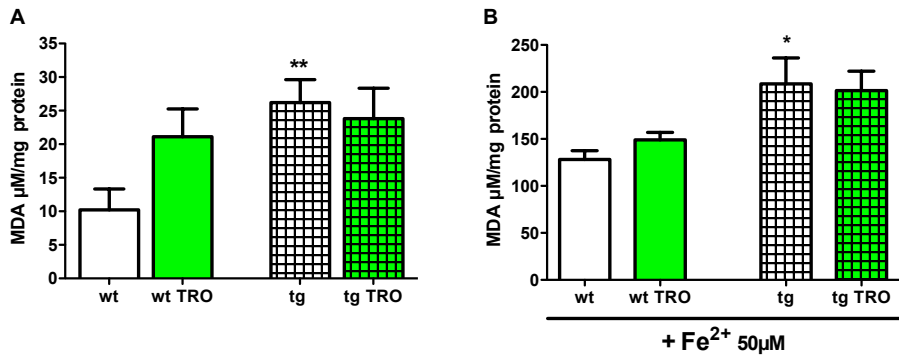
Figure 59. Malondialdehyde (MDA) levels. MDA levels were determined using a kit based on a modified thiobarbituric-acid method at 60°C in brain homogenates isolated from C57BJ/6 littermate control (wt) and Thy-1-C57BJ/6-APP$_{SL}$ (tg), either fed a control diet (wt or tg) or a diet containing Olesoxim (wt TRO or tg TRO). Brain homogenates were additionally challenged, using 50 μM Fe^{2+} (Fe) for 4 hours, as described in material & methods. Data represent the means ± SEM, n = 5-11, Two-way ANOVA with Bonferroni post-tests, *p<0,05, **p<0,01.

To detremine oxidative stress, the levels of malondialdehyd (MDA) – an endproduct of free radical induced lipid peroxidation - were measured in brain homogenates at basal levels and after iron induced Haber-Weiss-reaction in brain homogenates of Thy-1-C57BJ/6-APP$_{SL}$ and littermate control mice. It can be depicted from Figure 59, that Olesoxim treatement numerically increased MDA levels in brain homogenate, isolated from brains of littermate control mice, without being statistically significant. Brain homogenates, isolated from Thy-1-C57BJ/6-APP$_{SL}$ mice or littemate controls, were equal vulnerable against oxidative stress *in vitro* (Figure 59 B).

Table R1: Summary of Results. Characterization and treatment with Dimebon (Dim) or Olesoxim (TRO) of HEK293 cells transgenic for the 695 amino acid form of the human APP-gene, including the Swedisch APP-mutation (HEKsw) and C57BJ/6 mice transfected with the 751 amino acid form of human APP with the Swedish (KM670/671NL) and London (V717L) mutations, under the control of a neuron-specific murine Thy1 promotor (Thy1-APPSL). Main findings were expressed as change compared to untransfected control cells (HEKut) and litter mate control mice, respectively. Please refer to the results section for quantitative data and further details.

Parameter	HEKsw	HEKsw + Dim	HEKsw + TRO	Thy1-APP$_{SL}$	Thy1-APP$_{SL}$ + TRO
Aβ load	↑	↓	↑	↑	↑
OXPHOS capacity	↓	↑	↑	↓	↑
MMP	↓	↓	↓	↓	↑
MMP + CI inhibition	↔	↑	↑	↔	↑
ATP level	↓	↔	↓	↔	↔
ATP level + CI inhibition	↓	↔	↔	↔	↔
CS activity	↔	↑	↔	↔	↔
Mitochondrial length	↓	↑	↑		n.d.
Mitochondrial density	↓	↑	↑	n.d.	n.d.
TIMM50	↓	↑	↑	↔	↔
TOMM22	↔	↓	↔	↔	↓
Drp	↑	↑	⇧	↑	↑
Fis	↔	⇧	↑	↔	↑
Mfn	↔	⇧	⇧	↔	↑
Opa	↓	↑	↑	↓	↑
LC3-I | LC3-II	↓|↓	↑|↑	↑|↑	↔|↔	-|↓
Autophagic activity	↑	⇩	↔	↔	↔
PGC1alpha	↔	↔	↔	↑	↓
VDAC	↑	↓	↓	↑	↓
PBR	↑	↓	↓	↑	↓
ROS ± CI inhibition	↑	↓	n.d.	n.d.	n.d.
MDA ± Fe^{2+} stress	n.d.	n.d.	n.d.	↑	↔

n.d. = not determined, effects are indicated by arrows. Blank arrows indcate a trend

Discussion

Having a multifactorial pathology, AD makes it difficult to develop feasible therapies. Currently approved drugs solely attenuate symptoms, but do not cure the disease. Research into AD also has had several failures, in terms of developing disease-modifying therapies. Since AD starts many years far before the first symptoms occur, new scientific approaches therefore focus on early stage, which are discussed to be important in ageing and the onset of AD. The advanced mitochondrial cascade hypothesis is becoming the leading model for LOAD (Mueller et al. 2016). It also integrates physiological ageing as the main risk factor for LOAD (Stockburger et al. 2014; Mueller et al. 2016). Thus, mitochondrial dysfunction, as an early event in AD, represents a promising target for new therapeutics (Bubber et al. 2005; Lynn et al. 2010; Muller et al. 2010; Eckert et al. 2012a; Friedland-Leuner et al. 2014; Schuh et al. 2014). Accordingly, the efficacy of Dimebon and Olesoxim - two mitochondria targeting drugs - were tested in a cellular and a mouse model of LOAD in frame of this thesis.

Characterization of disease models

HEKsw cells and Thy1-APP$_{SL}$ mice were characterized as *in vitro* and *in vivo* model of AD, respectively. The main findings are summarized in table D1 and discussed below.

Table D1: Characterization of HEK293 cells transgenic for the 695 amino acid form of the human APP-gene, including the Swedisch APP-mutation (HEKsw) and C57BJ/6 mice transfected with the 751 amino acid form of human APP with the Swedish (KM670/671NL) and London (V717L) mutations, under the control of a neuron-specific murine Thy1 promotor (Thy1-APP$_{SL}$). Main findings are expressed as change, compared to untransfected control cells (HEKut) and littermate control mice, respectively. Refer to the results section for quantitative data and further details.

Parameter	HEKsw	Thy1-APP$_{SL}$
Aβ load	↑	↑
OXPHOS capacity	↓	↓
MMP	↓	↓
MMP + CI inhibition	←→	←→
ATP level	↓	←→
ATP level + CI inhibition	↓	←→
CS activity	←→	←→
Mitochondrial length	↓	n. d.
Mitochondrial density	↓	n. d.
TIMM50	↓	←→
TOMM22	←→	←→
Drp	↑	↑
Fis	←→	←→
Mfn	←→	←→
Opa	↓	↓
LC3-I / LC3-II	↓ | ↓	←→ | ←→
Autophagic activity	↑	←→
PGC1alpha	←→	↑
VDAC	↑	↑
PBR	↑	↑
ROS ± CI inhibition	↑	n.d.
MDA ± Fe^{2+} stress	n.d.	↑

n.d. = not determined, arrows in black indicate common changes in both models; arrows in red indicate differences between models.

Cellular HEK model of AD

Transfected human embryo kidney cells (HEK293 cells) represent a common model to investigate Aβ – related effects *in vitro* (Walsh et al. 2001; Su et al. 2004; Hoyer et al. 2005; Peters et al. 2009; Zheng et al. 2009; Zhu et al. 2009; Feng et al. 2010; Kurz et al. 2010; Zhu et al. 2011; Chami et al. 2012; Qin et al. 2012; Fan et al. 2013; Zou et al. 2013; Jun et al. 2014; Pohland et al. 2016). HEK293 cells have been transfected with various vectors, introducing the human wild type APP-gene and different APP-mutations, including the Swedish APP-mutation, which has been used for this work (Borg et al. 1998; Su et al. 2004; Peters et al. 2009; Zheng et al. 2009; Zhu et al. 2011; Chami et al. 2012; Eckert et al. 2012b; Leuner et al. 2012b).

Even though not neuronal, HEK293-APPsw (HEKsw) cells represent a model of chronic Aβ stress (Keil et al. 2004). Compared to other cell systems, e.g. PC12sw or SH-SY5Y-APPSW cells, HEKsw cells are characterized by a high expression rate of the APP and its mutated forms (Keil et al. 2004; Stockburger et al. 2014; Hagl et al. 2015a; Pohland et al. 2016).

HEK293 cells (HEKut) produced approximately 4 pg Aβ1-42 per mg protein in 24 hours (Peters et al. 2009; Pohland et al. 2016). In HEKsw cells, levels of Aβ1-40 were even higher and reached approx. 2000 pg/mg protein (Leuner et al. 2012b). These results are in line with earlier findings by Keil et al., who reported that HEKut and HEKsw secreted approx. 35 and 2958 pg/ml Aβ1-40 & Aβ1-42 in the cell culture medium (Keil et al. 2004). Increased levels of Aβ were related to increased expression of APP in transfected HEK cells (Keil et al. 2004; Pohland et al. 2016).

It has been shown that the secretion of Aβ has functional consequences in HEKsw cells, that may reflect towards a pathological mechanisms of AD. Excessive generation of nitric oxide has been implicated in the pathogenesis of AD (Malinski 2007; Virarkar et al. 2013) and nitrosative and oxidative stress had been linked to apoptosis in AD (Obulesu and Lakshmi 2014; Radi et al. 2014; Kim et al. 2015). HEKsw cells showed significantly increased levels of apoptotic cells (Keil et al. 2004), enhanced ROS levels, (Leuner et al. 2012b), enhanced NO levels, a rise in nitrosylated proteins and enhanced activity of NOS (Keil et al. 2004).

ROS and RNS are normally generated by tightly regulated enzymes and at moderate

concentrations. Furthermore, they are involved in the normal physiology of many processes such as signaling pathways or induction of mitogenic response (Valko et al. 2007). Mitochondria are the main source of oxidative stress in cells, as oxygen is used for the mitochondria related energy production. Oxidative stress affects mitochondrial proteins, mitochondrial lipids and mitochondrial DNA, which in turn leads to neuronal damage. HEKsw cells were characterized regarding mitochondrial bioenergetics including respiration, mitochondrial membrane potential and ATP production. Moreover, mitochondrial dynamics, mitophagy, formation of mitochondrial permeability transition pore, mitochondrial content and mitogenesis were examined (table D1).

In HEKsw cells the oxidative phosphorylation capacity, the activity of CIV and the electron transfer system in the non-coupled state were significantly diminished. Due to the measured overall reduction in the capacity of the respiratory system, HEKsw cells showed a significant lower MMP and significantly reduced ATP levels. These data confirm earlier findings from our lab. Leuner et al. reported a decreased respiratory control ratio (RCR) in HEKsw cells, which indicated a reduced respiration and an impaired coupling of the complexes of the respiration chain (Leuner et al. 2012b). Accordingly, the MMP and levels of ATP were significantly reduced in HEKsw cells (Leuner et al. 2012b). These recent data are also in agreement with earlier findings (Keil et al. 2004). However, Keil et al. reported a larger difference in mitochondrial related parameters between HEKut and HEKsw cells (Keil et al. 2004). Impaired mitochondrial respiration, membrane potential and ATP levels were also shown in neuronal cells, harboring human APP, e.g. in SH-SY5Y-APPwt cells (Stockburger et al. 2014) and PC12-APPsw cells (Keil et al. 2004; Kurz et al. 2010; Hagl et al. 2015a). Interestingly, both authors Keil and Hagl et al. reported an increased MMP in PC12-APPsw cells (Keil et al. 2004; Hagl et al. 2015a). Hagl et al. investigated this phenomenon further and identified an increase in the mitochondrial mass as possible reason for the increased MMP. Keil and coworkers also reported an increase in mitochondrial content, determined with confocal laser scanning microscopy in PC12APPsw cells (Keil et al. 2004). The increase in mitochondrial contents probably counteracts the impaired ATP production observed in PC12APPsw cells (Hagl et al. 2015a). Mitochondrial biogenesis was obviously not induced by PGC1 dependent gene expression, but increased mitochondrial fission representing a PGC1 independent way of generating new mitochondria (Santos et al. 2010; Youle and van der Bliek 2012). This contributed at least partly to an increased mitochondrial content, detected in PC12APPsw cells (Hagl et al. 2015a).

Besides impaired function of mitochondrial respiratory chain complexes, mitochondrial dysfunction included deficits of mitochondrial dynamics, such as impaired balance between fission and fusion mechanisms, abnormal shaping of mitochondria and reduced mitochondrial trafficking (Benard and Rossignol 2008; Stockburger et al. 2014; Hagl et al. 2015a; Lionaki et al. 2015; Stockburger et al. 2015). Fragmented mitochondria could either enforce autophagosomal activity or enhance apoptosis (Knott and Bossy-Wetzel 2008; Santos et al. 2010; Lionaki et al. 2015).

Substantial differences between HEKut controls and HEKsw cells were detected. In HEKsw cells most mitochondria showed truncated morphology, followed by punctuated mitochondria, supporting previous findings about pronounced effects of Aβ on mitochondrial dynamics (Trimmer et al. 2000; Wang et al. 2008). Inhibition of complex I of the mitochondrial respiratory chain led to mitochondrial fragmentation (Fang et al. 2012; Leuner et al. 2012b). Accordingly, in HEKut cells mitochondria were highly fragmented after inhibition of complex I with Rotenon. Mitochondria in HEKsw cells nearly do not change their form after inducing complex I dysfunction, which may indicate, that these cells were already maximal stressed.

To further examine the dynamic machinery, mitochondrial densities were determined. To evaluate the observed changes in mitochondrial length in more detail, protein levels of the fission & fusion machinery, as well as markers for mitophagy and swelling were measured.

Fission dynamin related protein1 (Drp) and fission 1 related protein (Fis) are marker proteins for mitochondrial fission (Santos et al. 2010). Protein levels of Fis stayed unchanged in our model, whereas Drp levels are significantly elevated in HEKsw cells. Mitochondrial fusion protein 1 (Mfn) and optic atrophie-1 (Opa) protein are markers for mitochondrial fusion (Santos et al. 2010). Mfn levels stayed unchanged, whereas protein levels of OPA were strongly reduced. Both changes led to a shift towards shorter mitochondria – a distribution pattern that can also be observed after hypoxia-reoxygenation stress (Liu and Hajnoczky 2011).

Fragmented mitochondria may enforce autophagosomal activity or enhance apoptosis in neurodegenerative disorders (Knott and Bossy-Wetzel 2008; Santos et al. 2010; Lionaki et al. 2015). Autophagy is a vesicle and lysosome-mediated degradative pathway, that is essential

for protein homeostasis and cell health (Zare-Shahabadi et al. 2015). The autophagosome-lysosome pathway degrades ageing organelles and protein aggregates, which is particularly crucial in neurons (Wong and Holzbaur 2015). In particular, compared to non-neuronal cells, neurons are dependent on high basal autophagy for survival. There is emerging agreement, that defects in autophagy are likely to contribute to the neurodegenerative processes in numerous diseases, including AD (Ghavami et al. 2014). Autophagy-lysosome defects occur early in the pathogenesis of AD and have been proposed to be a significant contributor to the disease process (Zare-Shahabadi et al. 2015). Autophagosomes are preferentially formed at the axon tip and undergo a retrograde transport back towards the cell body. Autophagosomes incorporate cargo, including damaged mitochondria (mitophagy) and protein aggregates and subsequently fuse with lysosomes during axonal transport to effectively degrade their internalized cargo (Wong and Holzbaur 2015). Thus, mitophagy may reduce the mitochondrial production of reactive oxygen species, through recycling of old and damaged mitochondria (Hensley and Harris-White 2015).

Different methods are available to measure autophagy including microtubule-associated protein light chain 3 (LC3) immunoblotting (Klionsky et al. 2007; Mizushima and Yoshimori 2007). Recently, guidelines for the use and the interpretation of assays to monitor autophagy have been published (Klionsky et al. 2016). The method using LC3 immunoblotting has pitfalls such as different immunoreactivity of LC-I and LC-II as well as other methods as well. However, it is the most widely used method. LC3 was detected as two bands following SDS-PAGE and immunoblotting: one represented cytosolic LC3-I. LC3-II was conjugated with phosphatidylethanolamine (PE) and was present on membranes and autophagosomes, and much less on autolysosomes (Kabeya et al. 2004; Mizushima and Yoshimori 2007). The precursor protein of LC3 (proLC3) is not detected under normal conditions (Mizushima and Yoshimori 2007). Both LC3-Isoforms, the cytosolic and the autophagosomal form were reduced in HEKsw cells, which indicates enhanced mitophagic activity. This finding is further supported by a reduced ratio of the LC3- isoforms, indicating enhanced autophagic activity (Mizushima and Yoshimori 2007).

Fragmented mitochondria in HEKsw cells may induce apoptosis after formation and opening of the mitochondrial permeability transition pore (mPTP) (Knott and Bossy-Wetzel 2008). Key for the mitochondrial-mediated intrinsic apoptotic pathway is the release of cytochrome *c* and other apoptotic factors, which is regulated by VDAC, the peripheral benzodiazepine

receptor (PBR or TSPO) and other proteins (see figure E1) (Cesura et al. 2003; Repalli 2014). Together with VDAC, PBR is a constituent of the mitochondrial permeability transition pore (mPTP). Its formation induces mitochondrial swelling and cytochrom *c* release, that initiates a molecular cascade leading to apoptosis (Forte 2004). Increased expression of PBR was observed in both, elderly people and in patients with Alzheimer's disease (Repalli 2014). Both mPTP markers, VDAC and PBR were broadly increased in HEKsw cells, indicating enhanced mPTP formation and finally enhanced apoptosis. However, further experiments have to enlighten, e.g. if mitochondria isolated from HEKsw cells show enhanced cristae swelling such recently reported for SH-SY5Y-APPsw cells (Stockburger et al. 2014). Based on recent unpublished data, showing that incubation of SH-SY5Y-APPsw with the mPTP inductor actractyloside enhanced mitochondrial fragmentation (Stockburger 2014), the possible relationship between enhanced fission and mPTP-opening markers should be experimentally investigated in HEKsw cells as well.

To establish, whether the detected dysfunctional energy parameters (OXPHOS, MMP, ATP) were based on deficient mitochondria or merely due to a loss of mitochondrial mass in HEKsw cells, citrate synthase (CS) activity was measured. CS as Krebs-cycle enzyme is constantly expressed in the matrix of mitochondria, thus CS activity is highly correlated with mitochondrial mass and has been found to be an accurate marker for mitochondrial content (Larsen et al. 2012).

CS activity was not significantly changed in HEKsw cells compared to HEKut control cells, suggesting that the mitochondrial content was not changed. According to Larsen and coworkers, the activities of respiratory complexes CI, CII, CIII, and CIV are also good markers to investigate mitochondrial content (Larsen et al. 2012). However, activities of all four respiratory chain complexes, as well as the area occupied by mitochondria, were significantly reduced in HEKsw cells. The latter finding, can be explained by a significantly reduced MMP: The dye Mito Tracker CMXRos, which was used to visualize mitochondria for confocal microscopy, attaches in a voltage dependent fashion at the inner mitochondrial membrane (Poot et al. 1996). Thus, the reduced MMP in HEKsw cells could contribute to a lower dye load and consequently result in lower measures of density. The aforementioned mitochondrial parameters are related to the inner mitochondrial membrane (Eckmann et al. 2013). To clarify the impact of mitochondrial membranes on impaired functionality and/or lower density appropriate protein markers were measured (Eckmann et al. 2013). In contrast to the translocase of the outer mitochondrial membrane (TOMM22) protein levels of the

translocase of the inner mitochondrial membrane (TIMM50) were strongly diminished in HEKsw cells. Thus, a deficient inner mitochondrial membrane would match with the data, presented for HEKsw cells: Reduced TIMM50 level indicated less inner mitochondrial membrane, which could explain the described deficits in OXPHOS, MMP, ATP and mitochondrial morphology.

Peroxisome proliferation-activated receptor gamma coactivator 1-alpha (PGC1) is a transcription factor, that represents the master regulator of mitochondrial biogenesis (Lopez-Lluch et al. 2008; Gonzalez-Freire et al. 2015). PGC1 exhibits various beneficial functions apart from mitochondrial biogenesis, for example peroxisomal remodeling and contribution to ROS removal (Austin and St-Pierre 2012). PGC1 was not altered in HEKsw cells, which may indicate a constant mitochondrial biogenesis. Equal CS activities in both investigated cell lines support the notion of an unchanged mitochondrial content in HEKsw cells (see above) (Larsen et al. 2012).

Murine C57BJ/6-Thy1-APP$_{SL}$ model of AD

C57BJ/6-Thy1-APP$_{SL}$ (Thy1-APP$_{SL}$) mice are transgenic for the 751 amino acid form of APP with the Swedish (KM670/671NL) and London (V717L) mutations under the control of a neuron-specific murine Thy1 promoter (Blanchard et al. 2003). These mice are also known as **APP22** (please refer to table 1). At the age of 3 months, elevated Aβ levels were detected in brains of Thy1-APP$_{SL}$ mice, first Aβ plaques can be found at the age of 6 months (Blanchard et al. 2003; Hauptmann et al. 2009). Keil et al. were the first, who reported significantly decreased MMP and ATP levels in dissociated brain cells (DBC) of 3-month-old Thy1-APP$_{SL}$ mice (Keil et al. 2004). Hauptmann et al. elucidated the model in more detail and confirmed decreased MMP and ATP levels in DBC of 3 months-old but also at 6 months-old Thy1-APP$_{SL}$ mice (Hauptmann et al. 2009). The extent of these deficits was comparable in 3 and 6 month-old Thy1-APP$_{SL}$ mice, although the histological state already showed substantial plaque formation (Blanchard et al. 2003; Hauptmann et al. 2009). Interestingly, effects on mitochondrial dysfunction were numerically more pronounced in 3-months-old mice. The authors hypothesized, that Aβ may already led to mitochondrial dysfunction, even before plaque formation occurres (Hauptmann et al. 2009). Moreover, the data suggested mitochondrial dysfunction as an early event in Aβ related pathogenesis. Data presented in this thesis confirm reduced MMP measures in dissociated brain cells, isolated from 3-months old Thy1-APP$_{SL}$ mice (table D1). However, ATP levels were unchanged. Subsequent studies confirmed reduced ATP levels in DBC isolated from 3-months old, but not from 9 months old Thy1-APP$_{SL}$ mice (Maximilian Pohland, personal communication; paper under revision). Thus, the extend of mitochondrial dysfunction in the brain seems to vary in Thy1-APP$_{SL}$ mice in different studies. It cannot be excluded that environmental factors, such as different conditions of handling, diet and seasons may have an impact on mitochondrial functions (Mo et al. 2015). In frame of this thesis, Thy1-APP$_{SL}$ mice were further characterized, regarding mitochondrial related function and parameters (table D1).

First of all, the activities of the complexes I-IV of the respiration chain were measured. Significantly reduced activities of CI, CI&II, and CIV were determined in mitochondria isolated from brains of Thy1-APP$_{SL}$ mice, which could explain the decreased MMP measures (see above). Since ATP levels were unchanged, it could be speculated that the OXPHOS capacity was able to still maintain basal ATP levels in brains of Thy1-APP$_{SL}$ mice. However, mitochondrial dysfunction has been shown to raise the production of reactive oxygen species

(ROS) (Nijtmans et al. 2004). The complexes, that are considered responsible for the majority of superoxide generation are CI, CII, and CIII (Nicholls 2002; Nijtmans et al. 2004). Thus, impaired activity of CI and CII may have led to enhanced ROS production, that would explain the determined increased levels of malondialdehyde (MDA) in brains of Thy1-APP$_{SL}$ mice. However, Schuessel et al. reported increased hydroxynonenal (HNE) levels, another marker molecule for lipid peroxidation, in brain homogenates from Thy1-APP$_{SL}$ mice, which was related to a reduced activity of mitochondrial Cu/Zn-super oxide dismutase (SOD) (Schuessel et al. 2005). In this study MDA levels were unchanged (Schuessel et al. 2005), as well as in 19-22 months-old PS1M146 mice, which represent another AD model (Table 1) (Schuessel et al. 2006). The same paper reported significantly increased HNE levels in brain homogenates (Schuessel et al. 2006).

To establish, whether the detected dysfunctional energy parameters (OXPHOS, MMP) and enhanced oxidative stress (MDA) were based on deficient mitochondria or were merely due to a loss of mitochondrial mass in brains of Thy1-APP$_{SL}$ mice, CS activity was measured. CS is constantly expressed in mitochondria, thus CS activity is highly correlated with mitochondrial mass and has been found to be an accurate marker for mitochondrial content (Larsen et al. 2012). CS activity was not significantly changed in brains of Thy1-APP$_{SL}$ mice, suggesting that the mitochondrial content was not changed. The unchanged mitochondrial membrane marker proteins (TIMM50 & TOMM22) support this notion. Accordingly, Choi et al. compared the number of mitochondria between wild-type mice and APP/PS1 transgenic mice and reported a quite similar number of mitochondria per 100 μm^2 (Choi et al. 2014). However, in Tg2576 mice, which represent another AD model (see table 1), the number of mitochondria was increased compared to wild type mice (Balietti et al. 2013). It was discussed that this difference may have been caused in part by age and strain differences between the studies (Choi et al. 2014).

According to Larsen and coworkers, the activities of respiratory system complexes CI, CII, CIII and CIV were also very good markers for mitochondrial content (Larsen et al. 2012). However, activities of CI, CI&II, and CIV of the respiratory chain were significantly reduced in mitochondria, isolated from brains of Thy1-APP$_{SL}$ mice. As discussed in connection with unchanged ATP levels (see above), it could be speculated that although respiratory chain complexes were dysfunctional, the Krebs-cycle was still maintained. However, mitochondrial dysfunction may provoke compensatory mechanisms, including induction of mitogenesis.

134

Significantly enhanced PGC1 protein levels supported this finding, since PGC1 is a transcription factor that represents the master regulator of mitochondrial biogenesis (Lopez-Lluch et al. 2008; Gonzalez-Freire et al. 2015).

Besides impaired function of mitochondrial respiratory chain complexes, mitochondrial dysfunction includes deficits of mitochondrial dynamics, such as an impaired balance between fission and fusion mechanisms (Benard and Rossignol 2008; Stockburger et al. 2014; Hagl et al. 2015a; Lionaki et al. 2015; Stockburger et al. 2015). Fragmented mitochondria could either enforce autophagosomal activity or enhance apoptosis (Knott and Bossy-Wetzel 2008; Santos et al. 2010; Lionaki et al. 2015). Thus, fission & fusion proteins were measured as markers for the dynamic machinery, LC3-I and LC3-II as autophagy marker proteins, and the mPTP constituents VDAC and PBR as early markers for apoptosis were measured in brain homogenates.

Drp and fission 1 related protein (Fis) are marker proteins for mitochondrial fission (Santos et al. 2010). Protein levels of Fis stayed unchanged, whereas Drp levels were significantly elevated in brains of Thy1-APP$_{SL}$ mice. Mfn and Opa proteins are markers for mitochondrial fusion (Santos et al. 2010). Mfn levels stayed unchanged, whereas protein levels of OPA were strongly reduced in brains of Thy1-APP$_{SL}$ mice. Both changes may lead to the shift towards shorter mitochondria – a distribution pattern that can also be observed after hypoxia-reoxygenation stress (Liu and Hajnoczky 2011).

Fragmented mitochondria may enforce autophagosomal activity or enhanced apoptosis in neurodegenerative disorders (Knott and Bossy-Wetzel 2008; Santos et al. 2010; Ghavami et al. 2014; Lionaki et al. 2015). Autophagy is a vesicle and lysosome-mediated degenerative pathway, that is essential for protein homeostasis and cell health as discussed above (Zare-Shahabadi et al. 2015). Microtubule-associated protein light chain 3 (LC3) immunoblotting was used to estimate autophagy in brains of Thy1-APP$_{SL}$ mice (Klionsky et al. 2007; Mizushima and Yoshimori 2007). The amount of both LC3-isoforms, the cytosolic and the autophagosomal form, were not changed in brain homogenates of Thy1-APP$_{SL}$ mice, indicating equal mitophagic activity. This notion is further supported by an unchanged ratio of the LC3- isoforms (Mizushima and Yoshimori 2007).

Fragmented mitochondria in brains of Thy1-APP$_{SL}$ mice may induce apoptosis after formation and opening of the mitochondrial transition pore (mPTP) (Knott and Bossy-Wetzel 2008). As discussed above, key for the mitochondrial-mediated intrinsic apoptotic pathway is the release of cytochrome *c*, which is regulated by VDAC and the PBR, which are constituents of the mitochondrial permeability transition pore (mPTP) (Cesura et al. 2003; Forte 2004; Repalli 2014). Both mPTP markers, the VDAC and the PBR were broadly increased in brain homogenate of Thy1-APPSL mice, suggesting enhanced mPTP formation. Enhanced VDAC expression has been reported for other AD mouse models as well (Cuadrado-Tejedor et al. 2011). However, further experiments have to enlighten, e.g. if mitochondria isolated show enhanced cristae swelling as it has been shown recently. Choi et al. investigated the ultrastructure of mitochondrial membranes and cristae in the hippocampus of APP/PSEN1 transgenic mice and report that they were severely disrupted (Choi et al. 2014). This alteration in structural and functional integrity was closely associated with the maintenance of mitochondrial volume homeostasis (Choi et al. 2014). Kaasik and colleagues (2007) suggested hypothetical phases of mitochondrial swelling, including the expansion of mitochondrial matrix with or without mitochondrial shape remodeling and rupture of the outer membrane or mitochondrial fusion (Kaasik et al. 2007). Although the expansion of mitochondrial matrix was observed, remarkable changes in mitochondrial size or remodeling of mitochondrial shape were not observed in Choi`s study (Choi et al. 2014).

Cellular and animal model of AD - relation to human post-mortem data

It can be depicted from table D1, that data were largely consistent for HEKsw cells and Thy1-APP$_{SL}$ mice. Both models showed an increased Aβ load, which was accompanied by a reduced OXPHOS capacity. Lower activities of CI and CIV were evident in both models. In the hippocampus of AD patients, CIV activity was decreased by 35–40%, compared to control. There was no significant difference in brain mitochondrial ATPase activity between AD and control groups (Bosetti et al. 2002). Genes in mitochondrial complexes I-V subunits were extensively down-regulated in the AD brain, most evident in the hippocampus (Berchtold et al. 2014).

In HEKsw cells and Thy1-APP$_{SL}$ mice reduced MMP measures were noted, which were most probably a direct result of the reduced OXPHOS activities. Since MMP is the driving force for complex V to produce ATP (Nijtmans et al. 2004), decreased ATP levels were expected in both models. However, only HEKsw cells showed decreased ATP levels. As indicated by the exclusive increase of PGC1, compensatory mechanisms in brains of Thy1-APP$_{SL}$ mice might have prevented damage as discussed above. On the other site PGC1 overexpression exacerbates the neuropathological and behavioral deficits, that occur in Tg19959 mice (Dumont et al. 2014), another AD mouse model, which is comparable to Thy1-APP$_{SL}$ mice (see table 1).

In agreement with the finding of unchanged CS activity in both HEKsw cells and Thy1-APP$_{SL}$ mice, Bosetti et al. reported that the mean activity of CS per gram of post-mortem brain tissue, a mitochondrial matrix enzyme insensitive to abnormalities of the respiratory chain, did not differ between the AD and control groups, indicating that the amount of mitochondria was not affected by AD pathology (Bosetti et al. 2002).

Both HEKsw cells and Thy1-APP$_{SL}$ mice showed a comparable pattern of Fission & Fusion marker proteins: Drp levels were enhanced, Fis and Mfn levels were unchanged, and Opa levels were reduced (table D1). Reduced Opa levels were also observed in post-mortem brain tissue of AD patients (Wang et al. 2009). However, immunoblot analysis revealed significantly reduced Drp1, Mfn1, and Mfn2 levels, whereas levels of Fis1 were significantly increased in AD brain tissue samples (Wang et al. 2009). Aravamudan et al. have shown, that fission & fusion events also depend on the cell cycle: in the interphase, mitochondrial fusion

is promoted, leading to extensive networking. As the mitotic and cytokinetic events occur during the M phase, mitochondria get fragmented, mixed and distributed equally among the progeny cells (Aravamudan et al. 2013). Since neurons are post-mitotic cells, cell cycle events can largely be excluded. Based on the consistent results in both, the cellular and murine AD model, there is no evidence that cell cycle events would have been influenced the experiments in HEKsw cells.

Intrinsic apoptosis pathways are involved in early pathogenesis of AD including mitochondria related release of apoptotic factors and activation of caspases (Leuner et al. 2007; Rohn 2010; Cuadrado-Tejedor et al. 2011; Repalli 2014; Wang et al. 2015). Key for the mitochondrial-mediated intrinsic apoptotic pathway is the release of cytochrome *c*, which is regulated by VDAC and the peripheral benzodiazepine receptor (PBR or TSPO)(Cesura et al. 2003). Protein levels of both markers of the mPTP, VDAC and PBR, were significantly enhanced in HEKsw and Thy1-APPSL mice (table D1). Cuadrado-Tejedor et al. reported enhanced expression of the VDAC1 in Alzheimer's disease transgenic mice and Lynn et al. showed significantly enhanced VADC1-3 protein levels in post-mortem tissue from patients with early AD (Lynn et al. 2010; Cuadrado-Tejedor et al. 2011). Increased expression of PBR was also observed in patients with Alzheimer's disease (Repalli 2014).

Both investigated models showed enhanced formation of oxidative stress (ROS production, elevated MDA levels, table D1). Oxidative stress plays a key role in the pathogenesis of AD and has been detected in brains of animal models of AD (Butterfield et al. 2001; Schuessel et al. 2006) and post-mortem brain tissue (DiCiero et al. 2000; Ansari and Scheff 2010; James et al. 2012). Ansari et al. reported that levels of oxidative markers correlated significantly with Mini-Mental Status Examination scores. Oxidative stress was more localized to the synapses, with levels increasing in a disease-dependent way (Ansari and Scheff 2010).

In conclusion, both, the cellular (HEKsw) and the animal model of AD (Thy1-APP$_{SL}$), broadly match pathophysiological features, that had been assessed in post-mortem samples from AD patients. Thus, HEKsw cells and Thy1-APP$_{SL}$ mice seem to be suitable models to study compounds as new therapeutics in AD.

Dimebon

After initial findings of beneficial effects of Dimebon on impaired cognitive functions in AD and HD (Bachurin et al. 2001; Doody et al. 2008; Kieburtz et al. 2010), several mechanisms were suggested including interactions with acetylcholinesterase, glutamatergic and serotonergic receptors and calcium channels. Findings, that Dimebon protects against the neurotoxic effects of Aβ (Bachurin et al. 2001; Lermontova et al. 2001), together with many observations of mitochondria as major target for the cell toxicity of Aβ (Reddy 2009; Leuner et al. 2012b), led to the assumption that mitochondrial protection might be a major mechanism. The plasma concentration in humans, taking 3 x 20 mg Dimebon/day, is 10-15 nM, with an estimated brain concentration of 100 nM (Doody et al. 2008; Zhang et al. 2010). Thus, the nM range resembles the calculated brain concentration in patients receiving Dimebon in the Phase II AD trial (Zhang et al. 2010). It has to be noted that many other *in vitro* studies used rather high concentrations in the micromolar range(Bachurin et al. 2001; Lermontova et al. 2001).

Evidence that Dimebon protects mitochondria have been recently published (Zhang et al. 2010; Day et al. 2011; Perez et al. 2012; Steele et al. 2013a). In this thesis, a cellular model of AD with severe mitochondrial dysfunction was characterized (see above) and demonstrated that nanomolar concentration of Dimebon restored mitochondrial form and function by ameliorating disease specific deficits in mitochondrial morphology, dynamics, ETC, as well as affecting quality control pathways e.g. mitophagy, mPTP formation, turnover, mitochondrial swelling (see dissertation of Janett Eckmann, 2013), and mitochondrial mass.

\#

Table D2: Effects of Dimebon (100 nM) on HEK293 cells transgenic for the 695 amino acid form of the human APP-gene including the Swedisch APP-mutation (HEKsw). Main findings are expressed as change compared to transfected control cells (HEKsw). Refer to the result section for quantitative data and further details.

Parameter	HEKsw + Dim
Aβ load	↓
OXPHOS capacity	↑
MMP	↓
MMP + CI inhibition	↑
ATP level	↔
ATP level + CI inhibition	↔
CS activity	↑
Mitochondrial length	↑
Mitochondrial density	↑
TIMM50	↑
TOMM22	↓
Drp	↑
Fis	⇧
Mfn	⇧
Opa	↑
LC3-I	LC3-II	↑	↑
Autophagic activity	⇩
PGC1alpha	↔
VDAC	↓
PBR	↓
ROS ± CI inhibition	↓
MDA ± Fe^{2+} stress	n.d.

n.d. = not determined, effects of Dimebon are indicated by arrows. Blank arrows indcate a trend

Dimebon reduced levels of Aβ and of ROS in HEKsw cells (table D2). Others have also reported a Dimebon-induced reduction of Aβ in cellular (Pohland et al. 2016; Porter et al. 2016) and mouse models of AD (Perez et al. 2012; Ustyugov et al. 2012). However, conflicting results have also been published (Steele et al. 2009; Peters et al. 2013).

Since mitochondria are a major target for the cell toxicity of Aβ (Reddy 2009; Leuner et al. 2012b), effects of Dimebon on mitochondrial form and function were tested. HEKsw cells showed an overall reduction in the capacity of the respiratory system, already downstream of

complex CI. Dimebon restored these deficits in OXPHOS activity and all respiratory stages were ameliorated back to control levels. Complex I respiration was elevated even above the control level. To further investigate how Dimebon increases mitochondrial respiration in HEKsw cells, the mitochondrial membrane potential (MMP), which is built by the electron transport chain (ETC) was measured. HEK cells were pre-incubated with Dimebon and MMP was examined under basal conditions, as well as under rotenon induced complex I dysfunction. Basal levels of MMP were reduced in the absence of rotenon. Dimebon significantly improved the MMP after rotenon insult, indicating protective properties (table D2).

Since OXPHOS induced MMP is the driving force for complex V (F1/F0-ATPase) to produce ATP (Nijtmans et al. 2004), an impact of Dimebon on ATP levels was expected. However, Dimebon did not change ATP levels. Zhang et al. (2010) reported that nanomolar concentrations of Dimebon improved several parameters of mitochondrial function, such as membrane potential, ATP production, MTT reduction, and apoptosis in human neuroblastoma cells and primary rat cortical neurons (Zhang et al. 2010). However, Dimebon induced autophagic activity in HEKsw cells (see below and table D2). Autophagy represents a highly energy consuming process (Ghavami et al. 2014) and thus consumes ATP, which might partly explain the observation that in spite of strongly increased OXPHOS, ATP level were unaffected.

Protective effects of Dimebon were more pronounced when the cells were additionally stressed, e.g. by serum deprivation (Zhang et al. 2010). In our cell model Dimebon showed protective effects after rotenon induced MMP decline. Thus, the observed Dimebon related enhancement of the OXPHOS capacity might be rather due to changes in the mitochondrial content, than to changes in functionality. To explore this hypothesis, CS activities were measured. CS is a very constant expressed mitochondrial matrix marker, which is widely used as a marker for mitochondrial mass (Larsen et al. 2012; Hagl et al. 2015a). Dimebon enhanced CS activity in HEKsw cells. Elevated mitochondrial respiratory activity, together with increased CS activity, is a known indicator for a higher mitochondrial content (Larsen et al. 2012).

Since mitochondrial density, as well as mitochondrial dynamics are mutual for initiation of quality control pathways (Knott and Bossy-Wetzel 2008; Liu and Hajnoczky 2011; Youle and van der Bliek 2012), morphological changes were assessed using laser scanning microscopy technique. In HEKsw cells predominantly punctuated and truncated mitochondria were detected. Dimebon incubation resorted morphological changes in HEKsw cells and showed a mitochondrial shape distribution close to the HEK$_{ut}$ control cells. Moreover, Dimebon improved morphological distribution in HEKsw cells stressed with rotenon, that exhibited further mitochondrial fragmentation (table D2). These effects were established for a Dimebon concentration of 0,1 μM, which was within in the concentration range used by Zhang *et al.* to show mitochondrial protective effects (Zhang et al. 2010).

Changes of mitochondrial morphology are also mutually connected with changes of mitochondrial function, typically observed for the OXPHOS system (Hensley and Harris-White 2015; Cogliati et al. 2016). HEKsw cells showed pronounced alterations of the OXPHOS machinery and a reduced area occupied by mitochondria. Dimebon selectively improved mitochondrial respiratory activity, restored mitochondrial density and elevated CS activity in HEKsw cells. Altogether, these data strongly indicate that Dimebon enhanced the mitochondrial mass (Larsen et al. 2012).

Membranes play an eminent role for form and function of mitochondria. The OMM encloses the entire organelle and contains numerous integral proteins, such as porins like the voltage dependent anion channel (VDAC), that are highly permeable to molecules up to 1,5 kDa. The IMM is quite tight and contains the translocase of the inner membrane (TIM), the adenosine nucleotide transporter (ANT) and other carriers for the transport of proteins and other compounds (Martin et al. 2011). The IMM also contains the proteins of the electron transfer system (ETS), responsible for oxidative phosphorylation and ATP production (Eckmann et al. 2013). Recent studies also revealed that changes in mitochondrial membrane fluidity might have a direct impact on membrane-based processes, such as F1/F0 ATP-synthase activity, fission-associated morphogenic changes, recruitment of pro-apoptotic factors and mPTP opening (Montecucco et al. 1982; Madden et al. 1983; Ricchelli et al. 1999; Colell 2003; Aleardi et al. 2005; Garofalo et al. 2007; Eckmann et al. 2013). It has been shown that fusion- (Mfn-1, OPA) and fission- (Drp-1, Fis1) proteins modulate the fluidity of mitochondrial membranes. Accordingly, blocking of Drp-1 significantly increases membrane fluidity, that results in strong inhibition of mitochondrial energy production, caused by

reduction in respiration (Benard et al. 2007). Moreover, mPTP opening itself modifies membrane fluidity by conformational change of pore-forming proteins (Ricchelli et al. 1999). Thus, there is evidence that mitochondrial membrane fluidity regulates or modulates the function of essential proteins in the mitochondrial membranes and vice versa (Eckmann et al. 2013). It was reported, that membrane fluidity was significantly reduced in HEKsw cells (Peters et al. 2009). However, Dimebon had no effect on the membrane fluidity of HEKsw cells.

The majority of mitochondrial proteins are nuclear encoded, synthesized in cytosolic ribosomes and imported into mitochondria by various translocases in the outer mitochondrial membrane (OMM) and the inner mitochondrial membranes (IMM) (Paschen and Frandsen 2001; Torraco et al. 2015). In contrast to the OMM, the IMM requires two translocases for the import of precursors into the matrix, TIMM23 and TIMM22 (Rapaport and Nargang 2004; Eckmann et al. 2013). TOMM22 is a translocase in the outer mitochondrial membrane and one of the membrane-embedded core components, that form the general insertion pore (GIP), anchored to the outer membrane and mediating initial steps for the import of pre-proteins into the organelle (Rapaport and Nargang 2004; Eckmann et al. 2013). TIMM50 functions as a receptor and component of TIMM23. It guides the precursors from the intermembrane side to the translocation pore TIMM23. TIMM23 makes an intimate contact with the single TOMM complex when a precursor is in transit (Rapaport and Nargang 2004; Eckmann et al. 2013). Inside the mitochondria chaperone proteins of the heat-shock family are mediating the folding of imported proteins (Rapaport and Nargang 2004; Eckmann et al. 2013). Thus, regular function and composition of mitochondrial membranes is crucial for the homeostasis, biosynthesis and metabolic demands of mitochondria.

In HEKsw cells TOMM22 protein levels were not changed, but TIMM50 protein levels were drastically decreased, which was completely restored by Dimebon incubation. Interestingly, Dimebon decreased TOMM22 protein levels in HEKsw cells. Thus, Dimebon obviously affects TIMM50 and TOMM22 protein levels. However, future investigations have to enlighten the underlying mechanisms.

Under physiological conditions fission & fusion (f & f) are carefully balanced (Jendrach et al. 2005; Twig et al. 2006). Mitochondrial dynamics allow the complementation of

mitochondrial DNA (mtDNA) mutations *in vitro* and *in vivo* (Legros et al. 2004; Rapaport and Nargang 2004; Eckmann et al. 2013), which supports the hypothesis that mitochondrial fission & fusion dynamics play a role in the mitochondrial quality control system (Bossy-Wetzel et al. 2003; Gilkerson 2009; Mai et al. 2010). Increased fission takes place during apoptosis, which is mediated by Drp1 (Frank et al. 2001). Cytosolic Drp1 needs to be translocated to mitochondria and Fis1 to initiate their division (Frank et al. 2001; Han et al. 2008). Fis1 serves as an anchor for Drp1 (Mozdy et al. 2000; Tieu et al. 2002). Calcium induced fission of mitochondria results from phosphorylation of Drp1, increasing its affinity to Fis1 and thus translocating it from the cytoplasm to the OMM (Han et al. 2008). Knock-down of Fis1 results in mitochondrial elongation, decreased autophagy and retained mitochondrial mass (Romanello et al. 2010). In AD the balance between fission and fusion is greatly shifted towards fission (Reddy and Beal 2008; Cho et al. 2009; Wang et al. 2009). This imbalance provides potential therapeutically interventions, namely drugs, which target the dynamic machinery of mitochondria, in order to shift the disturbed balance back to normal conditions.

The most prominent fusion factors are Mfn and Opa. Mfn is necessary for tethering between opposing membranes and Opa for the junction of the IMM. Opa1 induces mitochondrial elongation and network formation (Cipolat et al. 2004). Elongation of mitochondria conferred resistance to apoptotic stimuli in cell culture models (Lee et al. 2004; Sugioka et al. 2004; Jahani-Asl et al. 2007). Mfn1-OPA interactions are required to promote fusion (Arnoult et al. 2005). In HEKsw cells similar changes in the dynamic machinery, such as up-regulation of Drp and down-regulation of OPA1 and excessive overexpression in the levels of VDAC and PBR (table D2), were detected. This changes were in line with findings that mitochondrial fragmentation was associated with apoptosis, due to Fis1 overexpression and down-regulation of OPA1 (Frank et al. 2001; Olichon et al. 2003; Lee et al. 2004; Yu et al. 2005). Thus, mPTP opening may play a causative role in mitochondrial fragmentation, depolarization of the mitochondrial membrane potential, ATP depletion, and finally apoptosis. Supporting our data, inhibition of mPTP in other disease models already showed both, a reduction in expression of fission proteins and an increase in expression of fusion proteins (Galloway et al. 2012; de Arriba et al. 2013; Gonzalez-Polo et al. 2013; Stockburger et al. 2015). Dimebon showed no effects on the dynamic machinery markers in HEKut cells. In HEKsw, Dimebon further enhances protein levels of Drp and compensates for reduced Opa levels (table D2). This results mirrors the findings on mitochondrial length: While

Dimebon does not affect the mitochondrial length pattern in HEKut cells, it does broadly shifted mitochondrial morphology towards a tubular shape in HEKsw cells (table D2).

Elimination of dysfunctional mitochondria is of eminent importance to protect cells from mitochondrial dysfunction and release of pro-apoptotic factors. Mitophagy describes mitochondrial turnover by autophagic sequestration delivery to lysosomes for hydrolytic degradation and recycling of the resulting macromolecules (Shintani and Klionsky 2004). However, autophagy has to be balanced, since insufficient, as well as excessed autophagy can promote cell injury (Levine and Yuan 2005; Chakrabarti et al. 2009). Thus, enhanced autophagy can be protective, while impaired autophagy contributes to neurodegenerative diseases (Levine and Kroemer 2008). In different AD mouse models, it has been shown that Dimebon enhanced the activity of intracellular protein degradation pathways, including autophagy (Steele et al. 2012). Accordingly, Dimebon enhanced autophagy in HEKsw (table D2). Hence, a decrease in mitochondrial mass was expected. In contrast, Dimebon elevated mitochondrial density and enhanced CS activity. To enlighten the underlying mechanisms, the protein levels of PGC1, VDAC and PBR (mPTP marker) were assessed. While levels of the mitogenesis marker PGC1 were unaffected, Dimebon treatment significantly reduced protein levels of VDAC and PBR in HEKsw cells to basal levels (table D2).

VDAC mediates the trafficking of metabolites across the OMM and is also involved in the intracellular Ca^{2+} homeostasis and in apoptosis (Forte 2004). As mentioned above, VDAC and PBR were found to be key regulators for the mitochondrial-mediated intrinsic apoptotic pathway (Cesura et al. 2003). Enhanced expression of the VDAC was reported in Alzheimer's disease transgenic mice and significantly enhanced VADC protein levels were detected in post-mortem tissue from patients with early AD (Yoo et al. 2001; Lynn et al. 2010; Cuadrado-Tejedor et al. 2011). Increased expression of PBR was also observed in patients with Alzheimer's disease (Repalli 2014). Thus, Dimebon did not affect mitogenesis, but elevated mitochondrial mass and density probably by reducing apoptotic vulnerability.

Dimebon lowered Aβ and increased LC3-I and LC3-II levels in HEKsw cells, indicating enhanced autophagic activity. These findings point to elevated catabolic degradation of intracellular Aβ due to an increased autophagic clearance. This notion is supported by findings in different cell and animal models (Bharadwaj et al. 2012; Steele et al. 2012; Steele

et al. 2013). In cells and mouse brain, Dimebon is also able to decrease levels of α-synuclein by stimulating autophagy (Steele et al. 2013). α-Synuclein (α-syn) is a protein, which is related to neurodegenerative diseases, such as Parkinson´s disease, Lewy body dementia and even 30-50% of AD patients also harbor atypical α-syn accumulation (Broe et al. 2005; Uchikado et al. 2006). Future investigations have to evaluate if Dimebon is able to interfere with an ageing-dependent decrease of autophagy, that has been identified as a feature for the progression of AD pathology (Zhu et al. 2013).

In conclusion, Dimebon treatment restored diverse defects in Aβ overexpressing cells: autophagy marker were increased, Aβ levels were reduced, mitophagy as repair and renewal mechanism was elevated, mitochondrial mass and density were increased, OXPHOS capacity was restored, mitochondrial dynamics were balanced, mitochondrial shape showed a normal distribution, expression levels of the mPTP constituents were reduced, TIMM50 levels augmented to control levels and stress induced MMP and ROS levels were reduced. All these effects were assessed after incubation of cells with a rather low concentration of 100 nmol/L, which is above the plasma and brain levels in Dimebon treated TgCRND8 mice (202 pmol/mL in plasma; 810 pmol/mg in brain) (Wang et al. 2011), but much lower than the concentrations (e.g. 25 μmol/L) used in other *in vitro* investigations (Bachurin et al. 2001; Lermontova et al. 2001).

Based on these findings and in addition to already existing literature, Dimebon presents a potential therapeutic option for diseases with accompanied mitochondrial dysfunction, although clinical findings published so far are inconsistent (Cano-Cuenca et al. 2014; Chau et al. 2015).

Olesoxim

Olesoxim has demonstrated therapeutic efficacy in disease models of amyotrophic lateral sclerosis (Bordet et al. 2007; Sunyach et al. 2012), of Huntington (Clemens et al. 2015) and of peripheral neuropathies (Bordet et al. 2008; Xiao et al. 2009; Rovini et al. 2010; Xiao et al. 2012), by targeting mitochondria-related defects. Although well tolerated, Olesoxim did not show significant beneficial effect in ALS patients treated in combination with riluzole in a phase II-III trial (ClinicalTrials.gov Identifier: NCT00868166) (Lenglet et al. 2014). However, Olesoxim recently yielded impressive beneficial effects on motor function in a

phase II clinical trial in spinal muscular atrophy patients (ClinicalTrials.gov Identifier: NCT01302600). In the frame of the EU-funded "Mitotarget" project, the investigations concerning Olesoxim in cellular (*in vitro*) and murine (*in vivo)* models of AD, were expanded.

All tested concentrations are not toxic *in vitro* (personal information by Dr. Thierry Bordet, Throphos S.A). The applied dose (100 mg/kg b.w.) was far below the NOAEL for rats (1000 mg/kg b.w.) and was well tolerated by mice. Accordingly, Olesoxim exerted no effects on body weight, neither in Thy1-APP$_{SL}$ mice nor in littermate controls. These findings are in line with a notably safety profile of Olesoxim. Neither interactions with cytochrome P450 isoenzymes, nor genotoxicity (negative Ames test and micronucleus test) were reported. Moreover, no conspicuous features were detected in safety pharmacological measurements (CNS, respiratory and cardiovascular system, or QT prolongation) (personal information by Dr. Thierry Bordet, Throphos S.A). After subcutaneous application, Olesoxim reached a plasma concentration of approximately 5,85 µg/ml (Bordet et al. 2007), which is comparable with the plasma concentration of 6,2 µg/ml after oral administration of 100 mg/kg b.w. in our study. The low oral bioavailability (<10%) may account for the observation, that a threefold higher oral dose, compared to subcutaneous application, led to the same plasma concentration in mice (Figure 46) (Bordet et al. 2007). However, Olesoxim crosses the blood-brain-barrier and reached concentrations of approximately 3 µM after application of 30 µM s.c. (Bordet et al. 2007). This concentration was in the range of our *in vitro* assays.

Table D3: Effects of Olesoxim (TRO, 3 μM) on HEK293 cells transgenic for the 695 amino acid form of the human APP-gene, including the Swedish APP-mutation (HEKsw) and C57BJ/6 mice transfected with the 751 amino acid form of human APP with the Swedish (KM670/671NL) and London (V717L) mutations under the control of a neuron-specific murine Thy1 promotor (Thy1-APP$_{SL}$). Main findings are expressed as change compared to transfected control cells (HEKsw) and APP transgenic placebo fed mice, respectively. Refer to the results section for quantitative data and further details.

Parameter	HEKsw + TRO	Thy1-APP$_{SL}$ (tg) + TRO
Aβ load	↑	↑
OXPHOS capacity	↑	↑
MMP	↓	↑
MMP + CI inhibition	↑	↑
ATP level	↔	↔
ATP level + CI inhibition	↔	↔
CS activity	↔	↔
Mitochondrial length	↑	n.d.
Mitochondrial density	↑	n.d.
TIMM50	↑	↔
TOMM22	↔	↓
Drp	⇑	↑
Fis	↑	↑
Mfn	⇑	↑
Opa	↑	↑
LC3-I	LC3-II	↑	↑	↔	↓
Autophagic activity	↔	↔
PGC1alpha	↔	↓
VDAC	↓	↓
PBR	↓	↓
ROS ± CI inhibition	n.d.	n.d.
MDA ± Fe^{2+} stress	n.d.	↔

n.d. = not determined, arrows in black indicate common changes in both models; arrows in red indicate differences between models.

Olesoxim treatment enhanced mitochondrial respiration in HEKsw cells. A general increase in the respiratory capacity was also observed in mitochondria, isolated from brains of Olesoxim treated Thy1-APP$_{SL}$ mice. Since Olesoxim accumulates in mitochondria, they were the primary target of Olesoxim treatment (Bordet et al. 2010). In both disease models, Olesoxim normalized complex activities almost to control levels. In HEKsw cells 10 μM

Olesoxim completely restored complex I respiratory dysfunction, which perfectly matched the strong ameliorating effect of 10 μM Olesoxim on the MMP of HEKsw cells, after rotenon induced complex I dysfunction. It was expected that the enhanced OXPHOS capacity would also led to enhanced MMP and ATP levels (Nijtmans et al. 2004). However, in HEKsw cells MMP and ATP levels were further reduced. In mice, Olesoxim enhanced MMP but not ATP levels. The Olesoxim induced increase of the proton gradient within the intermembrane space was transferred into a higher MMP, which represents the driving force for the ATP production by the F1F0-ATPase. Further investigations have to elaborate if these changes led to the production of ROS (Nijtmans et al. 2004). However, levels of MDA were not changed in brains of Olesoxim treated Thy1-APP$_{SL}$ mice. Moreover, it has been shown that Olesoxim normalized alterations in transcripts, implicated in mitochondrial function and oxidative stress (e.g. Bcl-2, Bax, Casp3, Nos2) in α-synuclein overexpressing nigrostratial dopaminergig neurons (Richter et al. 2014).

To examine, whether the Olesoxim induced improvement of the OXPHOS capacity was due to an elevated mitochondrial mass, the activity citrate synthase was measured. CS activity was not changed after Olesoxim treatment in both AD models, which is in agreement with recent findings in BACHD rats, a Huntington model (Clemens et al. 2015). Thus, it can be concluded that Olesoxim did not chanced the mitochondrial mass (Larsen et al. 2012). Accordingly, protein levels of PGC1, which represent the master regulator protein for mitogenesis were unchanged *in vitro* or even reduced *in vivo* after Olesoxim treatment (table D3) (Lopez-Lluch et al. 2008; Gonzalez-Freire et al. 2015). However, Olesoxim incubation resulted in a very distinct and dose-dependent shift from highly fragmented to tubular and elongated mitochondrial lengths in HEKsw cells. The amount of punctuated mitochondria was strongly reduced by approximately 50%. On the other hand, the amount of tubular mitochondria was nearly doubled. Concerning the length pattern of mitochondria, Olesoxime pre-incubation had a moderate protective effect after challenging HEKsw cells with rotenon. Likewise, the reduced mitochondrial density was reversed by Olesoxim incubation in HEKsw cells. These changes might also explain the Olesoxim induced increase in the LC3-I and LC3-II protein levels, since mitochondrial density and dynamics are mutual for initiation of quality control pathways (Knott and Bossy-Wetzel 2008; Liu and Hajnoczky 2011; Youle and van der Bliek 2012). However, autophagy activity was unaffected, neither in HEKsw cells nor in Thy1-APP$_{SL}$ mice.

Olesoxim treatment restored the drastically reduced TIMM50 protein levels in HEKsw cells. TOMM22 levels were not affected. In brains of Thy1-APP$_{SL}$ mice, basal protein levels of TIMM50 and TOMM22 were not altered and Olesoxim decreased TOMM22 levels. In BACHD rats Olesoxim increased levels of TOMM20 in the striatum, but not in the cortex (Clemens et al. 2015). Future experiments have to elaborate the partly, conflicting results and explore the consequences of Olesoxim treatment, for the mitochondrial pre-protein translocation machinery (Hofmann and Bauer 2004).

In both, HEKsw cells and Thy1-APP$_{SL}$ mice, Olesoxim treatment elevated all investigated protein markers of the mitochondrial dynamic machinery (table D3). These findings are in agreement with a recent study using a rat Huntington model. Olesoxim increased levels of Mfn and Opa, but decreased Drp levels in the cortex of BACHD rats (Clemens et al. 2015). Moreover, it has been shown that cholesterol-oximes affect the expression of genes, important for mitochondrial function (Richter et al. 2014). A reduction in apoptotic events, indicated by decreased VDAC and PBR protein levels (table D3), is one explanation for enhanced mitochondrial dynamics in our models. The observation, that Olesoxime elongated the mitochondria in HEKsw cells, is supporting this finding (Griparic et al. 2004; Ghavami et al. 2014). Further supportive were the data, that Olesoxim protected embryonic cortical neurons from camptothecin induced caspase activation (Bordet et al. 2007; Gouarné et al. 2013; Gouarne et al. 2015).

Another interesting effect of Olesoxime is a modulation of mitochondrial membranes (Eckmann et al. 2013; Eckmann et al. 2014; Clemens et al. 2015). In previous studies it was reported, that Olesoxime was able to reverse the increase in mitochondrial membrane fluidity, observed in BACHD rats and two other Huntington disease models (Eckmann et al. 2014). We further showed that Olesoxim-treated BACHD rats had significantly higher mitochondrial membrane cholesterol levels than untreated BACHD rats, which might be causal for the reduction in membrane fluidity (Eckmann et al. 2014). Here, we demonstrated that Olesoxim dramatically increased the levels of the outer mitochondrial membrane transporter VDAC, which is also involved in mitochondrial cholesterol import (Rone et al. 2009). Thus, there were indications that the mitochondrial membrane environment was modulated by Olesoxime, which might connect to its beneficial effects (Clemens et al. 2015).

Olesoxim treatment led to a significant increase of Aβ levels in both, HEKsw cells and Thy1-APP$_{SL}$ mice (table D3). This effect could be explained by bio-physical interactions of the hydrophob, cholesterol-like compound with cellular membranes, where the processing of APP takes place. Although, Olesoxim was shown to accumulate in mitochondria (Bordet et al. 2007), the hydrophobic compound significantly reduced the fluidity of synaptosomal membranes (Eckmann et al. 2014) and a reduction in membrane fluidity was shown to stimulates the production of Aβ (Peters et al. 2009). In the light of the current disscussion in the field about the impact of Aβ on the pathology of AD (refer to the introduction) (Lansdall 2014), further investigations have to evaluate if the observed activation of the amyloidogenic pathway is harmful or not. Anyway, one conclusion from the data presented in this thesis is that at least a part of Olesoxime`s effects were independent from Aβ. Thus, future studies also have to adress the question, how the Olesoxim induced enhancement of OXPHOS capacity, mitochondrial dynamics, and autophagy or a reduction in marker proteins for the mPTP were related to changes in Aβ levels.

Another interesting observation that needs further examination was, that Olesoxime exerted partly negative effects in controls. For instance, Olesoxim reduced the OXPHOS capacity and enhanced protein levels of VADAC and PBR in brains of C57BJ/6 littermate control mice, which could limit the applicability of Olesoxim in further preclinical studies.

References

Abdel-Kader RM, Hauptmann S, Keil U, Scherping I, Leuner K, Eckert A, Muller WE (2007) Stabilization of mitochondrial function by Ginkgo biloba extract (EGb 761). Pharmacol Res 56 (6):493-502.

Afshordel S, Hagl S, Werner D, Rohner N, Kogel D, Bazan NG, Eckert GP (2015) Omega-3 polyunsaturated fatty acids improve mitochondrial dysfunction in brain aging - Impact of Bcl-2 and NPD-1 like metabolites. Prostaglandins Leukot Essent Fatty Acids 92:23-31.

Aleardi AM, Benard G, Augereau O, Malgat M, Talbot JC et al. (2005) Gradual alteration of mitochondrial structure and function by beta-amyloids: importance of membrane viscosity changes, energy deprivation, reactive oxygen species production, and cytochrome c release. J BioenergBiomembr 37 (4):207-225.

Alzheimer`s Association (2012) Alzheimer's disease: Facts and Figures. Alzheimers Dement 8 (2):131-168.

Alzheimer`s Disease International (2015a) About dementia - Alzheimer`s disease. http://www.alz.co.uk/info/alzheimers-disease. Accessed 08/10/2015

Alzheimer's Disease International (2015b) World Alzheimer Report 2015: The global Impact of Dementia. https://www.alz.co.uk/research/world-report-2015. Accessed 08/10/2015

Anand R, Gill KD, Mahdi AA (2014) Therapeutics of Alzheimer's disease: Past, present and future. Neuropharmacology 76 Pt A:27-50.

Anisuzzaman AS, Uwada J, Masuoka T, Yoshiki H, Nishio M et al. (2013) Novel contribution of cell surface and intracellular M1-muscarinic acetylcholine receptors to synaptic plasticity in hippocampus. J Neurochem 126 (3):360-371.

Ansari MA, Scheff SW (2010) Oxidative stress in the progression of Alzheimer disease in the frontal cortex. J Neuropathol Exp Neurol 69 (2):155-167.

Aravamudan B, Thompson MA, Pabelick CM, Prakash YS (2013) Mitochondria in lung diseases. Expert Rev Respir Med 7 (6):631-646.

Arnoult D, Grodet A, Lee YJ, Estaquier J, Blackstone C (2005) Release of OPA1 during apoptosis participates in the rapid and complete release of cytochrome c and subsequent mitochondrial fragmentation. J Biol Chem 280 (42):35742-35750.

Austin S, St-Pierre J (2012) PGC1alpha and mitochondrial metabolism--emerging concepts and relevance in ageing and neurodegenerative disorders. J Cell Sci 125 (Pt 21):4963-4971.

Azarashvili T, Stricker R, Reiser G (2010) The mitochondria permeability transition pore complex in the brain with interacting proteins – promising targets for protection in neurodegenerative diseases. Biol Chem 391 (6):619–629.

Bachurin S, Bukatina E, Lermontova N, Tkachenko S, Afanasiev A et al. (2001) Antihistamine agent Dimebon as a novel neuroprotector and a cognition enhancer. Ann N Y Acad Sci 939:425-435.

Bakchine S, Loft H (2008) Memantine treatment in patients with mild to moderate Alzheimer's disease: results of a randomised, double-blind, placebo-controlled 6-month study. J Alzheimers Dis 13 (1):97-107.

Baki L, Neve RL, Shao Z, Shioi J, Georgakopoulos A, Robakis NK (2008) Wild-type but not FAD mutant presenilin-1 prevents neuronal degeneration by promoting phosphatidylinositol 3-kinase neuroprotective signaling. J Neurosci 28 (2):483-490.

Balietti M, Giorgetti B, Casoli T, Solazzi M, Tamagnini F, Burattini C, Aicardi G, Fattoretti P (2013) Early selective vulnerability of synapses and synaptic mitochondria in the hippocampal CA1 region of the Tg2576 mouse model of Alzheimer's disease. J Alzheimers Dis 34 (4):887-896.

Barnard ND, Bush AI, Ceccarelli A, Cooper J, de Jager CA et al. (2014) Dietary and lifestyle guidelines for the prevention of Alzheimer's disease. Neurobiol Aging 35 Suppl 2:S74-78.

Barnett A, Brewer GJ (2011) Autophagy in aging and Alzheimer's disease: pathologic or protective? J Alzheimers Dis 25 (3):385-394.

Barthet G, Dunys J, Shao Z, Xuan Z, Ren Y et al. (2013) Presenilin mediates neuroprotective functions of ephrinB and brain-derived neurotrophic factor and regulates ligand-induced internalization and metabolism of EphB2 and TrkB receptors. Neurobiol Aging 34 (2):499-510.

Bedir E, Tatli, II, Khan RA, Zhao J, Takamatsu S, Walker LA, Goldman P, Khan IA (2002) Biologically active secondary metabolites from Ginkgo biloba. Journal of Agricultural and Food Chemistry 50 (11):3150-3155.

Benard G, Bellance N, James D, Parrone P, Fernandez H, Letellier T, Rossignol R (2007) Mitochondrial bioenergetics and structural network organization. J Cell Sci 120 (Pt 5):838-848.

Benard G, Rossignol R (2008) Ultrastructure of the mitochondrion and its bearing on function and bioenergetics. Antioxid Redox Signal 10 (8):1313-1342.

Benzi G, Pastoris O, Marzatico F, Villa RF, Dagani F, Curti D (1992) The mitochondrial electron transfer alteration as a factor involved in the brain aging. Neurobiol Aging 13 (3):361-368.

Berchtold NC, Sabbagh MN, Beach TG, Kim RC, Cribbs DH, Cotman CW (2014) Brain gene expression patterns differentiate mild cognitive impairment from normal aged and Alzheimer's disease. Neurobiol Aging 35 (9):1961-1972.

Berger-Sweeney J (2003) The cholinergic basal forebrain system during development and its influence on cognitive processes: important questions and potential answers. Neurosci Biobehav Rev 27 (4):401-411.

Beydoun MA, Beydoun HA, Gamaldo AA, Teel A, Zonderman AB, Wang Y (2014) Epidemiologic studies of modifiable factors associated with cognition and dementia: systematic review and meta-analysis. BMC Public Health 14:643.

Bharadwaj PR, Verdile G, Barr RK, Gupta V, Steele JW et al. (2012) Latrepirdine (dimebon) enhances autophagy and reduces intracellular GFP-Abeta42 levels in yeast. J Alzheimers Dis 32 (4):949-967.

Bilkei-Gorzo A (2014) Genetic mouse models of brain ageing and Alzheimer's disease. Pharmacology & therapeutics 142 (2):244-257.

Birks J (2006) Cholinesterase inhibitors for Alzheimer's disease. Cochrane Database Syst Rev (1):Cd005593.

Birks JS, Grimley Evans J (2015) Rivastigmine for Alzheimer's disease. Cochrane Database Syst Rev 4:Cd001191.

Blanchard V, Moussaoui S, Czech C, Touchet N, Bonici B et al. (2003) Time sequence of maturation of dystrophic neurites associated with A beta deposits in APP/PS1 transgenic mice. Experimental Neurology 184 (1):247-263.

Bordet T, Berna P, Abitbol JL, Pruss R (2010) Olesoxime (TRO19622): A Novel Mitochondrial-Targeted Neuroprotective Compound. Pharmaceuticals 3:345 - 368.

Bordet T, Buisson B, Michaud M, Abitbol JL, Marchand F, Grist J, Andriambeloson E, Malcangio M, Pruss RM (2008) Specific antinociceptive activity of cholest-4-en-3-one, oxime (TRO19622) in experimental models of painful diabetic and chemotherapy-induced neuropathy. J Pharmacol Exp Therap 326 (2):623-632.

Bordet T, Buisson B, Michaud M, Drouot C, Galea P et al. (2007) Identification and characterization of cholest-4-en-3-one, oxime (TRO19622), a novel drug candidate for amyotrophic lateral sclerosis. J Pharmacol Exp Ther 322 (2):709-720.

Borg JP, Yang Y, De Taddeo-Borg M, Margolis B, Turner RS (1998) The X11alpha protein slows cellular amyloid precursor protein processing and reduces Abeta40 and Abeta42 secretion. J Biol Chem 273 (24):14761-14766.

Bosetti F, Brizzi F, Barogi S, Mancuso M, Siciliano G, Tendi EA, Murri L, Rapoport SI, Solaini G (2002) Cytochrome c oxidase and mitochondrial F1F0-ATPase (ATP synthase) activities in platelets and brain from patients with Alzheimer's disease. Neurobiol Aging 23 (3):371-376.

Bossy-Wetzel E, Barsoum MJ, Godzik A, Schwarzenbacher R, Lipton SA (2003) Mitochondrial fission in apoptosis, neurodegeneration and aging. Curr Opin Cell Biol 15 (6):706-716.

Broe M, Shepherd CE, Mann DM, Milward EA, Gai WP, Thiel E, Halliday GM (2005) Insoluble alpha-synuclein in Alzheimer's disease without Lewy body formation. Neurotox Res 7 (1-2):69-76.

Bruban J, Voloudakis G, Huang Q, Kajiwara Y, Al Rahim M et al. (2015) Presenilin 1 is necessary for neuronal, but not glial, EGFR expression and neuroprotection via gamma-secretase-independent transcriptional mechanisms. Faseb J 29 (9):3702-3712.

Bruel-Jungerman E, Lucassen PJ, Francis F (2011) Cholinergic influences on cortical development and adult neurogenesis. Behav Brain Res 221 (2):379-388.

Bubber P, Haroutunian V, Fisch G, Blass JP, Gibson GE (2005) Mitochondrial abnormalities in Alzheimer brain: mechanistic implications. Ann Neurol 57 (5):695-703.

Butterfield DA, Howard BJ, LaFontaine MA (2001) Brain oxidative stress in animal models of accelerated aging and the age-related neurodegenerative disorders, Alzheimer's disease and Huntington's disease. Curr Med Chem 8 (7):815-828.

Butterfield DA, Pocernich CB (2003) The glutamatergic system and Alzheimer's disease: therapeutic implications. CNS Drugs 17 (9):641-652.

Cai Q, Tammineni P (2016) Alterations in Mitochondrial Quality Control in Alzheimer's Disease. Front Cell Neurosci 10:24.

Caldwell CC, Yao J, Brinton RD (2015) Targeting the prodromal stage of Alzheimer's disease: bioenergetic and mitochondrial opportunities. Neurotherapeutics. J American Soc Exp Neuro Therap 12 (1):66-80.

Cano-Cuenca N, Solis-Garcia del Pozo JE, Jordan J (2014) Evidence for the efficacy of latrepirdine (Dimebon) treatment for improvement of cognitive function: a meta-analysis. J Alzheimers Dis 38 (1):155-164.

Cesura AM, Pinard E, Schubenel R, Goetschy V, Friedlein A et al. (2003) The voltage-dependent anion channel is the target for a new class of inhibitors of the mitochondrial permeability transition pore. J Biol Chem 278 (50):49812-49818.

Chakrabarti L, Eng J, Ivanov N, Garden GA, La Spada AR (2009) Autophagy activation and enhanced mitophagy characterize the Purkinje cells of pcd mice prior to neuronal death. Mol Brain 2:24.

Chami L, Buggia-Prevot V, Duplan E, Delprete D, Chami M, Peyron JF, Checler F (2012) Nuclear factor-kappaB regulates betaAPP and beta- and gamma-secretases differently at physiological and supraphysiological Abeta concentrations. J Biol Chem 287 (29):24573-24584.

Chau S, Herrmann N, Ruthirakuhan MT, Chen JJ, Lanctot KL (2015) Latrepirdine for Alzheimer's disease. Cochrane Database Syst Rev 4:Cd009524.

Cho DH, Nakamura T, Fang J, Cieplak P, Godzik A, Gu Z, Lipton SA (2009) S-nitrosylation of Drp1 mediates beta-amyloid-related mitochondrial fission and neuronal injury. Science 324 (5923):102-105.

Choi KJ, Kim MJ, Je AR, Jun S, Lee C, Lee E, Jo M, Huh YH, Kweon HS (2014) Three-dimensional analysis of abnormal ultrastructural alteration in mitochondria of hippocampus of APP/PSEN1 transgenic mouse. J Biosci 39 (1):97-105.

Christen Y (2004) Ginkgo biloba and neurodegenerative disorders. Front Biosci 9:3091-3104.

Cipolat S, Martins de Brito O, Dal Zilio B, Scorrano L (2004) OPA1 requires mitofusin 1 to promote mitochondrial fusion. Proc Natl Acad Sci U S A 101 (45):15927-15932.

Citron M (2010) Alzheimer's disease: strategies for disease modification. Nat Rev Drug Discov 9 (5):387-398.

Citron M, Oltersdorf T, Haass C, McConlogue L, Hung AY, Seubert P, Vigo-Pelfrey C, Lieberburg I, Selkoe DJ (1992) Mutation of the beta-amyloid precursor protein in familial Alzheimer's disease increases beta-protein production. Nature 360 (6405):672-674.

Clemens LE, Weber JJ, Wlodkowski TT, Yu-Taeger L, Michaud M et al. (2015) Olesoxime suppresses calpain activation and mutant huntingtin fragmentation in the BACHD rat. Brain 138 (Pt 12):3632-3653.

Cogliati S, Enriquez JA, Scorrano L (2016) Mitochondrial Cristae: Where Beauty Meets Functionality. Trends Biochem Sci.

Colell A (2003) Cholesterol Impairs the Adenine Nucleotide Translocator-mediated Mitochondrial Permeability Transition through Altered Membrane Fluidity. J Biol Chem 278 (36):33928–33935.

Coyle J, Kershaw P (2001) Galantamine, a cholinesterase inhibitor that allosterically modulates nicotinic receptors: effects on the course of Alzheimer's disease. Biol Psychiatry 49 (3):289-299.

Cuadrado-Tejedor M, Vilarino M, Cabodevilla F, Del Rio J, Frechilla D, Perez-Mediavilla A (2011) Enhanced expression of the voltage-dependent anion channel 1 (VDAC1) in Alzheimer's disease transgenic mice: an insight into the pathogenic effects of amyloid-beta. J Alzheimers Dis 23 (2):195-206.

Day M, Chandran P, Luo F, Rustay NR, Markosyan S, LeBlond D, Fox GB (2011) Latrepirdine increases cerebral glucose utilization in aged mice as measured by [18F]-fluorodeoxyglucose positron emission tomography. Neuroscience 189:299-304.

de Arriba G, Calvino M, Benito S, Parra T (2013) Cyclosporine A-induced apoptosis in renal tubular cells is related to oxidative damage and mitochondrial fission. Toxicology letters 218 (1):30-38.

DeKosky ST, Williamson JD, Fitzpatrick AL, Kronmal RA, Ives DG et al. (2008) Ginkgo biloba for prevention of dementia: a randomized controlled trial. Jama 300 (19):2253-2262.

DiCiero MM, de BV, Vale MR, Viana GS (2000) Lipid peroxidation and nitrite plus nitrate levels in brain tissue from patients with Alzheimer's disease. Gerontology 46 (4):179-184.

Doody RS, Gavrilova SI, Sano M, Thomas RG, Aisen PS, Bachurin SO, Seely L, Hung D (2008) Effect of dimebon on cognition, activities of daily living, behaviour, and global function in patients with mild-to-moderate Alzheimer's disease: a randomised, double-blind, placebo-controlled study. Lancet 372 (9634):207-215.

Drachman DA (2006) Aging of the brain, entropy, and Alzheimer disease. Neurology 67 (8):1340-1352.

Drachman DA (2014) The amyloid hypothesis, time to move on: Amyloid is the downstream result, not cause, of Alzheimer's disease. Alzheimers Dement 10(3):372-80.

Drever BD, Riedel G, Platt B (2011) The cholinergic system and hippocampal plasticity. Behav Brain Res 221 (2):505-514.

Du H, Guo L, Fang F, Chen D, A Sosunov A et al. (2008) Cyclophilin D deficiency attenuates mitochondrial and neuronal perturbation and ameliorates learning and memory in Alzheimer's disease. Nature Medicine 14 (10):1097–1105.

Du H, Guo L, Yan S, Sosunov AA, McKhann GM, Yan SS (2010) Early deficits in synaptic mitochondria in an Alzheimer's disease mouse model. Proc Natl Acad Sci U S A 107 (43):18670-18675.

Du H, Guo L, Zhang W, Rydzewska M, Yan S (2011) Cyclophilin D deficiency improves mitochondrial function and learning/memory in aging Alzheimer disease mouse model. Neurobiology of aging 32 (3):398–406.

Du H, Yan S (2010) Mitochondrial permeability transition pore in Alzheimer's disease: cyclophilin D and amyloid beta. Biochim Biophys Acta 1802 (1):198–204.

Dumont M, Stack C, Elipenahli C, Jainuddin S, Launay N et al. (2014) PGC-1alpha overexpression exacerbates beta-amyloid and tau deposition in a transgenic mouse model of Alzheimer's disease. FASEB J 28 (4):1745-1755.

Eckert A, Steiner B, Marques C, Leutz S, Romig H, Haass C, Muller WE (2001) Elevated vulnerability to oxidative stress-induced cell death and activation of caspase-3 by the Swedish amyloid precursor protein mutation. J Neurosci Res 64 (2):183-192.

Eckert GP (2010) Traditional used Plants against Cognitive Decline and Alzheimer Disease. Front Pharmacol 1:138.

Eckert GP, Lipka U, Muller WE (2013) Omega-3 fatty acids in neurodegenerative diseases: focus on mitochondria. Prostaglandins Leukot Essent Fatty Acids 88 (1):105-114.

Eckert GP, Renner K, Eckert SH, Eckmann J, Hagl S, Abdel-Kader RM, Kurz C, Leuner K, Muller WE (2012a) Mitochondrial dysfunction--a pharmacological target in Alzheimer's disease. Mol Neurobiol 46 (1):136-150.

Eckert SH, Eckmann J, Renner-Sattler K, Eckert GP, Leuner K, Mueller WE (2012b) Dimebon Ameliorates Amyloid-beta Induced Impairments of Mitochondrial Form and Function. J Alzheimers Dis 31(1):21-32.

Eckmann J, Clemens LE, Eckert SH, Hagl S, Yu-Taeger L et al. (2014) Mitochondrial Membrane Fluidity is Consistently Increased in Different Models of Huntington Disease: Restorative Effects of Olesoxime. Mol Neurobiol 50 (1):107-118.

Eckmann J, Eckert SH, Leuner K, Muller WE, Eckert GP (2013) Mitochondria: Mitochondrial membranes in brain ageing and neurodegeneration. Int J Biochem Cell Biol 45:76-80.

Ehret MJ, Chamberlin KW (2015) Current Practices in the Treatment of Alzheimer Disease_ Where is the Evidence After the Phase III Trials? Clinical Therapeutics 37 (8):1604-1616.

Emilien G, Maloteaux JM, Beyreuther K, Masters CL (2000) Alzheimer disease: mouse models pave the way for therapeutic opportunities. Arch Neurol 57(2):176-81 57 (2):176-181.

Fan LF, Xu DE, Wang WH, Yan K, Wu H, Yao XQ, Xu RX, Liu CF, Ma QH (2013) Caspr interaction with Amyloid Precursor Protein reduces amyloid-beta generation in vitro. Neurosci Lett 548:255-260.

Fang L, Hemion C, Goldblum D, Meyer P, Orgul S, Frank S, Flammer J, Neutzner A (2012) Inactivation of MARCH5 prevents mitochondrial fragmentation and interferes with cell death in a neuronal cell model. PLoS One 7 (12):e52637.

Fehske CJ, Leuner K, Muller WE (2009) Ginkgo biloba extract (EGb761) influences monoaminergic neurotransmission via inhibition of NE uptake, but not MAO activity after chronic treatment. Pharmacol Res 60 (1):68-73.

Feng L, Li S, Xiao B, Chen S, Liu R, Zhang Y (2010) Fluorescence imaging of APP in Alzheimer's disease with quantum dot or Cy3: a comparative study. Zhong nan da xue xue bao Yi xue ban = Journal of Central South University Medical sciences 35 (9):903-909.

Foley AM, Ammar ZM, Lee RH, Mitchell CS (2015) Systematic review of the relationship between amyloid-beta levels and measures of transgenic mouse cognitive deficit in Alzheimer's disease. J Alzheimers Dis 44 (3):787-795.

Forte M (2004) VADC function in a cellular context. In: Koehler CM, Bauer MF (eds) Mitochondrial Function and Biogenesis, vol Topics in Current Genetics. Springer, Berlin, pp 251-266

Frank S, Gaume B, Bergmann-Leitner ES, Leitner WW, Robert EG, Catez F, Smith CL, Youle RJ (2001) The role of dynamin-related protein 1, a mediator of mitochondrial fission, in apoptosis. Dev Cell 1 (4):515-525.

Friedland-Leuner K, Stockburger C, Denzer I, Eckert GP, Muller WE (2014) Mitochondrial dysfunction: cause and consequence of Alzheimer's disease. Prog Mol Biol Transl Sci. 127:183-210.

Galloway CA, Lee H, Nejjar S, Jhun BS, Yu T, Hsu W, Yoon Y (2012) Transgenic control of mitochondrial fission induces mitochondrial uncoupling and relieves diabetic oxidative stress. Diabetes 61 (8):2093-2104.

Garofalo T, Tinari A, Matarrese P, Giammarioli AM, Manganelli V, Ciarlo L, Misasi R, Sorice M, Malorni W (2007) Do mitochondria act as "cargo boats" in the journey of GD3 to the nucleus during apoptosis? FEBS Lett 581 (21):3899-3903.

Gauthier S, Schlaefke S (2014) Efficacy and tolerability of Ginkgo biloba extract EGb 761® in dementia: a systematic review and meta-analysis of randomized placebo-controlled trials. Clinical Interventions in Aging 9:2065-2077.

Ghavami S, Shojaei S, Yeganeh B, Ande SR, Jangamreddy JR et al. (2014) Autophagy and apoptosis dysfunction in neurodegenerative disorders. Prog Neurobiol 112:24-49.

Giacobini E, Gold G (2013) Alzheimer disease therapy-moving from amyloid-beta to tau. Nat Rev Neurol 9 (12):677-686.

Gilkerson RW (2009) Mitochondrial DNA nucleoids determine mitochondrial genetics and dysfunction. Int J Biochem Cell Biol 41 (10):1899-1906.

Gilling KE, Jatzke C, Hechenberger M, Parsons CG (2009) Potency, voltage-dependency, agonist concentration-dependency, blocking kinetics and partial untrapping of the uncompetitive N-methyl-D-aspartate (NMDA) channel blocker memantine at human NMDA (GluN1/GluN2A) receptors. Neuropharmacology 56 (5):866-875.

Gincel D, Zaid H, Shoshan-Barmatz V (2001) Calcium binding and translocation by the voltage-dependent anion channel: a possible regulatory mechanism in mitochondrial function. Biochem J 358 (Pt 1):147-155.

Giorgetti M, Gibbons JA, Bernales S, Alfaro IE, Drieu LR et al. (2010) Cognition-enhancing properties of Dimebon in a rat novel object recognition task are unlikely to be associated with acetylcholinesterase inhibition or N-methyl-D-aspartate receptor antagonism. J Pharmacol Exp Ther 333 (3):748-757.

Glenner GG, Wong CW (1984) Alzheimers disease. Initial report of the purification and characterisation of a noval cerebrovascular amyloid protein. Biochem Biophys Res Commun 12:885-890.

Gonzalez-Freire M, de Cabo R, Bernier M, Sollott SJ, Fabbri E, Navas P, Ferrucci L (2015) Reconsidering the Role of Mitochondria in Aging. J Gerontol A Biol Sci Med Sci 70 (11):1334-1342.

Gonzalez-Polo RA, Bravo-San Pedro JM, Gomez-Sanchez R, Pizarro-Estrella E, Niso-Santano M, Fuentes JM (2013) Autophagy, mitochondria and 3-nitropropionic acid joined in the same model. Br J Pharmacol 168 (1):60-62.

Gouarné C, Giraudon-Paoli M, Seimandi M, Biscarrat C, Tardif G, Pruss RM, Bordet T (2013) Olesoxime protects embryonic cortical neurons from camptothecin intoxication by a mechanism distinct from BDNF. Br J Pharmacol 168 (8):1975-1988.

Gouarne C, Tracz J, Paoli MG, Deluca V, Seimandi M et al. (2015) Protective role of olesoxime against wild-type alpha-synuclein-induced toxicity in human neuronally differentiated SHSY-5Y cells. Br J Pharmacol 172 (1):235-245.

Green DR, Galluzzi L, Kroemer G (2011) Mitochondria and the autophagy-inflammation-cell death axis in organismal aging. Science 333 (6046):1109-1112.

Grimm A, Friedland K, Eckert A (2015) Mitochondrial dysfunction: the missing link between aging and sporadic Alzheimer`s disease. Biogerontology 17(2):281-96.

Griparic L, Head B, van der Bliek AM (2004) Mitochondrial fission and fusion machineries. In: Koehler C, Bauer MF (eds) Mitochondrial Function and Biogenetics. Springer Inc., Heidelberg, p 227ff

Hagl S, Berressem D, Grewal R, Sus N, Frank J, Eckert GP (2016) Rice bran extract improves mitochondrial dysfunction in brains of aged NMRI mice. Nutr Neurosci 19 (1):1-10.

Hagl S, Grewal R, Ciobanu I, Helal A, Khayyal MT, Muller WE, Eckert GP (2015a) Rice bran extract compensates mitochondrial dysfunction in a cellular model of early Alzheimer's disease. J Alzheimers Dis 43 (3):927-938.

Hagl S, Heinrich M, Kocher A, Schiborr C, Frank J, Eckert GP (2014) Curcumin micelles improve mitochondrial function in a mouse model of Alzheimer's disease. J Prevention Alzheimers Dis 1 (2):80-83.

Hagl S, Kocher A, Schiborr C, Eckert SH, Ciobanu I et al. (2013) Rice bran extract protects from mitochondrial dysfunction in guinea pig brains. Pharmacol Res 76C:17-27.

Hagl S, Kocher A, Schiborr C, Kolesova N, Frank J, Eckert GP (2015b) Curcumin micelles improve mitochondrial function in neuronal PC12 cells and brains of NMRI mice - Impact on bioavailability. Neurochem Int 89:234-242.

Hall AM, Roberson ED (2012) Mouse models of Alzheimer`s disease. Brain Res Bull 88 (1):3-12.

Han XJ, Lu YF, Li SA, Kaitsuka T, Sato Y et al. (2008) CaM kinase I alpha-induced phosphorylation of Drp1 regulates mitochondrial morphology. J Cell Biol 182 (3):573-585.

Hardy JA, Higgins GA (1992) Alzheimer's disease: the amyloid cascade hypothesis. Science 256 (5054):184-185.

Hauptmann S, Scherping I, Drose S, Brandt U, Schulz KL, Jendrach M, Leuner K, Eckert A, Mueller WE (2009) Mitochondrial dysfunction: An early event in Alzheimer pathology accumulates with age in AD transgenic mice. Neurobiol Aging 30 (10):1574-1586.

Hellweg R, Wirth Y, Janetzky W, Hartmann S (2012) Efficacy of memantine in delaying clinical worsening in Alzheimer's disease (AD): responder analyses of nine clinical trials with patients with moderate to severe AD. Int J Geriatr Psychiatry 27 (6):651-656.

Heneka MT, Carson MJ, El Khoury J, Landreth GE, Brosseron F et al. (2015) Neuroinflammation in Alzheimer's disease. Lancet Neurol 14 (4):388-405.

Hensley K, Harris-White ME (2015) Redox regulation of autophagy in healthy brain and neurodegeneration. Neurobiol Dis 84:50-59.

Herrup K (2015) The case for rejecting the amyloid cascade hypothesis. Nat Neurosci 18 (6):794-799.

Hirai K, Aliev G, Nunomura A, Fujioka H, Russell RL et al. (2001) Mitochondrial abnormalities in Alzheimer's disease. J Neurosci 21 (9):3017-3023.

Hofmann S, Bauer MF (2004) Protein translocation into mammalian mitochondria and its role in the development of human mitochondrial disorders. In: Koehler C, Bauer MF (eds) Mitochondrial Function and Biogenetics. Springer Inc., Heidelberg, pp 201-225

Howes MJ, Perry NS, Houghton PJ (2003) Plants with traditional uses and activities, relevant to the management of Alzheimer's disease and other cognitive disorders. Phytother Res 17 (1):1-18.

Hoyer A, Bardenheuer HJ, Martin E, Plaschke K (2005) Amyloid precursor protein (APP) and its derivatives change after cellular energy depletion. An in vitro-study. J Neural Transm 112 (2):239-253.

Hoyer S (1993) Brain oxidative energy and related metabolism, neuronal stress, and Alzheimer's disease: a speculative synthesis. J Geriatr Psychiatry Neurol 6 (1):3-13.

Hsiao K, Chapman P, Nilsen S, Eckman C, Harigaya Y, Younkin S, Yang F, Cole G (1996) Correlative memory deficits, Abeta elevation, and amyloid plaques in transgenic mice. Science 274 (5284):99-102.

Hu J, Zhang Z, Shen WJ, Azhar S (2010) Cellular cholesterol delivery, intracellular processing and utilization for biosynthesis of steroid hormones. Nutr Metab (Lond) 7:47.

Ihl R (2013) Effects of Ginkgo biloba extract EGb 761 (R) in dementia with neuropsychiatric features: review of recently completed randomised, controlled trials. International journal of psychiatry in clinical practice 17 Suppl 1:8-14.

Ihl R, Frolich L, Winblad B, Schneider L, Burns A, Moller HJ (2011) World Federation of Societies of Biological Psychiatry (WFSBP) guidelines for the biological treatment of Alzheimer's disease and other dementias. The world journal of biological psychiatry : the official journal of the World Federation of Societies of Biological Psychiatry 12 (1):2-32.

Iqbal K, Liu F, Gong CX (2014) Alzheimer disease therapeutics: focus on the disease and not just plaques and tangles. Biochem Pharmacol 88 (4):631-639.

Jahani-Asl A, Cheung EC, Neuspiel M, MacLaurin JG, Fortin A, Park DS, McBride HM, Slack RS (2007) Mitofusin 2 protects cerebellar granule neurons against injury-induced cell death. J Biol Chem 282 (33):23788-23798.

James AM, Sharpley MS, Manas ARB, Frerman FE, Hirst J, Smith RAJ, Murphy MP (2007) Interaction of the Mitochondria-targeted Antioxidant MitoQ with Phospholipid Bilayers and Ubiquinone Oxidoreductases. Journal of Biological Chemistry 282 (20):14708-14718.

James SA, Volitakis I, Adlard PA, Duce JA, Masters CL, Cherny RA, Bush AI (2012) Elevated labile Cu is associated with oxidative pathology in Alzheimer disease. Free Radic Biol Med 52 (2):298-302.

Jendrach M, Busch K, Bereiter-Hahn J (2005) Exchange of mitochondrial membrane proteins during fusion of mitochondria. European Journal of Cell Biology 84:72-72.

Jimeson M, Machado P (2010) Pfizer And Medivation Announce Results From Two Phase 3 Studies In Dimebon (latrepirdine*) Alzheimer's Disease Clinical Development Program. http://investors.medivation.com/releasedetail.cfm?releaseid=448818. Accessed 02/10/12 2012

Jun G, Asai H, Zeldich E, Drapeau E, Chen C et al. (2014) PLXNA4 is associated with Alzheimer disease and modulates tau phosphorylation. Ann Neurol 76 (3):379-392.

Kaasik A, Safiulina D, Zharkovsky A, Veksler V (2007) Regulation of mitochondrial matrix volume. Am J Physiol Cell Physiol 292 (1):C157-163.

Kabeya Y, Mizushima N, Yamamoto A, Oshitani-Okamoto S, Ohsumi Y, Yoshimori T (2004) LC3, GABARAP and GATE16 localize to autophagosomal membrane depending on form-II formation. J Cell Sci 117 (Pt 13):2805-2812.

Keil U, Bonert A, Marques CA, Scherping I, Weyermann J et al. (2004) Amyloid beta-induced changes in nitric oxide production and mitochondrial activity lead to apoptosis. J Biol Chem 279 (48):50310-50320.

Keil U, Hauptmann S, Bonert A, Scherping I, Eckert A, Muller WE (2006) Mitochondrial dysfunction induced by disease relevant AbetaPP and tau protein mutations. J Alzheimers Dis 9 (2):139-146.

Keil U, Scherping I, Hauptmann S, Eckert A, Muller WE (2005) Stabilization of mitochondrial function by piracetam. Pharmacopsychiatry 38 (5):253-253.

Kidd PM (2008) Alzheimer's disease, amnestic mild cognitive impairment, and age-associated memory impairment: current understanding and progress toward integrative prevention. Altern Med Rev 13 (2):85-115.

Kieburtz K, McDermott MP, Voss TS, Corey-Bloom J, Deuel LM et al. (2010) A randomized, placebo-controlled trial of latrepirdine in Huntington disease. Arch Neurol 67 (2):154-160.

Kim GH, Kim JE, Rhie SJ, Yoon S (2015) The Role of Oxidative Stress in Neurodegenerative Diseases. Experimental neurobiology 24 (4):325-340.

Kitazawa M, Medeiros R, Laferla FM (2012) Transgenic mouse models of Alzheimer disease: developing a better model as a tool for therapeutic interventions. Curr Pharm Des 18 (8):1131-1147.

Klionsky DJ, Abdelmohsen K, Abe A, Abedin MJ, Abeliovich H et al. (2016) Guidelines for the use and interpretation of assays for monitoring autophagy (3rd edition). Autophagy 12 (1):1-222.

Klionsky DJ, Cuervo AM, Seglen PO (2007) Methods for monitoring autophagy from yeast to human. Autophagy 3 (3):181-206.

Klugman A, Naughton DP, Isaac M, Shah I, Petroczi A, Tabet N (2012) Antioxidant enzymatic activities in Alzheimer's disease: the relationship to acetylcholinesterase inhibitors. J Alzheimers Dis 30 (3):467-474.

Knott AB, Bossy-Wetzel E (2008) Impairing the mitochondrial fission and fusion balance: a new mechanism of neurodegeneration. Ann N Y Acad Sci 1147:283-292.

Knott AB, Perkins G, Schwarzenbacher R, Bossy-Wetzel E (2008) Mitochondrial fragmentation in neurodegeneration. Nat Rev Neurosci 9 (7):505-518.

Kumar A, Singh A (2015) A review on mitochondrial restorative mechanism of antioxidants in Alzheimer's disease and other neurological conditions. Front Pharmacol 6:206.

Kurz C, Ungerer I, Lipka U, Kirr S, Schütt T, Eckert A, Leuner K, Mueller WE (2010) The metabolic enhancer piracetam ameliorates ß-amyloidpeptide induced impairment of mitochondrial function andneuritic outgrowth Br J Pharmacol 160 (2):246-257.

Lansdall CL (2014) An effective treatment for Alzheimer's disease must consider both amyloid and tau. Bioscience Horizons 7:1-11.

Larsen S, Nielsen J, Hansen CN, Nielsen LB, Wibrand F et al. (2012) Biomarkers of mitochondrial content in skeletal muscle of healthy young human subjects. J Physiol 590 (14):3349-3360.

Le Bars PL (2003) Magnitude of effect and special approach to Ginkgo biloba extract EGb 761 in cognitive disorders. Pharmacopsychiatry 36 Suppl 1:S44-S49.

Lee HP, Pancholi N, Esposito L, Previll LA, Wang X, Zhu X, Smith MA, Lee HG (2012) Early induction of oxidative stress in mouse model of Alzheimer disease with reduced mitochondrial superoxide dismutase activity. PLoS One 7 (1):e28033.

Lee YJ, Jeong SY, Karbowski M, Smith CL, Youle RJ (2004) Roles of the mammalian mitochondrial fission and fusion mediators Fis1, Drp1, and Opa1 in apoptosis. Mol Biol Cell 15 (11):5001-5011.

Legros F, Malka F, Frachon P, Lombes A, Rojo M (2004) Organization and dynamics of human mitochondrial DNA. J Cell Sci 117 (Pt 13):2653-2662.

Lenglet T, Lacomblez L, Abitbol JL, Ludolph A, Mora JS et al. (2014) A phase II-III trial of olesoxime in subjects with amyotrophic lateral sclerosis. European journal of neurology 21 (3):529-536.

Lermontova NN, Redkozubov AE, Shevtsova EF, Serkova TP, Kireeva EG, Bachurin SO (2001) Dimebon and tacrine inhibit neurotoxic action of beta-amyloid in culture and block L-type Ca(2+) channels. Bull Exp Biol Med 132 (5):1079-1083.

Leuner K, Kurz C, Guidetti G, Orgogozo JM, Muller WE (2010) Improved mitochondrial function in brain aging and Alzheimer disease - the new mechanism of action of the old metabolic enhancer piracetam. Front Neurosci 4:pii 44.

Leuner K, Muller WE, Reichert AS (2012a) From mitochondrial dysfunction to amyloid beta formation: novel insights into the pathogenesis of Alzheimer's disease. Mol Neurobiol 46 (1):186-193.

Leuner K, Pantel J, Frey C, Schindowski K, Schulz K, Wegat T, Maurer K, Eckert A, Muller WE (2007) Enhanced apoptosis, oxidative stress and mitochondrial dysfunction in lymphocytes as potential biomarkers for Alzheimer's disease. J Neural Transm Suppl (72):207-215.

Leuner K, Schütt T, Kurz C, Eckert SH, Schiller C et al. (2012c) Mitochondrion-Derived Reactive Oxygen Species Lead to Enhanced Amyloid Beta Formation. Antioxid Redox Signal 16 (12):1421-1433.

Levine B, Kroemer G (2008) Autophagy in the pathogenesis of disease. Cell 132 (1):27-42.

Levine B, Yuan J (2005) Autophagy in cell death: an innocent convict? J Clin Invest 115 (10):2679-2688.

Li Y, Zhang Y, Han W, Hu F, Qian Y, Chen Q (2013) TRO19622 promotes myelin repair in a rat model of demyelination. Int J Neurosci 123 (11):810-822.

Li Z, Okamoto K, Hayashi Y, Sheng M (2004a) The importance of dendritic mitochondria in the morphogenesis and plasticity of spines and synapses. Cell 119 (6):873-887.

Liang H, Ward WF (2006) PGC-1alpha: a key regulator of energy metabolism. Adv Physiol Educ 30 (4):145-151.

Lionaki E, Markaki M, Palikaras K, Tavernarakis N (2015) Mitochondria, autophagy and age-associated neurodegenerative diseases: New insights into a complex interplay. BBA - Bioenergetics 1847 (11):1412-1423.

Liu X, Hajnoczky G (2011) Altered fusion dynamics underlie unique morphological changes in mitochondria during hypoxia-reoxygenation stress. Cell Death Differ 18 (10):1561-1572.

Lopez-Lluch G, Irusta PM, Navas P, de Cabo R (2008) Mitochondrial biogenesis and healthy aging. Exp Gerontol 43 (9):813-819.

Lynn BC, Wang J, Markesbery WR, Lovell MA (2010) Quantitative changes in the mitochondrial proteome from subjects with mild cognitive impairment, early stage, and late stage Alzheimer's disease. J Alzheimers Dis 19 (1):325-339.

Madden TD, Hope MJ, Cullis PR (1983) Lipid requirements for coupled cytochrome oxidase vesicles. Biochem 22 (8):1970–1974.

Magalon K, Zimmer C, Cayre M, Khaldi J, Bourbon C et al. (2012) Olesoxime accelerates myelination and promotes repair in models of demyelination. Ann Neurol 71 (2):213-226.

Mai S, Klinkenberg M, Auburger G, Bereiter-Hahn J, Jendrach M (2010) Decreased expression of Drp1 and Fis1 mediates mitochondrial elongation in senescent cells and enhances resistance to oxidative stress through PINK1. J Cell Sci 123 (Pt 6):917-926.

Malinski T (2007) Nitric oxide and nitroxidative stress in Alzheimer's disease. J Alzheimers Dis 11 (2):207-218.

Manczak M, Anekonda TS, Henson E, Park BS, Quinn J, Reddy PH (2006) Mitochondria are a direct site of A beta accumulation in Alzheimer's disease neurons: implications for free radical generation and oxidative damage in disease progression. Hum Mol Genet 15 (9):1437-1449.

Manczak M, Park BS, Jung Y, Reddy PH (2004) Differential expression of oxidative phosphorylation genes in patients with Alzheimer's disease: implications for early mitochondrial dysfunction and oxidative damage. Neuromolecular Med 5 (2):147-162.

Mao P, Reddy PH (2011) Aging and amyloid beta-induced oxidative DNA damage and mitochondrial dysfunction in Alzheimer's disease: implications for early intervention and therapeutics. Biochim Biophys Acta 1812 (11):1359-1370.

Martin LJ, Adams NA, Pan Y, Price A, Wong M (2011) The mitochondrial permeability transition pore regulates nitric oxide-mediated apoptosis of neurons induced by target deprivation. The Journal of neuroscience : the official journal of the Society for Neuroscience 31 (1):359-370.

Martinou JC, Youle RJ (2011) Mitochondria in apoptosis: Bcl-2 family members and mitochondrial dynamics. Dev Cell 21 (1):92-101.

Masters CL, Bateman R, Blennow K, Rowe CC, Sperling RA, Cummings JL (2015) Alzheimer`s disease. Nature Reviews Disease Primers:15056.

Mattson MP, Gleichmann M, Cheng A (2008) Mitochondria in neuroplasticity and neurological disorders. Neuron 60 (5):748-766.

Mazza M, Capuano A, Bria P, Mazza S (2006) Ginkgo biloba and donepezil: a comparison in the treatment of Alzheimer's dementia in a randomized placebo-controlled double-blind study. European journal of neurology 13 (9):981-985.

McManus MJ, Murphy MP, Franklin JL (2011) The mitochondria-targeted antioxidant MitoQ prevents loss of spatial memory retention and early neuropathology in a transgenic mouse model of Alzheimer's disease. J Neurosci 31 (44):15703-15715.

McShane R, Areosa Sastre A, Minakaran N (2006) Memantine for dementia. Cochrane Database Syst Rev (2):Cd003154.

Medina M, Avila J (2014) New perspectives on the role of tau in Alzheimer's disease. Implications for therapy. Biochem Pharmacol 88 (4):540-547.

Michaelson DM (2014) APOE epsilon4: the most prevalent yet understudied risk factor for Alzheimer's disease. Alzheimers Dement 10 (6):861-868.

Mizushima N, Levine B, Cuervo AM, Klionsky DJ (2008) Autophagy fights disease through cellular self-digestion. Nature 451 (7182):1069-1075.

Mizushima N, Yoshimori T (2007) How to interpret LC3 immunoblotting. Autophagy 3 (6):542-545.

Mo C, Renoir T, Hannan AJ (2016) What's wrong with my mouse cage? Methodological considerations for modeling lifestyle factors and gene-environment interactions in mice. J Neurosci Methods 30 (265):99-108.

Montecucco C, Smith GA, Dabbeni-sala F, Johannsson A, Galante YM, Bisson R (1982) Bilayer thickness and enzymatic activity in the mitochondrial cytochrome c oxidase and ATPase complex. FEBS letters 144 (1):145–148.

Moreira PI, Zhu X, Wang X, Lee HG, Nunomura A, Petersen RB, Perry G, Smith MA (2010) Mitochondria: a therapeutic target in neurodegeneration. Biochim Biophys Acta 1802 (1):212-220.

Mozdy AD, McCaffery JM, Shaw JM (2000) Dnm1p GTPase-mediated mitochondrial fission is a multi-step process requiring the novel integral membrane component Fis1p. J Cell Biol 151 (2):367-380.

Mueller WE, Eckert A, Eckert GP, Fink H, Friedland K, Heoerr R, Ihl R, Kasper S, Moeller HJ (2016) Ginkgo-Spezialextrakt 761 (Tebonin) - Ein präklinisches und klinisches Update im Wandel klinischer und ätiopathogenetischer Konzepte der Alzheimer-Demenz. Psychopharmakotherapie 23 (3):102-117.

Muller WE, Eckert A, Kurz C, Eckert GP, Leuner K (2010) Mitochondrial dysfunction: common final pathway in brain aging and Alzheimer's disease--therapeutic aspects. Mol Neurobiol 41 (2-3):159-171.

Muller WE, Eckert GP, Eckert A (1999) Piracetam: novelty in a unique mode of action. Pharmacopsychiatry 32 Suppl 1:2-9.

Musiek ES, Holtzman DM (2015) Three dimensions of the amyloid hypothesis: time, space and 'wingmen' . Nature Neuroscience 18 (6):800-806.

Nicholls DG (2002) Mitochondrial function and dysfunction in the cell: its relevance to aging and aging-related disease. Int J Biochem Cell Biol 34 (11):1372-1381.

Nijtmans LGJ, Ugallde C, van den Heuvel LP, Smeitink JAM (2004) Function and dysfunction of the oxidative phospharylation system. In: Koehler C, Bauer MF (eds) Mitochondrial Function and Biogenetics. Springer Inc., Heidelberg, pp 149-167

Obulesu M, Lakshmi MJ (2014) Apoptosis in Alzheimer's disease: an understanding of the physiology, pathology and therapeutic avenues. Neurochem Res 39 (12):2301-2312.

Olichon A, Baricault L, Gas N, Guillou E, Valette A, Belenguer P, Lenaers G (2003) Loss of OPA1 perturbates the mitochondrial inner membrane structure and integrity, leading to cytochrome c release and apoptosis. J Biol Chem 278 (10):7743-7746.

Pagani L, Eckert A (2011) Amyloid-Beta interaction with mitochondria. Int J Alzheimers Dis 2011:925050.

Paradies G, Petrosillo G, Paradies V, Ruggiero FM (2011) Mitochondrial dysfunction in brain aging: role of oxidative stress and cardiolipin. Neurochem Int 58 (4):447-457.

Parsons CG, Danysz W, Dekundy A, Pulte I (2013) Memantine and cholinesterase inhibitors: complementary mechanisms in the treatment of Alzheimer's disease. Neurotox Res 24 (3):358-369.

Paschen W, Frandsen A (2001) Endoplasmic reticulum dysfunction - a common denominator for cell injury in acute and degenerative diseases of the brain? JNeurochem 79 (4):719-725.

Perez SE, Nadeem M, Sadleir KR, Matras J, Kelley CM, Counts SE, Vassar R, Mufson EJ (2012) Dimebon alters hippocampal amyloid pathology in 3xTg-AD mice. International journal of physiology, pathophysiology and pharmacology 4 (3):115-127.

Perry, G., Avila, J., Kinoshita, J., Smith, M.A. Alzheimer`s Disease: A Century of Scientific and Clinical Research (2006). IOS Press Amsterdam, Netherlands.

Peskind ER, Potkin SG, Pomara N, Ott BR, Graham SM, Olin JT, McDonald S (2006) Memantine treatment in mild to moderate Alzheimer disease: a 24-week randomized, controlled trial. Am J Geriatr Psychiatry 14 (8):704-715.

Peters I, Igbavboa U, Schutt T, Haidari S, Hartig U et al. (2009) The interaction of beta-amyloid protein with cellular membranes stimulates its own production. Biochim Biophys Acta 1788 (5):964-972.

Peters OM, Connor-Robson N, Sokolov VB, Aksinenko AY, Kukharsky MS, Bachurin SO, Ninkina N, Buchman VL (2013a) Chronic administration of dimebon ameliorates pathology in TauP301S transgenic mice. J Alzheimers Dis 33 (4):1041-1049.

Peters OM, Shelkovnikova T, Tarasova T, Springe S, Kukharsky MS et al. (2013b) Chronic administration of Dimebon does not ameliorate amyloid-beta pathology in 5xFAD transgenic mice. J Alzheimers Dis 36 (3):589-596.

Petrosillo G, Matera M, Casanova G, Ruggiero FM, Paradies G (2008) Mitochondrial dysfunction in rat brain with aging Involvement of complex I, reactive oxygen species and cardiolipin. Neurochemistry Int 53 (5):126-131.

Pickford F, Masliah E, Britschgi M, Lucin K, Narasimhan R et al. (2008) The autophagy-related protein beclin 1 shows reduced expression in early Alzheimer disease and regulates amyloid beta accumulation in mice. J Clin Invest 118(6):2190-9.

Picone P, Nuzzo D, Caruana L, Scafidi V, Di Carlo M (2014) Mitochondrial dysfunction: different routes to Alzheimer's disease therapy. Oxid Med Cell Longev 2014:780179.

Pike CJ, Walencewicz AJ, Glabe CG, Cotman CW (1991) In vitro aging of beta-amyloid protein causes peptide aggregation and neurotoxicity. Brain Res 563 (1-2):311-314.

Pinho CM, Teixeira PF, Glaser E (2014) Mitochondrial import and degradation of amyloid-beta peptide. Biochim Biophys Acta 1837 (7):1069-1074.

Plomp PJ, Gordon PB, Meijer AJ, Hoyvik H, Seglen PO (1989) Energy dependence of different steps in the autophagic-lysosomal pathway. J Biol Chem 264 (12):6699-6704.

Pohland M, Hagl S, Pellowska M, Wurglics M, Schubert-Zsilavecz M, Eckert GP (2016) MH84: A Novel gamma-Secretase Modulator/PPARgamma Agonist-Improves Mitochondrial

Dysfunction in a Cellular Model of Alzheimer's Disease. Neurochem Res 41 (1-2):2231-2242.

Poot M, Zhang YZ, Kramer JA, Wells KS, Jones LJ, Hanzel DK, Lugade AG, Singer VL, Haugland RP (1996) Analysis of mitochondrial morphology and function with novel fixable fluorescent stains. J Histochem Cytochem 44 (12):1363-1372.

Porsteinsson AP, Grossberg GT, Mintzer J, Olin JT (2008) Memantine treatment in patients with mild to moderate Alzheimer's disease already receiving a cholinesterase inhibitor: a randomized, double-blind, placebo-controlled trial. Curr Alzheimer Res 5 (1):83-89.

Porter T, Bharadwaj P, Groth D, Paxman A, Laws SM, Martins RN, Verdile G (2016) The Effects of Latrepirdine on Amyloid-beta Aggregation and Toxicity. J Alzheimers Dis 50 (3):895-905.

Pozueta J, Lefort R, Shelanski ML (2013) Synaptic changes in Alzheimer's disease and its models. Neuroscience 251:51-65.

Qin R, Zhou D, Wang J, Hu H, Yang Y, Yao X, Sun X (2012) Compound Danshen tablets downregulate amyloid protein precursor mRNA expression in a transgenic cell model of Alzheimer's disease: Effects and a comparison with donepezil. Neural Reg Res 7 (9):659-663.

Qiu C, De Ronchi D, Fratiglioni L (2007) The epidemiology of the dementias: an update. Curr Opin Psychiatry 20 (4):380-385.

Qiu C, Kivipelto M, von Strauss E (2009) Epidemiology of Alzheimer's disease: occurrence, determinants, and strategies toward intervention. Dialogues Clin Neurosci 11 (2):111-128.

Radi E, Formichi P, Battisti C, Federico A (2014) Apoptosis and oxidative stress in neurodegenerative diseases. J Alzheimers Dis 42 Suppl 3:S125-152.

Rapaport D, Nargang FE (2004) Mitochondrial biongenesis: Protein import into and across the outer membrane. In: Koehler CM, Bauer MF (eds) Mitochondrial Function and Biogenesis, vol 8. Topics in Current Gentics. Springer, Berlin,

Rasola A, Sciacovelli M, Pantic B, Bernardi P (2010) Signal transduction to the permeability transition pore. FEBS Lett 584 (10):1989-1996.

Reddy DPH (2014) Misfolded proteins, mitochondrial dysfunction, and neurodegenerative diseases. BBA - Molecular Basis of Disease 1842 (8):1167.

Reddy PH, Manczak M, Mao P, Calkins MJ, Reddy AP, Shirendeb U (2010) Amyloid-beta and mitochondria in aging and Alzheimer's disease: implications for synaptic damage and cognitive decline. J Alzheimers Dis 20 Suppl 2:S499-512.

Reddy PH (2009) Amyloid beta, mitochondrial structural and functional dynamics in Alzheimer's disease. Exp Neurol 218 (2):286-292.

Reddy PH, Beal MF (2008) Amyloid beta, mitochondrial dysfunction and synaptic damage: implications for cognitive decline in aging and Alzheimer's disease. Trends MolMed 14 (2):45-53.

Reddy PH, Beal MF (2005) Are mitochondria critical in the pathogenesis of Alzheimer's disease? Brain Res Rev 49 (3):618-632.

Reitz C, Mayeux R (2014) Alzheimer disease: epidemiology, diagnostic criteria, risk factors and biomarkers. Biochem Pharmacol 88 (4):640-651.

Repalli J (2014) Translocator protein (TSPO) role in aging and Alzheimer's disease. Curr Aging Sci 7 (3):168-175.

Revett TJ, Baker GB, Jhamandas J, Kar S (2013) Glutamate system, amyloid ss peptides and tau protein: functional interrelationships and relevance to Alzheimer disease pathology. J Psych Neurosci 38 (1):6-23.

Rhein V, Song X, Wiesner A, Ittner LM, Baysang G et al. (2009) Amyloid-beta and tau synergistically impair the oxidative phosphorylation system in triple transgenic Alzheimer's disease mice. Proc Natl Acad Sci U S A 106 (47):20057-20062.

Ricchelli F, Gobbo S, Moreno G, Salet C (1999) Changes of the fluidity of mitochondrial membranes induced by the permeability transition. Biochem 38 (29):9295-9300.

Richter F, Gao F, Medvedeva V, Lee P, Bove N et al. (2014) Chronic administration of cholesterol oximes in mice increases transcription of cytoprotective genes and improves transcriptome alterations induced by alpha-synuclein overexpression in nigrostriatal dopaminergic neurons. Neurobiol Dis 69:263-275.

Rohn TT (2010) The role of caspases in Alzheimer's disease; potential novel therapeutic opportunities. Apoptosis 15 (11):1403-1409.

Romanello V, Guadagnin E, Gomes L, Roder I, Sandri C et al. (2010) Mitochondrial fission and remodelling contributes to muscle atrophy. EMBO J 29 (10):1774-1785.

Rone MB, Liu J, Blonder J, Ye X, Veenstra TD, Young JC, Papadopoulos V (2009) Targeting and insertion of the cholesterol-binding translocator protein into the outer mitochondrial membrane. Biochemistry 48 (29):6909-6920.

Rovini A, Carre M, Bordet T, Pruss RM, Braguer D (2010) Olesoxime prevents microtubule-targeting drug neurotoxicity: selective preservation of EB comets in differentiated neuronal cells. Bioch Pharmacol 80 (6):884-894.

Rozemuller JM, Eikelenboom P, Stam FC, Beyreuther K, Masters CL (1989) A4 protein in Alzheimer's disease: primary and secondary cellular events in extracellular amyloid deposition. J Neuropathol Exp Neurol 48 (6):674-691.

Rui Y, Tiwari P, Xie Z, Zheng JQ (2006) Acute impairment of mitochondrial trafficking by beta-amyloid peptides in hippocampal neurons. J Neurosci 26 (41):10480-10487.

Sabbagh MN, Berk C (2010) Latrepirdine for Alzheimer's Disease: Trials and Tribulations. Future Neurology 5 (5):645-651.

Sachdeva D, Burns A (2011) Dimebolin in dementia. CNS Neurosci Ther 17 (3):199-205.

Santos RX, Correia SC, Wang X, Perry G, Smith MA, Moreira PI, Zhu X (2010) A synergistic dysfunction of mitochondrial fission/fusion dynamics and mitophagy in Alzheimer`s disease. J Alzheimers Dis 20 Suppl 2:S401-412.

Sastre J, Lloret A, Borras C, Pereda J, Garcia-Sala D, Droy-Lefaix MT, Pallardo FV, Vina J (2002) Ginkgo biloba extract EGb 761 protects against mitochondrial aging in the brain and in the liver. Cell Mol Biol 48 (6):685-692.

Saunders AM, Strittmatter WJ, Schmechel D, St George-Hyslop PH, Pericak Vance MA et al. (1993) Association of apolipoprotein E allele 4 with late-onset falmilial and sporadic Alzheimer`s Disease. Neurology 43:1467-1472.

Schaffhauser H, Mathiasen JR, Dicamillo A, Huffman MJ, Lu LD, McKenna BA, Qian J, Marino MJ (2009) Dimebolin is a 5-HT6 antagonist with acute cognition enhancing activities. Biochem Pharmacol 78 (8):1035-1042.

Schioth HB, Craft S, Brooks SJ, Frey WH, 2nd, Benedict C (2012) Brain Insulin Signaling and Alzheimer's Disease: Current Evidence and Future Directions. Molecular Neurobiol 46(1):4-10.

Schliebs R, Arendt T (2006) The significance of the cholinergic system in the brain during aging and in Alzheimer's disease. J Neural Transm 113 (11):1625-1644.

Schneider LS, Dagerman KS, Higgins JP, McShane R (2011) Lack of evidence for the efficacy of memantine in mild Alzheimer disease. Arch Neurol 68 (8):991-998.

Schuessel K, Frey C, Jourdan C, Keil U, Weber CC, Müller-Spahn F, Müller WE, Eckert A (2006) Aging sensitizes toward ROS formation and lipid peroxidation in PS1M146L transgenic mice. Free Radic Biol Med 40 (5):850-862.

Schuessel K, Schafer S, Bayer TA, Czech C, Pradier L, Muller-Spahn F, Muller WE, Eckert A (2005) Impaired Cu/Zn-SOD activity contributes to increased oxidative damage in APP transgenic mice. Neurobiol Dis 18 (1):89-99.

Schuh RA, Jackson KC, Schlappal AE, Spangenburg EE, Ward CW, Park JH, Dugger N, Shi GL, Fishman PS (2014) Mitochondrial oxygen consumption deficits in skeletal muscle isolated from an Alzheimer's disease-relevant murine model. BMC Neurosci 15:24.

Selkoe DJ, Abraham C, Ihara Y (1982) Alzheimer-Disease - Insolubility of Paired Helical Filaments (Phf) and the Potential Role of Enzymatic Cross-Linking. Neurology 32 (4):A227-A227.

Shintani T, Klionsky DJ (2004) Autophagy in health and disease: a double-edged sword. Science 306 (5698):990-995.

Shoshan-Barmatz V, Ben-Hail D (2012) VDAC, a multi-functional mitochondrial protein as a pharmacological target. Mitochondrion 12 (1):24–34.

Simonsen A, Cumming RC, Brech A, Isakson P, Schubert DR, Finley KD (2008) Promoting basal levels of autophagy in the nervous system enhances longevity and oxidant resistance in adult Drosophila. Autophagy 4 (2):176-184.

Slotkin TA, Seidler FJ, Crain BJ, Bell JM, Bissette G, Nemeroff CB (1990) Regulatory changes in presynaptic cholinergic function assessed in rapid autopsy material from patients with Alzheimer disease: implications for etiology and therapy. Proc Natl Acad Sci U S A 87 (7):2452-2455.

Sperling RA, Aisen PS, Beckett LA, Bennett DA, Craft S et al. (2011) Toward defining the preclinical stages of Alzheimer's disease: recommendations from the National Institute on Aging-Alzheimer's Association workgroups on diagnostic guidelines for Alzheimer's disease. Alzheimers Dement 7 (3):280-292.

Steele JW, Ju S, Lachenmayer ML, Liken J, Stock A et al. (2013a) Latrepirdine stimulates autophagy and reduces accumulation of alpha-synuclein in cells and in mouse brain. Mol Psychiatry 18 (8):882-888.

Steele JW, Kim SH, Cirrito JR, Verges DK, Restivo JL et al. (2009) Acute dosing of latrepirdine (Dimebon), a possible Alzheimer therapeutic, elevates extracellular amyloid-beta levels in vitro and in vivo. Mol Neurodegener 4:51.

Steele JW, Lachenmayer ML, Ju S, Stock A, Liken J et al. (2013) Latrepirdine improves cognition and arrests progression of neuropathology in an Alzheimer`s mouse model. Molecular Psychiatry 18(8):889-97.

Stockburger C (2014) Störung der mitochondrialen Dynamik als zentraler Bestandteil von Hirnalterungsprozessen und der Pathogenese der Alzheimer Erkrankung, Dissertation University of Frankfurt, Frankfurt

Stockburger C, Gold VA, Pallas T, Kolesova N, Miano D, Leuner K, Muller WE (2014) A cell model for the initial phase of sporadic Alzheimer's disease. J Alzheimers Dis 42 (2):395-411.

Stockburger C, Miano D, Baeumlisberger M, Pallas T, Arrey TN, Karas M, Friedland K, Muller WE (2015) A Mitochondrial Role of SV2a Protein in Aging and Alzheimer's Disease: Studies with Levetiracetam. J Alzheimers Dis 50 (1):201-215.

Stoll S, Scheuer K, Pohl O, Muller WE (1996) Ginkgo biloba extract (EGb 761) independently improves changes in passive avoidance learning and brain membrane fluidity in the aging mouse. Pharmacopsychiatry 29 (4):144-149.

Su B, Wang X, Bonda D, Perry G, Smith M, Zhu X (2010) Abnormal mitochondrial dynamics--a novel therapeutic target for Alzheimer's disease? MolNeurobiol 41 (2-3):87-96.

Su Y, Ryder J, Li B, Wu X, Fox N et al. (2004) Lithium, a common drug for bipolar disorder treatment, regulates amyloid-beta precursor protein processing. Biochemistry 43 (22):6899-6908.

Sugioka R, Shimizu S, Tsujimoto Y (2004) Fzo1, a protein involved in mitochondrial fusion, inhibits apoptosis. J Biol Chem 279 (50):52726-52734.

Sunyach C, Michaud M, Arnoux T, Bernard-Marissal N, Aebischer J et al. (2012) Olesoxime delays muscle denervation, astrogliosis, microglial activation and motoneuron death in an ALS mouse model. Neuropharmacology 62 (7):2346-2352.

Swerdlow RH, Burns JM, Khan SM (2010) The Alzheimer's disease mitochondrial cascade hypothesis. J Alzheimers Dis 20 Suppl 2:S265-279.

Swerdlow RH, Burns JM, Khan SM (2014) The Alzheimer's disease mitochondrial cascade hypothesis: progress and perspectives. Biochim Biophys Acta 1842 (8):1219-1231.

Swerdlow RH, Khan SM (2004) A "mitochondrial cascade hypothesis" for sporadic Alzheimer's disease. Med Hypotheses 63 (1):8-20.

Swerdlow RH, Khan SM (2009) The Alzheimer's disease mitochondrial cascade hypothesis: an update. Exp Neurol 218 (2):308-315.

Tan CC, Yu JT, Wang HF, Tan MS, Meng XF, Wang C, Jiang T, Zhu XC, Tan L (2014) Efficacy and safety of donepezil, galantamine, rivastigmine, and memantine for the treatment of Alzheimer's disease: a systematic review and meta-analysis. J Alzheimers Dis 41 (2):615-631.

Tang WK, Ungvari GS, Leung HCM (2002) Effect of piracetam on ECT-induced cognitive disturbances: A randomized, placebo-controlled, double-blind study. Journal of Ect 18 (3):130-137.

Tanida I, Mizushima N, Kiyooka M, Ohsumi M, Ueno T, Ohsumi Y, Kominami E (1999) Apg7p/Cvt2p: A novel protein-activating enzyme essential for autophagy. Mol Biol Cell 10 (5):1367-1379.

Tieu Q, Okreglak V, Naylor K, Nunnari J (2002) The WD repeat protein, Mdv1p, functions as a molecular adaptor by interacting with Dnm1p and Fis1p during mitochondrial fission. J Cell Biol 158 (3):445-452.

Torraco A, Peralta S, Iommarini L, Diaz F (2015) Mitochondrial Diseases Part I: mouse models of OXPHOS deficiencies caused by defects in respiratory complex subunits or assembly factors. Mitochondrion 21:76-91.

Torres-Aleman I (2008) MOUSE MODELS OF ALZHEIMER'S DEMENTIA: CURRENT CONCEPTS AND NEW TRENDS. Endocrinology 149 (12):5952-5957.

Trimmer PA, Swerdlow RH, Parks JK, Keeney P, Bennett JP, Jr., Miller SW, Davis RE, Parker WD, Jr. (2000) Abnormal Mitochondrial Morphology in Sporadic Parkinson's and Alzheimer's Disease Cybrid Cell Lines. Exp Neurol 162 (1):37-50.

Twig G, Graf SA, Wikstrom JD, Mohamed H, Haigh SE et al. (2006) Tagging and tracking individual networks within a complex mitochondrial web with photoactivatable GFP. Am J Physiol Cell Physiol 291 (1):C176-184.

Uchikado H, Lin WL, DeLucia MW, Dickson DW (2006) Alzheimer disease with amygdala Lewy bodies: a distinct form of alpha-synucleinopathy. J Neuropathol Exp Neurol 65 (7):685-697.

Ueda K, Fukui Y, Kageyama H (1994) Amyloid beta - protein induced neuronal cell death: neurotoxic properties of aggregated amyloid beta - protein. Brain Res 639:240-244.

Ustyugov AA, Shelkovnikova TA, Kokhan VS, Khritankova IV, Peters O, Buchman VL, Bachurin SO, Ninkina NN (2012) Dimebon reduces the levels of aggregated amyloidogenic protein forms in detergent-insoluble fractions in vivo. Bull Exp Biol Med 152 (6):731-733.

Valko M, Leibfritz D, Moncol J, Cronin MT, Mazur M, Telser J (2007) Free radicals and antioxidants in normal physiological functions and human disease. Int J Biochem Cell Biol 39 (1):44-84.

Valla J, Berndt JD, Gonzalez-Lima F (2001) Energy hypometabolism in posterior cingulate cortex of Alzheimer's patients: superficial laminar cytochrome oxidase associated with disease duration. J Neurosci 21 (13):4923-4930.

Van Cauwenberghe C, Van Broeckhoven C, Sleegers K (2016) The genetic landscape of Alzheimer disease: clinical implications and perspectives. Genet Med 18(5):421-30.

van den Heuvel L, Smeitink J (2001) The oxidative phosphorylation (OXPHOS) system: nuclear genes and human genetic diseases. Bioessays 23 (6):518-525.

Vellas B, Coley N, Ousset P-J, Berrut G, Dartigues J-F et al. (2012) Long-term use of standardised Ginkgo biloba extract for the prevention of Alzheimer's disease (GuidAge): a randomised placebo-controlled trial. Lancet Neurol 11 (10):851-859.

Vellas B, Coley N, Ousset P-J, Berrut G, Dartigues J-F et al. (2010) Results of GUIDEAGE - A 5-year placebo-controlled study on the efficacy of EGb761 120mg to prevent or delay Alzheimer`s Dementia onset in elderly subjects with memory copmlaint. J Nutr Health Aging 14 (Supp 2):S23.

Vignisse J, Steinbusch HW, Bolkunov A, Nunes J, Santos AI, Grandfils C, Bachurin S, Strekalova T (2011) Dimebon enhances hippocampus-dependent learning in both appetitive and inhibitory memory tasks in mice. Prog Neuropsychopharmacol Biol Psychiatry 35 (2):510-522.

Virarkar M, Alappat L, Bradford PG, Awad AB (2013) L-arginine and nitric oxide in CNS function and neurodegenerative diseases. Crit Rev Food Sci Nutr 53 (11):1157-1167.

Waegemans T, Wilsher CR, Danniau A, Ferris SH, Kurz A, Winblad B (2002) Clinical efficacy of piracetam in cognitive impairment: A meta-analysis. Dementia and Geriatric Cognitive Disorders 13 (4):217-224.

Walsh DM, Hartley DM, Condron MM, Selkoe DJ, Teplow DB (2001) In vitro studies of amyloid beta-protein fibril assembly and toxicity provide clues to the aetiology of Flemish variant (Ala692-->Gly) Alzheimer's disease. Biochem J 355 (Pt 3):869-877.

Wang BS, Wang H, Song YY, Qi H, Rong ZX, Zhang L, Chen HZ (2010) Effectiveness of standardized ginkgo biloba extract on cognitive symptoms of dementia with a six-month treatment: a bivariate random effect meta-analysis. Pharmacopsychiatry 43 (3):86-91.

Wang J, Ferruzzi MG, Varghese M, Qian X, Cheng A, Xie M, Zhao W, Ho L, Pasinetti GM (2011) Preclinical study of dimebon on beta-amyloid-mediated neuropathology in Alzheimer's disease. Mol Neurodegener 6 (1):7.

Wang X, Su B, Lee HG, Li X, Perry G, Smith MA, Zhu X (2009) Impaired balance of mitochondrial fission and fusion in Alzheimer's disease. J Neurosci 29 (28):9090-9103.

Wang X, Su B, Siedlak SL, Moreira PI, Fujioka H, Wang Y, Casadesus G, Zhu X (2008) Amyloid-Beta overproduction causes abnormal mitochondrial dynamics via differential modulation of mitochondrial fission/fusion proteins. Proc Natl Acad Sci U S A 105 (49):19318-19323.

Wang XJ, Cao Q, Zhang Y, Su XD (2015) Activation and regulation of caspase-6 and its role in neurodegenerative diseases. Annu Rev Pharmacol Toxicol 55:553-572.

Wareski P, Vaarmann A, Choubey V, Safiulina D, Liiv J, Kuum M, Kaasik A (2009) PGC-1 alpha and PGC-1 beta regulate mitochondrial density in neurons. J Biol Chem 284 (32):21379-21385.

Webster SJ, Wilson CA, Lee CH, Mohler EG, Terry AV, Jr., Buccafusco JJ (2011) The acute effects of dimebolin, a potential Alzheimer's disease treatment, on working memory in rhesus monkeys. BrJPharmacol 164 (3):970-978.

Weinmann S, Roll S, Schwarzbach C, Vauth C, Willich SN (2010) Effects of Ginkgo biloba in dementia: systematic review and meta-analysis. BMC Geriatr 10:14.

WHO (2015a) Dementia Fact Sheet March 2015. http://www.who.int/mediacentre/factsheets/fs362/en/. Accessed 12/20/2015

WHO (2015b) World report on ageing and health. http://www.who.int/ageing/events/world-report-2015-launch/en/. Accessed 12/20/2015

Winblad B (2005) Piracetam: A review of pharmacological properties and clinical uses. Cns Drug Reviews 11 (2):169-182.

Wisniewski T, Goni F (2015) Immunotherapeutic approaches for Alzheimer's disease. Neuron 85 (6):1162-1176.

Wong YC, Holzbaur EL (2015) Autophagosome dynamics in neurodegeneration at a glance. J Cell Sci 128 (7):1259-1267.

Wu J, Li Q, Bezprozvanny I (2008) Evaluation of Dimebon in cellular model of Huntington's disease. Mol Neurodegener 3:15.

Xiao WH, Zheng FY, Bennett GJ, Bordet T, Pruss RM (2009) Olesoxime (cholest-4-en-3-one, oxime): analgesic and neuroprotective effects in a rat model of painful peripheral neuropathy produced by the chemotherapeutic agent, paclitaxel. Pain 147 (1-3):202-209.

Xiao WH, Zheng H, Bennett GJ (2012) Characterization of oxaliplatin-induced chronic painful peripheral neuropathy in the rat and comparison with the neuropathy induced by paclitaxel. Neurosci 203:194-206.

Xu Y, Yan J, Zhou P, Li J, Gao H, Xia Y, Wang Q (2012) Neurotransmitter receptors and cognitive dysfunction in Alzheimer's disease and Parkinson's disease. Prog Neurobiol 97 (1):1-13.

Yoo BC, Fountoulakis M, Cairns N, Lubec G (2001) Changes of voltage-dependent anion-selective channel proteins VDAC1 and VDAC2 brain levels in patients with Alzheimer's disease and Down syndrome. Electrophoresis 22 (1):172-179.

Youle RJ, van der Bliek AM (2012) Mitochondrial fission, fusion, and stress. Science 337 (6098):1062-1065.

Yu T, Fox RJ, Burwell LS, Yoon Y (2005) Regulation of mitochondrial fission and apoptosis by the mitochondrial outer membrane protein hFis1. J Cell Sci 118 (Pt 18):4141-4151.

Zanetta C, Nizzardo M, Simone C, Monguzzi E, Bresolin N, Comi GP, Corti S (2014) Molecular therapeutic strategies for spinal muscular atrophies: current and future clinical trials. Clin Ther 36 (1):128-140.

Zare-Shahabadi A, Masliah E, Johnson GV, Rezaei N (2015) Autophagy in Alzheimer's disease. Rev Neurosci 26 (4):385-395.

Zhang S, Hedskog L, Petersen CA, Winblad B, Ankarcrona M (2010) Dimebon (latrepirdine) enhances mitochondrial function and protects neuronal cells from death. JAlzheimersDis 21 (2):389-402.

Zhang ZW, Xu XC, Liu T, Yuan S (2016) Mitochondrion-Permeable Antioxidants to Treat ROS-Burst-Mediated Acute Diseases. Oxidative medicine and cellular longevity 2016:6859523.

Zheng L, Kagedal K, Dehvari N, Benedikz E, Cowburn R, Marcusson J, Terman A (2009) Oxidative stress induces macroautophagy of amyloid beta-protein and ensuing apoptosis. Free Radic Biol Med 46 (3):422-429.

Zhu F, Wu F, Ma Y, Liu G, Li Z, Sun Y, Pei Z (2011) Decrease in the production of beta-amyloid by berberine inhibition of the expression of beta-secretase in HEK293 cells. BMC Neurosci 12:125.

Zhu XC, Yu JT, Jiang T, Tan L (2013) Autophagy modulation for Alzheimer's disease therapy. Mol Neurobiol 48 (3):702-714.

Zhu Y, Xiao K, Ma L, Xiong B, Fu Y et al. (2009) Design, synthesis and biological evaluation of novel dual inhibitors of acetylcholinesterase and beta-secretase. Bioorg Med Chem 17 (4):1600-1613.

Ziegler-Graham K, Brookmeyer R, Johnson E, Arrighi HM (2008) Worldwide variation in the doubling time of Alzheimer's disease incidence rates. Alzheimers Dement 4 (5):316-323.

Zou Y, Xu L, Chen W, Zhu Y, Chen T et al. (2013) Discovery of pyrazole as C-terminus of selective BACE1 inhibitors. European journal of medicinal chemistry 68:270-283.

List of Publications

1: Clemens LE, Weber JJ, Wlodkowski TT, Yu-Taeger L, Michaud M, Calaminus C, **Eckert SH**, Gaca J, Weiss A, Magg JC, Jansson EK, Eckert GP, Pichler BJ, Bordet T, Pruss RM, Riess O, Nguyen HP. **Olesoxim suppresses calpain activation and mutant huntingtin fragmentation in the BACHD rat.** Brain. 2015;138(Pt 12):3632-53.

2: Eckmann J, Clemens LE, **Eckert SH**, Hagl S, Yu-Taeger L, Bordet T, Pruss RM, Muller WE, Leuner K, Nguyen HP, Eckert GP. **Mitochondrial membrane fluidity is consistently increased in different models of Huntington disease: restorative effects of Olesoxim.** Mol Neurobiol. 2014;50(1):107-18.
.
3: Stockburger C, Kurz C, Koch KA, **Eckert SH**, Leuner K, Müller WE. **Improvement of mitochondrial function and dynamics by the metabolic enhancer piracetam.** Biochem Soc Trans. 2013;41(5):1331-4.

4: Hagl S, Kocher A, Schiborr C, **Eckert SH**, Ciobanu I, Birringer M, El-Askary H, Helal A, Khayyal MT, Frank J, Muller WE, Eckert GP. **Rice bran extract protects from mitochondrial dysfunction in guinea pig brains.** Pharmacol Res. 2013; 76:17-27.

5: Eckmann J*, **Eckert SH***, Leuner K, Muller WE, Eckert GP. Mitochondria: mitochondrial membranes in brain ageing and neurodegeneration. Int J Biochem Cell Biol. 2013; 45(1):76-80.

6: Eckert GP, Renner K, **Eckert SH**, Eckmann J, Hagl S, Abdel-Kader RM, Kurz C, Leuner K, Muller WE. **Mitochondrial dysfunction--a pharmacological target in Alzheimer's disease.** Mol Neurobiol. 2012 Aug;46(1):136-50.

7: **Eckert SH**, Eckmann J, Renner K, Eckert GP, Leuner K, Muller WE. **Dimebon ameliorates amyloid-β induced impairments of mitochondrial form and function.** J Alzheimers Dis. 2012; 31(1):21-32.

8: Leuner K, Schütt T, Kurz C, **Eckert SH**, Schiller C, Occhipinti A, Mai S, Jendrach M, Eckert GP, Kruse SE, Palmiter RD, Brandt U, Dröse S, Wittig I, Willem M, Haass C, Reichert AS, Müller WE. **Mitochondrion-derived reactive oxygen species lead to enhanced amyloid beta formation.** Antioxid Redox Signal. 2012; 16(12):1421-33.

9: Peters I, Igbavboa U, Schütt T, **Haidari S**, Hartig U, Rosello X, Böttner S, Copanaki E, Deller T, Kögel D, Wood WG, Müller WE, Eckert GP. **The interaction of beta-amyloid protein with cellular membranes stimulates its own production.** Biochim Biophys Acta. 2009;1788(5):964-72.